CHARACTERIZATION OF LOW DENSITY POLYETHYLENE/OIL-FLY ASH COMPOSITES AND IMPACT OF SURFACE MODIFICATION OF OIL FLY ASH ON COMPOSITE PROPERTIES

BY

Muhammad Jamal Khan

A Thesis Presented to the

DEANSHIP OF GRADUATE STUDIES

KING FAHD UNIVERSITY OF PETROLEUM & MINERALS

DHAHRAN, SAUDI ARABIA

In Partial Fulfillment of the
Requirements for the Degree of

MASTER OF SCIENCE

In

CHEMICAL ENGINEERING

November, 2010

KING FAHD UNIVERSITY OF PETROLEUM & MINERALS

DHAHRAN- 31261, SAUDI ARABIA

DEANSHIP OF GRADUATE STUDIES

This thesis, written by **Muhammad Jamal Khan** under the direction of his thesis advisor and approved by his thesis committee, has been presented and accepted by the Dean of Graduate Studies, in partial fulfillment of the requirements for the degree of **MASTER OF SCIENCE IN CHEMICAL ENGINEERING.**

Thesis Committee

Dr. Abdulhadi Al-Juhani
(Thesis Advisor)

Prof. Ibnelwaleed Ali Hussein
(Thesis Co-Advisor)

Prof. Basel Fateh Abu-Sharkh
(Member)

Dr. Reyad A. Shawabkeh
(Member)

Dr. Anwar Ul-Hamid
(Member)

Dr. Usamah A. Al-Mubaiyedh
(Department Chairman)

Dr. Salam A. Zummo
(Dean of Graduate Studies)

Date 8/11/10

Dedicated to my loving family

ACKNOWLEDGMENTS

In the name of ALLAH, the Most Beneficent, the Most Merciful.

Praise and gratitude to ALLAH, the Almighty, with Whose gracious help, I was able to accomplish this work patience and endurance.

Acknowledgement is due to King Fahd University of Petroleum and Minerals, Saudi Arabia for providing the support and also for the King Abdulaziz City for Science and Technology for additional funding.

I had an excellent opportunity to work with various talented and professional individuals from KFUPM. I do not think that the words in this acknowledgement could express how truly grateful I am to my thesis advisor Dr. Abdulhadi A. Al-Juhani and co-advisor Dr. Ibnelwaleed A. Hussein for their constant support, guidance and encouragement throughout the course of this research and for many hours, day and night, of attention they devoted to the development of this study. I always revere their patience, expert guidance and ability to solve all intricate problems. They made my pursuit of higher education a truly enjoyable and unforgettable experience.

I would like to express my profound gratitude and appreciation to Dr. Reyadh Shawabkeh for his valuable guidance and encouragement in the conduction and successfully completion of this thesis. I really enjoyed working with him especially on the field of OFA surface modification.

Sincere appreciation and grateful thank to my committee member Dr. Anwar Ul-Hamid for his help and insight in different analysis specially SEM and XRF. His expertise really helped me to understand the morphological behavior of composites.

I also would like to thank to my committee member Dr. Basel Abu-Sharkh for his help and support.

Thanks are due to the current and previous chairmen of the Chemical Engineering Department, KFUPM Dr. Adnan Al-Amer and Dr. Usamah Al-Mubaiyedh for their support and assistance in all intricate problems. Also thanks to all my teachers of Chemical Engineering Department who helped me to developed the deep thinking of this field.

I am grateful to all my colleagues for their help and friendship especially to Mr. Sarfraz Haider Abbasi and Mr. Saad Sadiq for their motivational support and exchanging ideas. Also, I would like to thanks all staff persons and colleagues who helped me in the completion to my thesis especially Mr. Arab, Mr. Awwal, Mr. Massihullah, Mr. Moriano, Mr. Mofeez, Mr. Anwar, Mr. Saeed, Mr. Saood and Mr. A. Quddos.

Very special thanks to my dearest mother and father and other family members for their unconditional and endless support, love, sacrifices, prayers and understanding throughout my academic career. You all have both been a constant support for me and showed never wavering belief in me and understanding during the last 2 years. I would like to thank to all my aunts, uncles and cousins for all their concern and encouraging over the years. I would not be where I am in life if it weren't for their love and prays.

Also, I want to express my thanks to some of my dearest friends especially: Faraz Ali, Arhum, Zulfiqar, Wahab, Faraz, Babar, Salman, Zeehasham, Asad, Monim, Rahil, Shahid, and all others for their friendship and for being there for me when I needed someone to help clear my thoughts and to give me much needed bout of laughter.

To you all, I say Thank You.

TABLE OF CONTENTS

Acknowledgment iv
Table of Contents vi
List of Tables ix
List of Figures x
Abstract (English) xvi
Abstract (Arabic) xvii

Chapter 1
Introduction 1
1.1. Fly Ash and LDPE Composites 1
1.2. Motivation and Research Objective 3

Chapter 2 6
Literature Review 6

Chapter 3 17
Experimental Setup and Material Preparation 17
3.1: Surface treatment of Fly Ash 17
3.2: Characterization of Modified Fly Ash 19
3.2.1: Fourier Transform Infrared Spectroscopy (FTIR): 19
3.2.2: Surface Morphology: 20
3.2.3: XRD Analysis 20
3.2.4: BET Analysis and pore size distribution 20
3.3: Formulation of Fly Ash-Polymer Composite using Melt-Blending method 21
3.4: Rheological Analysis 22
3.5: Mechanical Analysis 24
3.6: Thermal Analysis 26
3.7: FE-SEM Analysis 27

Chapter 4

Results & Discussion: Characterization of Surface Modified Fly Ash 28

4.1: FTIR Analysis for Functional group 30

4.2: SEM and Spot Analysis 33

4.3: XRD Analysis 35

4.4: BET Analysis 37

Chapter 5

Results & Discussion: Rheological and Morphological Behavior of LDPE/OFA Composite 40

Part A: Rheological Behavior of LDPE/OFA Composite *41*

5.1: Effect of OFA on Storage Modulus of Composites 41

5.2: Effect of OFA on Loss Modulus of Composite 47

5.3: Crossover Point and Crossover Frequency: 53

5.4: Degree of dispersion by Cole-Cole Plot 55

Part B: Morphological Characterization of LDPE/OFA Composites *58*

Chapter 6

Results & Discussion: Mechanical, Thermal and Morphological Behavior of LDPE/OFA Composite 63

Part A: Mechanical Behavior of LDPE/OFA Composite 63

6.1: Effect of OFA on Young's Modulus: 64

6.1.1: Effect of OFA Loading on Young's Modulus 64

6.1.2: Effect of OFA Functionalization on Young's Modulus 67

6.1.3: Effect of PE-g-MA Compatiblizer on Young's Modulus 69

6.2: Effect of OFA on Elongation to Break 71

6.2.1: Effect of OFA Loading on Elongation to Break 71

6.2.2: Effect of OFA Functionalization on Elongation to Break 75

6.2.3: Effect of PE-g-MA Compatiblizer on Elongation to Break 77

6.3: Effect of OFA on Toughness 78

6.3.1: Effect of OFA Loading on Toughness 78

6.3.2: Effect of OFA Functionalization on Toughness 83

6.3.3: Effect of PE-g-MA Compatiblizer on Toughness 84

6.4: Effect of OFA on Yield Strength 86
6.4.1: Effect of OFA Loading on Yield Strength 71
6.4.2: Effect of OFA Functionalization on Yield Strength 75
6.4.3: Effect of PE-g-MA Compatiblizer on Yield Strength 77
6.5: Effect of OFA on Ultimate Strength 93
6.5.1: Effect of OFA Loading on Ultimate Strength 71
6.5.2: Effect of OFA Functionalization on Ultimate Strength 75
6.5.3: Effect of PE-g-MA Compatiblizer on Ultimate Strength 77
Part B: Thermal Behavior of LDPE/OFA Composite: 101
6.6: Effect on Melting Point: 101
6.7: Effect on %Crystallization: 105
6.8: Effect on On-Set Temperature: 108
6.9: Effect on Crystallization Peak: 111

Chapter 7 115

Conclusion and Recommendations 115

Appendix A 120

References 159

Vitae 165

LIST OF TABLES

Table 2.1: Heavy fuel oil fly ash analysis 7

Table 2.2: Elemental composition of OFA by EDX 7

Table 3.1: Variation of reaction parameters for OFA 19

Table 3.2: Composition of LDPE/OFA Composites 22

Table 4.1: XRF analysis of ash samples treated at different acid compositions (wt.%) with air oxidation 29

Table 4.2: Average weight percent of carbon, oxygen and sulfur on the surface of ash samples 35

Table 4.3: Physical properties of the ash samples deduced from N_2 adsorption 38

Table 6.1: Effect of OFA loading on Young's Modulus 64

Table 6.2: Effect of OFA loading on Elongation to Break 71

Table 6.3: Effect of OFA loading on Toughness 79

Table 6.4: Effect of OFA loading on Yield Strength 86

Table 6.5: Effect of OFA loading on Ultimate Strength 94

Table 6.6: Effect of OFA loading on Melting Point 101

Table 6.7: Effect of OFA loading on %Crystallinity 105

Table 6.8: Effect of OFA loading on On-Set Temperature 108

Table 6.9: Effect of OFA loading on Crystallization Peak 112

LIST OF FIGURES

Figure 1.1: Fly ash grains at magnified view 3

Figure 1.2: Flow Chart of the Project 5

Figure 3.4.1: Carver Hydraulic Press 23

Figure 3.4.2: ARES Controlled Strain Rheometer 24

Figure 3.5.1: Dog Bone Sample for Mechanical Analysing 25

Figure 3.5.2: Instron Mechanical Testing Machine 25

Figure 3.6.1: Modulated DSC Equipment 27

Figure 4.1: XRF analysis of untreated OFA sample. 29

Figure 4.2(a): FTIR spectra of as-received and modified fly ash with and without air-oxidation 32

Figure 4.2(b): FTIR spectra of fly ash modified by different acid composition and air-oxidation 32

Figure 4.3: SEM analysis of the ash samples 34

Figure 4.4: X-Ray Diffraction Patterns for modified and unmodified Oil Fly Ash 37

Figure 4.5: BET modified and unmodified Oil Fly Ash 39

Figure 5.1.1(a): Effect of OFA Loading on Storage Modulus 42

Figure 5.1.1(b): Effect of COOH-OFA Loading on Storage Modulus 43

Figure 5.1.1(c): Effect of OFA Loading with 2% PE-g-MA on Storage Modulus 43

Figure 5.1.1(d): Effect of COOH-OFA Loading with 2% PE-g-MA on Storage Modulus 44

Figure 5.1.2(a): Effect of OFA-functionalization at 5% loading on Storage Modulus 45

Figure 5.1.2(b): Effect of PE-g-MA at 5% OFA loading on Storage Modulus 46
Figure 5.1.2(c): Effect of PE-g-MA at 5% COOH-OFA loading on Storage Modulus 46
Figure 5.2.1(a): Effect of OFA Loading on Loss Modulus 48
Figure 5.2.1(b): Effect of COOH-OFA Loading on Loss Modulus 49
Figure 5.2.1(c): Effect of OFA Loading with 2% PE-g-MA on Loss Modulus 49
Figure 5.2.1(d): Effect of COOH-OFA Loading with 2% PE-g-MA on Loss Modulus ...50
Figure 5.2.2(a): Effect of OFA-functionalization at 5% loading on Loss Modulus 51
Figure 5.2.2(b): Effect of PE-g-MA at 5% OFA loading on Loss Modulus 52
Figure 5.2.2(b): Effect of PE-g-MA at 5%COOH-OFA loading on Loss Modulus 52
Figure 5.3.1: Effect of OFA Loading on Crossover Point and Frequency 54
Figure 5.3.1: Effect of COOH-OFA Loading on Crossover Point and Frequency 54
Figure 5.4.1: Cole-Cole plot for LDPE/OFA composite 56
Figure 5.4.2: Cole-Cole plot for LDPE/OFA composite with PE-g-MA 56
Figure 5.4.2: Cole-Cole plot for LDPE/COOH-OFA composite.....57
Figure 5.4.2: Cole-Cole plot for COOH-OFA and LDPE polymer composite with PE-g-MA 57
Figure 5.5.1: SEM for pure LDPE at 5µm scale 59
Figure 5.5.2(a) SEM for LDPE/OFA composite at 2% loading and 5µm scale 59
Figure 5.5.2(b) SEM for LDPE/OFA composite at 2% loading and 10µm scale 60
Figure 5.5.3: SEM for LDPE/OFA composite at 5% loading and 5µm scale 60
Figure 5.5.4(a) SEM for LDPE/COOH-OFA composite at 2% loading and 10µm scale .61
Figure 5.5.4(b) SEM for LDPE/COOH-OFA composite at 2% loading and 5µm scale...61
Figure 5.5.5(a) SEM for LDPE/COOH-OFA composite at 5% loading and 5µm scale...62

Figure 5.5.5(b) SEM for LDPE/COOH-OFA composite at 5% loading and 4µm scale...62
Figure 6.1.1(a): Effect of OFA Loading on Young's Modulus 65
Figure 6.1.1(b): Effect of COOH-OFA Loading on Young's Modulus.....66
Figure 6.1.1(c): Effect of OFA Loading with 2% PE-g-MA on Young's Modulus 66
Figure 6.1.1(d): Effect of COOH-OFA Loading with 2% PE-g-MA on Young's Modulus 67
Figure 6.1.2(a): Effect of OFA functionalization without PE-g-MA on Young's Modulus 68
Figure 6.1.2(b): Effect of OFA functionalization with 2% PE-g-MA on Young's Modulus 68
Figure 6.1.3(a): Effect of Compatiblizer with OFA Loading on Young's Modulus.....70
Figure 6.1.3(b): Effect of Compatiblizer with COOH-OFA Loading on Young's Modulus 70
Figure 6.2.1(a): Effect of OFA Loading on Elongation 73
Figure 6.2.1(b): Effect of COOH-OFA Loading on Elongation.....73
Figure 6.2.1(c): Effect of OFA Loading with 2% PE-g-MA on Elongation 74
Figure 6.2.1(d): Effect of COOH-OFA Loading with 2% PE-g-MA on Elongation.....74
Figure 6.2.2(a): Effect of OFA functionalization without PE-g-MA on Elongation 76
Figure 6.2.2(b): Effect of OFA functionalization with 2% PE-g-MA on Elongation.....76
Figure 6.2.3(a): Effect of Compatiblizer with OFA Loading on Elongation.....77
Figure 6.2.4(b): Effect of Compatiblizer with COOH-OFA Loading on Elongation 78
Figure 6.3.1(a): Effect of OFA Loading on Toughness.....81
Figure 6.3.1(b): Effect of COOH-OFA Loading on Toughness 81

Figure 6.3.1(c): Effect of OFA Loading with 2% PE-g-MA on Toughness 82

Figure 6.3.1(d): Effect of COOH-OFA Loading with 2% PE-g-MA on Toughness 82

Figure 6.3.2(a): Effect of OFA functionalization without PE-g-MA on Toughness 83

Figure 6.3.2(b): Effect of OFA functionalization with PE-g-MA on Toughness 84

Figure 6.3.3(a): Effect of Compatiblizer with OFA Loading on Toughness.....85

Figure 6.3.3(b): Effect of Compatiblizer with COOH-OFA Loading on Toughness 85

Figure 6.4.1(a): Effect of OFA Loading on Yield Strength.....88

Figure 6.4.1(b): Effect of COOH-OFA Loading on Yield Strength 88

Figure 6.4.1(c): Effect of OFA Loading with 2% PE-g-MA on Yield Strength.....89

Figure 6.4.1(d): Effect of COOH-OFA Loading with 2% PE-g-MA on Yield Strength ..89

Figure 6.4.2(a): Effect of OFA functionalization without PE-g-MA on Yield Strength...90

Figure 6.4.2(b): Effect of OFA functionalization with PE-g-MA on Yield Strength 91

Figure 6.4.3(a): Effect of Compatiblizer with OFA Loading on Yield Strength.....92

Figure 6.4.3(b): Effect of Compatiblizer with COOH-OFA Loading on Yield Strength .93

Figure 6.5.1(a): Effect of OFA Loading on Ultimate Strength.....95

Figure 6.5.1(b): Effect of COOH-OFA Loading on Ultimate Strength 96

Figure 6.5.1(c): Effect of OFA Loading with 2%PE-g-MA on Ultimate Strength.....96

Figure 6.5.1(d): Effect of COOH-OFA Loading with 2%PE-g-MA on Ultimate Strength
.....97

Figure 6.5.2(a): Effect of OFA functionalization without PE-g-MA on Ultimate Strength
.....98

Figure 6.5.2(b): Effect of OFA functionalization without PE-g-MA on Ultimate Strength
.....98

Figure 6.5.3(a): Effect of Compatiblizer with OFA Loading on Ultimate Strength 100
Figure 6.5.3(b): Effect of Compatiblizer with COOH-OFA Loading on Ultimate Strength 100
Figure 6.6.1(a): Endothermic Melting curves of LDPE/OFA composite without compatiblizer 102
Figure 6.6.1(b): Endothermic Melting curves of LDPE/OFA composite with compatiblizer 102
Figure 6.6.2: Effect of functionalization of OFA on Melting Point 103
Figure 6.6.3(a): Effect of compatiblizer with OFA loading on Melting Point 104
Figure 6.6.3(b): Effect of compatiblizer with COOH-OFA loading on Melting Point ...104
Table 6.7: Effect of OFA loading on %Crystallinity 105
Figure 6.7.1: Effect of functionalization of OFA on %Crystallinity 106
Figure 6.7.2(a): Effect of compatiblizer with OFA loading on %Crystallinity 107
Figure 6.7.2(b): Effect of compatiblizer with COOH-OFA loading on %Crystallinity ..107
Figure 6.8.1(a): Exothermic Crystallization curves of LDPE/OFA composite without compatiblizer 109
Figure 6.8.1(b): Exothermic Crystallization curves of LDPE/OFA composite with compatiblizer 109
Figure 6.8.2: Effect of functionalization of OFA on On-set temperature 110
Figure 6.8.3(a): Effect of compatiblizer with OFA loading on On-set temperature 110
Figure 6.8.3(b): Effect of compatiblizer with COOH-OFA loading on On-set temperature 111
Figure 6.9.1: Effect of functionalization of OFA on Crystallization Peak 113

Figure 6.9.2(a): Effect of compatiblizer with OFA loading on Crystallization Peak 113

Figure 6.9.2(b): Effect of compatiblizer with COOH-OFA loading on Crystallization Peak.....114

ABSTRACT

Full Name : Muhammad Jamal Khan

Thesis Title : Characterization of Polyethylene/Fly Ash Composites and Impact of Surface Modification of Fly Ash on composite Properties

Major Field : Chemical Engineering

Date of Degree : June, 2010

Mineral Fillers are commonly used in plastics to enhance the performance and reduce the cost of plastic resins. Uniform distribution of these fillers through the polymer matrix is one of the main considerations to achieve the desirable properties of composites. Oil Fly Ash (OFA) was used in this research project as filler in Low density Polyethylene (LDPE) and its effect on different properties was investigated. OFA was obtained as a by-product from the combustion of fuel in power plants, is cheap filler as compared to the other traditional fillers. Surface modification or functionalization of OFA by acid treatment was one of the main goals of this study. It is believed that the surface modification is an effective technique to achieve good dispersion of filler into the polymer matrix and hence final properties of polymer composites may be enhanced. Different parameters were used for OFA functionalization followed by optimization of these parameters. Fourier transforms infrared spectroscopy, Scanning Electron Microscopy/Energy dispersive spectroscopy and X-ray Diffraction crystallography of OFA was undertaken before and after the modification to observe the effect of surface modification. Also, the Polyethylene-grafted-Maleic Anhydride (PE-g-MA) was used to investigate the attraction of Maleic group with and without the functionalization of fillers. The effect of OFA on the rheological, morphological, mechanical and thermal properties was investigated. Different weight fractions of OFA were used in order to investigate the effect of filler content in the polymer matrix.

ملخص الرسالة

الإسم بالكامل : جمال محمد خان

عنوان الرسالة : دراسة البولي إثيلين / مركبات الرماد المتطاير وأثر تعديل السطح بالرماد المتطاير على خصائص المركب

مجال التخصص : الهندسة الكيميائية

تاريخ الدرجة العلمية: يونيو، 2010

الحشو المعدني يَستعملُ بشكل كبير في البلاستيكِ لتَحسين الأداءِ ويُخفّضُ كلفةَ الراتنج البلاستيكي. التوزيع الموحّد لهذا الحشو خلال مصفوفةِ البوليمر يكون إحدى التحديات الرئيسيةِ لإنْجاز الخواص المرغوبةِ للمركّباتِ. رماد النفط المتطاير (أو. إف. أي) أستعمل في هذا المشروع البحثي كمادة محشوة في البولي إثيلين ذو الكثافةِ المنخفضةِ وتأثيره على الخواص المختلفةِ أيضا درس في هذا البحث. رماد النفطِ المتطاير يتولد كناتج عرضي مِنْ احتراق الوقودِ في محطات توليد الطاقة، بالإضافة إلى ذلك فهو يعتبر مادة حشو رخيصة بالمقارنة مع الحشو التقليديِ الآخرِ. التعديل السطحي أَو إضافة احد المجموعات الوظيفية لرمادِ النفطِ المتطاير بالمعالجةِ الحامضيةِ كَانتْ إحدى الأهدافِ الرئيسيةِ لهذه الدراسةِ. فهو يُعتَقدُ بأنّ التعديلَ السطحيَ تقنيةُ فعّالةُ لإنْجاز توزيع جيد للمادة المحشوة في مصفوفةِ البوليمر وبتالي فإن خواص النهائية لمركبات البوليمر المتكونة من هذا الحشو سوف تتحسن. عوامل مختلفة إستعملتت لإضافة المجموعات الوظيفية لرمادِ النفطِ المتطاير تَلتْ بتحقيقِ الأمثلية بينها. أظهرت دراسات عديدة أجريت لرماد النفط المتطاير قَبلَ وَبَعد التعديلِ لمُلاحَظَة تأثيرِ التعديلِ السطحي عليها. أيضاً، درست إضافة مجموعة الماليك إلى البوليمر لكي يرى تأثيرها على الحشو قبل وبعد إضافة المجموعة الوظيفة. درس تأثير رمادِ النفطِ المتطاير على التميع، تركيبة السطح ,الخواص الحرارية والميكانيكية في هذا البحث. كتل مختلفة من رماد النفط المتطاير استخدمت لكي يَتحرّى تأثيرَ محتوى الحشو في مصفوفة البوليمر.

CHAPTER 1

INTRODUCTION

1.1. Fly Ash and LDPE Composites

Fly ash is a residual or by-product generated by the combustion of coal and fuel. It is collected from the chimneys of coal-fired power plants and is different from the other ash which is collected from the bottom of the coal furnace called "bottom ash". Fly ash and Bottom ash are collectively called "Coal Ash". Oil fly ash (OFA) is a fine, grained, black powdery particulate type waste material (fig.1) and is collected by means of electrostatic precipitators or mechanical devices such as cyclones to control the air pollution. According to a survey conducted by American Chemical Society in 2009, more than 71 million tons of fly ash is produced annually in United Stated by 460 coal-fired plants and 45 percent of this quantity is re-used for different applications [1]. Mostly it is used as a replacement of Portland cement, as a filler in polymers, asphalt and cementitious materials, stabilization agent and also for solidification for wastage and sludge. A report published by C&EN in December 2009 estimates that 7% of global carbon dioxide and greenhouse gases are emitted by cement production which can be reduced by the use of fly ash [2]. In KSA, about 70 power plants consume 9.285 million metric tons of diesel fuel, 7,211 million metric tons of crude oil, 5.437 million metric tons of heavy fuel oil and 22,913 million m^3 of gas and produced OFA as a by-product. This quantity must be disposed in an environment friendly manner. In many countries, fly ash is generally stored at coal power plants or placed in landfills. A big percentage of fly ash is recycled

to supplement cement in concrete production and black pigment for cementatious materials.

OFA was mainly composed of unburned carbon black, residue ash and some amount of sulfur depending on the type of fuel oil used [3]. Some traces of toxic components may be present depending on the specific fuel such as arsenic, beryllium, boron, cadmium, chromium VI, cobalt, lead, manganese, mercury, molybdenum, selenium, strontium, thallium and vanadium [4-6]. Some other component like SiO_2, Al_2O_3, Fe_2O_3 and Cao may also present in a very small amount.

Polymer composite filled with inorganic mineral fillers have an attraction for industries for their wide ranging applications and low cost. Fillers are incorporated into polymers to improve various properties such as, mechanical strength, rheological behavior and thermal degradation. Uniform distribution of these tiny particles plays an important role in the enhancement of the properties. Clays, silica, mica, fly-ash and montmorrilonite are some common examples of mineral fillers [7-11]. Since the discovery of carbon nanotubes (CNT) in 1991, a remarkable enhancement has been done in the polymer composite industry. Carbon nanotubes having magnificent properties attracted the attention of engineers and scientists for use as filler material for polymer nanocomposites. But high cost of expensive synthesis and difficulties in bulk production has restricted the use of CNT for large scale composite production. As compared to CNT, fly-ash produced as a by-product by large scale power plant industry makes it inexpensive and very accessible. Surface modification by functionalization also enhances the dispersion of the fillers and hence improves the composites properties more effectively.

The object of the current research was to study the effect of OFA filler on the mechanical, thermal, rheological and morphological properties of the low density polyethylene. Surface modification of fly ash was undertaken in order to increase its dispersion in the polymer matrix and in an effort to enhance the properties of polymer composite.

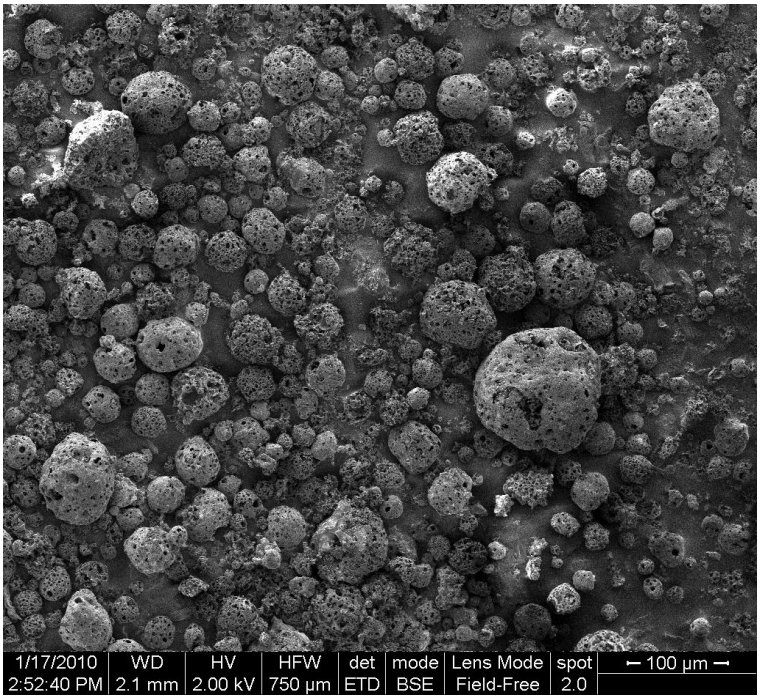

Figure 1.1: Fly ash grains at magnified view

1.2. Motivation and Research Objective

The main objective of this research work was to look into the possibility of improving the mechanical, rheological and thermal properties of low density polyethylene (LDPE) composites using inexpensive Oil Fly Ash (OFA) filler with and without surface modification, as compared to conventional expensive fillers such as CNT. The resulting composite adds high value to polyolefin as well as a makes good use of a by-product

produced by the fuel combustion processes of coal and fuel oil. A detailed investigation of the surface modification of OFA by acid treatment has been conducted. The parameters for surface treatment like acid composition and air oxidation were optimized in order to determine the optimum functionalization conditions for fly ash particles. Formulation of modified and unmodified fly ash withe polymer matrix was carried out followed by rheological, mechanical, thermal and morphological characterization of LDPE/OFA composites.

This research has the following specific objectives:

1. To perform surface treatment of OFA to attached functional group and also to enhance the surface properties of OFA
2. Characterization of OFA before and after surface modification
3. To produce composites of LDPE with modified and un-modified OFA by Melt-mixing with and without PE-g-MA compatiblizer
4. To determine the effect of OFA loading on
    a. the mechanical strength of LDPE by dynamic mechanical thermal analyzer
    b. the thermal stability of LDPE by modulated DSC equipment
    c. the rheological properties of LDPE by ARES Rheometer
    d. the morphological properties of the LDPE/OFA matrix by high resolution SEM

The results of this project are expected to develop local expertise in surface modification and polymer composites. A schematic flow chart for the project design is shown in Figure 1.2.

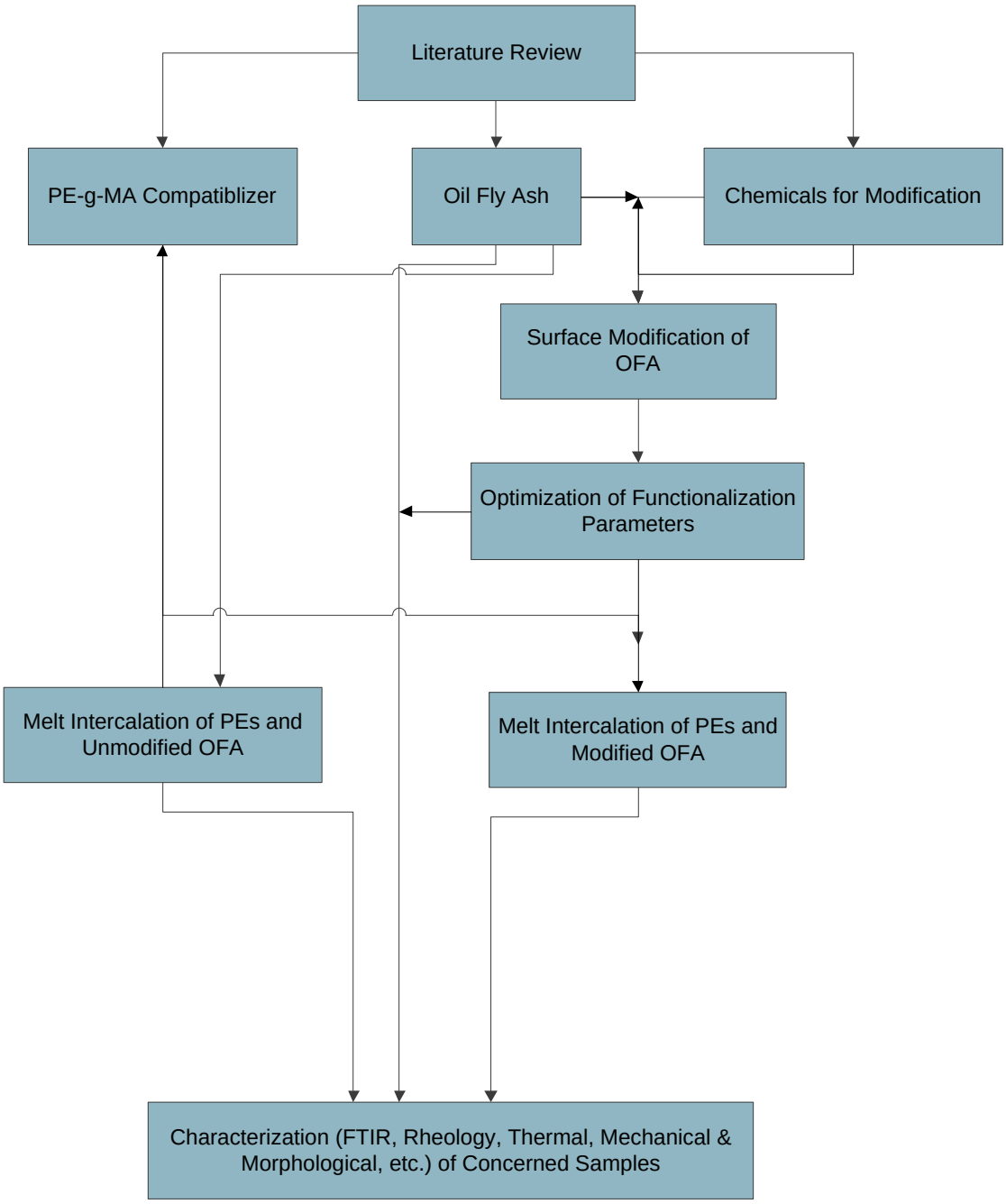

Figure 1.2: Flow Chart of the Project

CHAPTER 2

LITERATURE REVIEW

Polyethylene (PE) is a thermoplastic with a very simple structure, probably the polymer we see most in daily life. The variety of its application from simple shopping bags and children toys to bullet proof vests made it heavily used consumer product in chemical industry. Different types of fillers have been used to improve the properties of PE. Selection of fillers depends on the required enhancement in desirable properties and also on its economical production. Fly Ash is considered as a cheap filler material in construction industry because it is obtain as a by-product from the burning of fuel in power plants. Following literature describes the effect of fillers on the properties of PE and also the use of OFA as a filler in different applications. It is believed that up to 50% of the cement in concrete can be replaced by fly ash without compromising concrete performance [12].

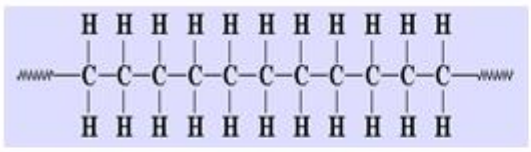

Polyethylene

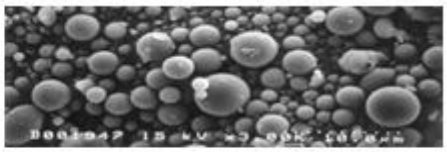

Fly Ash

Abu-Rizaiza and Daous [13-14] characterized the fly ash resulting from combustion of heavy fuel oil in the power generation plant of the Saudi Electricity Company in Rabigh. The chemical analysis of oil fly ash used is shown in Table 2.1. Also in a previous project, the Energy Dispersive X-ray Spectroscopy Analysis (EDX) was carried at the

Research Institute, KFUPM. Chemical composition obtained from this analysis is shown in Table 2.2.

Table 2.1: Heavy fuel oil fly ash analysis

Parameter	Quantity
pH @ 18 °C	2.8
Moisture	0.33 wt %
Unburned Carbon @ 700 °C	90.18 wt %
Ash Content	9.82 wt %
SO_3	3.06 wt %
Vanadium as V	4007 ppm
Nickel as Ni	1021 ppm
Iron as Fe	559.4 ppm
Magnesium as Mg	1800 ppm

Table 2.2: Elemental composition of OFA by EDX

Element	Weight, %
Carbon	92.5
Magnesium	0.79
Silicon	0.09
Sulfur	5.80
Vanadium	0.61

These analyses show that the fly ash used in this research work is mostly composed of carbon material with a very little amount of sulfur. Also the presence of some heavy metal is observed in traces.

Suryasarathi et al. [15] described the effect of fly ash on the mechanical, thermal, dielectric, rheological and morphological properties of Nylon 6. Fly Ash of an average particle size of 8μm and 60μm was used in 5, 10, 20, 25, 30, 35 and 40 wt% ratios. It was observed that as the percentage of the filler increased, tensile strength of the composites decreased and the effect was greater with larger particle size. It was observed that the rate of reduction of percentage elongation was higher in case of smaller particle size up to 20% filler loading whereas; it was higher at higher filler loading in case of larger particle size fly ash. Although the flexural strength increased with increase in filler concentration in both cases but it started to decrease after 40% addition of large particle size. The impact strength initially increased or remained almost same upto 25% addition of both particle sizes. Agglomeration of smaller particle sized is assumed and confirmed by higher increase in Young's Modulus as compared to larger particle size filler. Results show good dispersion of smaller particle size in case of low filler loading (upto 20%) as compared to larger particle size while it decreases in the case of higher filler loading due to agglomeration of smaller particle size and hence reduce strain mobility. An increase in dielectric constant has been observed by addition of both particle size fillers. Heat distortion temperature also increased by the addition of both type of fillers. The extent of increment is higher in case of larger particle size for lower filler loading but the higher in case of lower particle size for higher filler loading (upto 40%) due to agglomeration. Addition of fly ash increased the shear viscosity of the composite but the slip of particulate filler occurred at 10 wt% concentration for larger particle size and at 20 wt% concentration for smaller particle size. This is due to the presence of hollow sphere in larger particle size. Scanning electron microscopy images of 30 wt% composites were

used to describe the surface morphology of the composite. It was observed that the polymer matrix is not sufficient to encapsulate the filler. Good separation of particles was observed for smaller particle size in case of lower filler loading as compared to larger particle size but agglomeration observed in higher filler loading for smaller particle size.

Mechanical properties and surface Morphology of recycled HDPE filled with calcium carbonate and Fly Ash has been investigated by Atikhler et al. [16]. Authors investigated the effect of surface treated FA on the mechanical properties of HDPE as compare to conventional calcium carbonate filler. Fly ash was subjected to surface treatment with 3-amino propyl triethoxy silane. Tensile strength slightly increased by the addition FA as filler compared to conventional calcium carbonate. However, increment is much higher when modified FA was used especially, up to 30% filler content. At 40% loading, the increase in Young's modulus of the composites was 62.2%, 78.5% and 88.0% for calcium carbonate, untreated FA and treated FA respectively. The decrease in elongation to break is higher for FA filled composites compare with calcium carbonate filled composites. This decrement slightly increased when treated-FA used as filler. SEM results showed a good interfacial adhesion between FA and HDPE matrix. Conclusively authors found FA as good replacement for CC.

Fly Ash generated from heavy oil was characterized by Woo et al. [17] and compared to carbon black for use in cementious industry. Author described that heavy oil fly ash (HOFA) is mainly composed of carbon and with some contents of sulfur and residue ash. Heavy oil fly ash is composed of black amorphous carbon similar to carbon black with spherical shaped particle. The particle size distribution ranged from 10μm to 120 μm. The mortar test showed stable compressive strength with increasing heavy oil fly ash addition

which is attributed to the glass state inorganic substances such as SiO_2, Fe_2O_3, Al_2O_3 and CaO in heavy oil fly ash contributed to the formation of hydrate cementious material that increase compressive strength. Results showed that fly ash has good physical and chemical properties like carbon black and can be replaced carbon black after some treatments in cementious material.

Yang et al. investigated the surface modification of fly ash by use of isothermal heating and its effect on polymer properties [18]. Authors observed an increase in surface area and whiteness of fly ash particles after modification. Also the filling test showed an improvement in interface between polypropylene and fly ash after modification. Kishore et al. investigated the effect of surface treatment of fly ash by adhesion-increasing and adhesion-decreasing on impact behavior of polymer composite [19]. It was observed by results that adhesion-increasing modification (silane-acetone treatment) showed greater absorption of energy and maximum load while adhesion-reducing modification increased the Ductility Index. Effect of Si69 and NaOH treatment of surface of fly ash on the properties of Natural Rubber/Fly Ash composite was investigated by Thongsang et al. [20]. It was observed that by using various contents of bis-(triethoxysilylpropyl) tetrasulfane (Si69) for surface modification, the mechanical properties of composites increased up to 4% loading of filler, while NaOH solution showed no improvement in properties. Surface modification to improve the dispersion is not a new technique. It is observed that the attachment of carboxylic acids to the different carbon compounds (such as carbon nanotubes) not only enhanced the interface linking property of filler but also provides the reactive sites to attach a variety of functional groups [21-23].

The rheological investigation of polyethylene oxide (PEO)/organoclay nanocomposites has been done by Hyun et al. [24]. Author used three different organoclays modified with the alkyl ammonium salts; the effect of surfactants on organoclay surfaces in polymer/organoclay nanocomposites was investigated. The internal structure analysis and rheological measurement of the nanocomposites was done by the author. Rheological properties of these nanocomposites show different behavior with different modifier concentrations and surfactant sizes (chain lengths). An increase in shear viscosity and power law behavior was observed with increase in organoclay concentration. Thermal stability and storage moduli also increased with increasing organoclay contents.

Dezhen et al. [25] investigated the influence of chlorinated polyethylene (CPE) on mechanical properties, morphology, and rheology of nanocomposites of poly(vinyl chloride) (PVC) and nano-metric calcium carbonate particles. Poly(vinyl chloride)/calcium carbonate nanocomposites were prepared by melt blending method and Chlorinated PE used as an interfacial modifier. Results showed that elongation to break and Young's Modulus increased with increase in concentration of $CaCO_3$ nanoparticles. The use of CPE was more effective in increasing in Izod impact strength and author obtained a higher value of 745 J/m in the presence of CPE. Rheological study showed a remarkable increment in melt viscosity by the addition of $CaCO_3$ nanoparticles in PVC while the viscosity decreased by the addition of CPE. TEM was used for the morphological study of the nanocomposite and results showed $CaCO_3$ particles were dispersed uniformly through the matrix of PVC. Results showed that the nano $CaCO_3$ particles in the PVC matrix were encapsulated with a CPE layer.

Sombatsompop et al. [26] investigated the effects of untreated precipitated silica and fly ash silica as fillers on the properties of natural rubber and styrene butadiene rubber compounds. The effects of filler on the final properties were investigated for a range of 0 to 80 phr loading. A progressive increase in cure time and minimum and maximum torque observed in NR system at precipitated silica (PSi) loading of 30-75 phr while no change or a relatively low cure time and viscosity observed in case of Fly Ash silica (FASi). For low concentration (0-30), vulcanization properties of both PSi and FASi were the same but it improved more for higher concentration in case PSi filler while it remained the same for FASi. Author suggested FA as filler in NR for low concentration loading (0-30 phr) to improve its mechanical properties but not for SBR except when improvement in tensile and tear properties required.

Hwang described the beneficial uses of Fly Ash [27] in cementious, polymer and other different industries. Author investigated the effect of Fly Ash on the properties of Polypropylene, LDPE and HDPE as compared to traditional $CaCO_3$ filler. The polymers were mixed with the fillers at filler contents of 0, 10, 20, 40 and 80 pph. Results showed that the yield strength and Young's modulus of the materials increase, and elongation decrease, as the filler content increases. SEM images show good bonding of $CaCO_3$ with HDPE and Fly ash with PP.

Chen et al. [28] improved the interaction between poly (butylene succinate) (PBS) and a commercial organoclay, Cloisite 25A (C25A), using functionalization of clay by epoxy groups. Author grafted the epoxy group to C25A and produced a twice functionalized organoclay (TFC). Results showed an improvement of mechanical properties of composite in case of PBS/TFC as compared to PBS/C25A composite. XRD and TEM

analyses were used to study the morphology of the composites which showed an increase in interfacial interaction between PBS and TFC. It means that TFC enhanced the crystallization of PBS more effectively than C25A, and this indicated that TFC was more efficient for the nucleation than C25A.

The rheological properties of polystyrene/layered silicate nanocomposites are investigated by Lim and Park [29]. Author showed that both storage and loss moduli increased with silicate loading at all frequencies and showed non-terminal behavior at low frequencies which shows the presence of non-homogeneous systems with ordered microstructures. The result showed that the rheological properties of polystyrene/layered silicate nanocomposite depend not only on the intercalation of polymers, but also on the alignment of silicate layers.

Mcnally et al. [30], investigated polyethylene (PE) multiwalled carbon nanotubes (MWCNT's) composite with filler loading ranged from 0.1 to 10%. Author observed some degree of dispersion as well as agglomerations. Also the percolation threshold of the system was investigated. Author discussed the previous observation of (Potschke et al., 2004; Bhattacharyya et al., 2004; Mitchel et al., 2002) that the formation of a percolated system can be detected by characterising the complex viscosity (η^*), storage modulus (G') and loss modulus (G'') as a function of frequency (ω). It was observed that η^*, G' and G" increases with the increase of the concentration of MWCNT. The increment was more dominant at lower frequencies as compare to higher frequency. Also the low frequency response is indicative of 'pseudo-solid-like' behavior, and has been seen for a conventionally filled polymer with strong interactions between filler and polymer.

Ahmad et al. [31] investigated the thermal stability, mechanical and adsorption resistant properties of HDPE/PEG/Clay nanocomposites on exposure to electron beam where Poly ethylene glycol (PEG) was used as compatiblizer. These properties were investigated by TGA, Young's Modulus, tensile strength and hardness test. Author used the organically modified montmorillonite (OMMT) type of clay in this study. Results showed that presence of PEG as a compatiblizer has improved the dispersion of clay layers into the matrix and enhanced the mechanical properties and thermal resistance of nanocomposites. 2M2HT was used as a swelling agent or clay modifier but the best intercalation was observed after the addition of PEG into the matrix. It means that the addition of PEG enhanced the dispersibility of clay layer into the polymer matrix to form a more homogeneous system by increasing the distance between the clay layers. Authors observed that a Maleic-anhydride group compatiblizer interact with the swelling agent to improve the penetration of clay layer into the polymer molecule more easily. It is observed that a significant decrease in thermal stability occurs as we eliminate the PEG compatiblizer from the polymer matrix. A satisfactory enhancement in the Young's modulus was observed after adding 5 wt% of clay that drops on further clay content but a satisfied improvement in tensile strength is not observed. But the enhancement in mechanical properties observed by improvement in cross-linking of polymer was linked to irradiation effect. It is also observed that the addition of PEG prevented the degradation of nanocomposites up to 100KGy of irradiation and significantly improved the tensile strength and Young's Modulus valued at 500KGy of irradiation. In this study, author used 15% of PEG as compatiblizer.

Bidkaret al. [32] investigate the possibility of partial replacement of active filler carbon black by cheaper fly ash as a co-filler for elastomer composites. Variable percentages of fillers have been used to optimize the best composition. Author investigated the effect on mechanical and morphological properties of the composite. Results showed an improvement in elongation and tensile strength when a composition of 20phr fly ash and 10phr carbon black used as compare to other compositions. A decrease in these properties was observed beyond 20phr content due to change in crosslink density. On the other hand, modulus increased continuously as the percentage of fly ash and increased and hence the crosslink reaction progressed. A highest crosslink density was observed when the composition 20-10-100, fly ash-carbon black-SBR used. Similarity of the hardness value for all composition was observed either containing the pure carbon black or with fly ash ranging from 72 to 80 but better then gum vulcaniczate that is 57 only. SEM results showed that presence of de-bounded fly ash particles indicates poor polymer filler interaction while straight fracture path and rough surface showed higher polymer filler interaction in case of carbon black. Fracture surface of the formulation with 20phr of fly ash and 10 phr of carbon black is very similar to that of the composition, which contains only carbon black and hence gives the best results.

Bing-Xing et al. [33-34] investigated the enhancement of the mechanical properties of polypropylene using poly-propylene-grafted multiwalled carbon nanotubes. Author used reactive blending process for grafting of PP onto the MWCNTs by using 0.6% maleic anhydride and amine-functionalized MWCNTs. Pristine MWCNTs was first acid treated to attach COOH group and then reacted with ethylenediamine to produce NH_2-MWCNTs. PP-MA and MWNT–NH_2 then melt blended to produce PP-grafted-

MWCNTs. The grafting was confirmed by using XPS. Results showed a considerable improvement in the mechanical properties of the composites as compared to addition with pristine MWCNTs. The composites with an grafted MWCNTs content of 1.5 wt%, its tensile strength, ultimate strain, toughness and Young's modulus were improved by 141, 49, 287, and 108%, respectively as compared to PP. This improvement is much better as compare to pristine MWCNTs and clay as filler. The storage modulus of PP was increased by 38% and 83% by the addition of 0.5% and 1.0% PP-g-MWCNTs respectively. Author also noted that for composites containing PP-g-MWNTs, there is a decrease in mechanical properties when the effective MWNTs content was increased to 2.0 wt%. SEM and TEM were used to study the morphology of the composites. Results showed that PP-g-MWCNTs were dispersed well into polymer matrix whereas bundles of pristine MWNCTs were observed in the PP-MWCNTs case. But it is still difficult to completely disperse PP-g-MWNTs in the PP matrix at higher PP-g-MWNTs contents.

CHAPTER 3

EXPERIMENTAL SETUP AND MATERIAL PREPARATION

3.1: Surface treatment of Fly Ash

Functionalization of carbonaceous material or any other filler through surface modification has been an attractive proposition in research field for long time. Attachment of different functional groups to surface of carbon may increase not only its dispersion and attachment to the product but sometimes also affects its solubility. Functionalization also introduces the multi-functional-attachment property into the product. Two main techniques are generally used for surface modification of carbonaceous material (like CNTs). One is covalent attachment of functional groups and second is non-covalent attachment of molecules which is mainly based on van der Waals forces [35-36].

In this research, surface modification of OFA has been done by functionalization with carboxylic acid group using acid treatment method. It has been thought that attachment of carboxylic group to the surface of fly ash may enhance the interaction between polymer and filler. The attached acidic group would be attracted by hydrocarbon backbone of polymer due to functional group interaction and effects the dispersion of filler into polymer matrix. We have used different parameters to see the effect on the surface modification and optimization of conditions. A mixture of sulfuric acid to nitric acid has been used for the oxidation of carbon ash. The volumetric ratio used for acid to fly ash is

2:1 while the concentration of nitric acid used in acid mixture ranging from 5-20%. Also the effect of oxygen flow to enhance the oxidization has been examined.

The Oil Fly Ash (OFA) was received by Saudi Aramco by power generation plants of Saudi Electricity. Oil fly ash was in the form of black powder mainly composed of carbon and with some traces of metal oxide like magnesium, silicon, sulfur and vanadium. This analysis has been carried out in a previous project by Energy Dispersive X-Ray Spectroscopy analysis (EDX). Sulfuric acid and nitric acid have been received by Sigma Aldrich Company. Sulfuric acid has the purity greater than 95% and density 1.83 gm/ml while nitric acid has the purity greater than 90% and density 1.48 gm/ml. The bulk density of OFA is close to 0.48-0.5 gram per cm^3.

A sample of 100g of OFA was mixed with a mixture of 200 ml of concentrated sulfuric and nitric acids in a 3 liter beaker. The volume ratios of nitric to sulfuric acids were ranging from 5:95 to 20:80 vol./vol.%. The acids-ash mixture was then heated and stirred continuously to 160^oC. At this temperature the mixture becomes slurry. At this stage, air was introduced through small capillary tube with constant flow rate of 5 ml/min for further oxidation of the ash. Heating was continued until acid gets evaporated and a black solid material was produced to indicate complete reaction of the ash. Further, this material was treated with 100 ml demineralized water which was added gradually to the mixture to enhance the activation of ash. Then, the produced material was cooled to 22±1 ^oC and washed several times with demineralized water to remove the remaining acids and until the pH of supernatant reaches 5. After washing, wet fly ash was dried into the oven at 105°C for 1.5 h and saved in closed vessels for uses. This procedure was repeated several times by varying the reaction parameters as shown in Table 3.1.

Table 3.1: Variation of reaction parameters for OFA

Sample No.	H_2SO_4 v.%	HNO_3 v.%	Oxidation by air
1	0	0	No
2	95	5	No
3	95	5	Yes
4	90	10	Yes
5	85	15	Yes
6	80	20	Yes

3.2: Characterization of Modified Fly Ash

Surface modified Oil fly ash subjected to FTIR, SEM and XRD Analysis in order to observe the attached functional group to fly ash, morphological behavior, elemental analysis and also the different types of carbonate and oxides present in the samples

3.2.1: Fourier Transform Infrared Spectroscopy (FTIR):

The functional groups on the surface of the treated OFA were analyzed using FPC FTIR Perkin Elmer spectrophotometer. A weight of 1-2 mg of the OFA was mixed thoroughly with 1.0 g of fine dried powder of KBr. Then the resulting mixture was hydraulically pressed at 10 ton/m2 to obtain a thin transparent disk. The thin disk was placed in an oven at 110 oC for 4 hours to prevent any interference of any existing water vapor or carbon dioxide molecules. All the FT-IR spectra were taken in transmission.

3.2.2: Surface Morphology:

Morphological behavior of the surface of fly ash particles was observed by *JEOL JSM*-646LV Scanning Electron Microscope. The sample was initially dried, fixed with double-side masking tape, and then gold-coated using a sputtering machine for 6 minutes in order to improve the conductivity of the sample. Once the gold coating was completed, the specimens were viewed on the SEM at different magnifications.

3.2.3: XRD Analysis

The XRD patterns of the samples were measured using a Shimadzu XRD-6000 spectrometer. Aluminum sample holder was filled by dried fly ash. The target element used in the instrument was Copper having λ of 0.154 nm. The samples were tested at 40 kV and 30 mA and the spectra for all samples are obtained.

3.2.4: BET Analysis and pore size distribution

The BET surface area and pore volumes for the produced OFA were both determined using Micromeritics ASAP 2020 using nitrogen adsorption at 77.35 K. A sample of 0.3210 g was degassed and dried at 150 oC under vacuum for 6 hrs. The specific surface area was measured and calculated by a BET equation and a cross-section area of nitrogen molecule of 0.162 nm2 [37] was used.

3.3: Formulation of Fly Ash-Polymer Composite using Melt-Blending method

LDPE was supplied by Nova Chemicals, Canada. The LDPE has a weight average molecular weight of 99.5 kg/mol and a MWD of 6.5 and a melt index of 0.75 g/10 min and a total short branch content of 22 branches/1000 C as determined by GPC and NMR, respectively (Hussein and Williams) [38]. The PE-g-MA was received by Sigma Aldrich and it has a viscosity of 1400-1700 cP, a density of 0.925 g/cm^3 and a melting point of 105°C.

Preparation of LDPE/OFA composites was performed in a Brabender Melt Mixer. The blender consists of three heating zones with independent temperature control systems. LDPE/OFA composite samples were prepared with four different OFA concentration (1, 2, 5 and 10 %w). PE-g-MA was used as a compatiblizer to enhance the dispersion and compatibility between LDPE and OFA. Physical premixing of LDPE, OFA and compatiblizer is done into a beaker. Then the composites were fed to the Brabender Melt Mixer at a temperature of 190^{0}C and a blending speed of 50 rpm. The time of melt mixing for each sample is 10 minutes. Sixteen composite samples were prepared with different compositions as given in Table 2. For the first four samples, the effect of filler concentration of unmodified OFA was examined while samples 5-8 will reveal the influence of the compatiblizer. On the other hand, samples 9-16 will show the impact of the modified filler (COOH-OFA) on un-compatiblized and compatiblized composites.

Table 3.2: Composition of LDPE/OFA Composites

Sample No.	LDPE (wt%)	Fly Ash (wt%)		MA-g-PE (wt%)
		Unmodified	Modified	
1	99	1	-	-
2	98	2	-	-
3	95	5	-	-
4	90	10	-	-
5	97	1	-	2
6	96	2	-	2
7	93	5	-	2
8	88	10	-	2
9	99	-	1	-
10	98	-	2	-
11	95	-	5	-
12	90	-	10	-
13	97	-	1	2
14	96	-	2	2
15	93	-	5	2
16	88	-	10	2

3.4: Rheological Analysis

For Rheological analysis, samples are prepared by using Carver press model showed in figure 3.4.1. Small quantity of composite is placed between the steel plates having the hollow circles to shape the sample for rheological instrument. These plates are pressed by Carver press at a temperature of 190^0C and increase in pressure with time. The pressure

applied is 0 ton for 3 minutes, 1 ton for 1, minute, 3 ton for 1 minute, 5 ton for 1 minute & 7 ton for 1 minute. So the total pressing time is seven minutes at a fixed temperature. After that, plates are allowed to cool for 5 minutes and samples are withdrawn between the plates and fine cutting has been done to make samples in a regular shape.

For Rheological analysis, measurements were carried out by Advanced Rheometrics Expansion system (ARES) controlled strain rheometer as shown in figure 3.4.2. Dynamic shear tests were carried out using cone and plate geometry. Diameter of the sample was 25mm, cone angle was 0.1 radians, gap was 0.048mm. Strain was 15%, temperature was 190ºC and the frequency was varied from 100 rad/s to 0.1 rad/s under the 60 psi pressure of nitrogen gas.

Figure 3.4.1: Carver Hydraulic Press

Figure 3.4.2: ARES Controlled Strain Rheometer

3.5: Mechanical Analysis

For Mechanical analysis, samples are prepared by using Carver press model showed in figure 3.4.1. Small quantity of composite is placed between the steel plates having the square hollow to shape the sample for mechanical instrument. These plates are pressed by Carver press at a temperature of 190^0C and increase in pressure with time. The pressure applied is 0 ton for 3 minutes, 1 ton for 1, minute, 3 ton for 1 minute, 5 ton for 1 minute & 7 ton for 1 minute. So the total pressing time is seven minutes at a fixed temperature. After that, plates are allowed to cool for 5 minutes and square sample sheet are withdrawn between the plates. The dog bone shaped samples are prepared from these square sample sheets by using hydraulic cutter. The dog bone samples are shown in figure 3.5.1.

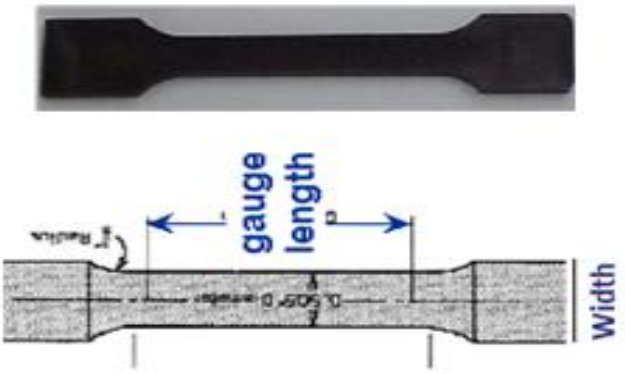

Figure 3.5.1: Dog Bone Sample for Mechanical Analysing

For Mechanical analysis, measurements were carried out by Instron Mechanical Testing Machine as shown in figure 3.5.2. The measurement of length, width and thickness of Dog bone sample is done by venire caliper. Dog bone samples have a fixed length of 15 mm but the width and thickness varied for different samples. The data of each sample is putted into the machine software and sample analyzed for mechanical properties at a fixed strain rate of 40.00 mm/minute.

Figure 3.5.2: Instron Mechanical Testing Machine

3.6: Thermal Analysis

Thermal analysis is done by Modulated DSC equipment TA Q1000 as shown in Figure 3.6.1. The equipment is calibrated from -80 to 190°C for melting and crystallization curves and heat of fusion by using pure Indium standard. Nitrogen at a flow rate 50 ml/min was used to purge the instrument to prevent degradation of the samples upon thermal treatments. The composites samples are weighted between 5 to 10 mg and Non-hermetic pans are loaded to DSC analyses by auto-sampler. Pure LDPE is also subjected to this analysis as a reference material. Heating-Cooling-Heating system is used for the analysis i.e. firstly the sample is heated up to 180°C, second the sample is cooled down up to -80°C and in the last sample is again heated up to 180°C. First heating is for the uniform dispersion of non-uniform shaped sample in to the non-hermetic pan after melting so that sample is subjected to uniform heat distribution. Second and third heating is used for the analyzing the peaks for crystallinity and melting point. The absolute crystallinity was calculated using the heat of fusion of a perfect polyethylene crystal, 290 J/g by using TA Universal Analysis software.

Figure 3.6.1: Modulated DSC Equipment

3.7: FE-SEM Analysis

FE-Scanning Electron Microscopy of polymer composites was carried out to observe the surface morphology of LDPE/OFA composite and dispersion of fly ash into the LDPE matrix. For FE-SEM analysis, fresh surface of samples is prepared to remove any impurity or particle from the surface of sample. For this purpose, firstly the samples are dipped into the liquid nitrogen for one minute and then quickly broken from the mid so that a fresh surface of sample appeared. These samples were subjected to nano-scaled gold coating for charging effect of composite. The gold coating is done for 20 seconds by sputtering machine in Mechanical Engineering Department, KFUPM. FE-SEM analysis is done at different resolution ranging from 500x to 40,000x.

CHAPTER 4

RESULTS & DISCUSSION

CHARACTERIZATION OF SURFACE MODIFIED FLY ASH

The chemical analysis of untreated of OFA is illustrated ion Table 2.2. It contains mainly 92.5 wt% carbon and 5.8 wt% sulfur while the rest are traces of metal oxides. This material was initially soaked with sulfuric acid at room temperature where no effect was noticed on the mixture. Gradual addition of the nitric acid caused a rapid increase in solution temperature up to 150 ^{o}C. This jump in temperature was noticed within few minute as a result of exothermic reaction between the acids and the ash. Further external heating of the mixture has elaborated carbon monoxide, carbon and sulfur dioxide, and nitrous oxide. This treatment with acids results in several slufonation and nitrification reactions at the surface of the ash samples. X-ray fluorescence (XRF) analysis of ash samples before and after treatment showed an increase of silicon content from 0.99 wt% to 7wt% with increasing nitric acid from 0 to 20% (Table 4.1 and Figure 4.1). This is due leaching out Mn, Ni and Zn from the solid sample. Sulfur contents have increased from 71wt% (untreated sample) to 82wt% for samples treated with 10 wt% nitric acids. Further increase of nitric acid has decreased this percentage to 77wt% (sample 6). This is due to the oxidation of some of organic sulfur to produce sulfur dioxide [39]. Moreover, sulfur in fly ash can exists in three main classes; pyritic, sulfates and the organic sulfurs where nitric acid dissolves sulfate and pyrite sulfur aggressively and attacks organic sulfur only mildly [40].

Table 4.1: XRF analysis of ash samples treated at different acid compositions (wt.%) with air oxidation

H2SO4:HNO3 Ratio	Si	S	Ca	V	Mn	Fe	Ni	Zn
0 : 0	0.9914	71.27	7.79	13.14	0.0071	3.99	2.61	0.1861
95 : 05	3.34	79.88	8.32	3.65	0	3.77	0.8069	0.1291
90 : 10	3.55	82.22	6.98	2.29	0	0.819	0.3227	0
85 : 15	6.04	78.22	8.51	4.35	0	1.45	0.244	0
80 : 20	7	76.96	7.76	4.56	0	2.28	0.3004	0

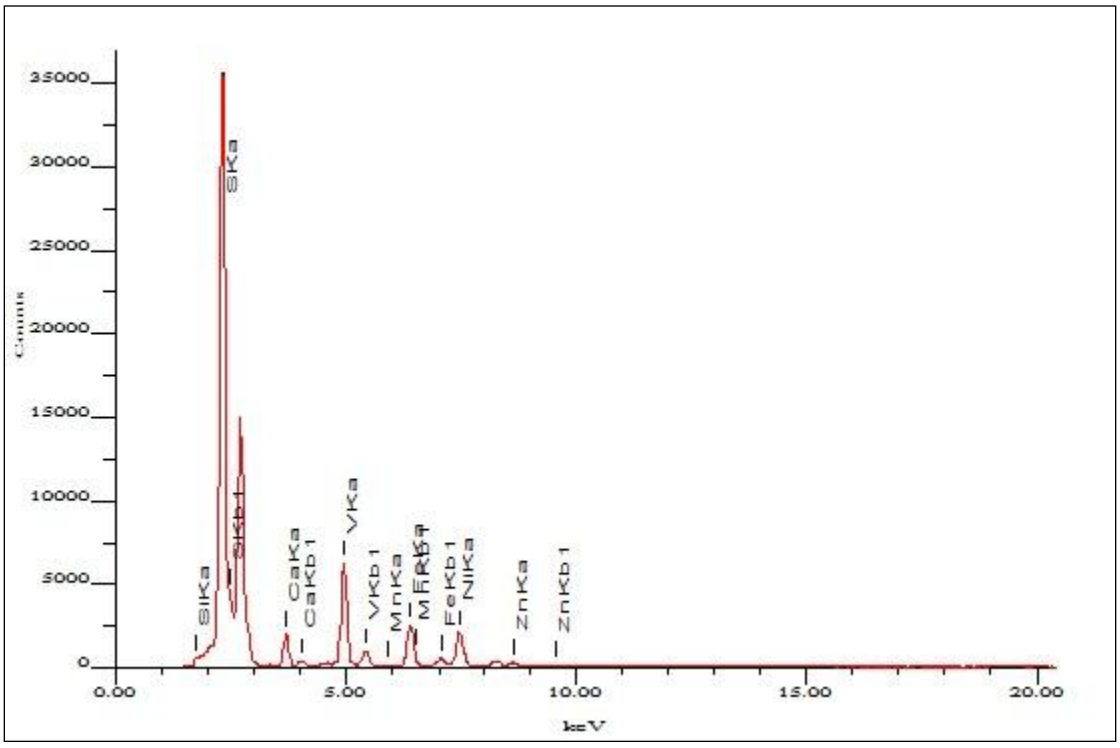

Figure 4.1: XRF analysis of untreated OFA sample.

4.1: FTIR Analysis for Functional group

In order to identify whether a new functional group was attached to the surface of treated OFA, FTIR spectra of the samples were scanned from 500 to 4000 cm-1 wave length and the percentage of transmittance was observed.

Figure 4.2(a) shows the FTIR spectra of untreated OFA compared to samples treated with 95 wt%H2SO4 and 5 wt% HNO3 without injection of air. The spectrum of as-received sample shows two major peaks at 3400-3650 cm-1 which is due to O-H bond stretching of alcoholic groups [41-43]. Three minor peaks are observed at 3305, 2884 and 2541 cm-1. These peaks are in the range of 2400-3400 cm-1 which is due to the hydrogen bonded O-H stretching of acidic groups [41]. Also, one peak is observed at 2194 cm-1 which shows the presence of C≡C bonding. The spectrum shows the presence of OH group and some carbon to carbon triple bonding. For the modified sample the peak at 3305 is shifted to 3309 cm-1. Also it shows the appearance of some more peaks in the region of 2400-3400 cm-1. The peaks which were observed in the untreated sample were slightly increased after modification which illustrates the attachment of carboxylic group to the surface of fly ash. The peaks of C≡C bonding is shifted from 2144 to 2100 cm-1 but no increment is observed. However, one more small peak at 1585 cm-1 is observed which represents the presence of C=C bond [44]. It is observed that by air oxidation, peaks in the range of 2400-3600 cm-1 wave length increased which shows the increment in attached carboxylic group to the surface of fly ash. . Other than that, all other peaks such as C≡C bond and C=C bond peaks are also increased. It shows that the functionalization of fly ash increased with the oxidation due to injection of air.

Figure 4.2(b) shows the FTIR spectra of fly ash modified by different acid composition and oxidation by air. The sample that modified by the addition of 90wt% H2SO4 and 10 wt% HNO3 shows some more improvements in the peaks. It is observed that in the range of 3400-3600 cm-1 there are three peaks that appeared at 3468, 3599 and 3521 cm-1, respectively. The peak which is observed at 2475 cm-1 is shifted to 2459 cm-1. In addition, two more peaks were appeared at 2550 and 2594 cm-1 and two small peaks were observed at 1720 and 1760 cm-1. This illustrates the stretching of C=O in the ester group. However, the peak of C=C is shifted to 1467 cm-1.

On the other hand, the sample that is treated with 85 wt%H2SO4 and15 wt% HNO3 shows a maximum increase in peaks count as compared to that treated with 90wt% H2SO4 and 10 wt% HNO3. For this sample, four more peaks are observed in the region of 2400-3600 cm-1 which shows a considerable stretching of O-H functional group of carboxylic acid. Also, the C=C peak disappeared whereas the peak for the ester groups shifted from 1760 cm-1 to 1716 cm-1 which is in the range of C=O of carboxylic group. A comparison between the spectra of the different samples shows that the maximum functionalization of carboxylic acid group was achieved with the addition of 15% HNO3. Nevertheless, further increase in nitric acid composition has decreased the attached functional groups. The spectrum of the sample that was treated with 80 wt% H2SO4 and 20 wt% HNO3 shows a little decrease in the number of peaks in the region of 2400-3600 cm-1 which is a clear evidence of the decrease in O-H group of carboxylic acid. Also, the peak of C=O is almost disappeared whereas three new peaks are observed in the region of 1900-2000 cm-1. These peaks are either due to the presence of aromatics compounds or the formation of some unsaturated hydrocarbons.

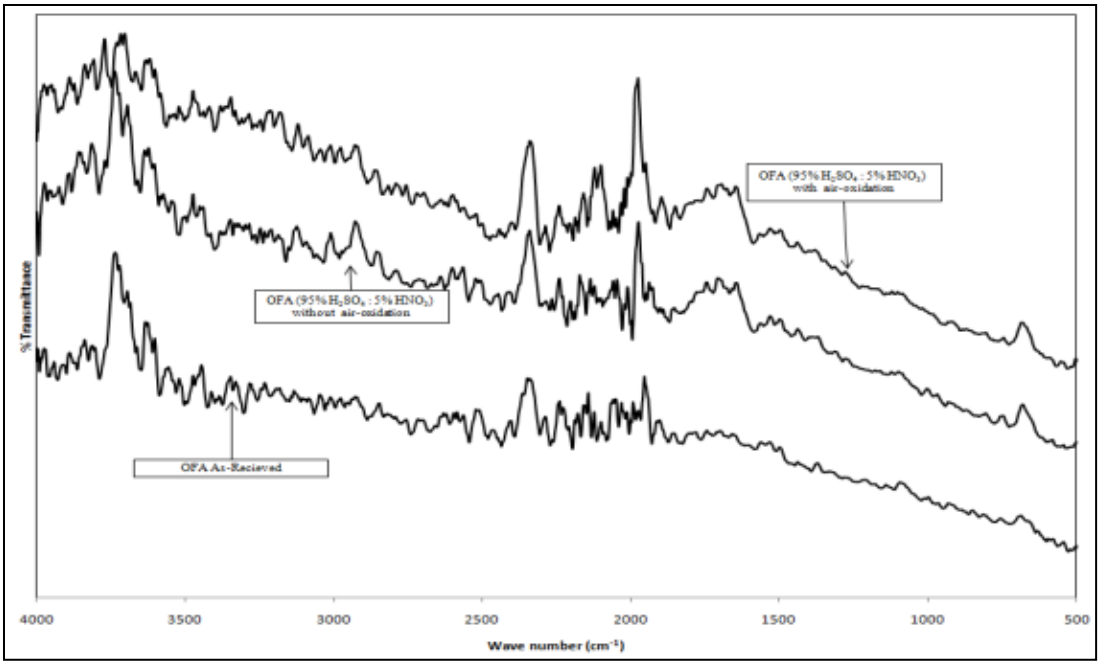

Figure 4.2(a): FTIR spectra of as-received and modified fly ash with and without air-oxidation

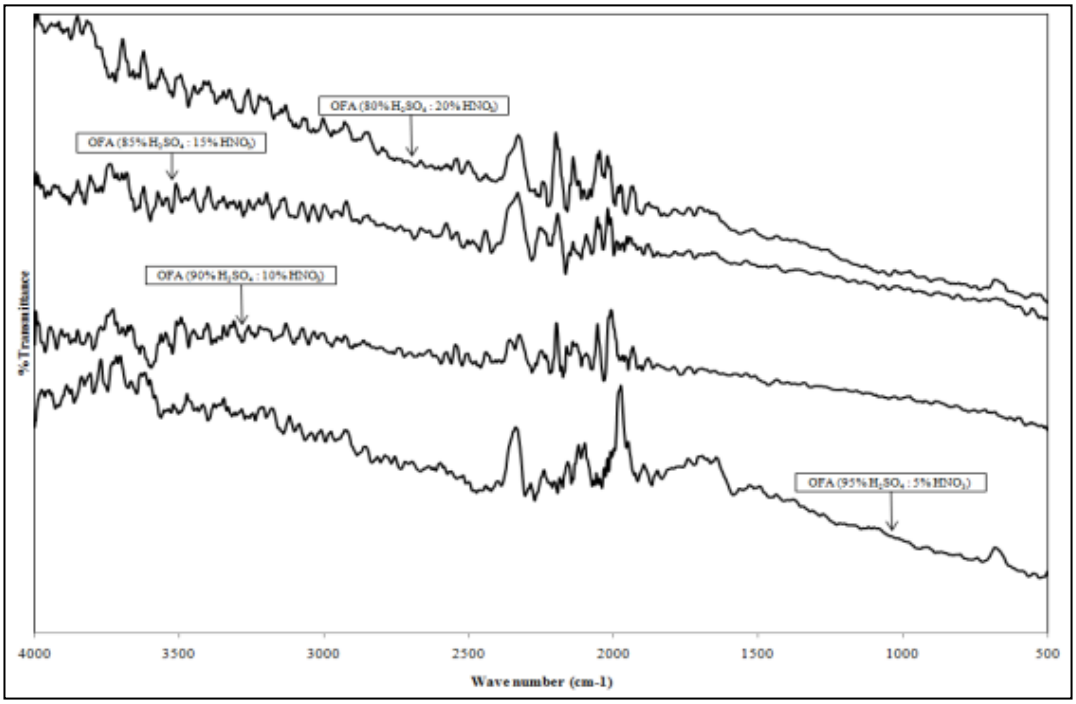

Figure 4.2(b): FTIR spectra of fly ash modified by different acid composition and air-oxidation

4.2: SEM and Spot Analysis

Surface morphology of the ash samples is shown in Figure 4.3(a-f). It is apparent that most of the ash particles are spherical in shape with high porosity. The size of these particles is in the range of 10-100 μm.

Spot analysis of modified and unmodified particles was performed to determine the ratio of carbon, oxygen and sulfur in these samples. Carbon to oxygen ratio in these samples illustrates the degree of oxidation before and after treatment. It is observed that oxygen to carbon ratio has changed according to the acid treatment method. It is also apparent that sulfur content decreases with increasing degree of oxidation which demonstrated the replacement of oxygen to sulfur on the surface (Table 4.2). The sample that treated with air, and 95 wt% H_2SO_4 and 5 wt% HNO_3 showed an increase of oxygen functional groups compared to air untreated sample. In addition, the replacement of sulfur by oxygen has increased with increasing nitric acid which could be attributed to the high reactivity of nitric acid.

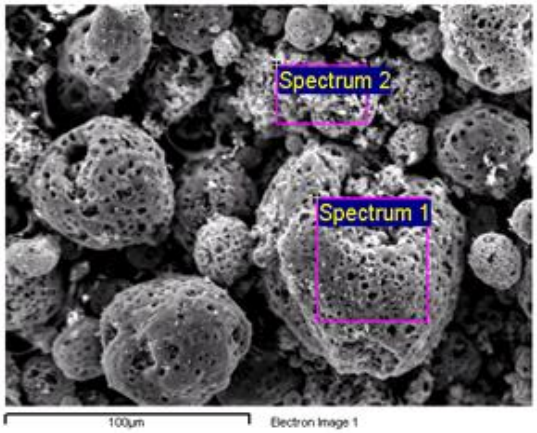

(a) Original Sample

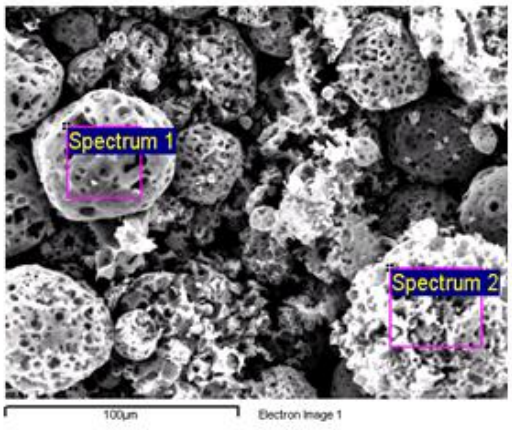

(b) Treated with 95wt% H_2SO_4 and 5wt% HNO_3 without air oxidation

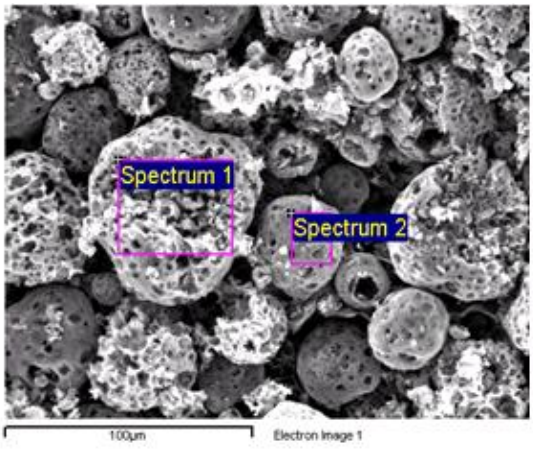

(c) Treated with 95wt% H_2SO_4 and 5wt% HNO_3 with air oxidation

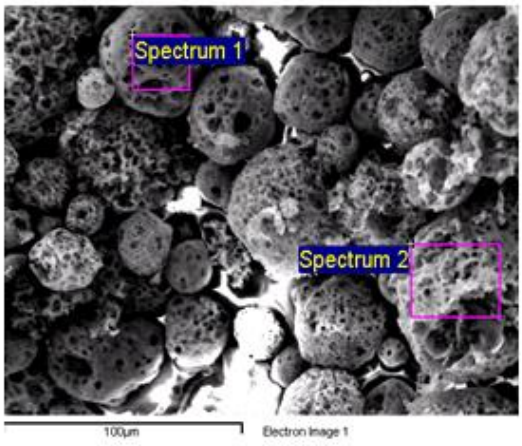

(d) Treated with 90wt% H_2SO_4 and 10wt% HNO_3 without air oxidation

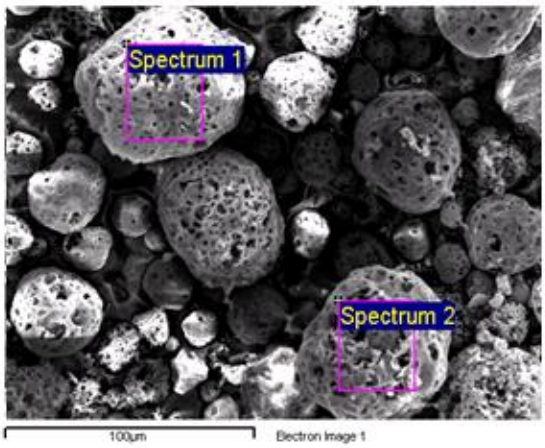

(e) Treated with 85wt% H_2SO_4 and 15wt% HNO_3 without air oxidation

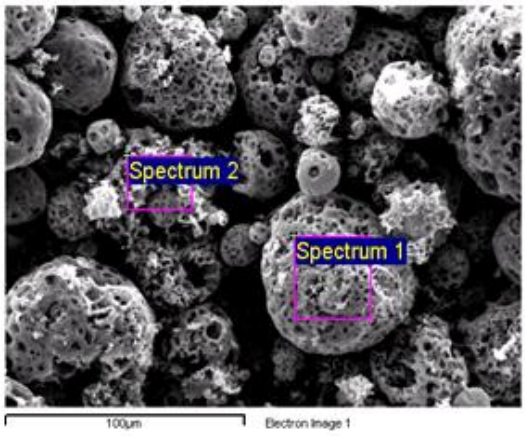

(f) Treated with 80wt% H_2SO_4 and 20wt% HNO_3 without air oxidation

Figure 4.3: SEM analysis of the ash samples

Table 4.2: Average weight percent of carbon, oxygen and sulfur on the surface of ash samples

Sample	wt% carbon	wt% oxygen	wt% Sulfur
Untreated	53.82	24.07	22.11
Treated with 95 wt% H_2SO_4 and 5 wt% HNO_3 without air oxidation	59.23	29.50	11.26
Treated with 95 wt% H_2SO_4 and 5 wt% HNO_3 With air oxidation	54.41	32.43	13.16
Treated with 90 wt% H_2SO_4 and 10 wt% HNO_3 With air oxidation	53.53	38.18	8.33
Treated with 85 wt% H_2SO_4 and 15 wt% HNO_3 With air oxidation	56.83	38.11	5.06
Treated with 80 wt% H_2SO_4 and 20 wt% HNO_3 With air oxidation	54.07	40.33	5.6

4.3: XRD Analysis

Evaluation of common and predominant phases within the ash samples during treatment was obtained using X-ray diffraction technique (Figure 4.4). In general, the XRD spectra of the samples illustrate the presence of carbon, zeolite, mullite, quartz, faujasite, cancrinite and sodalite [41]. Untreated fly ash demonstrated the presence of faujasite and zeolite X, P and NA at 11^o, 16^o and 18^o 2θ. A large peak of carbon and mullite is

observed at 25^{o} 2θ which shows the high concentration of crystalline carbon as compared to other minerals. Very small peaks of faujasite, mullite, cancrinite and zeolite X, P were observed between 27^{o} and 33^{o} 2θ. Also the peaks of mullite and sodalite are observed at 42^{o} and 43^{o} 2θ followed by small quartz peak at 77^{o} 2θ. It is observed that after modification of fly ash surface with 95 wt % H_2SO_4 and 5 wt% HNO_3 most of the little peaks have disappeared. The intensity of the carbon and mullite peak at 25^{o} 2θ is increased to 143% whereas sodalite peak at 43^{o} 2θ is also raised to 100% as compare to as-received fly ash. Moreover, a new peak of faujasite appeared at 37^{o} 2θ and a small peak of quartz at 77^{o} 2θ increased to about 130%. The modification of ash with 85 wt% H_2SO_4 and 15 wt% HNO_3 resulted in increment of the large carbon peak to more than 200% compared to the original one, while faujasite peak is increased by 45% only. No considerable difference is observed in sodalite and quartz peaks. The surface modification of fly ash with 80 wt% H2SO4 and 20 wt% HNO3 shows the reappearance of small peaks of faujasite, mullite, cancrinite and zeolite X, P observed between 27^{o} to 33^{o} 2θ. The carbon and mullite peak decreased to a similar level of unmodified fly ash. Also, the peak of quartz decreased and two very large thin peaks appeared which could be related to a noise.

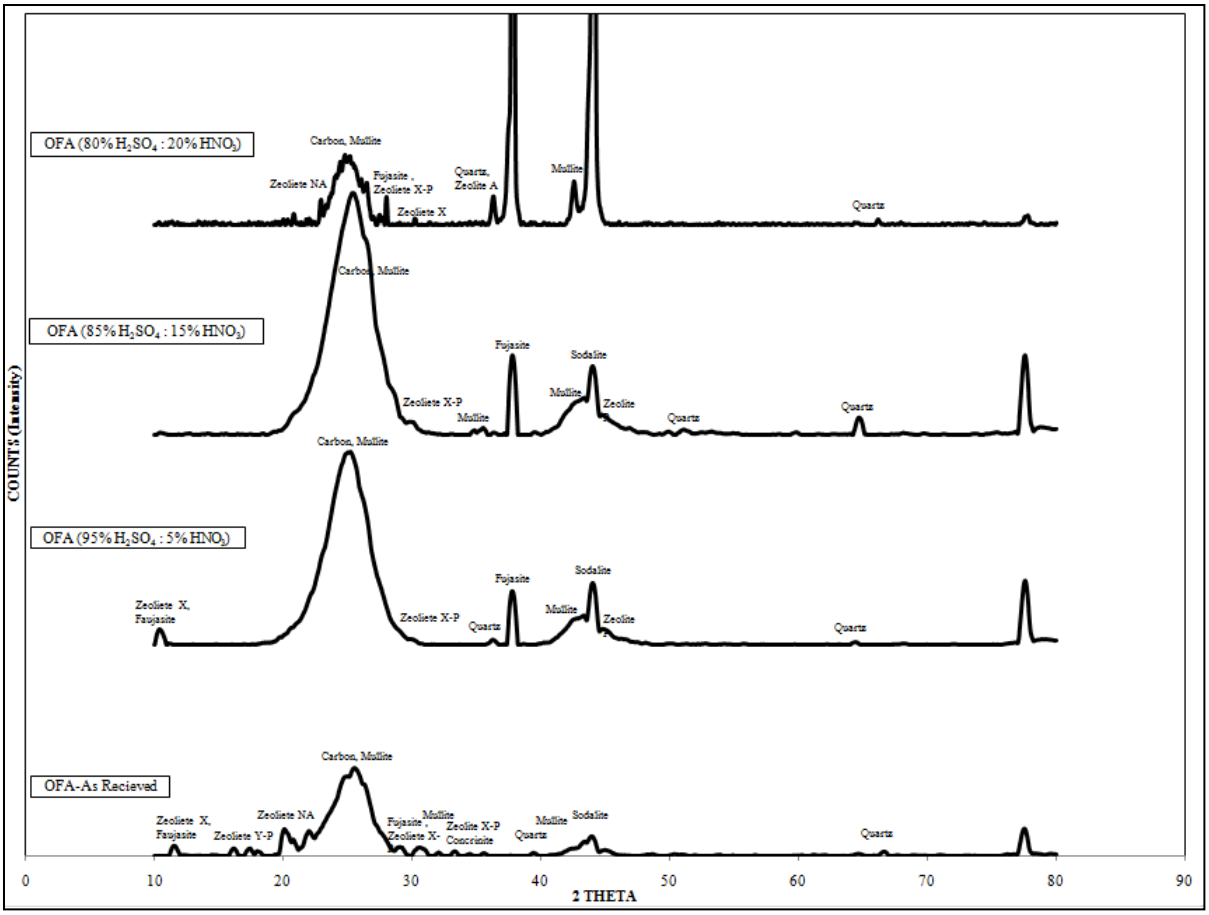

Figure 4.4: X-Ray Diffraction Patterns for modified and unmodified Oil Fly Ash

4.4: BET Analysis

Figure 4.5 shows selected adsorption–desorption isotherms of N_2 at 77 K for the produced chemically modified ash samples. This isotherm belongs to type I in the IUPAC classification. It represents characteristics of material made up of slit shaped pores where the pore size distribution is mainly in the microporous field. The narrow and uniform micoporosity of this carbon is supported by overlapping the adsorption-desorption curves. The BET surface area has increase from 7.36 m^2/g for the original sample to 157.76 m^2/g for the sample treated with 85 wt% H_2SO_4 and 15 wt% HNO_3 in the

presence of air. This value has decreased to 56.87m^2/g with further increase in nitric acid concentration, which is attributed to disruption of the pore structure. The average pore diameter value is varying from 104.56 Å for the untreated sample to 23.56 Å for the sample treated with 20wt% HNO_3 in the presence of air (Table 4.3).

Table 4.3: Physical properties of the ash samples deduced from N_2 adsorption

H_2SO_4:HNO_3 Ratio	**BET Surface Area** m^2/gm	**Langmuir Surface Area** m^2/gm	**Average Pore width (4v/A)** Å	**t-Plot micropore volume** cm^3/g
0 : 0	7.35	10.23	104.58	0.000129
95 : 05	26.03	35.81	47.69	0.002101
90 : 10	71.13	99.55	36.45	-0.001823
85 : 15	157.76	213.19	26.19	0.026528
80 : 20	56.87	78.40	23.56	0.003716

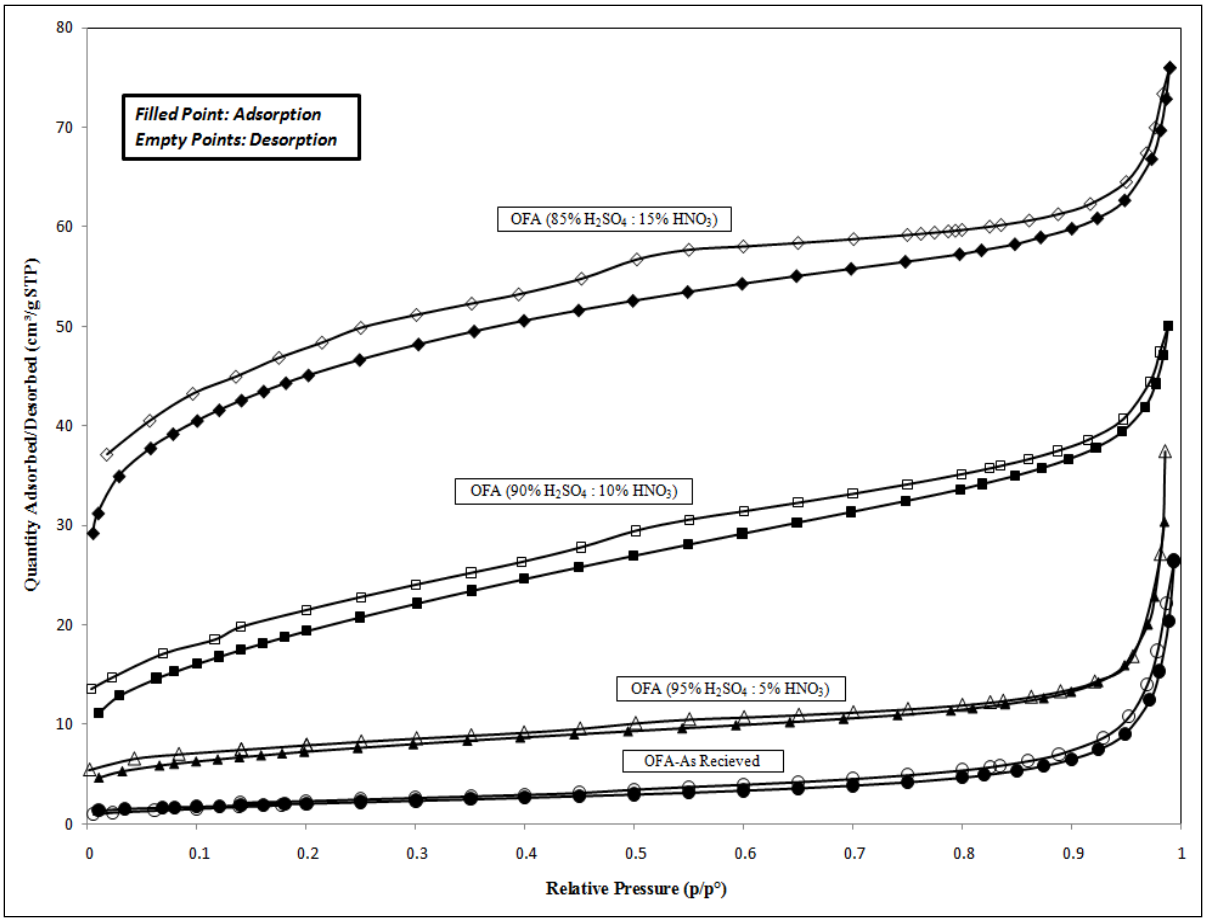

Figure 4.5: BET modified and unmodified Oil Fly Ash

CHAPTER 5

RESULTS & DISCUSSION

RHEOLOGICAL AND MORPHOLOGICAL BEHAVIOR OF LDPE/OFA COMPOSITE

Rheological properties of Polymer composites have a vital importance for the understanding of their flow behavior, miscibility and processibility. Influence of the tiny fillers on the rheological properties of polymers has been investigated for many decades. In this chapter, we investigated the effect of OFA loading as a filler on the rheological properties of LDPE. Also the effect of OFA functionalization by acid treatment and addition of Polyethylene-grafted-Maleic Anhydride as a compatiblizer is investigated. The results are compiled with morphological characterization of LDPE/OFA composites. The dispersion of fly ash particles into the polymer matrix is observed at high resolution microscopy.

Rheological characterization of composite is investigated by ARES control strain rheometer. Different properties have been calculated as storage modulus, loss modulus, cross-over point and cross-over frequency. The morphological characterization is done by FE-SEM technique at different resolution. Gold coating of quenched fractured samples is done for charging the surface. The dispersion of filler with and without modification is observed at high and low magnification and results are compared with previous observation.

Part A: Rheological Behavior of LDPE/OFA Composite

5.1: Effect of OFA on Storage Modulus of Composites

5.1.1: Effect of OFA Loading:

The storage modulus, G′, basically represents the stored energy of the elastic portion of viscoelastic materials. Figure 5.1.1(a) shows the effect of as-received OFA loading on the G′ of LDPE composite. G′ increased at all loadings and the increase is more dominant at low frequency [45, 46]. At low frequency, the G′ increased linearly for 1 and 2% OFA loading but dropped at 5 and 10%. This suggests a poor distribution or agglomeration of OFA at high loadings. However, at high frequency, the rheology of LDPE composite is insensitive to the OFA loading.

Figure 5.1.1(b) shows the effect of acid-functionalized OFA (COOH-OFA) loading on the G′ of LDPE composites. As the concentration of COOH-OFA in the polymer matrix is increased, the G′ increased and the composite shows more solid-like behavior. The increase is more dominant at low frequencies. Also, at low frequency, 1 and 2% loadings of COOH-OFA show almost the same degree of improvement. The maximum increase is observed at 5% loading; however, a slight decrease was obtained at 10% loading. At high frequency, all loadings showed similar results similar to the previous results of as-received OFA.

The effect of the use of 2% PE-g-MA as a compatiblizer on G′ of LDPE composites with OFA and COOH-OFA is shown in Figure 5.1.1(c) and 5.1.1(d), respectively. For as-received OFA, G′ increased linearly with the addition of filler upto 5% filler loading then it slightly decreased at 10% loading. The shift in the increase in G′ with COOH-OFA

loading from 2% to 5% suggests a positive role for the chemical modification. These results provide evidence of good distribution of OFA at low and moderate loadings. Whereas, poor distribution was obtained at high loading (10%) even in the presence of a compatiblizer. However, Figure-5.1.1(d) shows that the G′ increased with the increase in filler concentration even at high loadings in the case of COOH-OFA. For as-received OFA and PE-g-MA at all loadings almost similar results were observed with little improvement in G′ over pure LDPE (Figure 5.1.1(c)). On the other hand, COOH-OFA system (Figure 5.1.1(d)) showed more improvement in G′ of the composites as well as distinct increase in G′ with loading. The increment is more dominant at low frequency as reported earlier.

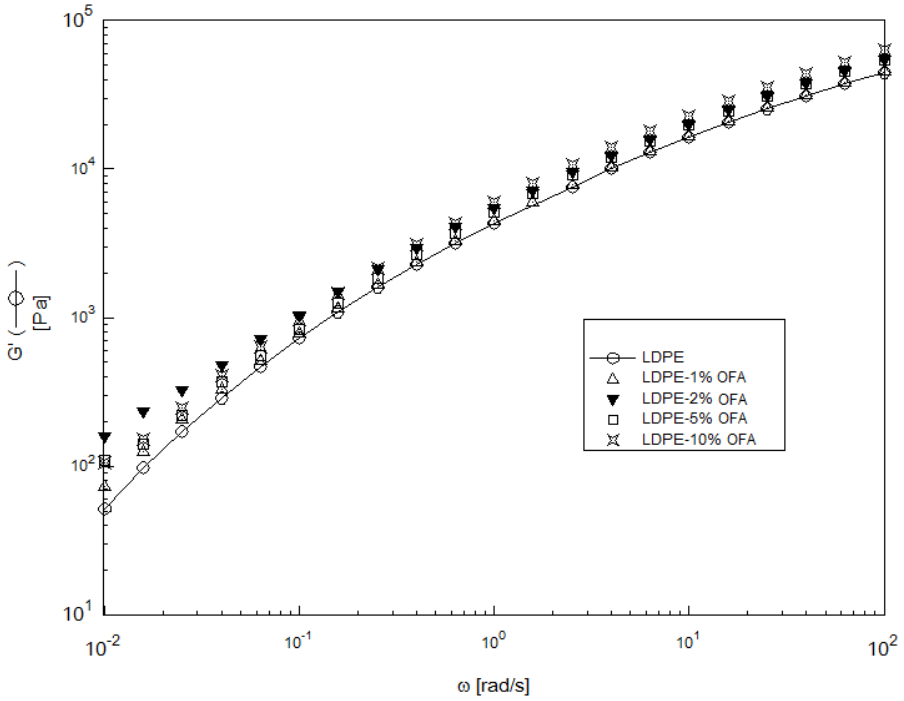

Figure 5.1.1(a): Effect of OFA Loading on Storage Modulus

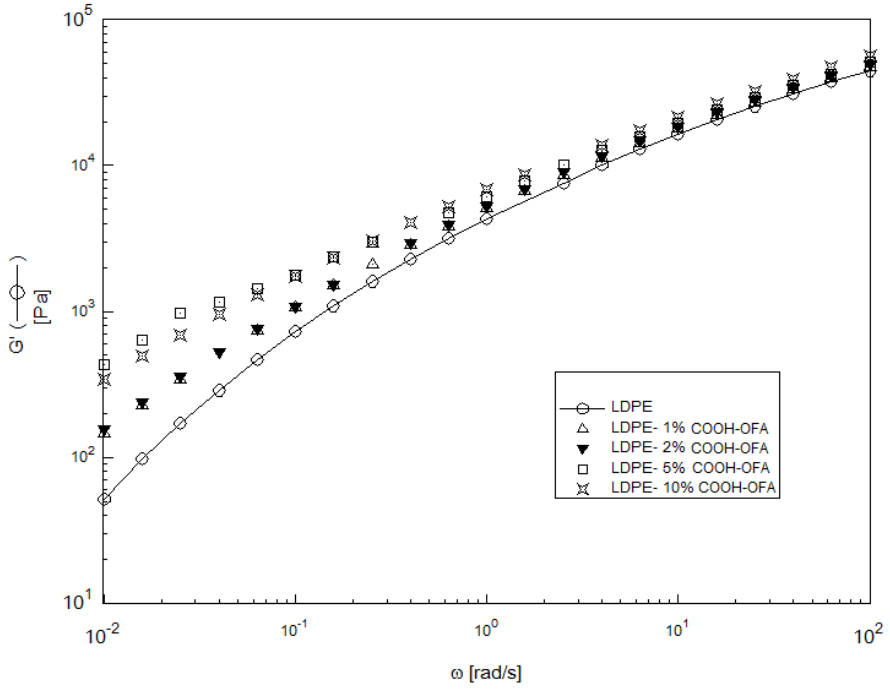

Figure 5.1.1(b): Effect of COOH-OFA Loading on Storage Modulus

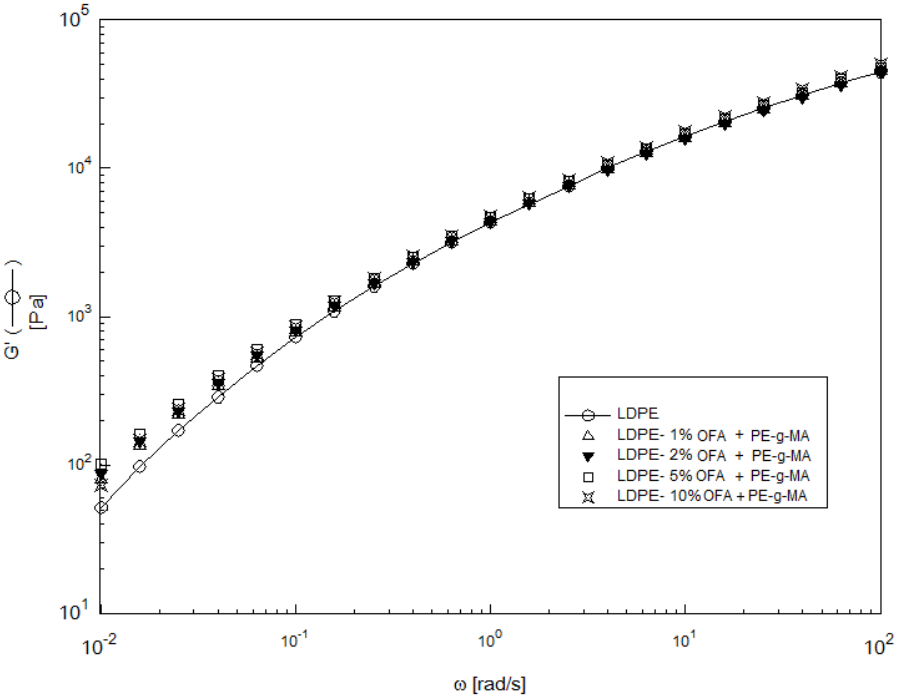

Figure 5.1.1(c): Effect of OFA Loading with 2% PE-g-MA on Storage Modulus

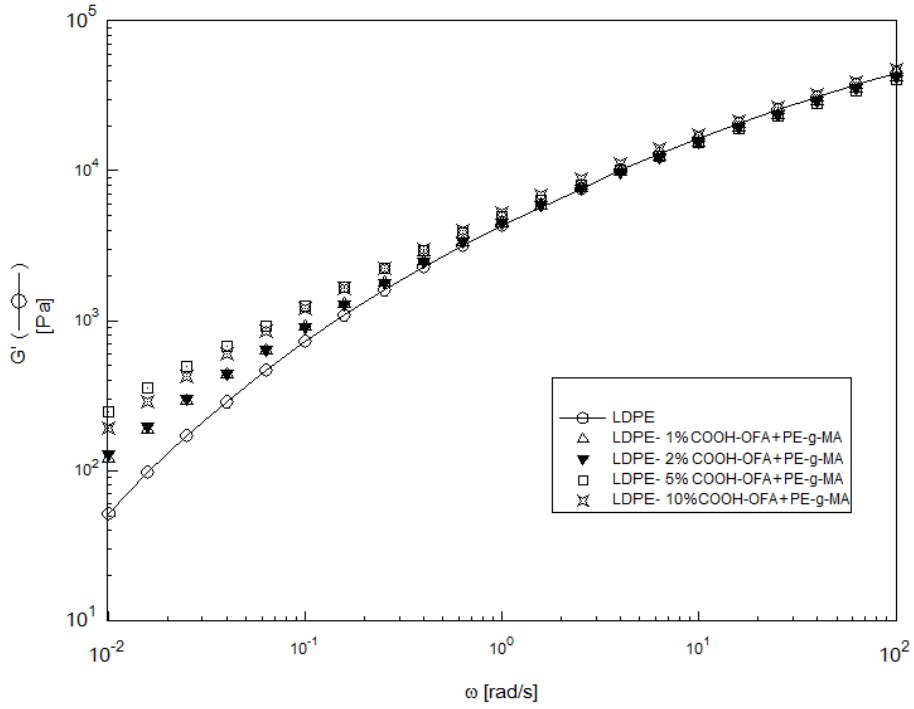

Figure 5.1.1(d): Effect of COOH-OFA Loading with 2% PE-g-MA on Storage Modulus

5.1.2: Effect of OFA functionalization and PE-g-MA on Storage Modulus:

A comparison of G′ for modified and unmodified OFA at 5% loading is shown in Figure 5.1.2(a). The functionalized OFA showed higher values of G′ as compared to untreated OFA. This is clear evidence that the chemical modification of OFA resulted in good dispersion of OFA in the polymer matrix even at very high loading. This dispersion is not achieved in the case of as-received OFA. Similar results are obtained at 1, 2 and 10 %w loadings and the difference is getting more pronounced with the increase in filler concentration. The enhancement in elastic strength of LDPE composites is mainly at low frequency. The effect on 1, 2 and 10% filler loading is shown in Appendix A.

The effect of PE-g-MA compatiblizer on G′ with OFA and COOH-OFA at 5% loading is shown in Figures 5.1.2(b) and 5.1.2(c), respectively. The addition of the compatiblizer

did not result in the increase in G′ of the composite in the case of unmodified OFA. However, the modified OFA showed increase in G′ at low frequency. Similar behavior is obtained at 1, 2 and 10% loadings. The effect of compatiblizer can be easily observed at almost the entire range of frequency and it is more pronounced in the case of COOH-OFA. It is also observed that the difference is increased at high loadings as compared to low loadings in the case of COOH-OFA. These results suggest the impact of chemical modification of OFA on G′ dominates the influence of the compatiblizer as shown by Figure 5.1.2(c). The effect on 1, 2 and 10% filler loading is shown in Appendix A.

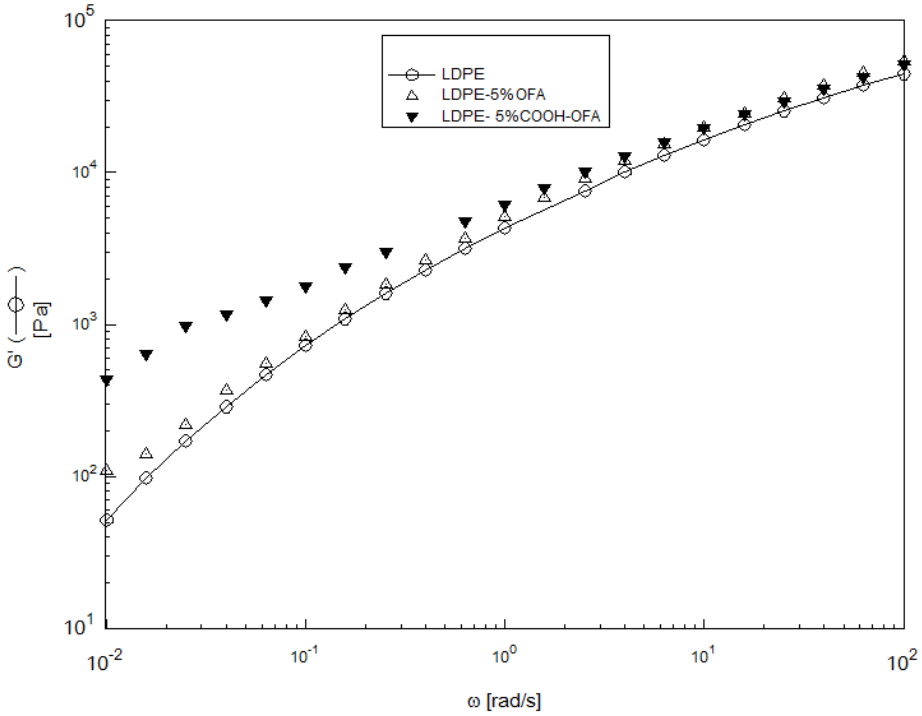

Figure 5.1.2(a): Effect of OFA-functionalization at 5% loading on Storage Modulus

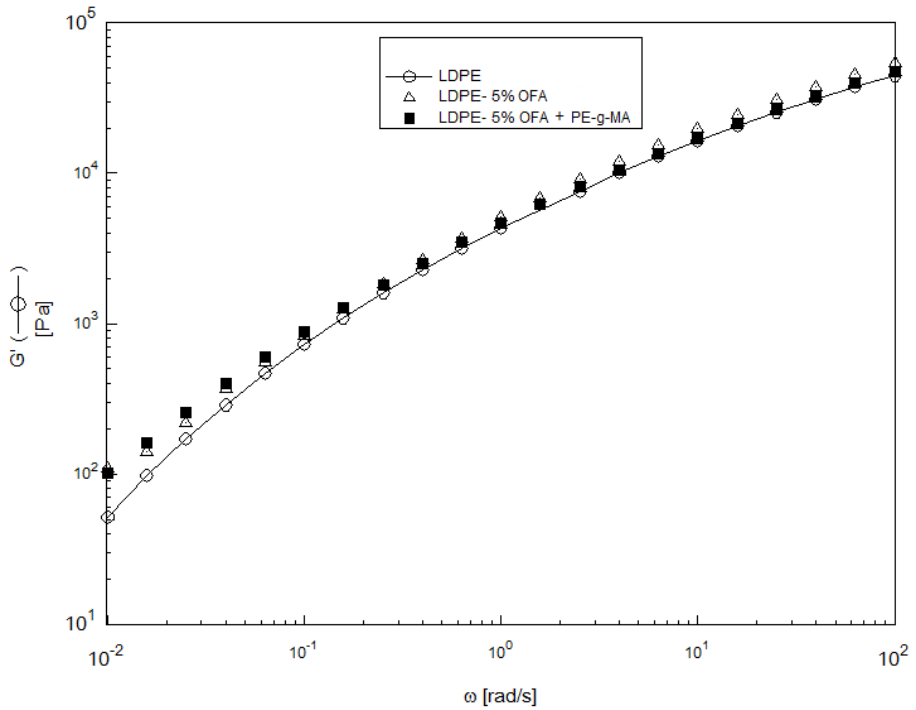

Figure 5.1.2(b): Effect of PE-g-MA at 5% OFA loading on Storage Modulus

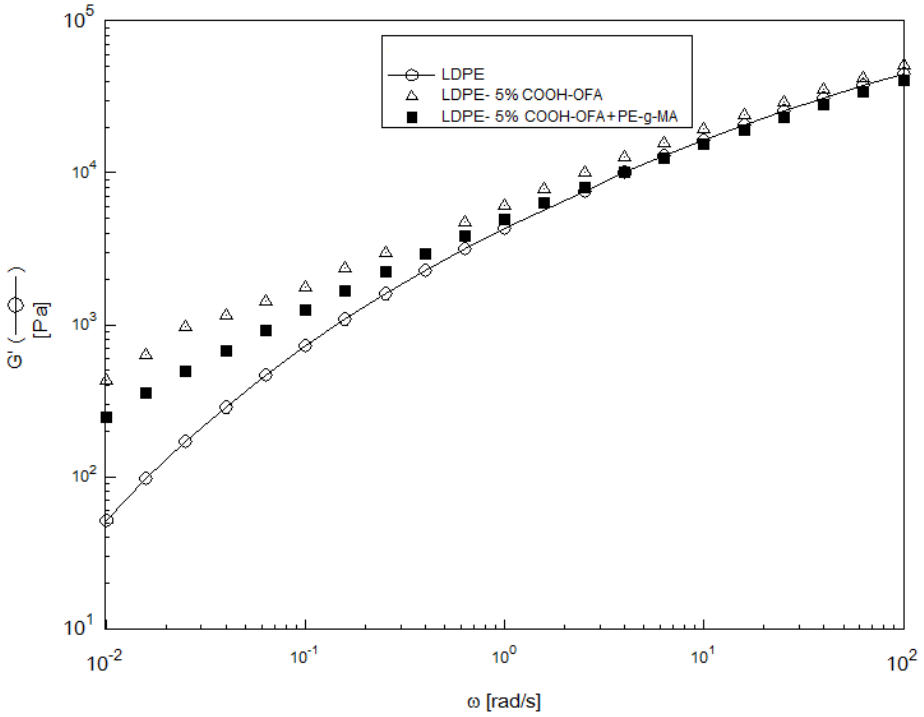

Figure 5.1.2(c): Effect of PE-g-MA at 5% COOH-OFA loading on Storage Modulus

5.2: Effect of OFA on Loss Modulus of Composite

5.2.1: Effect of OFA Loading on Loss Modulus:

The Loss modulus is directly related to the dissipated energy of the material as it is the amount of energy lost due to viscous flow of material. Figure 5.2.1(a) shows the effect of OFA loading on the loss modulus, G″, of LDPE composites. It is shown that the G″ increased in each case of OFA loading. The increase is more pronounced at low frequency as compared to higher frequency [45, 46]. All composition showed similar increase in G″, i.e. the OFA loading had no influence on G″ for untreated ash. However, for modified the 1 and 2% OFA loadings showed similar results. Also, the 5 and 10% loadings showed similar results but higher than those of 1 and 2%. It is suggested that the poor distribution of OFA at such high loadings is the reason behind these observations similar to the previous results of G′.

Figure 5.2.1(b) shows the effect of COOH-OFA loading on the G″ of LDPE composites. The results show that the G″ increased with the increase in the concentration of filler into the polymer matrix. The increment rises linearly with the OFA loading. Almost similar results are obtain at 1 and 2% loading and reach to maximum enhancement at 5% filler concentration. A very slight decrease is observed at 10% loading. The results of G″ support the previous findings from G′.

Figure 5.2.1(c) shows the effect of OFA and PE-g-MA as compatiblizer on G″ LDPE composites. No considerable change is observed in the values of G″ in the case of OFA loading in the presence of the compatiblizer. When functionalized OFA was used with PE-g-MA, the increase in properties is observed at low frequency. The effect of

functionalization on the properties is shown in Figure 5.2.1(d). Again, there is no effect for the compatiblizer on filler dispersion at very high filler loadings.

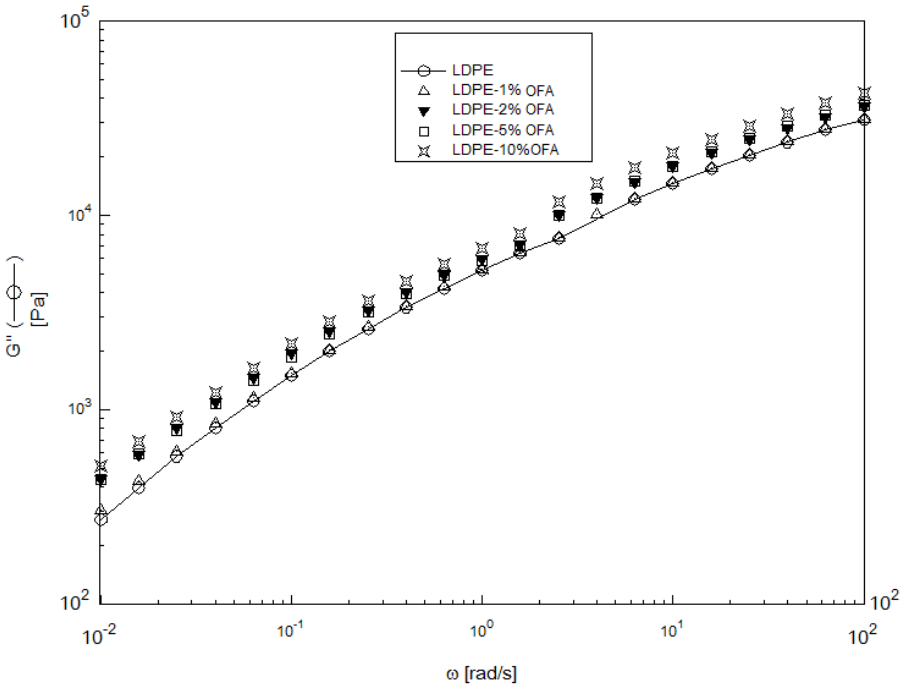

Figure 5.2.1(a): Effect of OFA Loading on Loss Modulus

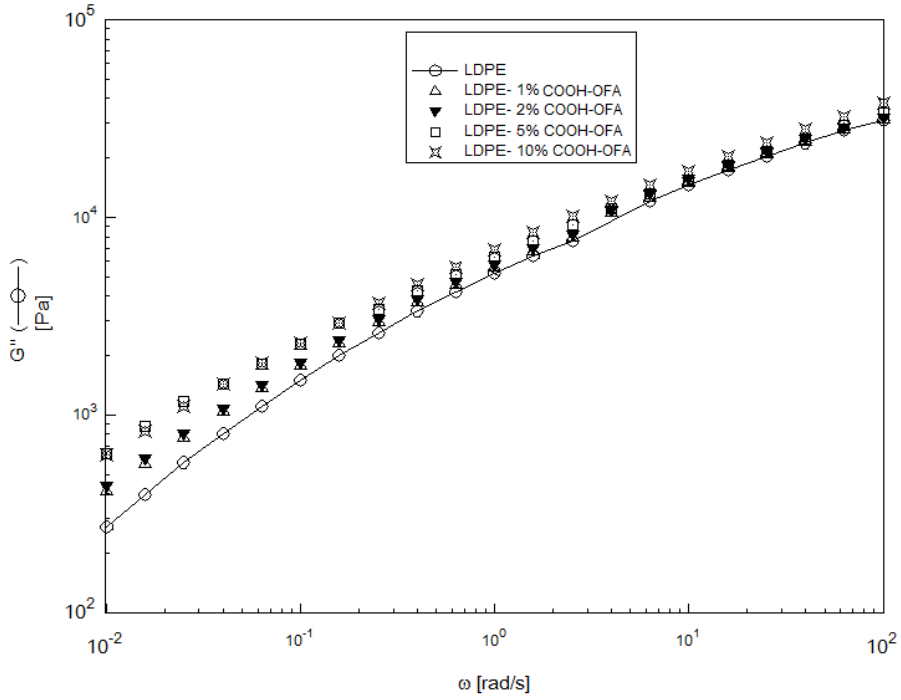

Figure 5.2.1(b): Effect of COOH-OFA Loading on Loss Modulus

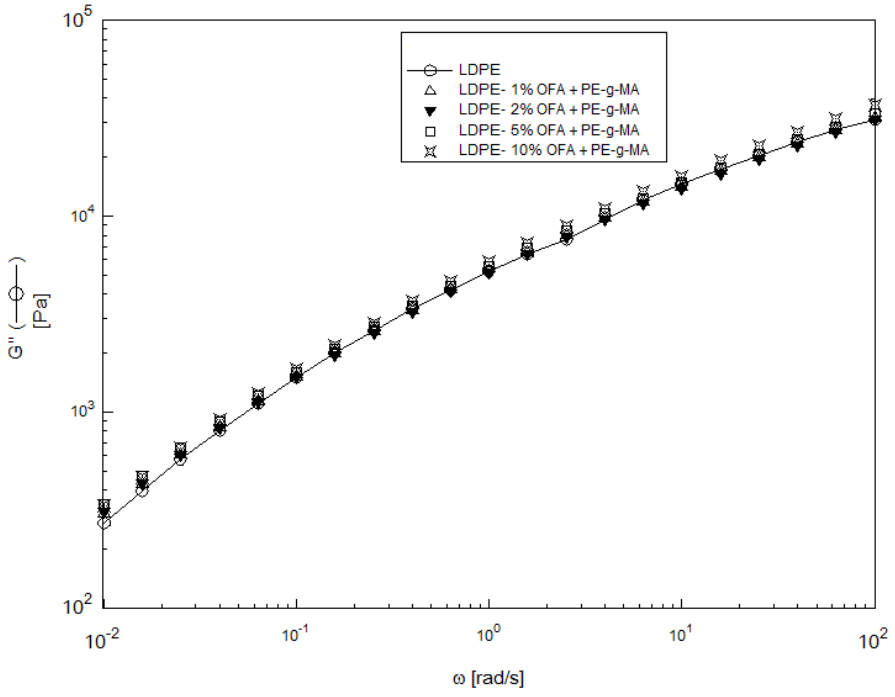

Figure 5.2.1(c): Effect of OFA Loading with 2% PE-g-MA on Loss Modulus

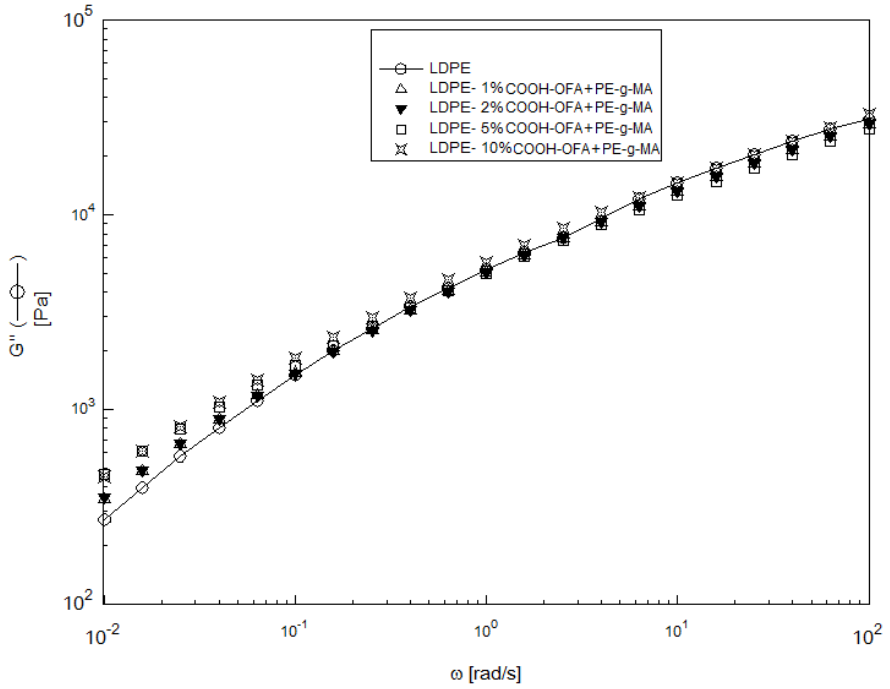

Figure 5.2.1(d): Effect of COOH-OFA Loading with 2% PE-g-MA on Loss Modulus

5.2.2: Effect of OFA functionalization and PE-g-MA on Loss Modulus:

A comparison of G″ modified and unmodified OFA at 5% filler loading is shown in Figure 5.2.2(a). Results show that the functionalization of OFA has a clear impact on the enhancement of G″. At each loading, COOH-OFA gives higher values and the difference is more pronounced with the increase in the concentration of OFA. It is a direct result of good dispersion of COOH-OFA as proved by FE-SEM results discovered earlier. These results are obtained even at higher loading which is not the case for as-received OFA. At high frequency, very minor decrease in G″ is observed in the case of COOH-OFA which suggests improved flow behavior of polymer composite [45, 46]. Similar results are obtained at 1, 2 and 10 %w filler concentration.

The effect of the compatiblizer with as-received and acid-functionalized OFA at 5% filler loading is shown in Figures 5.2.2(b) and 5.2.2(c), respectively. The addition of

compatiblizer resulted in a decrease in G″ of the composite in both cases due to the low viscosity of compatiblizer as compare to pure LDPE. The effect of compatiblizer can be easily observed at the entire range of frequency. The effect of compatiblizer is more dominant in the case of functionalized OFA and the difference is more obvious at high filler loading as compared to low loading. At high frequency, G″ for the compatiblized COOH-OFA was lower than G″ for pure LDPE. So, increase in G″ was observed at low frequency and a drop in G″ at high frequency. This observation indicates that the COOH functionalization is acts as reinforcement but leads to slight shear thinning at high frequency. The synergistic effect of the compatiblizer and the functionalization is good for the processing of these composites. Similar behavior is observed at 1, 2 and 10% filler loading. The effect on 1, 2 and 10% filler loading is shown in Appendix A.

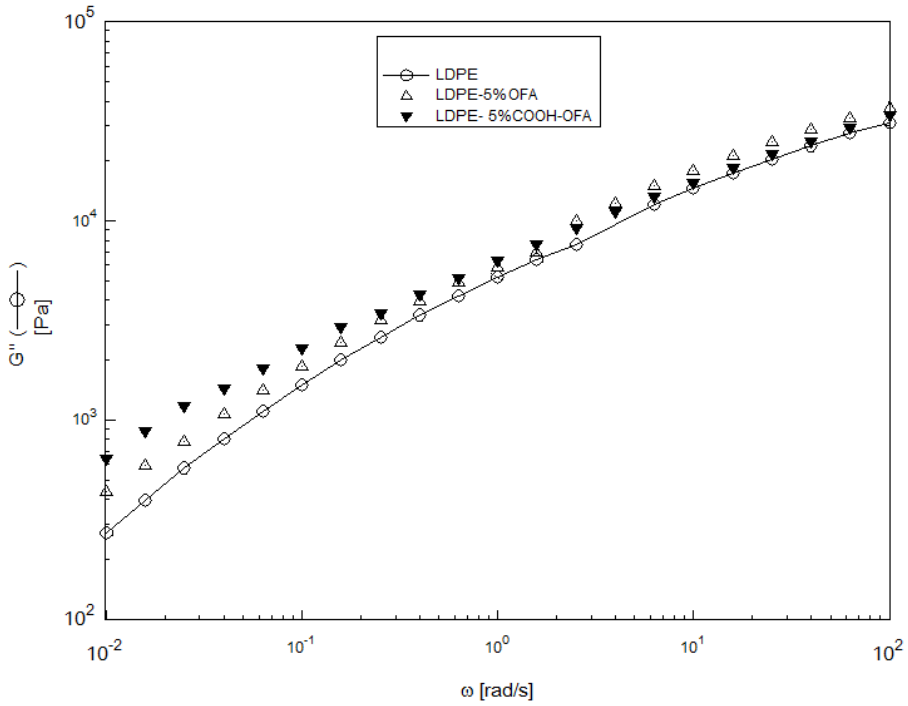

Figure 5.2.2(a): Effect of OFA-functionalization at 5% loading on Loss Modulus

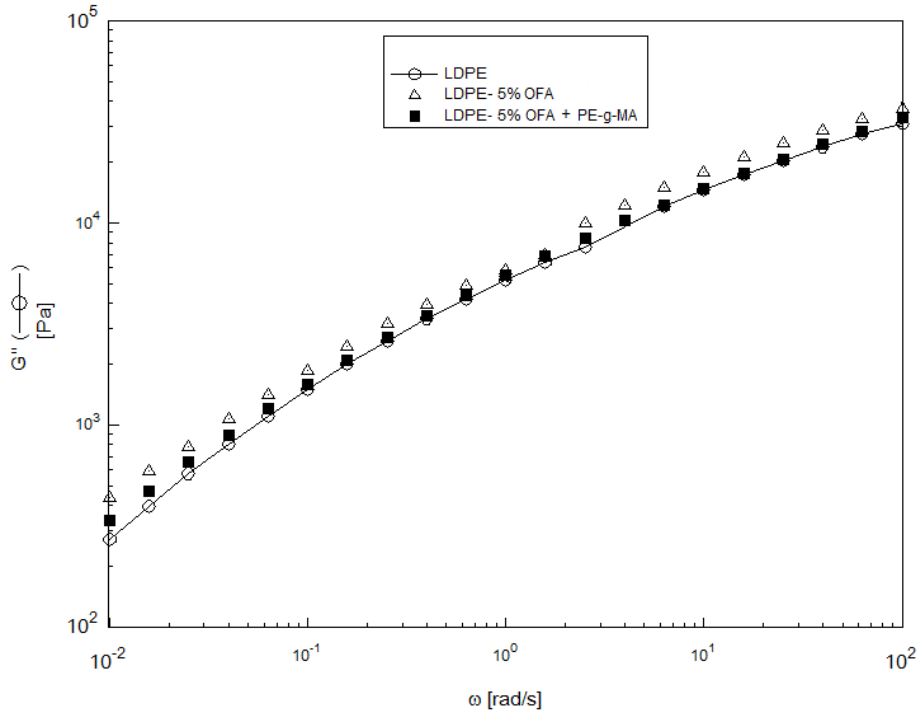

Figure 5.2.2(b): Effect of PE-g-MA at 5% OFA loading on Loss Modulus

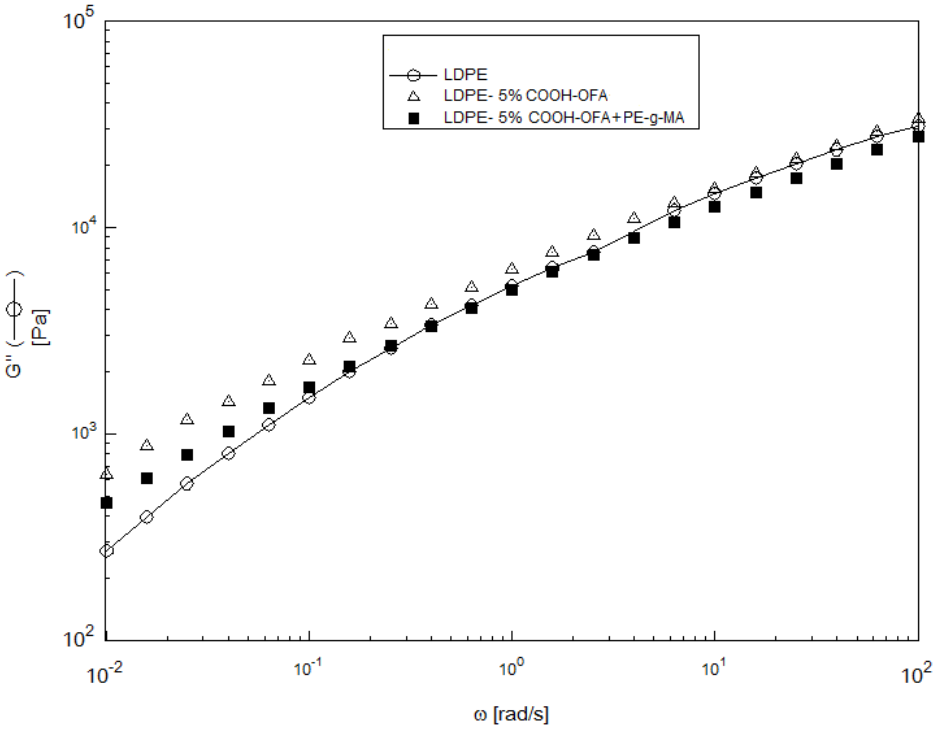

Figure 5.2.2(b): Effect of PE-g-MA at 5%COOH-OFA loading on Loss Modulus

5.3: Crossover Point and Crossover Frequency:

Crossover point Gc is the intersection point of G′ and G″ curve when plotted against frequency. The frequency at which this intersection occurs is called crossover frequency, ωc. Crossover Point defines the separation of elastic and viscous behavior of the material [47-49]. At this point, ωc represents the homogeneity of the composite material. The low value of Gc and ωc represents that material is more homogenous due to fine dispersion [49]. In the case of as-received OFA, Gc and ωc increased with the increase in filler loading for modified fly ash as shown in figure 5.3.1. It shows the poor distribution of filler within the polymer matrix and phase separation at higher loading due to agglomeration of filler particles. However in the case of COOH-OFA, Gc and ωc decreased with the addition of modified ash. The slight increase in Gc at 10% loading is consistent with our previous observations from Cole-Cole plot that showed slight drop in the curve for the 10% OFA loading. This suggests the fine and constant degree of distribution of COOH-OFA in the polymer matrix. The effect of filler loading on Gc and ωc can be described more precisely by Figures 5.3.1 and 5.3.2. In Figure 5.3.1, with the addition of compatiblizer the distribution of as-received OFA has improved and the value of Gc and ωc decreased at each loading. Whereas no considerable improvement is observed in the case of COOH-OFA loading except at 5% filler concentration as shown in Figure 5.3.2. In each case except 5% loading, the value of Gc and ωc for compatiblized composites is slightly higher with compatiblizer. So, in the absence of functionalization the compatiblizer tends to reduce Gc and ωc, which suggests improvement of dispersion. However, in the case of functionalized OFA, the role of the compatiblizer is, in general, not significant or negative (see Figure 5.3.2).

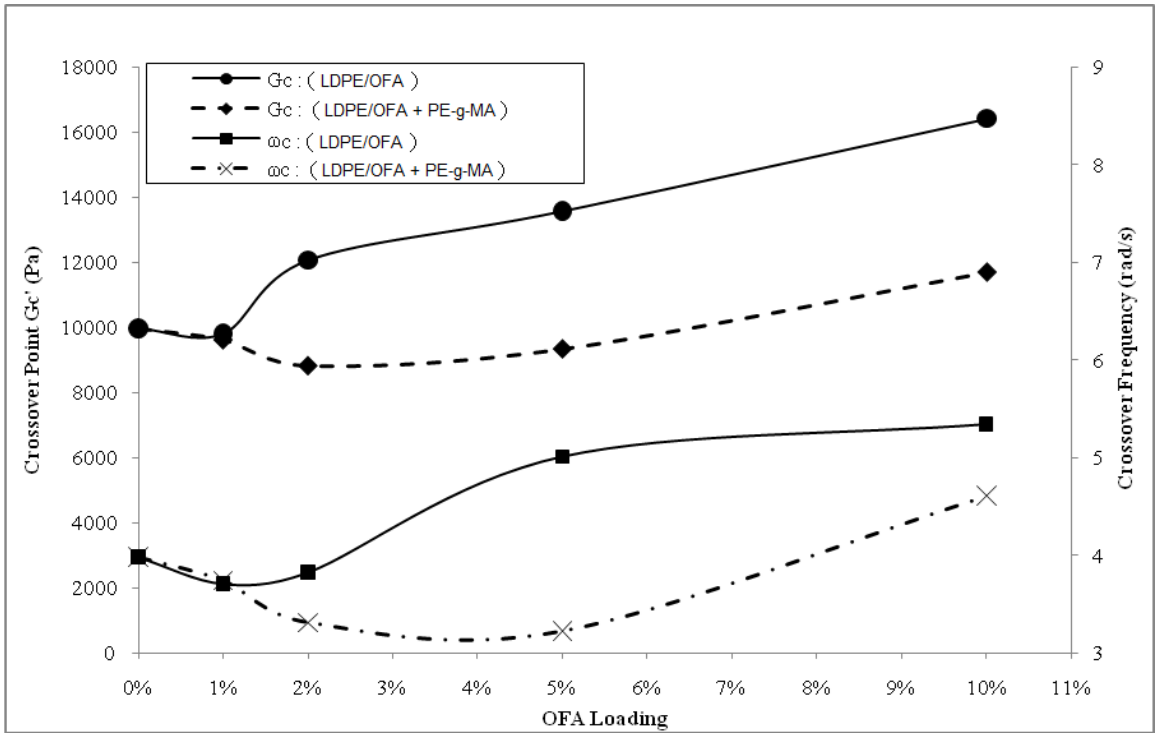

Figure 5.3.1: Effect of OFA Loading on Crossover Point and Frequency

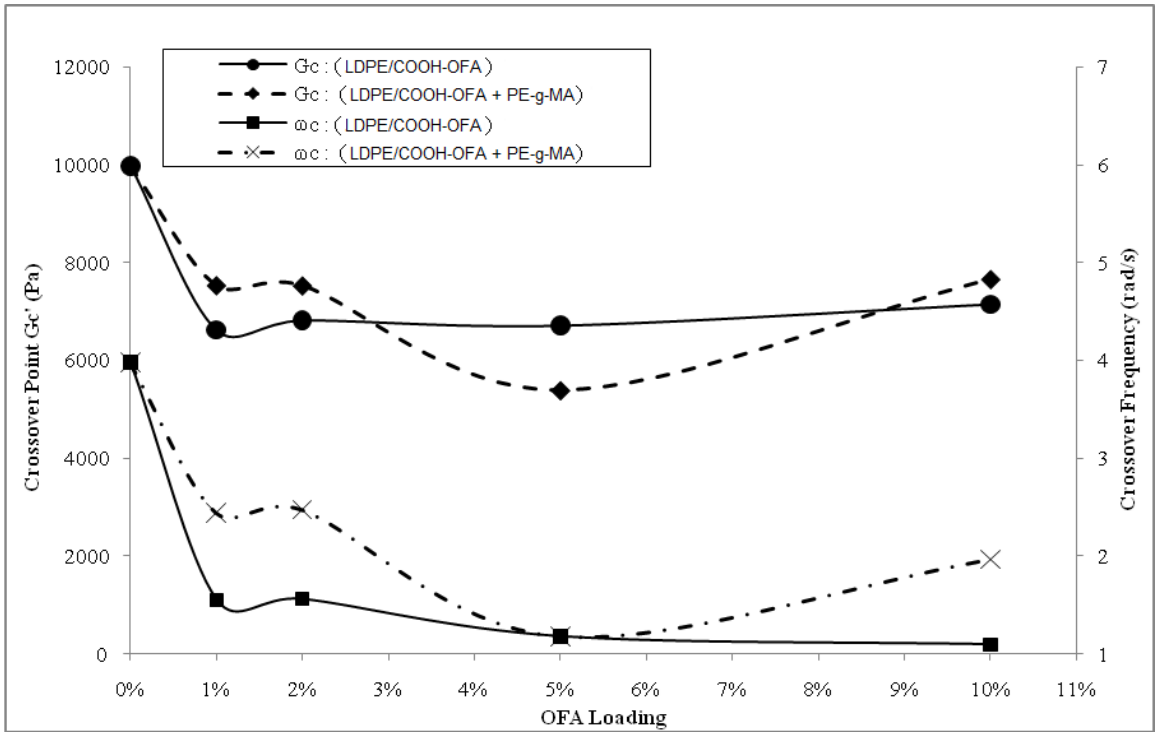

Figure 5.3.1: Effect of COOH-OFA Loading on Crossover Point and Frequency

5.4: Degree of dispersion by Cole-Cole Plot

The relaxation behavior of polymer composites can be represented by Cole-Cole plots which depend on the degree of dispersion of the filler. It is a plot of imaginary viscosity, η'', vs real viscosity, η'. Higher the degree of dispersion shows the high longer relaxation time [45-47]. Figure 5.4.1 shows the Cole-Cole plot of LDPE/OFA composites at different filler loading. For 1 and 2% filler loading, the degree of dispersion increased with filler concentration but at 5 and 10% loading, it again decreased. It means the agglomeration may occur at higher filler loading in case of as-received OFA. Also, two relaxation mechanisms at high filler loading show the two-phase system because of non-homogeneous behavior [45]. Figure 5.4.2 shows the Cole-Cole plot of LDPE/OFA composite with 2% PE-g-MA. The degree of dispersion of OFA has improved in the presence of the compatiblizer and maximum relaxation time observed at 5% filler loading. Also the two phase system which is observed without compatiblizer by two slopes in Cole-Cole plot has disappeared.

The Cole-Cole plot of COOH-OFA and LDPE polymer composite is shown in Figure 5.4.3. It is observed that in each case, the relaxation time increased with the addition of filler. The highest degree of dispersion is observed at 5% loading which is a little decreased at 10% loading. No variation is observed in relaxation behavior of LDPE/CHOOH-OFA composites which shows the homogeneity of the system. Also, the high relaxation time as compared to OFA shows a good dispersion of filler due to functionalization. The effect of PE-g-MA compatiblizer on the degree of dispersion of functionalized OFA is shown in Figure 5.4.4. A slight improvement is observed after the addition of PE-g-MA at high loading.

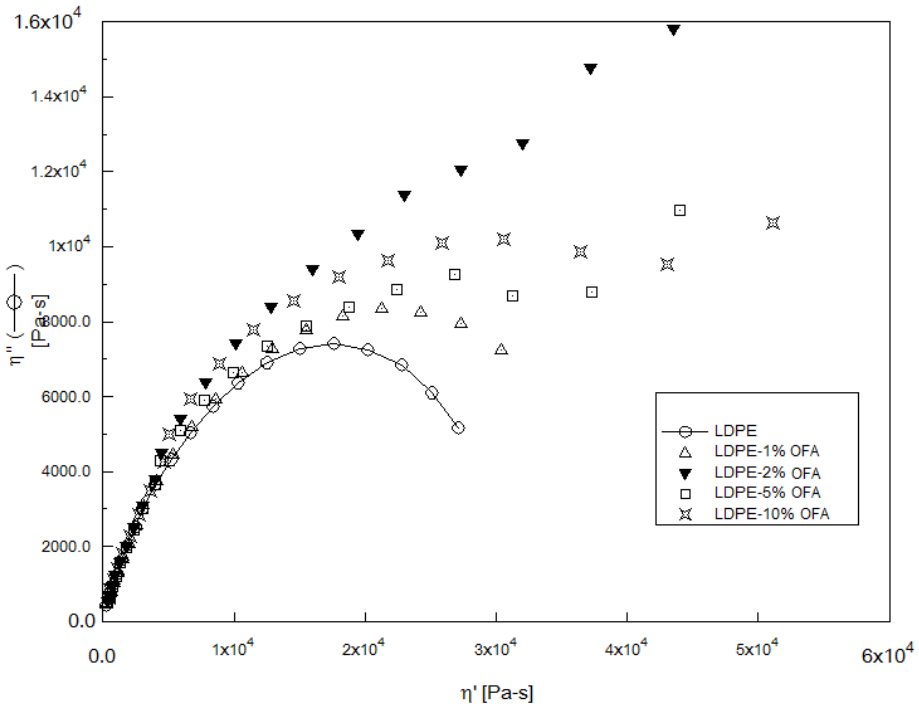

Figure 5.4.1: Cole-Cole plot for LDPE/OFA composite

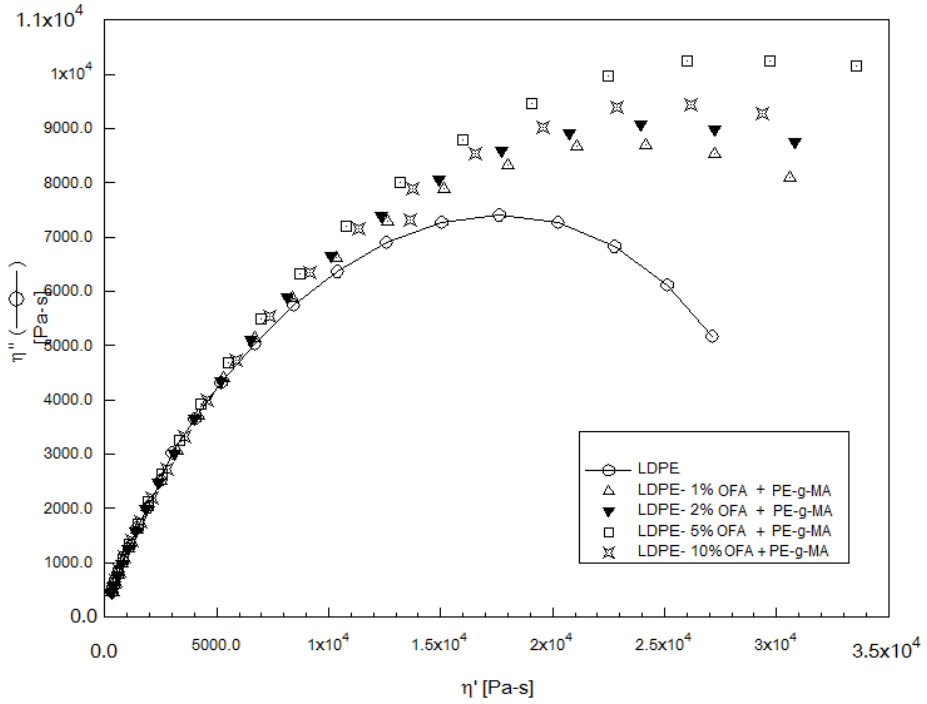

Figure 5.4.2: Cole-Cole plot for LDPE/OFA composite with PE-g-MA

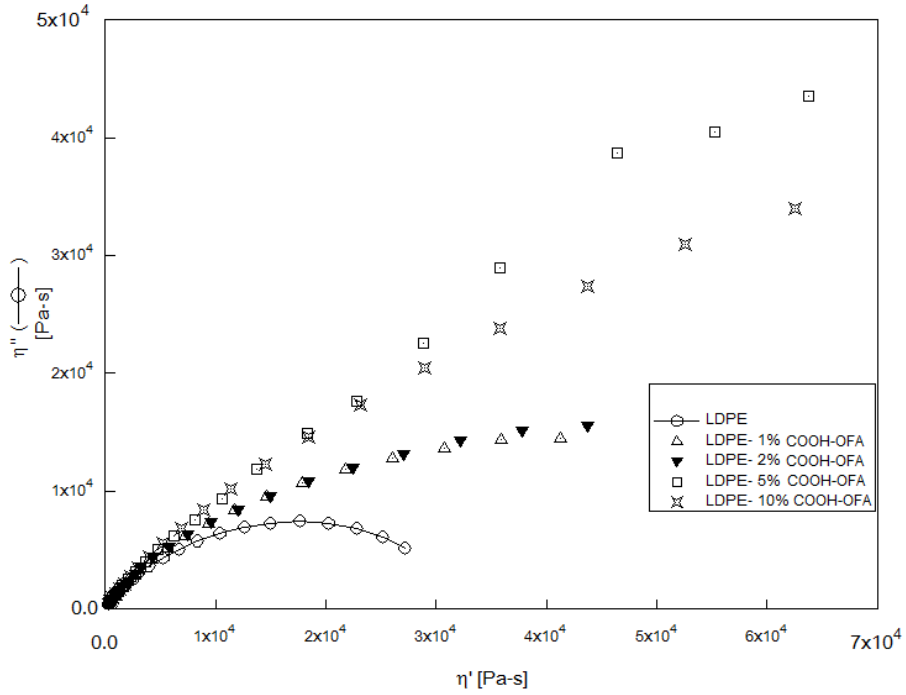

Figure 5.4.2: Cole-Cole plot for LDPE/COOH-OFA composite

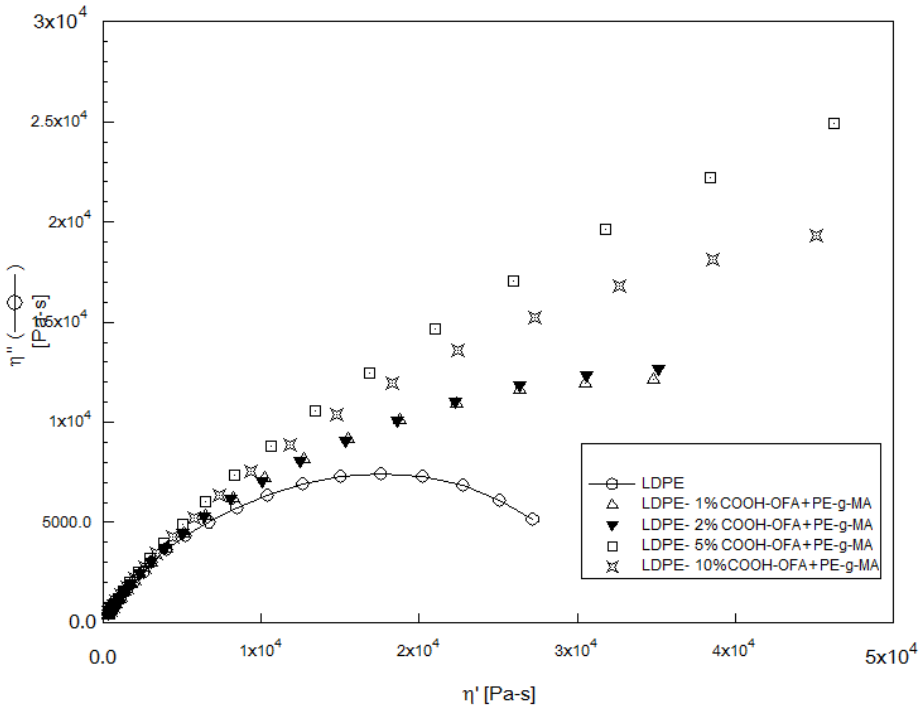

Figure 5.4.2: Cole-Cole plot for COOH-OFA and LDPE polymer composite with PE-g-MA

Part B: Morphological Characterization of LDPE/OFA Composites

The FE-SEM analysis of Pure LDPE sample is done as a reference as shown in Figure 5.5.1. The dispersion of OFA at 2 and 5% loading is shown in Figures 5.5.2(a-b) and 5.5.3, respectively. It is observed that the OFA particles are distributed well in the polymer matrix. However, some agglomeration of particles is also observed as shown in Figures 5.5.2(b). The dispersion of surface modified fly ash particles at 2 and 5% loading is shown in Figures 5.5.4(a-b) and 5.5.5(a-b), respectively. A better dispersion of fly ash particles is observed after the surface modification as compare to unmodified OFA. A well dispersed COOH-OFA particles were observed at high and low magnification. The degree of dispersion is improved by acid functionalization of OFA as reflected in the reduction of the size of agglomeration. A comparison of results for 2% OFA shown in Figures 5.5.2(a) and 5.5.4(b) suggests a reduction of particle size by a factor of at least 2. Similarly, a comparison of Figures 5.5.5(b) and 5.5.3 suggests improved dispersion at 5% OFA loading as a result of surface modification. All of these comparisons were made for images of the same magnifications. However, the COOH modification of OFA did not eliminate the agglomeration but rather reduced its size as shown in Figures 5.5.2(b) and 5.5.4(a). Similar results are observed when PE-g-MA was used as compatiblizer.

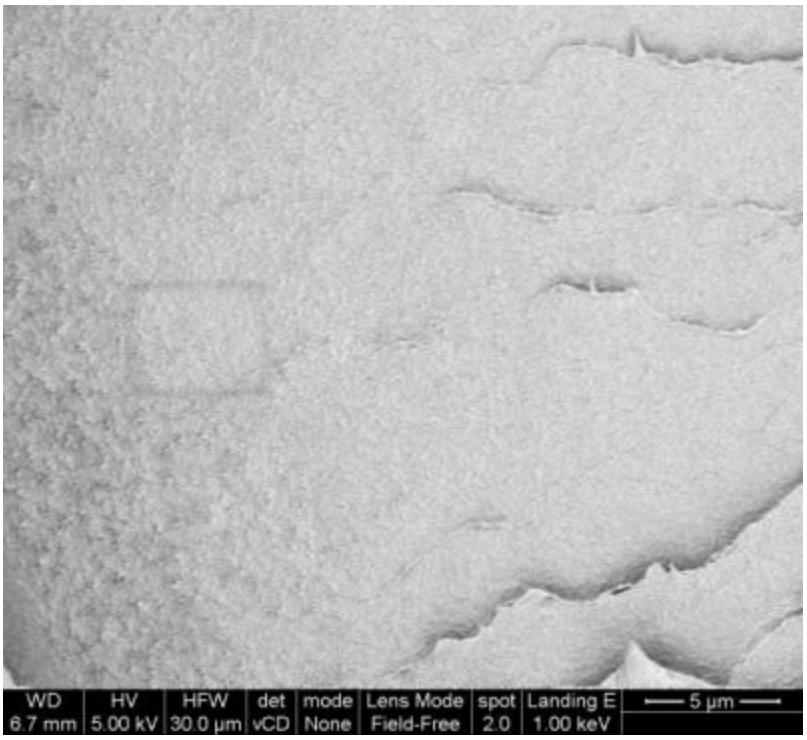

Figure 5.5.1: SEM for pure LDPE at 5µm scale

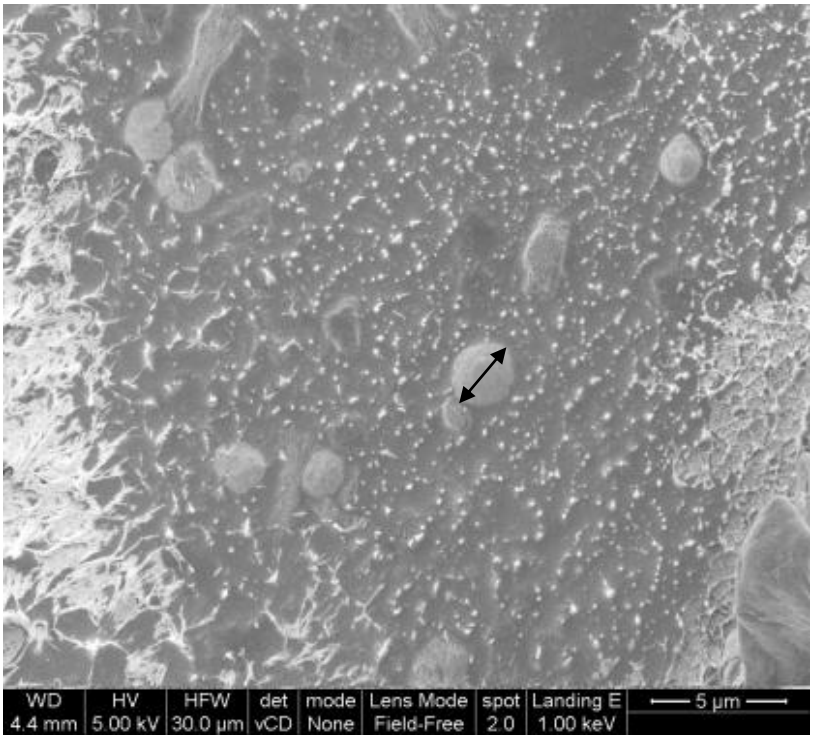

Figure 5.5.2(a) SEM for LDPE/OFA composite at 2% loading and 5µm scale

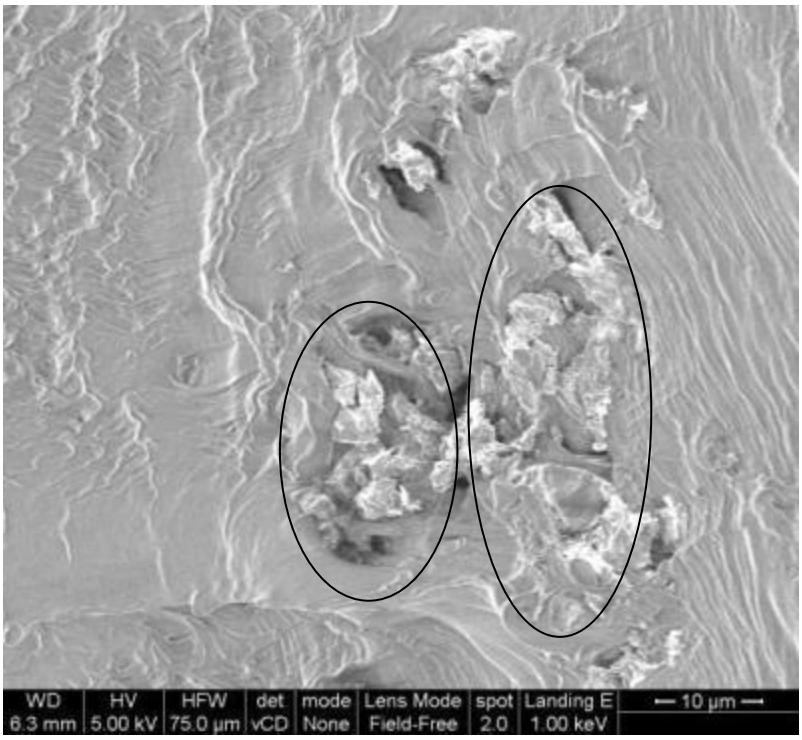

Figure 5.5.2(b) SEM for LDPE/OFA composite at 2% loading and 10µm scale

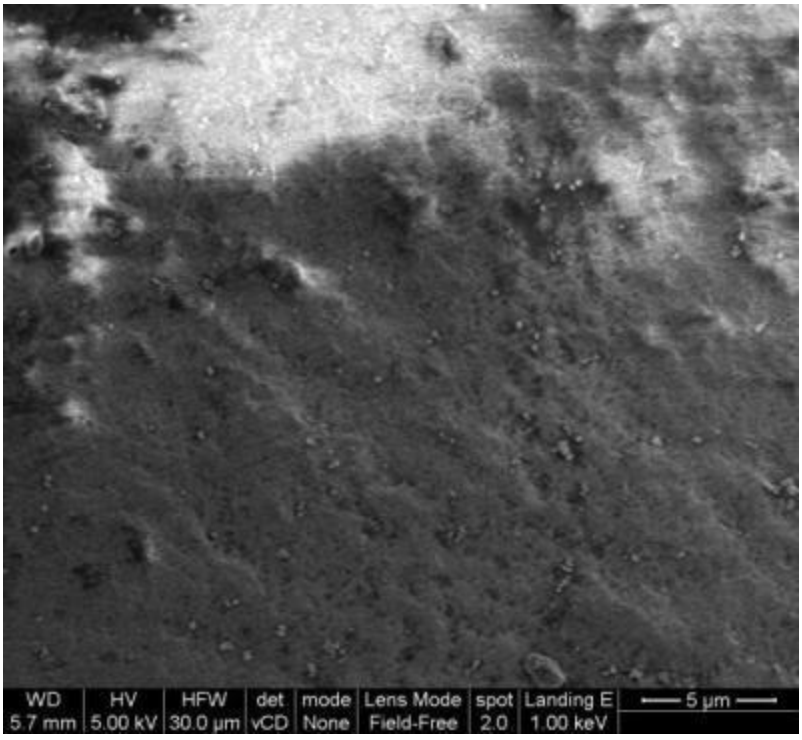

Figure 5.5.3: SEM for LDPE/OFA composite at 5% loading and 5µm scale

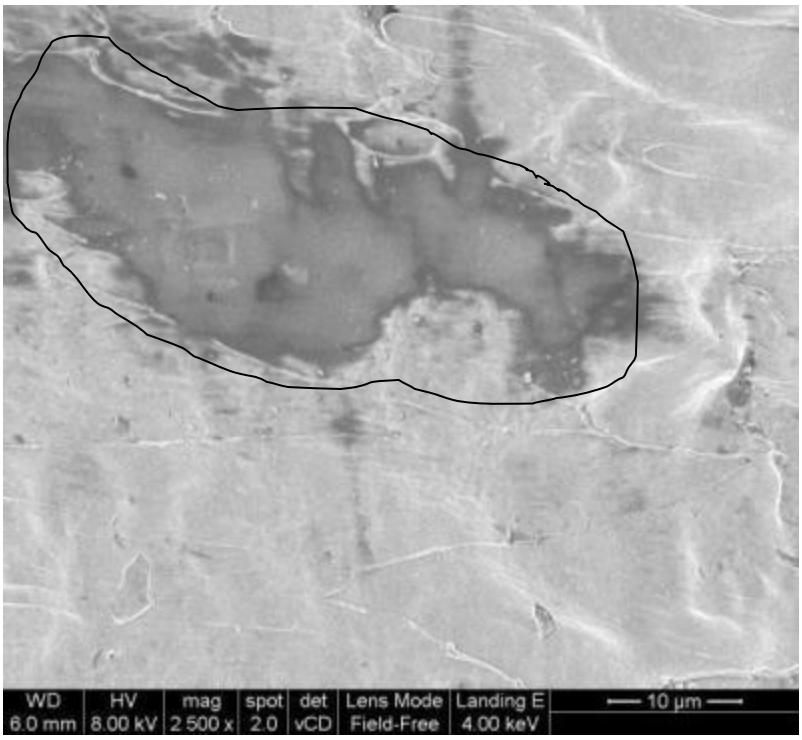

Figure 5.5.4(a) SEM for LDPE/COOH-OFA composite at 2% loading and 10µm scale

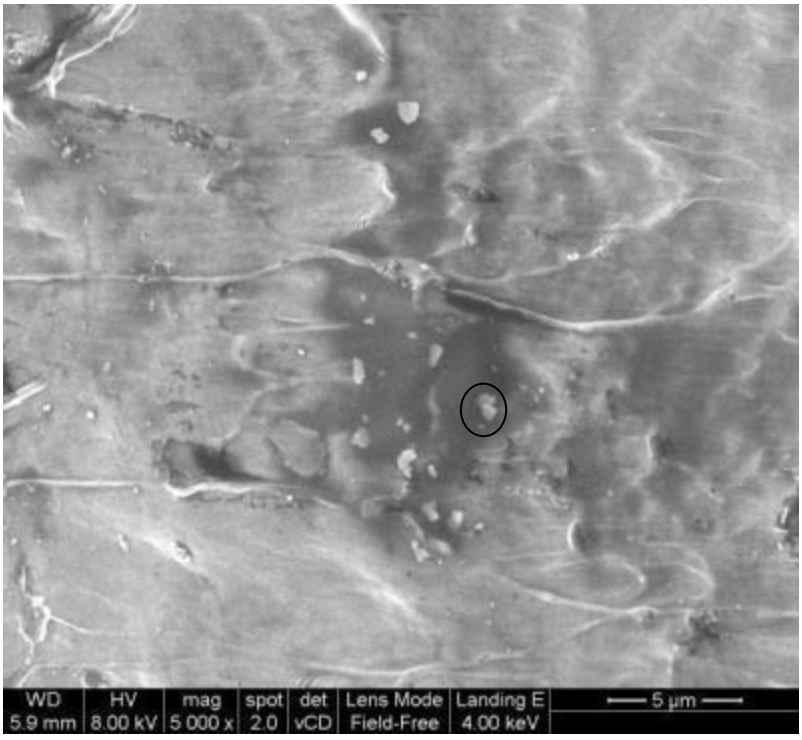

Figure 5.5.4(b) SEM for LDPE/COOH-OFA composite at 2% loading and 5µm scale

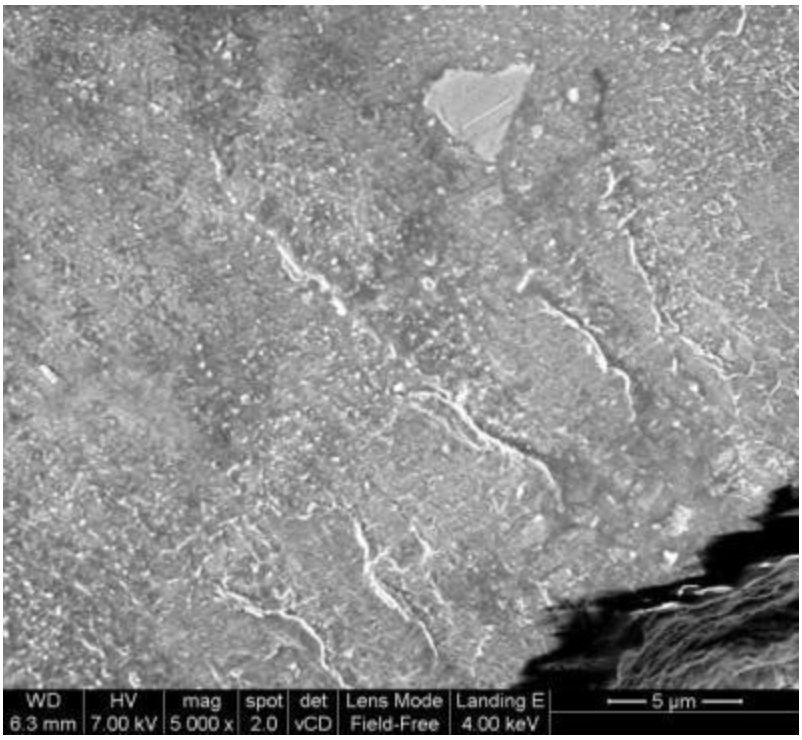

Figure 5.5.5(a) SEM for LDPE/COOH-OFA composite at 5% loading and 5µm scale

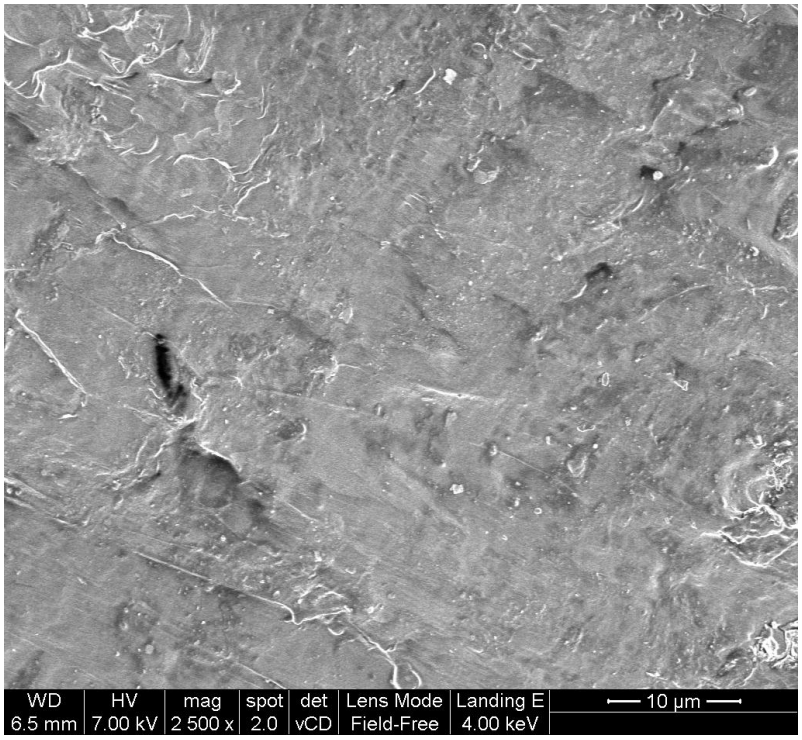

Figure 5.5.5(b) SEM for LDPE/COOH-OFA composite at 5% loading and 4µm scale

CHAPTER 6

RESULTS & DISCUSSION

MECHANICAL AND THERMAL BEHAVIOR OF LDPE/OFA COMPOSITE

It is believed that the enhancement in the polymer's thermal properties can be achieved by fillers loading which have better strength and heat flow or resistance characteristics. In this chapter, we investigated the effect on OFA loading as a filler on the mechanical and thermal properties of LDPE. Also the effect of OFA functionalization by acid treatment and effect of Polyethylene-grafted-Maleic anhydride addition as a compatiblizer is investigated.

Part A: Mechanical Behavior of LDPE/OFA Composite

Mechanical behavior of LDPE/OFA composite is observed by tensile testing on Instron Mechanical Analyzer. Different properties have been calculated as Young's Modulus, Elongation to break, Toughness, Yield Strength and Ultimate strength. 3 specimens for each composite are analyzed and average values are compared with pure LDPE. Comparison between modified and unmodified OFA loading is done and also the effect of PE-g-MA is observed. Solid lines with empty and filled box marker show the OFA without and with compatiblizer respectively. Dash lines with empty and filled circle marker show the COOH-OFA without and with compatiblizer respectively.

6.1: Effect of OFA on Young's Modulus:

6.1.1: Effect of OFA Loading on Young's Modulus

Young's Modulus is the measure of the stiffness of an isotropic elastic material. Table 6.1 shows the results of Young's Modulus analysis at 4% strain for 1, 2, 5 and 10 wt% OFA loading. Also the %increase in values are calculated and reported in the table. Table shows that Young's Modulus is linearly relates to the loading of OFA. In each case, the Young's Modulus increased as we increase the percentage of OFA in the composite.

Table 6.1: Effect of OFA loading on Young's Modulus

Composite		OFA Loading				
		0%	**1%**	**2%**	**5%**	**10%**
LDPE/OFA	Value (MPa)	112.50	121.57	127.40	141.25	156.90
	% Increase	0.00	8.06	13.24	25.56	39.47
	S.D.	3.80	9.19	8.34	1.63	0.75
LDPE/COOH-OFA	Value (MPa)	112.50	129.07	132.00	139.37	157.77
	% Increase	0.00	14.73	17.33	23.88	40.24
	S.D.	3.80	2.19	2.62	3.19	3.35
LDPE/OFA + PE-g-MA	Value (MPa)	112.50	130.67	133.17	142.77	166.27
	% Increase	0.00	16.15	18.37	26.91	47.80
	S.D.	3.80	1.02	6.00	3.29	1.54
LDPE/COOH-OFA + PE-g-MA	Value (MPa)	112.50	127.73	133.17	151.90	165.20

	% Increase	0.00	13.54	18.37	35.02	46.84
	S.D.	3.80	4.17	3.94	3.83	2.69

Results showed that about 8.06-16.05% increase in Young's modulus achieved by only 1% addition of filler whereas 13.24-18.37% increment achieved by only 2% addition of filler. At higher loading, 23.88-35.02% increment achieved by 5% addition while 39.47-47.80% increment is observed at 10% filler loading. As the three specimens are used for each composite sample, standard deviation of three specimens' results is also reported. The effect of OFA loading is described more efficiently by Figure 6.1.1(a-d). Figure 6.1.1 (a) and (b) shows the result of as-received and acid-functionalized OFA loading without PE-g-MA compatiblizer respectively while the figure 6.1.1 (c) and (d) shows the result of as-received and acid-functionalized OFA loading with PE-g-MA compatiblizer respectively.

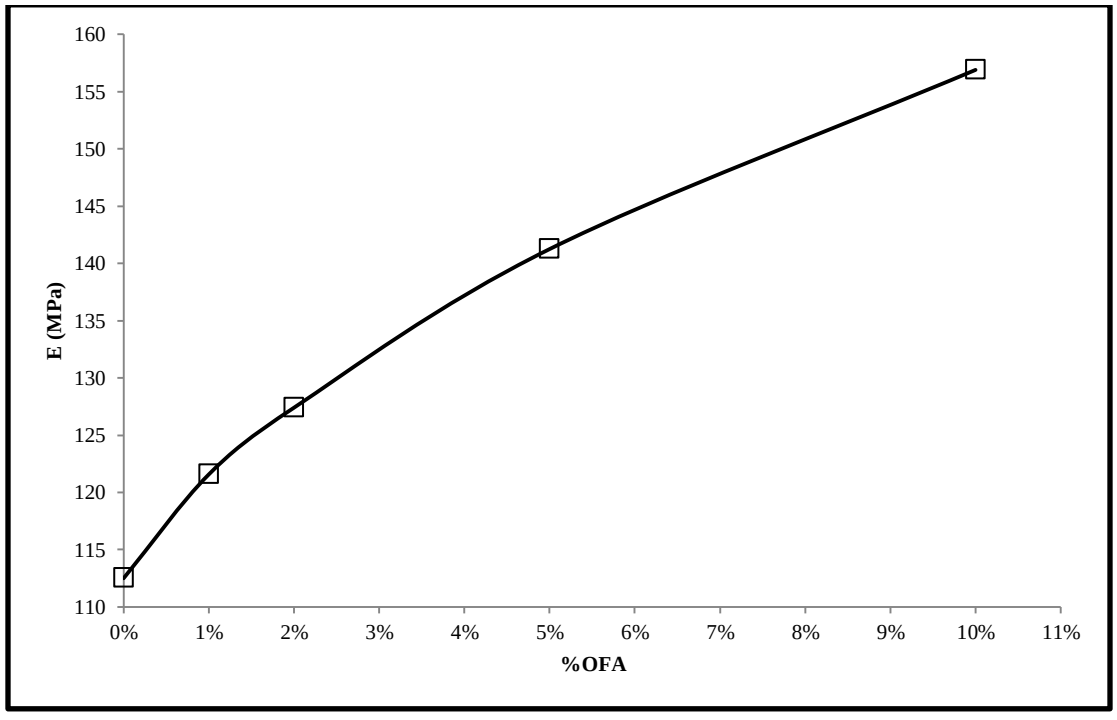

Figure 6.1.1(a): Effect of OFA Loading on Young's Modulus

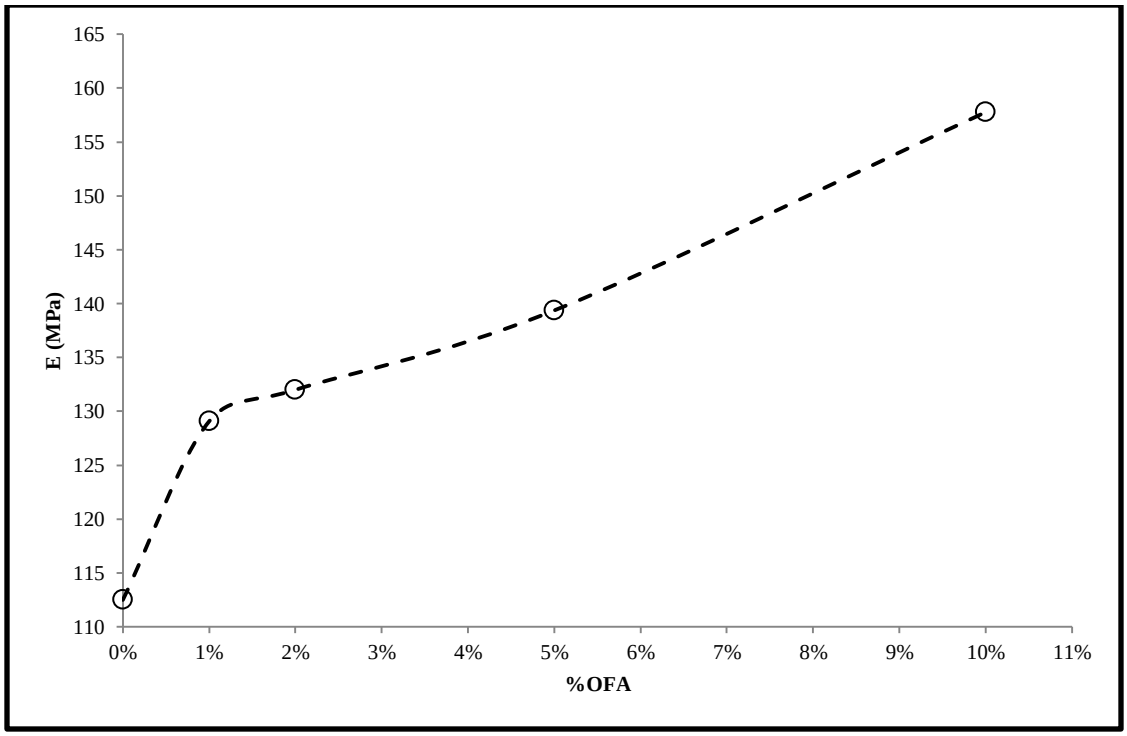

Figure 6.1.1(b): Effect of COOH-OFA Loading on Young's Modulus

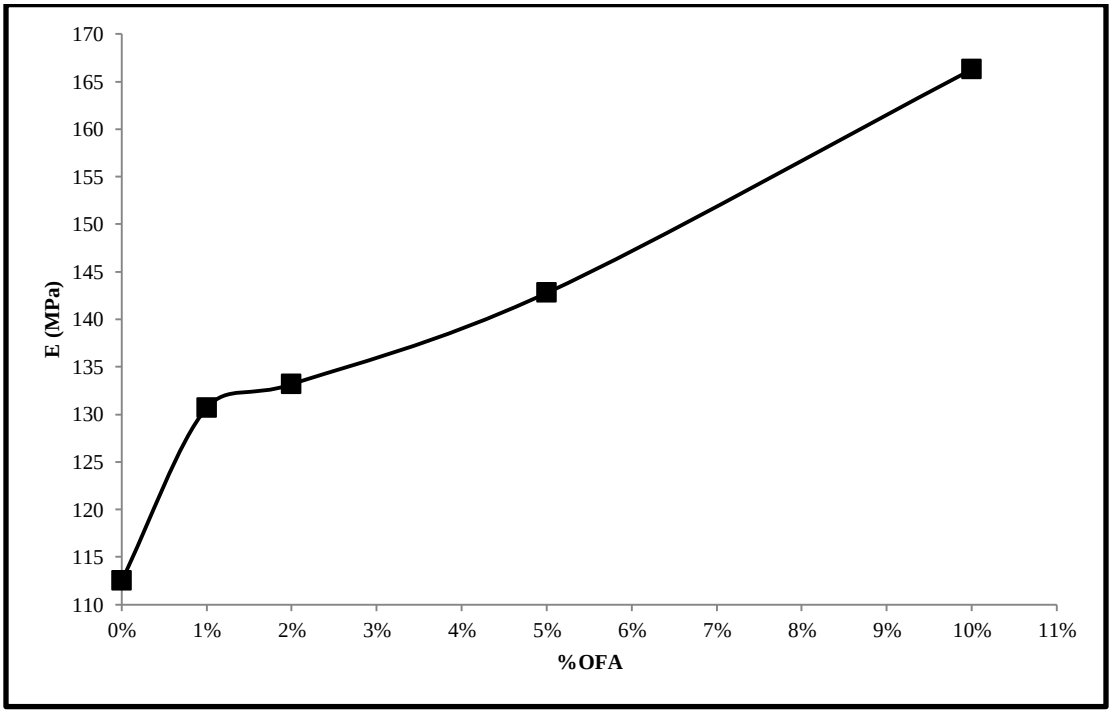

Figure 6.1.1(c): Effect of OFA Loading with 2% PE-g-MA on Young's Modulus

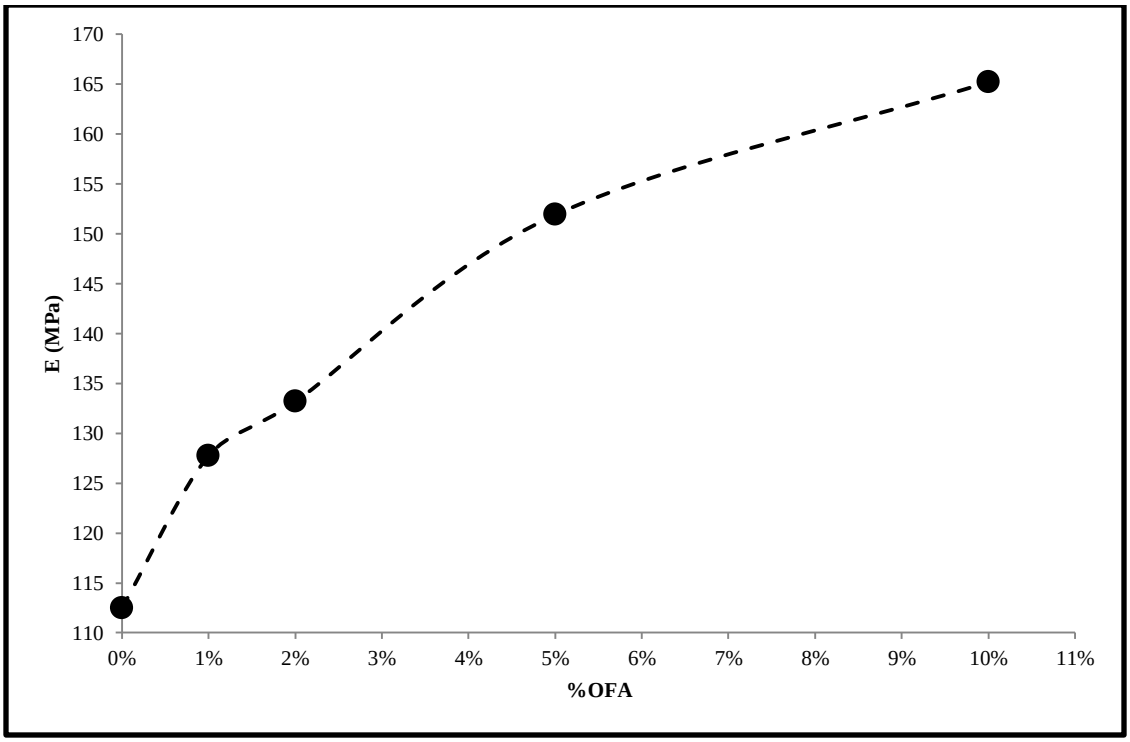

Figure 6.1.1(d): Effect of COOH-OFA Loading with 2% PE-g-MA on Young's Modulus

6.1.2: Effect of OFA Functionalization on Young's Modulus

Effect of OFA functionalization with and without PE-g-MA compatiblizer on Young's Modulus of composites is shown in figure 6.1.2(a-b). Figure 6.1.2(a) shows the effect of functionalization without PE-g-MA compatiblizer. It is observed that at lower loading i.e. 1 and 2 wt%, functionalized fly ash shows good improvement as compare to as-received fly ash whereas at higher loading i.e. 5 and 10wt%, both type of fly ash gives almost same results.

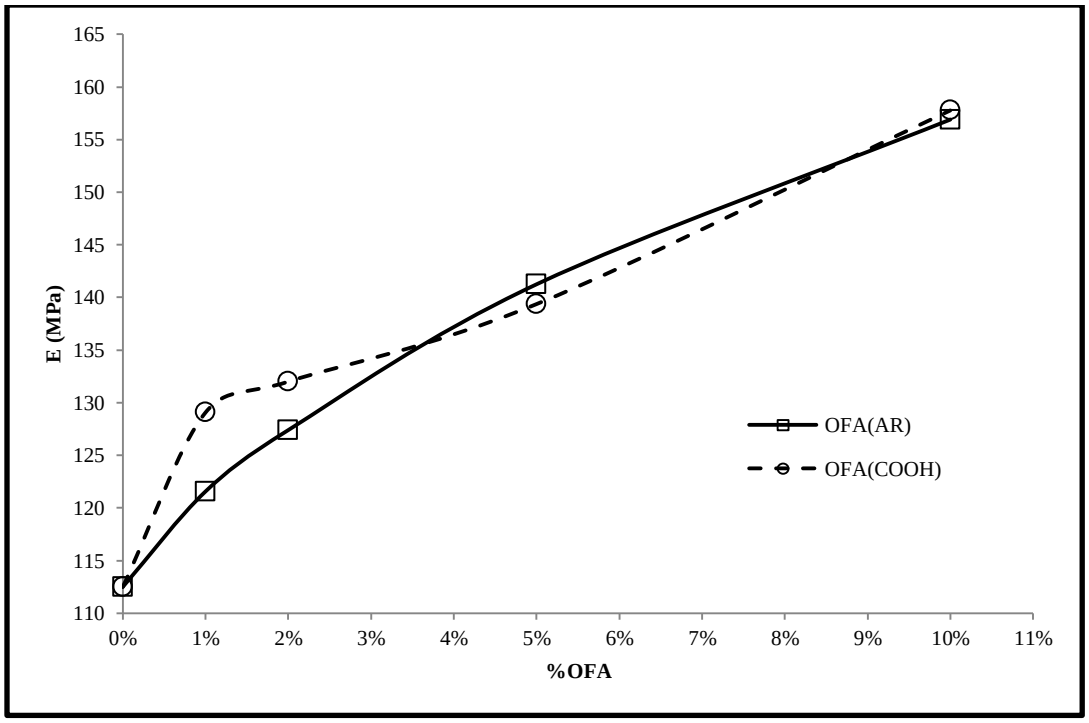

Figure 6.1.2(a): Effect of OFA functionalization without PE-g-MA on Young's Modulus

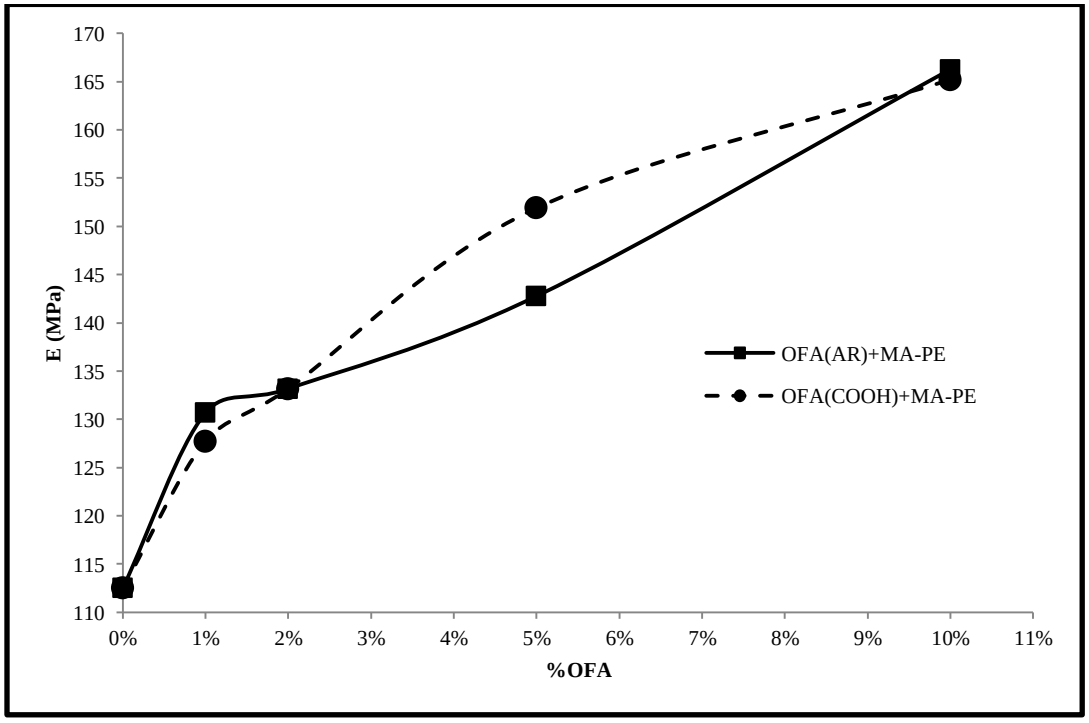

Figure 6.1.2(b): Effect of OFA functionalization with 2% PE-g-MA on Young's Modulus

Figure 6.1.2(b) shows the effect of functionalization in the presence of PE-g-MA. It is observed that at lower loading i.e. 1 and 2 wt%, modified and unmodified fly ash gives the similar results whereas at 5 wt% loading, a considerable improvement is observed. It means that the compatiblizer enhance the dispersion of fly ash into the polymer matrix. At 10 wt% fly ash loading, both type of fillers gives the similar results which means that optimum condition in this case of functionalization is 5 wt% loading.

6.1.3: Effect of PE-g-MA Compatiblizer on Young's Modulus

Effect of Polyethylene-grafted-Maleic Anhydride with and without OFA surface modification on Young's Modulus of composites is shown in figure 6.1.3(a-b). Figure 6.1.3(a) shows the effect of PE-g-MA compatiblizer with unmodified fly ash. It is clearly observed that at each loading, the Young's Modulus of composites increased by the addition of PE-g-MA. It shows that compatiblizer created a good interlink between filler and polymer matrix. Figure 6.1.3(b) shows the effect of PE-g-MA with modified fly ash. It is observed that at lower loading i.e. 1 and 2 wt%, both type of fly ash gives the similar results while at higher loading i.e. 5 and 10 wt%, a considerable improvement is observed. The effect of compatiblizer is not observed at lower loading because the functionalization already improved the dispersion and improvement reached to it optimized condition. But at higher loading, when the more agglomeration may possible, the PE-g-MA effects and improved the dispersion more with attached functional group of fly ash.

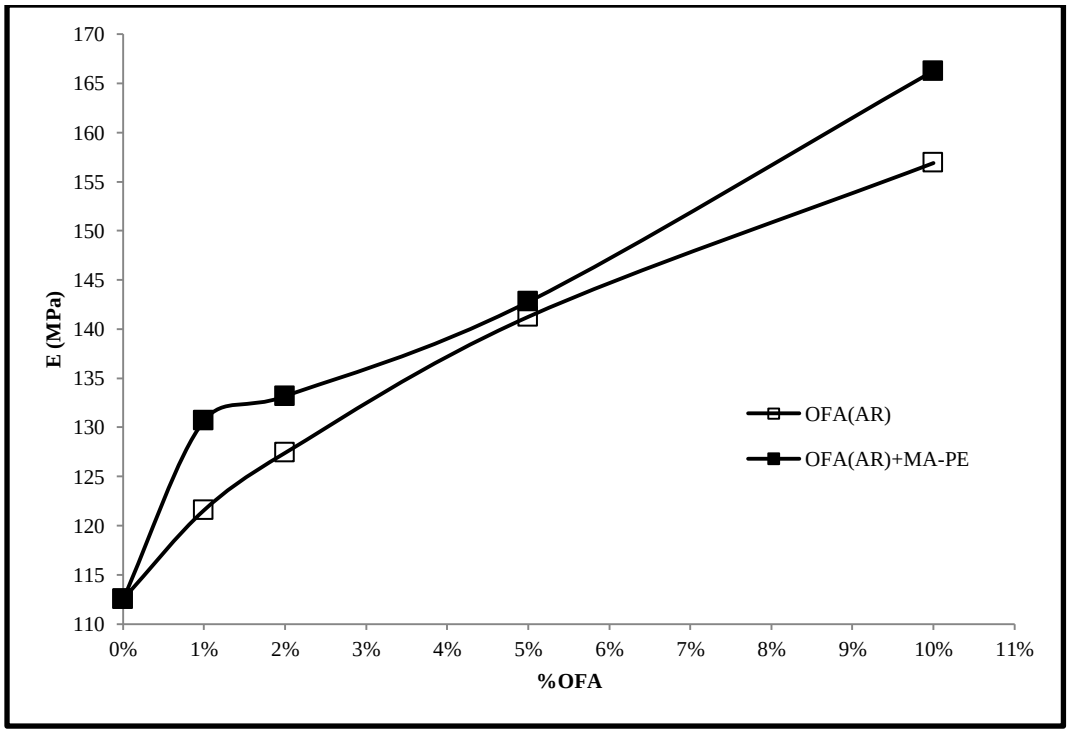

Figure 6.1.3(a): Effect of Compatiblizer with OFA Loading on Young's Modulus

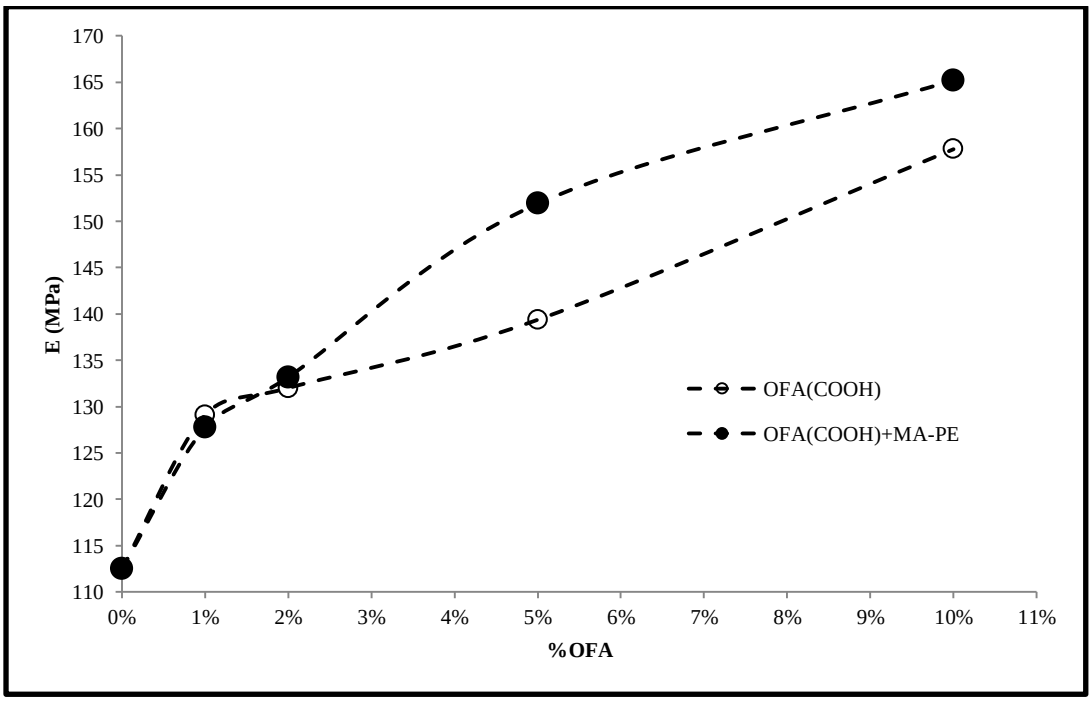

Figure 6.1.3(b): Effect of Compatiblizer with COOH-OFA Loading on Young's Modulus

6.2: Effect of OFA on Elongation to Break

6.2.1: Effect of OFA Loading on Elongation to Break

Elongation to break is basically the maximum strain or deformation of material before rupture. Table 6.2 shows the results of Elongation to break for 1, 2, 5 and 10 wt% OFA loading. Also the %decrease in values and standard deviation of 3 specimens' results is calculated and reported in the table. Table shows that percent Elongation to break is linearly relates to the loading of OFA.

Table 6.2: Effect of OFA loading on Elongation to Break

Composite	OFA Loading					
		0%	**1%**	**2%**	**5%**	**10%**
LDPE/OFA	Value %	735	549	492	078	059
	% Decrease	0.00	25.31	33.06	89.39	91.97
	S.D.	1.35	0.19	0.15	0.32	0.03
LDPE/COOH-OFA	Value %	735	556	489	154	076
	% Decrease	0.00	24.35	33.47	79.05	89.66
	S.D.	1.35	0.25	0.59	0.54	0.01
LDPE/OFA + PE-g-MA	Value %	735	550	479	143	055
	% Decrease	0.00	25.17	34.83	80.54	92.52
	S.D.	1.35	0.10	0.44	0.47	0.09
LDPE/COOH-OFA + PE-g-MA	Value %	735	583	539	128	066

	% Decrease	0.00	20.68	26.67	82.59	91.02
	S.D.	1.35	0.18	0.14	0.24	0.02

In each case, the Elongation decreased as we increase the percentage of OFA in the composite. This is due to reason that by addition of filler, composite becomes more brittle and stiff. So, as we increase the OFA concentration, the plasticity of the material decreased and it breaks soon. Results shows that a decreases in elongation from 20.68%-25.31% is observed by only 1% addition and 26.67%-34.83% is observed by 2% addition of filler. At higher loading, a large decrement in elongation is observed i.e 79.05%-89.39% by 5% loading and 89.66%-92.52% by 10% loading. The effect of OFA loading is described more efficiently by Figure 6.2.1(a-d). Figure 6.2.1 (a) and (b) shows the result of as-received and acid-functionalized OFA loading without PE-g-MA compatiblizer respectively while the figure 6. 2.1 (c) and (d) shows the result of as-received and acid-functionalized OFA loading with PE-g-MA compatiblizer respectively.

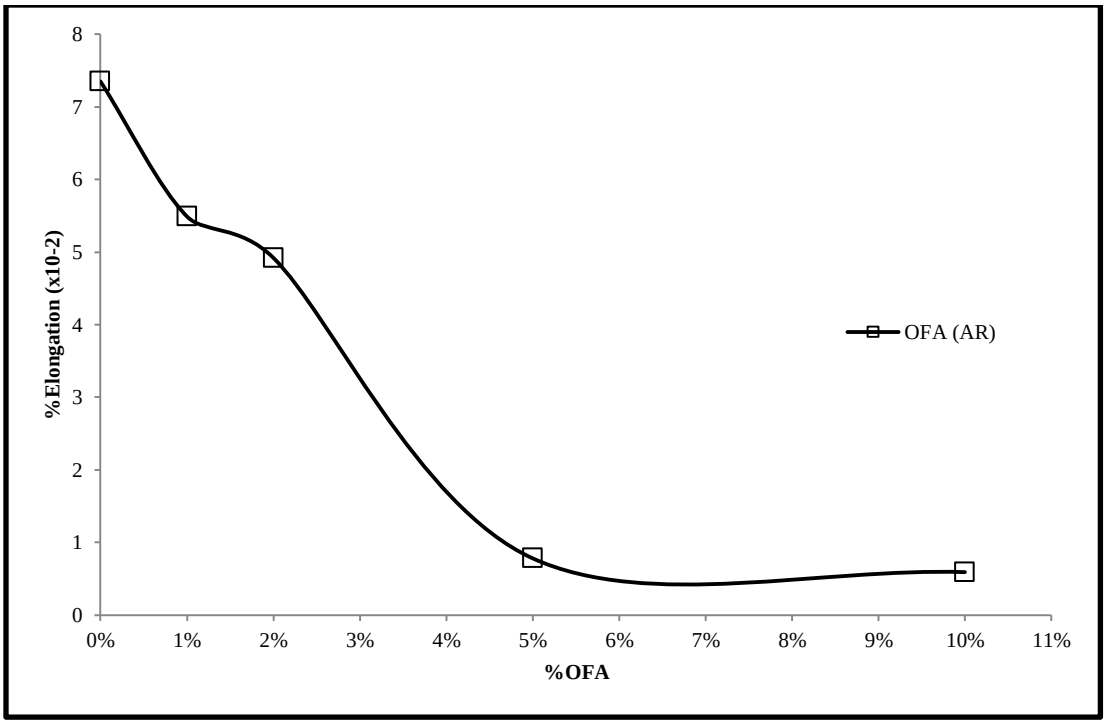

Figure 6.2.1(a): Effect of OFA Loading on Elongation

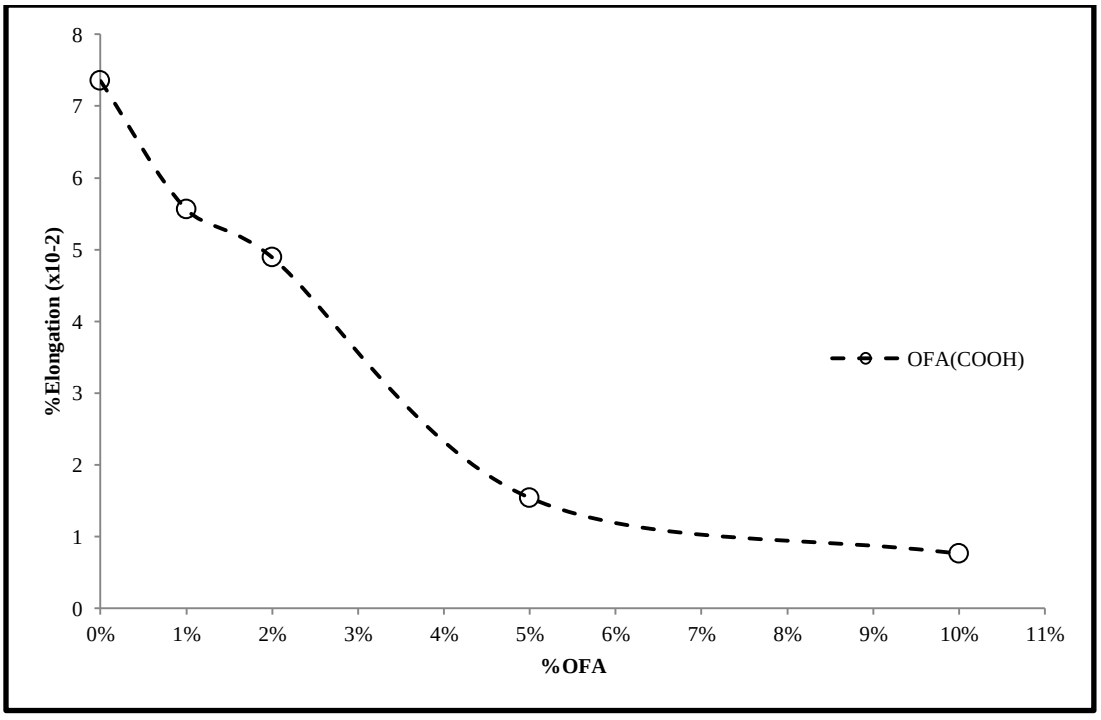

Figure 6.2.1(b): Effect of COOH-OFA Loading on Elongation

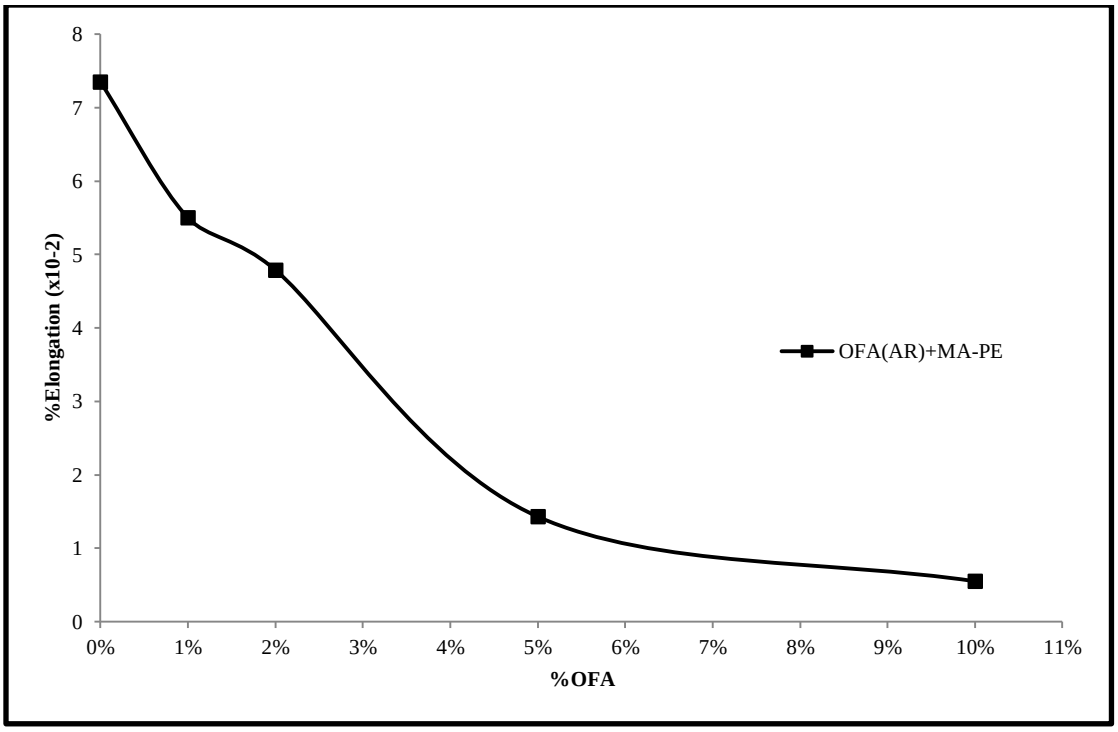

Figure 6.2.1(c): Effect of OFA Loading with 2% PE-g-MA on Elongation

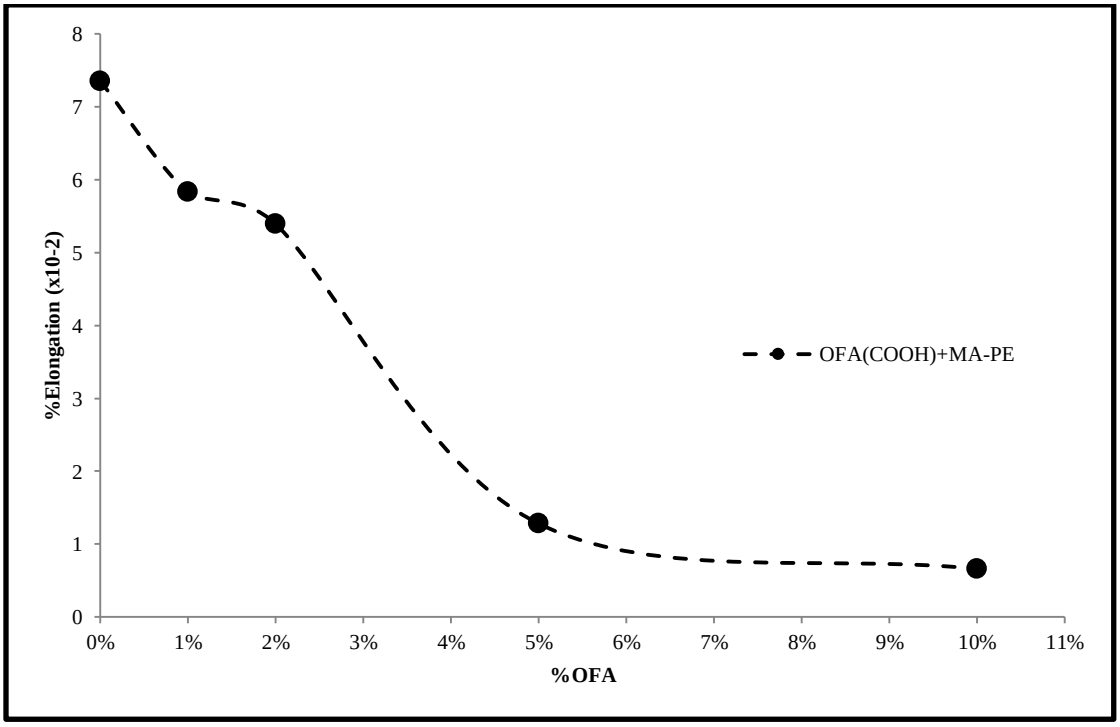

Figure 6.2.1(d): Effect of COOH-OFA Loading with 2% PE-g-MA on Elongation

It is observed by each figure that at initial loading, the decrease in elongation is very small as compared to high loading. At 5% OFA loading, the elongation reduced to more than 80% which is huge effect. It shows that OFA is dispersed into the polymer matrix, reduce its plastic behavior and enhanced the brittleness. The difference between 5-10% loading is not very much as compare to 2-5% due to two possible reasons. First is that, the optimum condition of dispersion is achieved at 5% loading and secondly, the decrease in elongation is reached to such a high value that no more big decrement is possible. It is observed the highest standard deviation is obtained in case of pure LDPE because it is most amorphous material as compare to composite. As we introduce the OFA filler, the crystallinity of the material increased and system becomes more organized and deviation in results decreased.

6.2.2: Effect of OFA Functionalization on Elongation to Break

Effect of OFA functionalization with and without PE-g-MA compatiblizer on Elongation to break of composites is shown in figure 6.2.2 (a-b). Figure 6.2.2(a) shows the effect of functionalization without PE-g-MA compatiblizer. It shows that at lower loading i.e. 1 and 2 wt%, functionalized fly ash shows no improvement as compare to as-received fly ash and gives the same decrement. At 5% filler loading, the elongation to break is a little increased by functionalization as compare to unmodified fly ash. At 10% loading, improvement is observed but less as compare to 5% loading. This is because of enrichment of filler particles into the matrix. As the compatiblizer added to the system as shown in figure 6.2.2(b), it effects the functionalization more at lower concentration so better improvement is achieved at low filler loading with compatiblizer. At higher loading, both types of fillers give the same effect with compatiblizer.

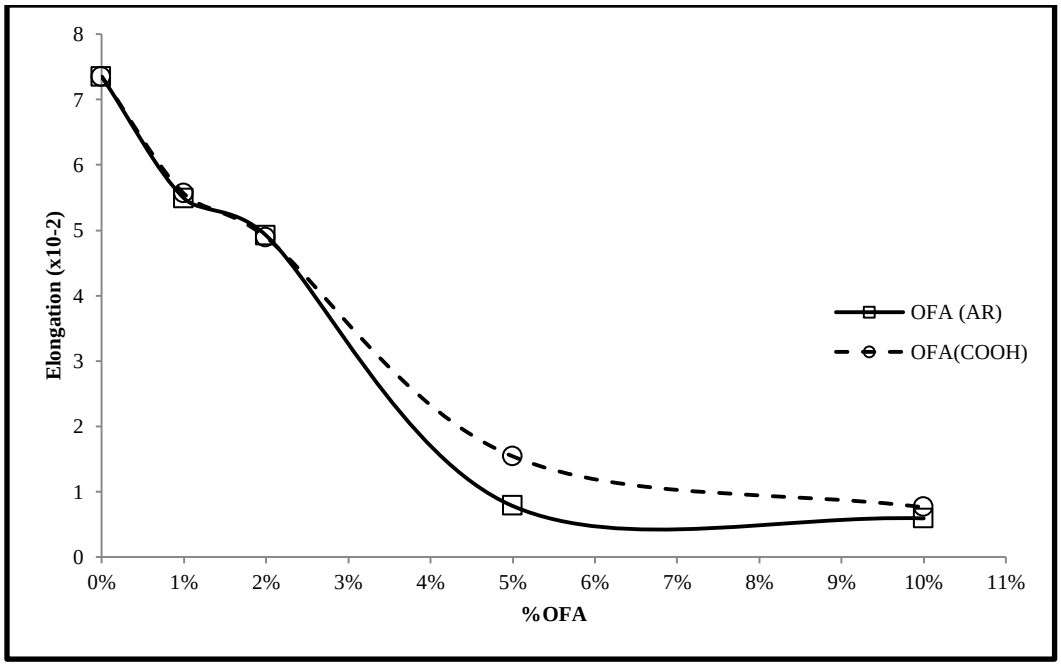

Figure 6.2.2(a): Effect of OFA functionalization without PE-g-MA on Elongation

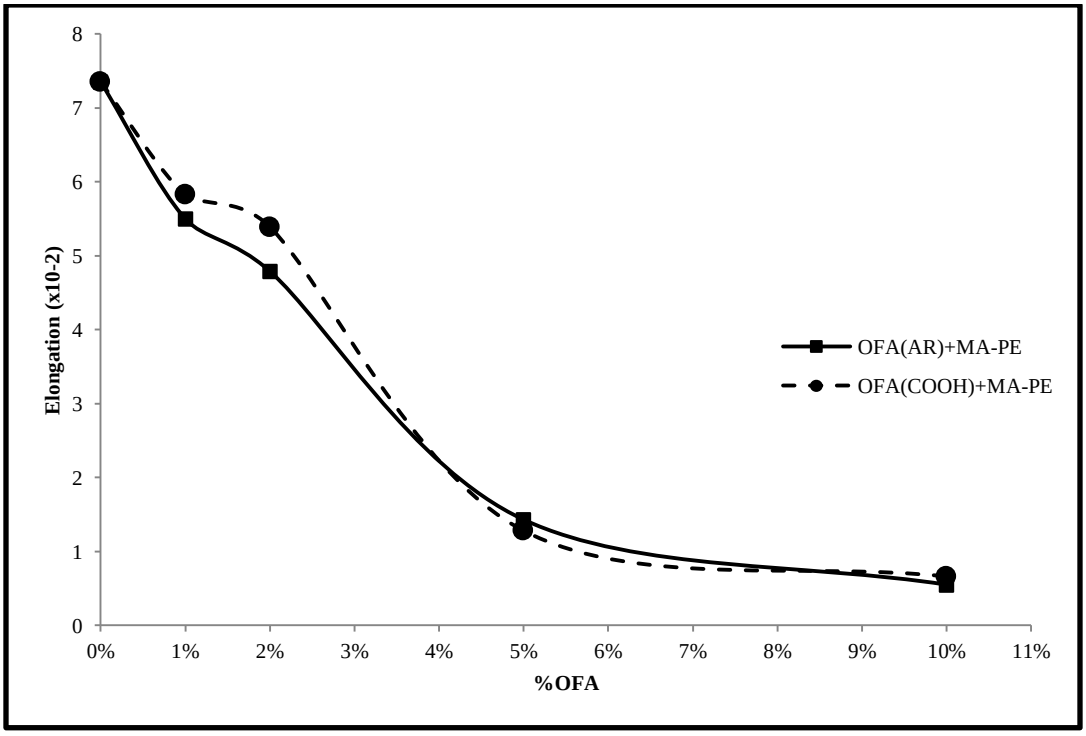

Figure 6.2.2(b): Effect of OFA functionalization with 2% PE-g-MA on Elongation

6.2.3: Effect of PE-g-MA Compatiblizer on Elongation to Break

Effect of Polyethylene-grafted-Maleic Anhydride with and without OFA surface modification on Elongation to break of composites is shown in figure 6.2.3 (a-b). Figure 6.2.3(a) shows the effect of PE-g-MA compatiblizer with unmodified fly ash. It is clearly observed that no improvement is achieved in elongation by the addition of compatiblizer except at the 5% filler concentration and hence gives the optimum condition at 5% loading. Figure 6.2.3(b) shows the effect of PE-g-MA with modified fly ash. It is observed that at lower loading i.e. 1 and 2 wt%, a very little improvement is achieved but at higher concentration, no enhancement is observed by PE-g-MA. So we can conclude the compatiblizer doesn't affect more on elongation and little difference is due to affect on dispersion by compatiblizer.

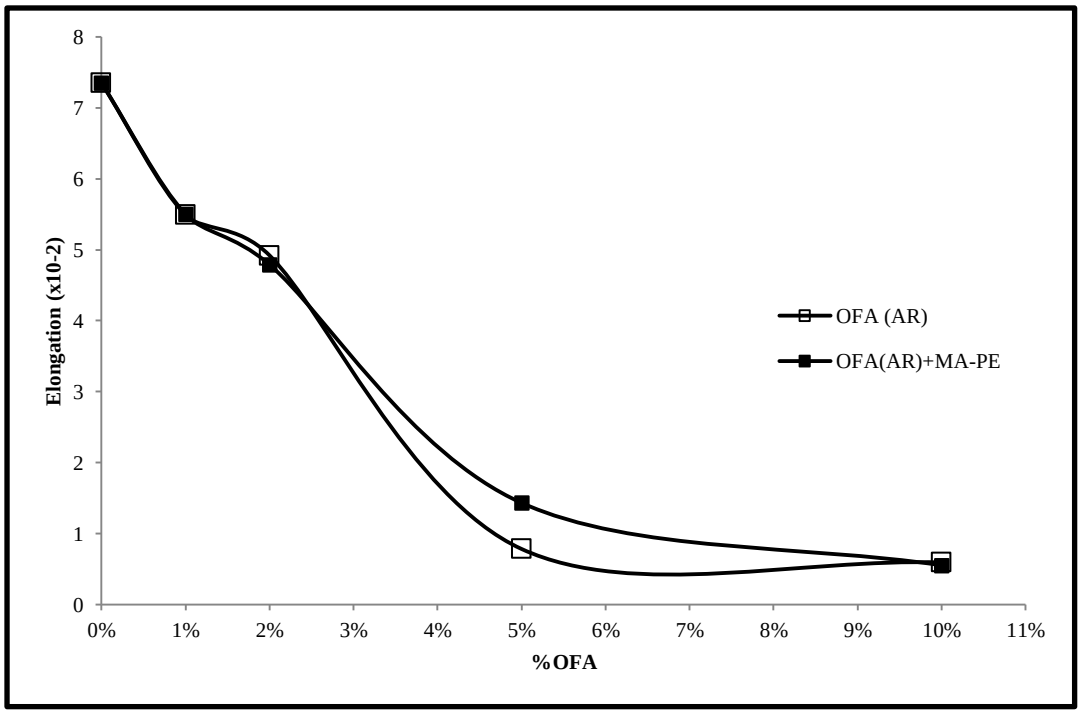

Figure 6.2.3(a): Effect of Compatiblizer with OFA Loading on Elongation

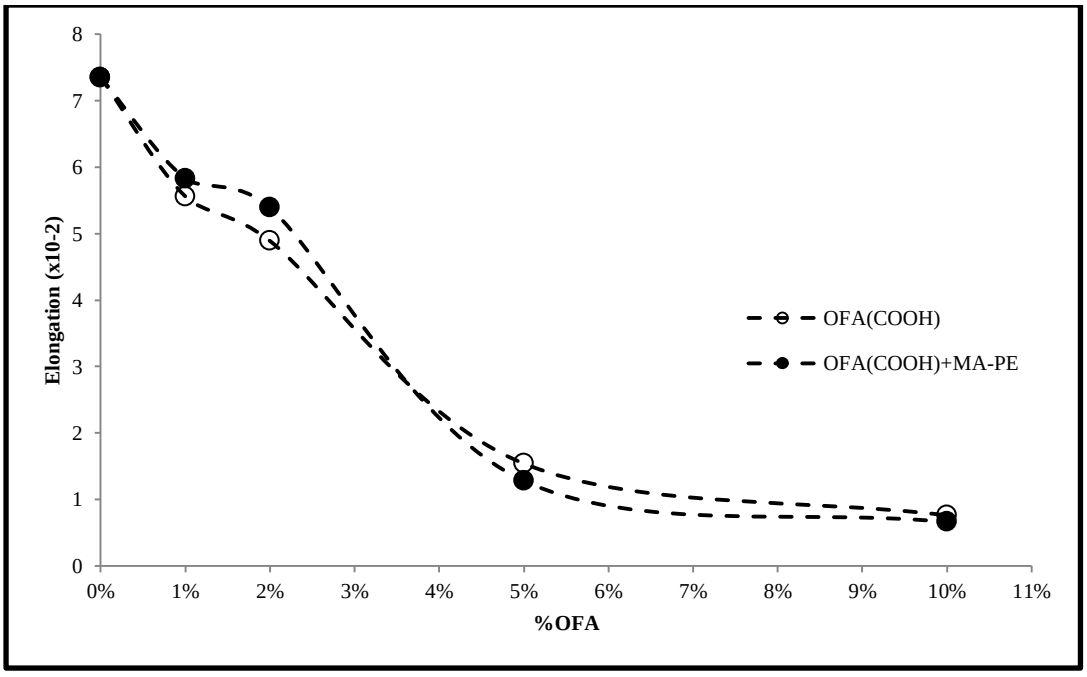

Figure 6.2.4(b): Effect of Compatiblizer with COOH-OFA Loading on Elongation

6.3: Effect of OFA on Toughness

6.3.1: Effect of OFA Loading on Toughness

Toughness can be defined as the resistance to fracture of a material when stressed. Table 6.3 shows the results of Toughness for 1, 2, 5 and 10 wt% OFA loading. Also the %decrease in values and standard deviation are calculated and reported in the table. Table shows that percent toughness is linearly relates to the loading of OFA. In each case, the toughness decreased as we increase the OFA loading in the composite.

Table 6.3: Effect of OFA loading on Toughness

Composite		OFA Loading				
		0%	1%	2%	5%	10%
LDPE/OFA	Value (MPa)	75.33	52.19	47.84	6.32	5.02
	% Decrease	0.00	30.72	36.45	91.61	93.34
	S.D.	14.23	8.34	4.27	2.77	0.24
LDPE/COOH-OFA	Value (MPa)	75.33	52.63	45.01	13.38	7.79
	% Decrease	0.00	30.13	40.25	82.24	89.66
	S.D.	14.23	2.78	11.23	4.82	0.05
LDPE/OFA + PE-g-MA	Value (MPa)	75.33	53.73	46.90	14.06	5.46
	% Decrease	0.00	28.67	37.74	81.34	92.75
	S.D.	14.23	2.30	4.79	4.66	0.94
LDPE/COOH-OFA + PE-g-MA	Value (MPa)	75.33	62.14	58.53	13.52	6.88
	% Decrease	0.00	17.51	22.30	82.05	90.87
	S.D.	14.23	2.39	1.78	2.75	0.27

As the toughness is the Amount of energy per volume that a material can absorb before rupturing, so it depends on the elongation of material. It can be calculate by evaluating the area under the curve of stress-strain plot. As we have seen in the table 6.2 that by increasing the OFA loading in the filler, elongation to break decreases, so the toughness is also decreases. At lower loading, 17.51-30.72% and 22.30-40.25% decrement is observed by 1 and 2 wt% filler loading. While at higher loading, 81.34-91.61% and 89.66-93.34% decrement is found by 5 and 10 wt% OFA loading. The effect

may describe more efficiently by Figure 6.3.1 (a-d). Figure 6.3.1 (a) and (b) shows the result of as-received and acid-functionalized OFA loading without PE-g-MA compatiblizer respectively while the figure 6.3.1 (c) and (d) shows the result of as-received and acid-functionalized OFA loading with PE-g-MA compatiblizer respectively.

It is observed by each figure that at initial loading, the decrease in toughness is very less as compare to high loading. At 5% OFA loading, the toughness reduced to more than 80% which is huge effect. It shows that OFA is dispersed into the polymer matrix, strain hardening and hence the plasticity and enhanced the brittleness. The difference between 5-10% loading is not very much as compare to 2-5% due to two possible reasons. First is that, the optimum condition of dispersion is achieved at 5% loading and secondly, the decrease is toughness is reached to such a high value that no more big decrement is possible. The same phenomenon is observed in case of elongation to break. It is observed the highest standard deviation is obtained in case of pure LDPE because it is most amorphous material as compare to composite. As we introduce the OFA filler, the crystallinity of the material increased and system becomes more organized and deviation in results decreased.

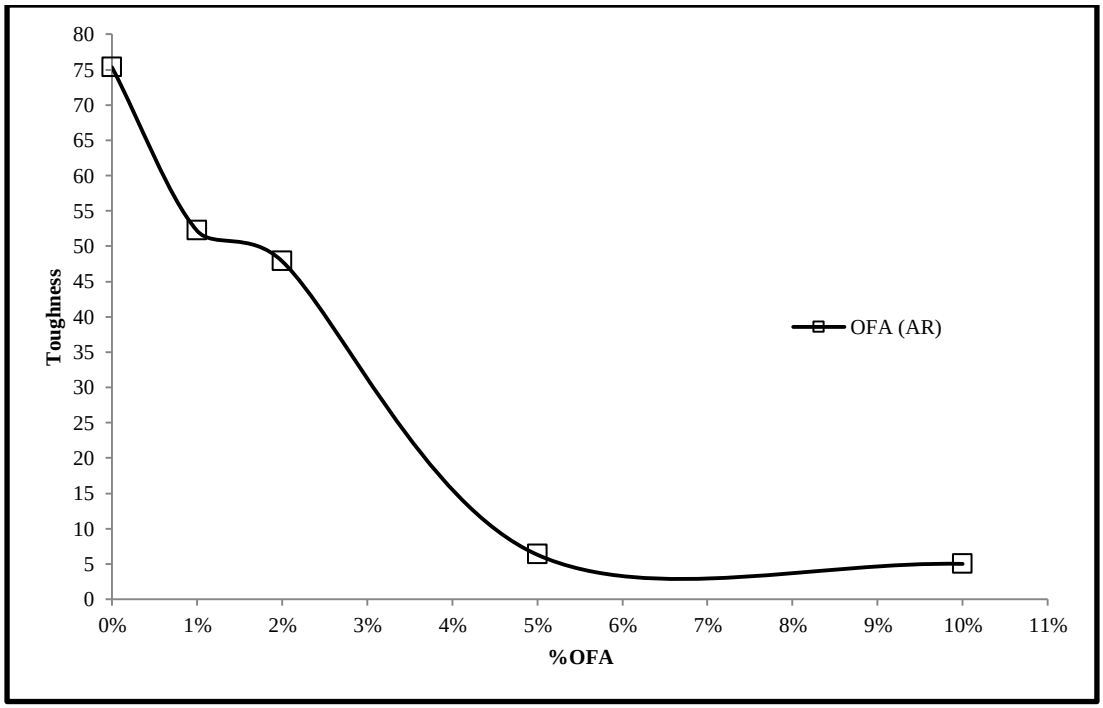

Figure 6.3.1(a): Effect of OFA Loading on Toughness

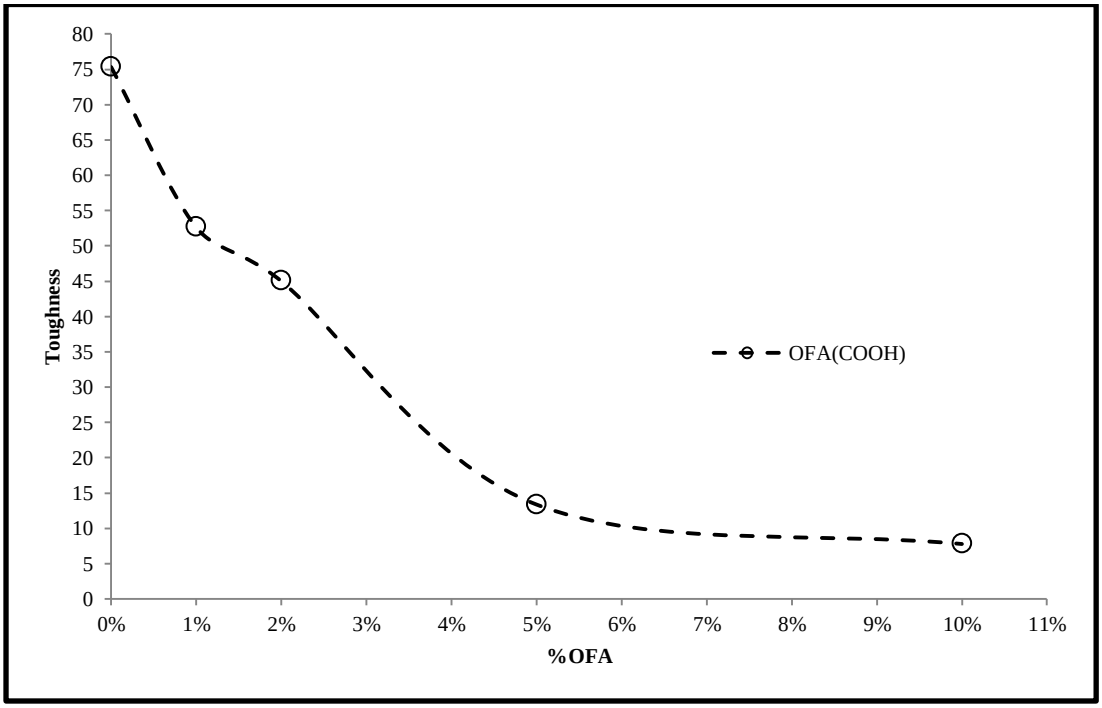

Figure 6.3.1(b): Effect of COOH-OFA Loading on Toughness

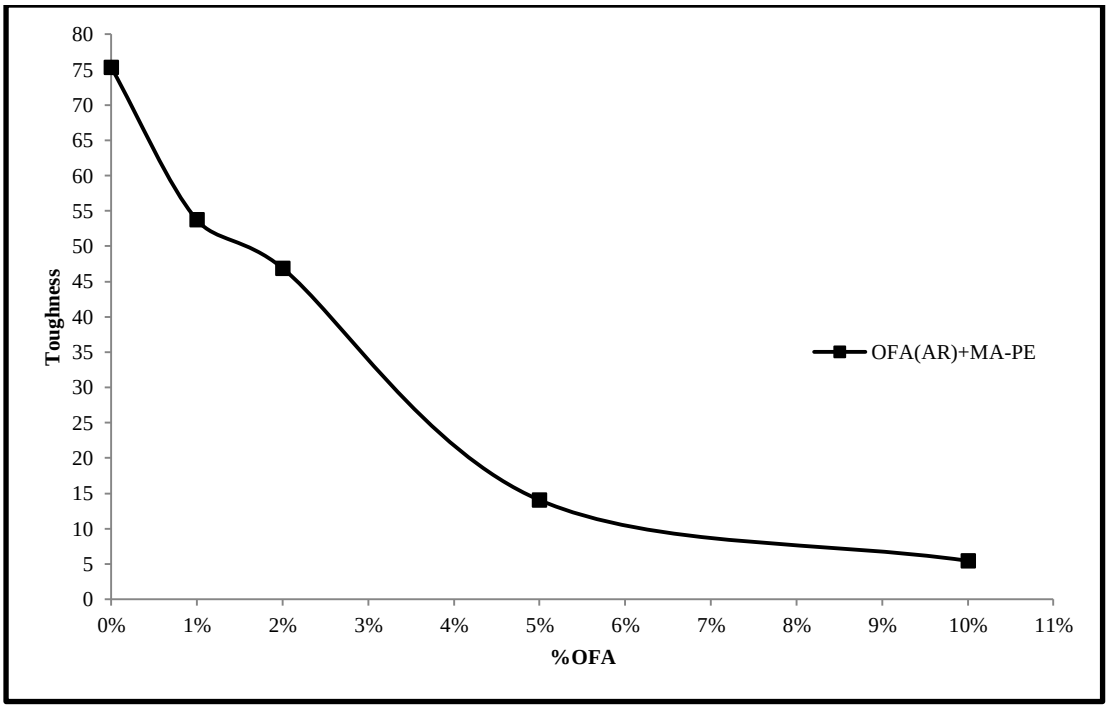

Figure 6.3.1(c): Effect of OFA Loading with 2% PE-g-MA on Toughness

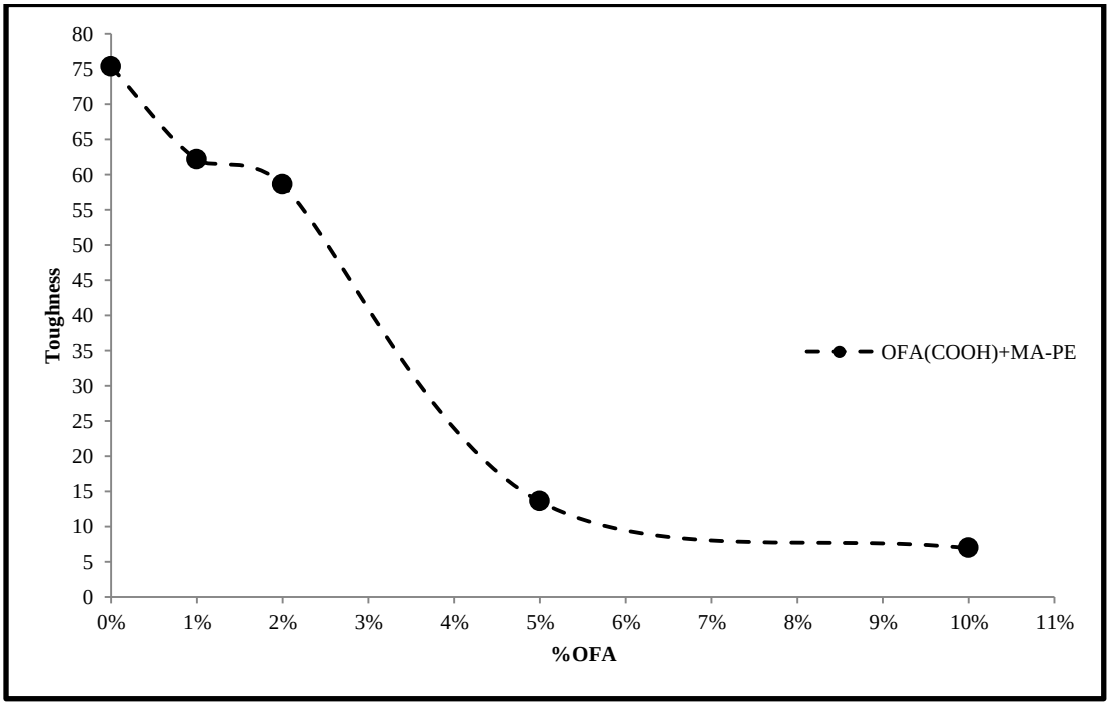

Figure 6.3.1(d): Effect of COOH-OFA Loading with 2% PE-g-MA on Toughness

6.3.2: Effect of OFA Functionalization on Toughness

Effect of OFA functionalization with and without PE-g-MA compatiblizer on toughness of composites is shown in figure 6.3.2 (a-b). Figure 6.3.2 (a) shows the effect of functionalization without PE-g-MA compatiblizer. It shows that at lower loading i.e. 1 and 2 wt%, functionalized fly ash shows no improvement as compare to as-received fly ash and gives the almost same decrement. At 5% filler loading, the toughness is increased by functionalization. At 10% loading, improvement is observed but less as compare to 5% loading. This is because of enrichment of filler particles into the matrix. As the compatiblizer added to the system as shown in figure 6.3.2(b), it effects the functionalization more at lower concentration so better improvement is achieved at low filler loading with compatiblizer. At higher loading, both type of fillers gives the same extent of decrement with compatiblizer.

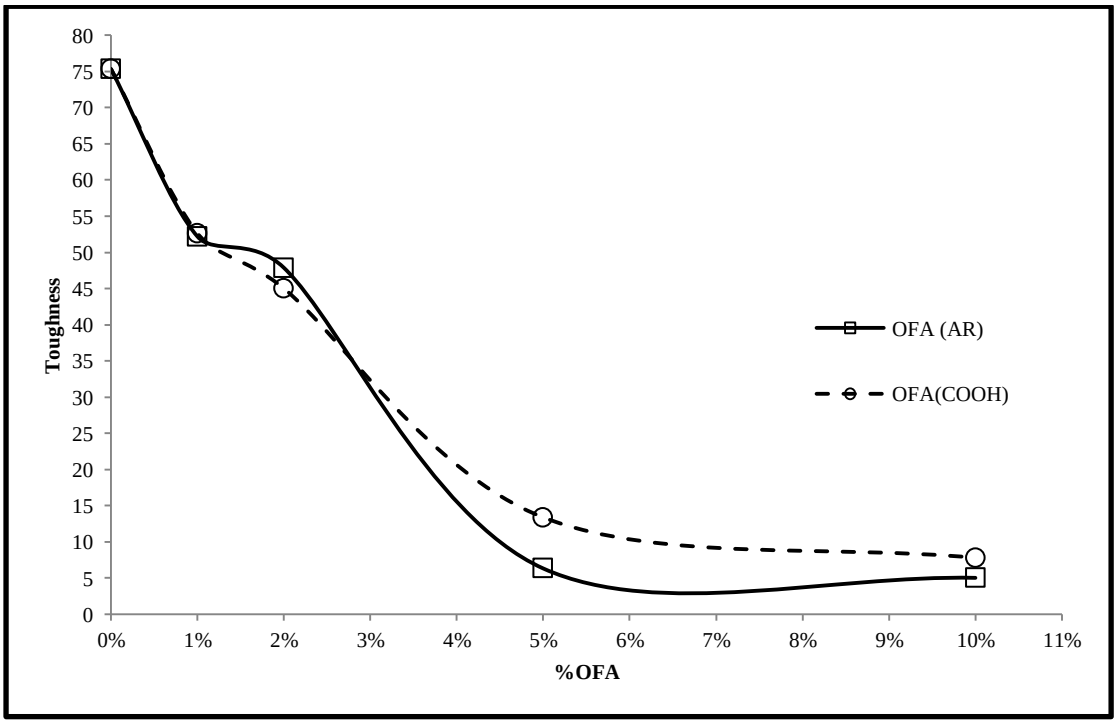

Figure 6.3.2(a): Effect of OFA functionalization without PE-g-MA on Toughness

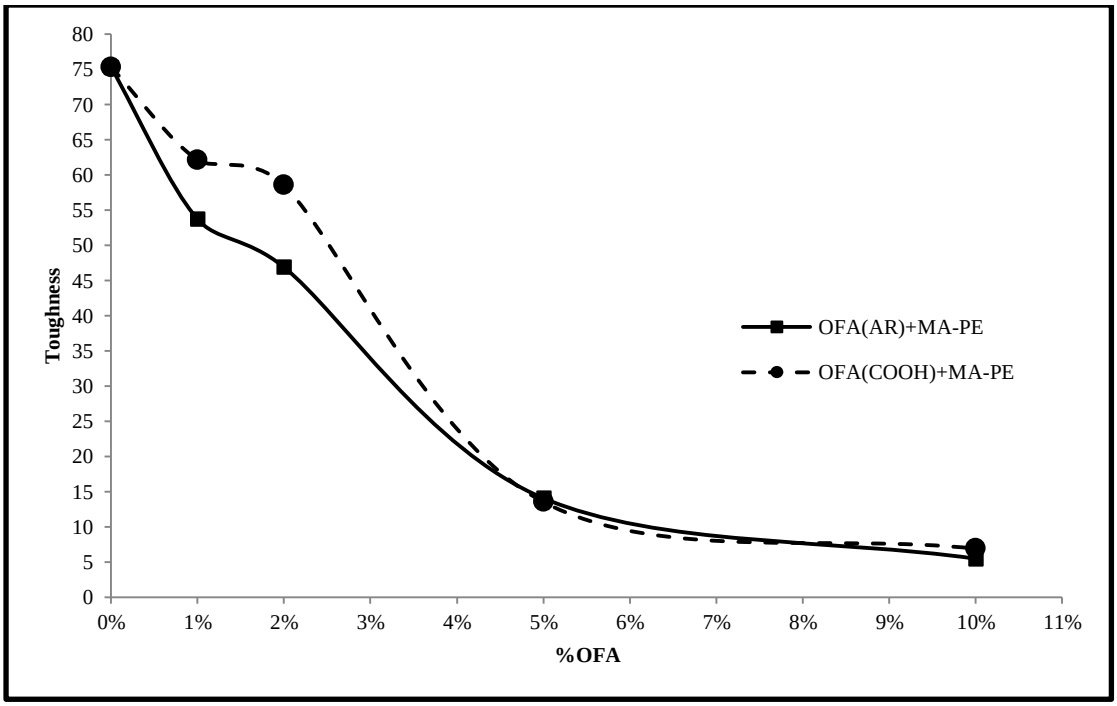

Figure 6.3.2(b): Effect of OFA functionalization with PE-g-MA on Toughness

6.3.3: Effect of PE-g-MA Compatiblizer on Toughness

Effect of Polyethylene-grafted-Maleic Anhydride with and without OFA surface modification on toughness of composites is shown in figure 6.3.3 (a-b). Figure 6.3.3(a) shows the effect of PE-g-MA compatiblizer with unmodified fly ash. It is clearly observed that at no improvement is achieved in toughness except at the 5% filler concentration and hence gives the optimum condition at 5% loading. Figure 6.3.3(b) shows the effect of PE-g-MA with modified fly ash. It is observed that at lower loading i.e. 1 and 2 wt%, a very small improvement is achieved but at higher concentration, no enhancement is observed. It is the same effect as we observed in elongation in section 6.2.3. So we can conclude the compatiblizer doesn't affect more on toughness and little difference is due to affect on dispersion by compatiblizer.

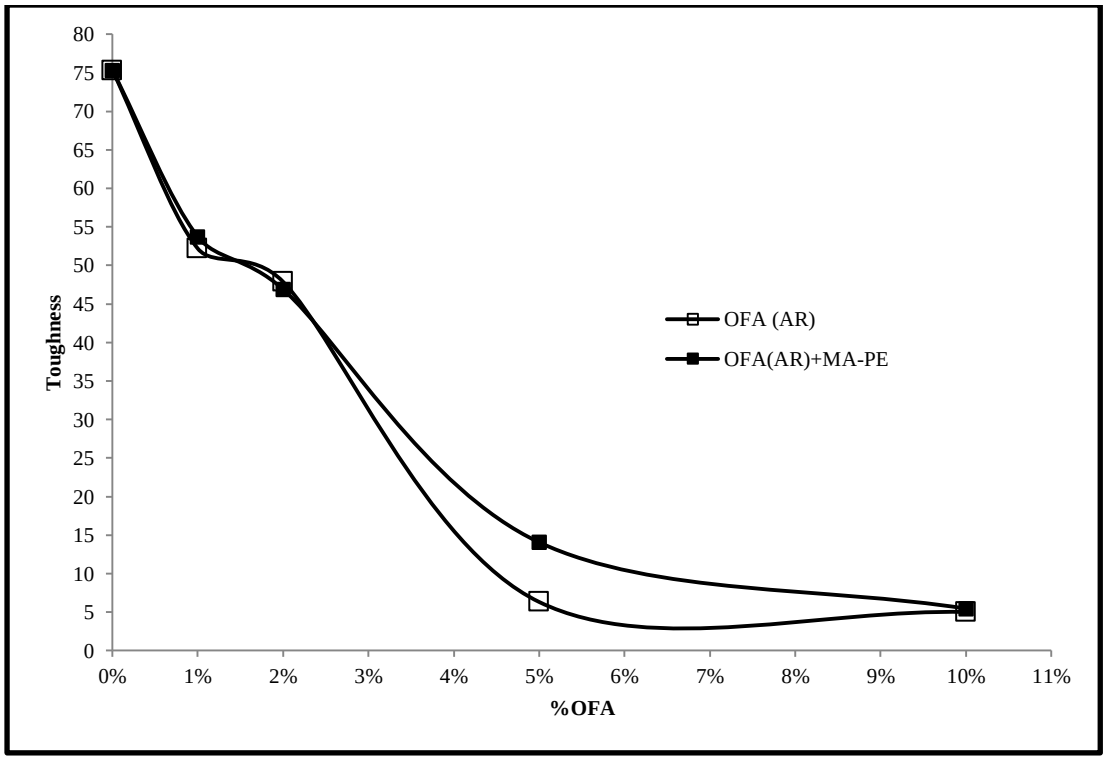

Figure 6.3.3(a): Effect of Compatiblizer with OFA Loading on Toughness

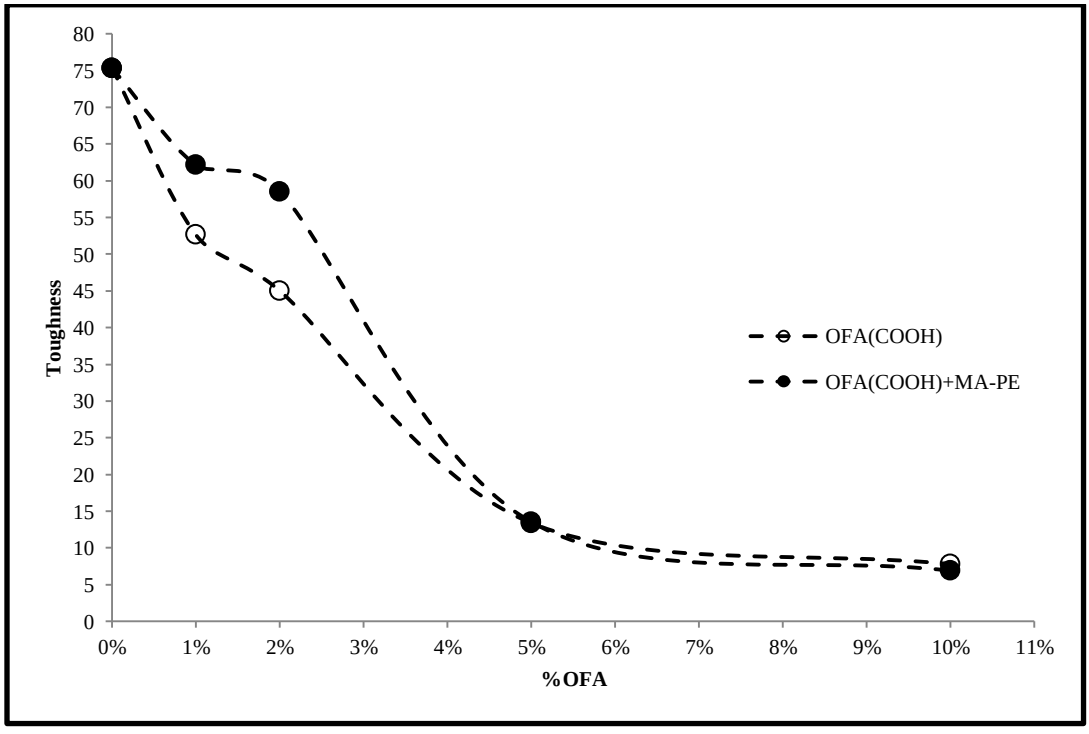

Figure 6.3.3(b): Effect of Compatiblizer with COOH-OFA Loading on Toughness

6.4: Effect of OFA on Yield Strength

6.4.1: Effect of OFA Loading on Yield Strength

The Yield strength may be defined as the stress at which a material begins to deform plastically and deform permanently. Before this point the material deforms elastically and regains its original shape when the applied stress is removed. Table 6.4 shows the results of Yield strength for 1, 2, 5 and 10 wt% OFA loading. Also the %increase in values and standard deviations are calculated and reported in the table.

Table 6.4: Effect of OFA loading on Yield Strength

Composite	OFA Loading					
		0%	**1%**	**2%**	**5%**	**10%**
LDPE/OFA	Value (MPa)	9.21	9.37	9.37	10.02	10.49
	% Increase	0.00	1.74	1.74	8.79	13.90
	S.D.	0.62	0.74	0.59	0.07	0.03
LDPE/COOH-OFA	Value (MPa)	9.21	9.75	9.84	10.14	12.09
	% Increase	0.00	5.86	6.84	10.10	31.27
	S.D.	0.62	0.13	0.07	0.13	0.16
LDPE/OFA + PE-g-MA	Value (MPa)	9.21	10.11	10.77	11.43	12.13
	% Increase	0.00	9.77	16.94	24.10	31.70
	S.D.	0.62	0.42	0.08	0.07	0.06
LDPE/COOH-OFA + PE-g-MA	Value (MPa)	9.21	10.70	11.44	12.25	12.65

	% Increase	0.00	16.18	24.21	33.01	37.35
	S.D.	0.62	0.51	0.11	0.27	0.49

Table shows that Yield strength is linearly relates to the loading of OFA. In each case, the Yield strength increased as we increase the percentage of OFA in the composite. Results showed that about 1.74-16.18% increase in Yield strength achieved by only 1% addition of filler whereas 1.74-24.21% increment achieved by only 2% addition of filler. At higher loading, 8.79-33.01% increment achieved by 5% addition while 13.90-37.35% increment is observed at 10% filler loading. As the three specimens are used for each composite sample, standard deviation of three specimens' results is also reported. The effect of OFA loading is described more efficiently by Figure 6.4.1 (a-d). Figure 6.4.1 (a) and (b) shows the result of as-received and acid-functionalized OFA loading without PE-g-MA compatiblizer respectively. It is observed that at initial loading i.e. 1 and 2 wt%, the yield modulus is slightly increased but considerable improvement is achieved at higher loading i.e. 5 and 10 wt%. On the other hand, figure 6.4.1 (c) and (d) shows the result of as-received and acid-functionalized OFA loading with PE-g-MA compatiblizer respectively. These figures shows that good enhancement in Yield strength starts even at lower loading i.e. 1 and 2 wt% and it continuously increased as we increased the OFA concentration into the polymer matrix.

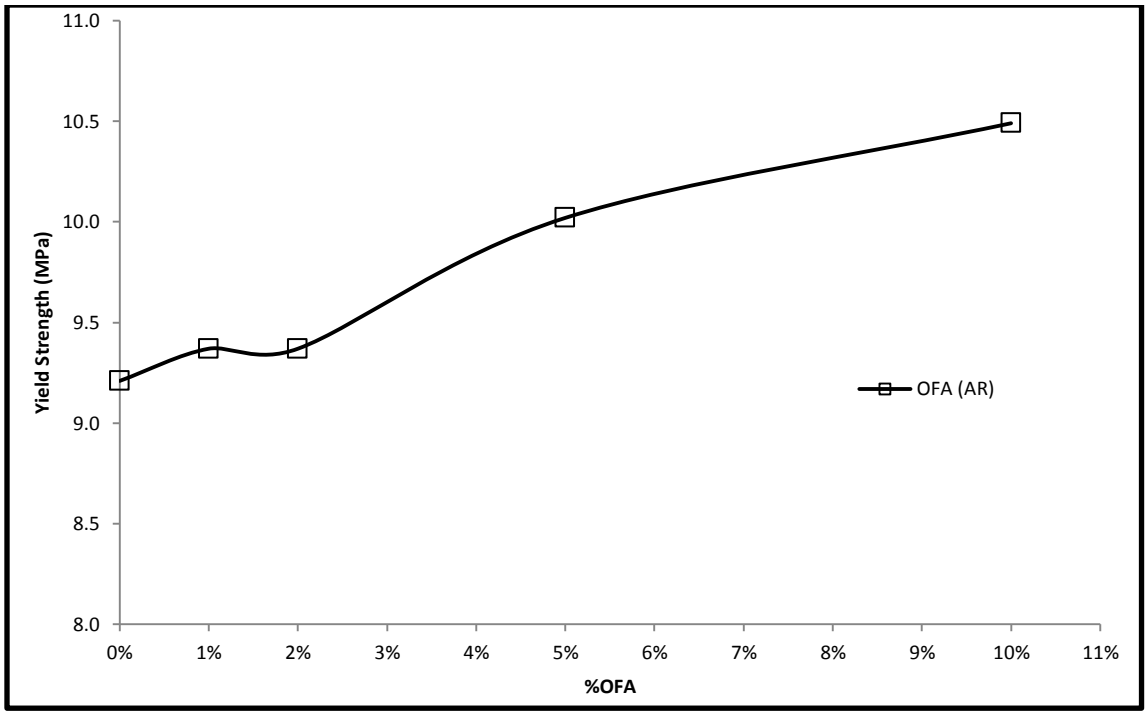

Figure 6.4.1(a): Effect of OFA Loading on Yield Strength

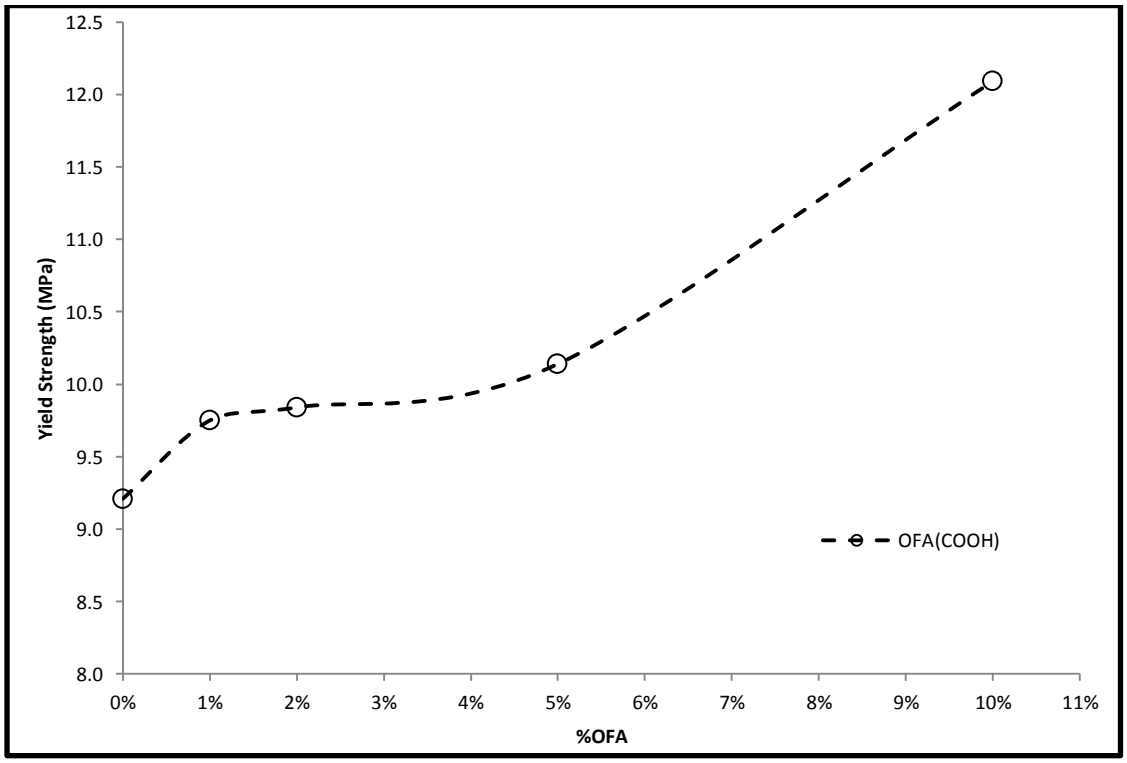

Figure 6.4.1(b): Effect of COOH-OFA Loading on Yield Strength

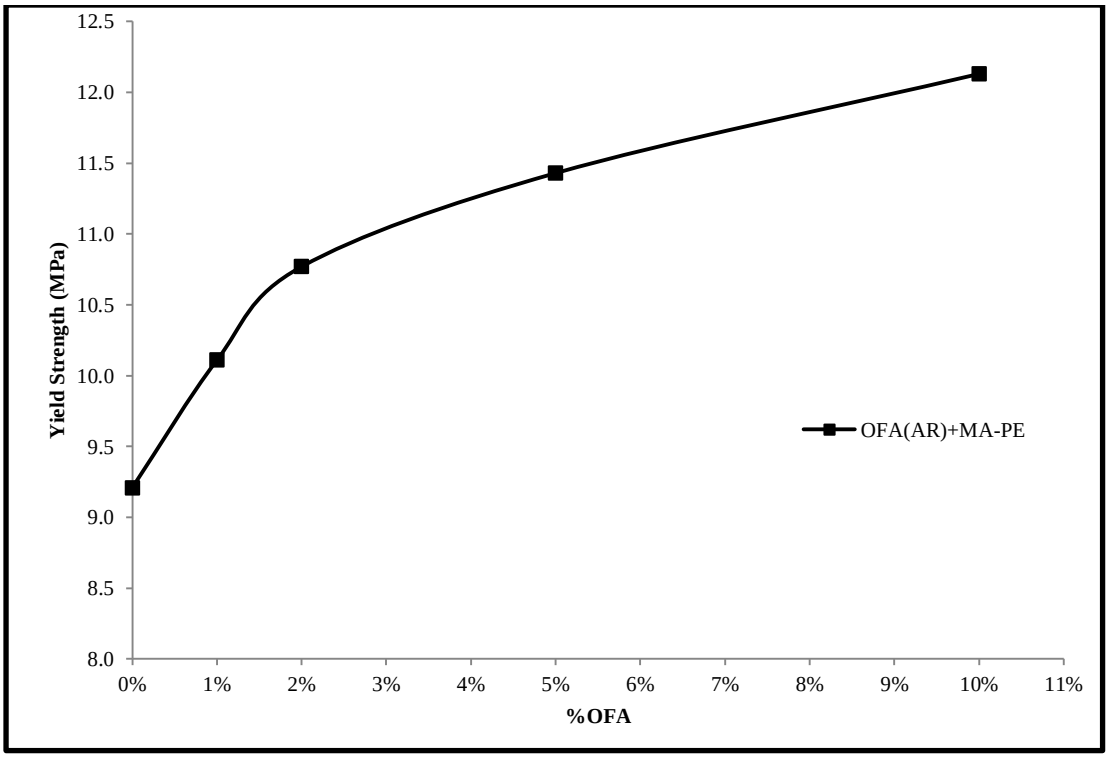

Figure 6.4.1(c): Effect of OFA Loading with 2% PE-g-MA on Yield Strength

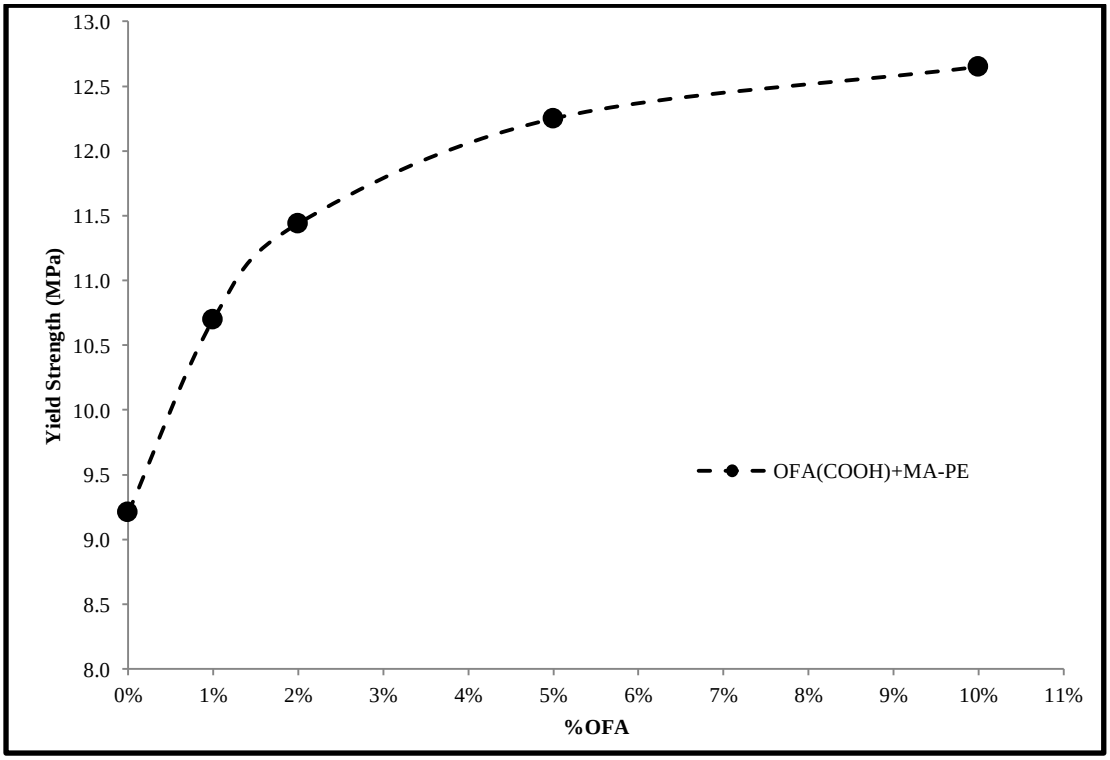

Figure 6.4.1(d): Effect of COOH-OFA Loading with 2% PE-g-MA on Yield Strength

6.4.2: Effect of OFA Functionalization on Yield Strength

Effect of OFA functionalization with and without PE-g-MA compatiblizer on Yield Strength of composites is shown in figure 6.4.2 (a-b). Figure 6.4.2(a) shows the effect of functionalization without PE-g-MA compatiblizer. It is observed that at lower loading i.e. 1 and 2 wt%, functionalized fly ash shows good improvement as compared to as-received fly ash. At 5% loading, a very small increment is observed whereas at higher 10 wt%, loading, remarkable improvement is achieved. It shows that functionalization creates a good interlinking between filler and polymer matrix and make it more hard enhanced its elastic properties.

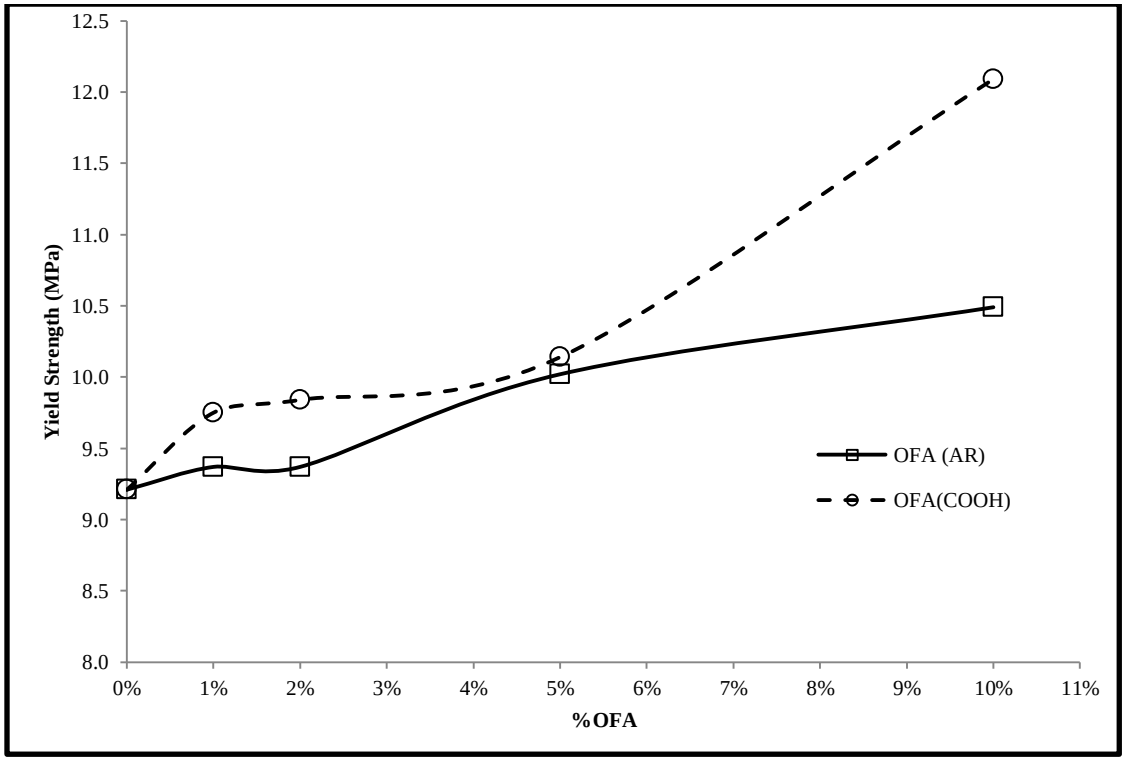

Figure 6.4.2(a): Effect of OFA functionalization without PE-g-MA on Yield Strength

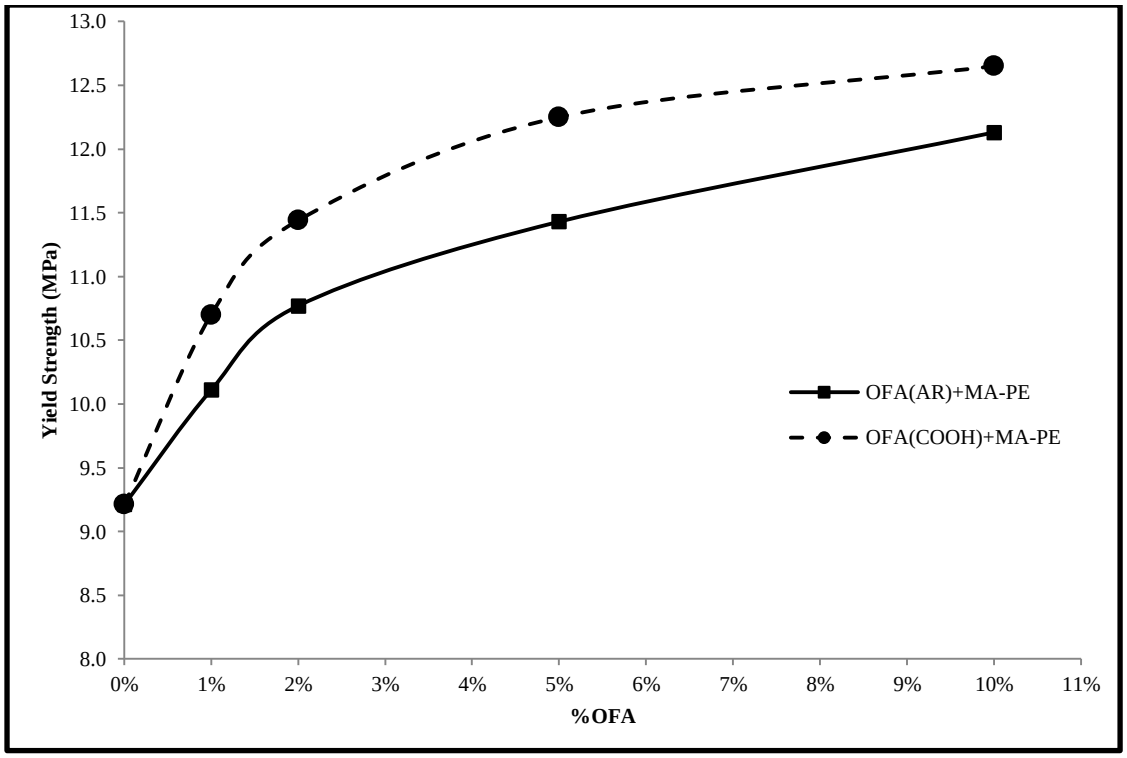

Figure 6.4.2(b): Effect of OFA functionalization with PE-g-MA on Yield Strength

Figure 6.4.2(b) shows the effect of functionalization in the presence of PE-g-MA. It is observed that at each loading, modified fly ash gives the better results as compare to un-modified fly ash. The increment by compatiblizer in case of unmodified fly ash is more as compare to modified fly ash at higher loading. It means that functionalization affects more on elastic strength and gets the optimized conditions.

6.4.3: Effect of PE-g-MA Compatiblizer on Yield Strength

Effect of Polyethylene-grafted-Maleic Anhydride with and without OFA surface modification on Yield Strength of composites is shown in figure 6.4.3 (a-b). Figure 6.4.3(a) shows the effect of PE-g-MA compatiblizer with unmodified fly ash. It is clearly shown that at each loading, a considerable increase in Yield Strength of composites achieved by the addition of PE-g-MA. It shows that compatiblizer created a good

interlink between filler and polymer matrix. Figure 6.4.3(b) shows the effect of PE-g-MA with modified fly ash. Similar to previous result, improvement in Yield Strength is observed by addition of PE-g-MA. The effect of compatiblizer is more clear at 1,2 and 5% loading but the difference is decreased at 10% OFA loading because the functionalization already enhanced the elastic strength by creating good interlinking between polymer matrix and filler and improvement reached to it optimized condition. This condition is not appeared in case of unmodified OFA because there was no functional group attached with the surface of fillers.

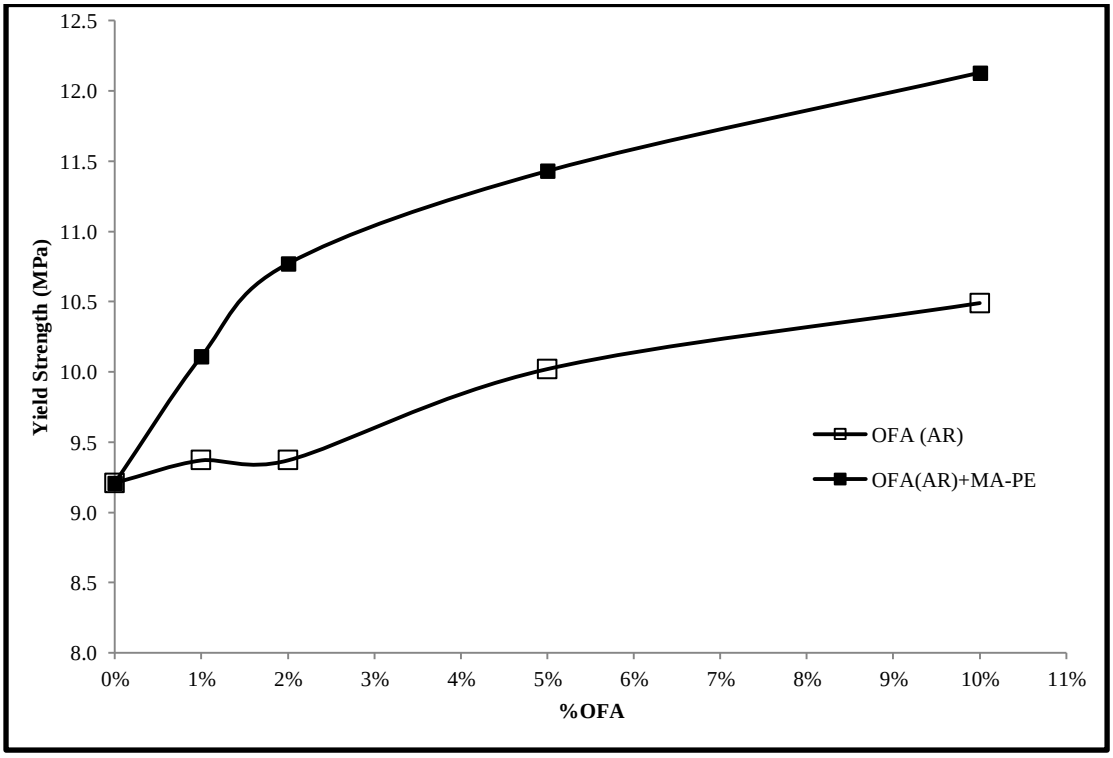

Figure 6.4.3(a): Effect of Compatiblizer with OFA Loading on Yield Strength

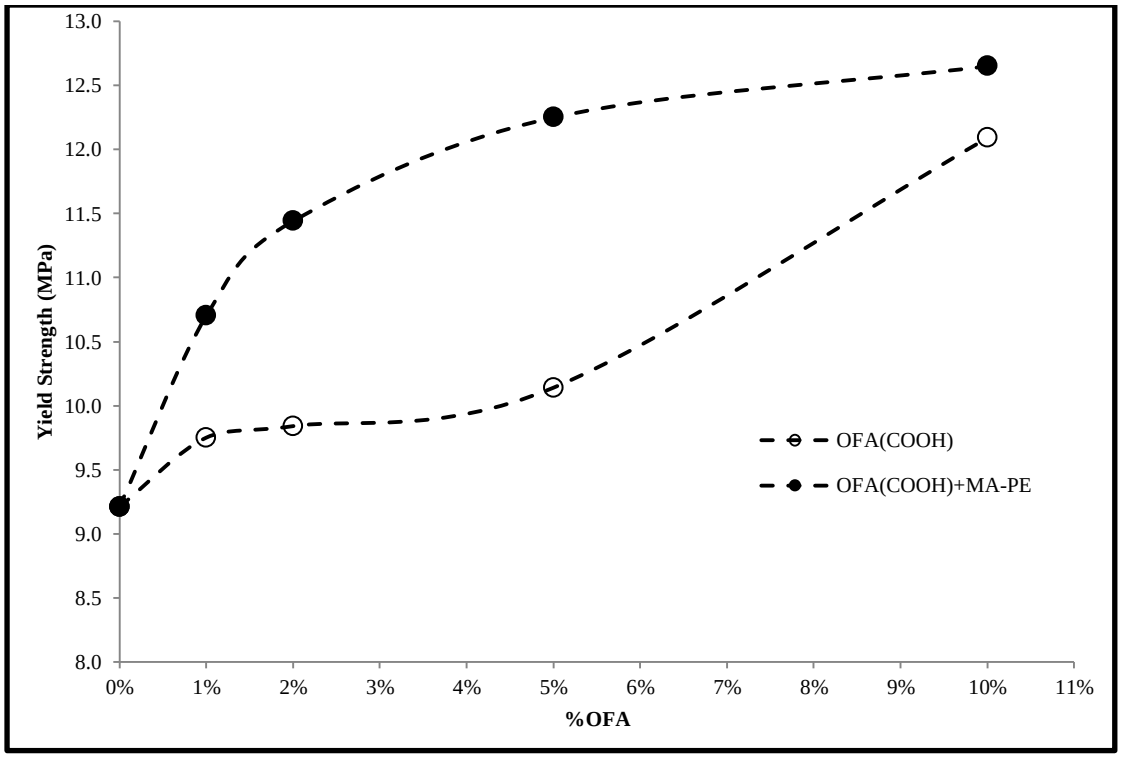

Figure 6.4.3(b): Effect of Compatiblizer with COOH-OFA Loading on Yield Strength

6.5: Effect of OFA on Ultimate Strength

6.5.1: Effect of OFA Loading on Ultimate Strength

The Ultimate strength may be defined as the maximum stress a material can withstand when subjected to tension, compression or shearing. It can be evaluated by maximum stress on stress-strain plot. Table 6.5 shows the results of Ultimate Strength for 1, 2, 5 and 10 wt% OFA loading. Also the %decrease in values and standard deviation are calculated and reported in the table. Table shows that Ultimate strength doesn't relate linearly to the loading of OFA. In each case, it decreased initially and then increased or became straight at higher loading.

Table 6.5: Effect of OFA loading on Ultimate Strength

Composite		OFA Loading				
		0%	1%	2%	5%	10%
LDPE/OFA	Value (MPa)	13.87	11.68	10.98	10.17	10.73
	% Decrease	0.00	15.79	20.84	26.68	22.64
	S.D.	1.69	1.05	0.35	0.07	0.03
LDPE/COOH-OFA	Value (MPa)	13.87	11.61	10.83	10.21	12.28
	% Decrease	0.00	16.29	21.92	26.39	11.46
	S.D.	1.69	0.23	0.91	0.12	0.20
LDPE/OFA + PE-g-MA	Value (MPa)	13.87	11.81	11.32	11.51	12.45
	% Decrease	0.00	14.85	18.39	17.02	10.24
	S.D.	1.69	0.49	0.50	0.13	0.11
LDPE/COOH-OFA + PE-g-MA	Value (MPa)	13.87	12.80	12.89	12.40	12.85
	% Decrease	0.00	7.71	7.07	10.60	7.35
	S.D.	1.69	0.64	0.10	0.28	0.37

We have observed that in case of more amorphous structure, the material shows the strain hardening in second phase of stress-strain graph and the maximum stress is obtain in this plastic portion. Whereas, when the material becomes more crystalline or brittle, the strain hardening starts decreasing and maximum stress obtain at yield strength point or in elastic region. As we know that pure LDPE is more amorphous material as compare to

composite so it shows maximum strain hardening and hence we obtain highest value of Ultimate strength. So by low filler loading, maximum stress value decreased and moves towards elastic portion due to diminishing of strain hardening. At higher loading, it increased due to hardening effect of filler in elastic portion. The effect may describe more efficiently by Figure 6.5.1 (a-d). Figure 6.5.1 (a) and (b) shows the result of as-received and acid-functionalized OFA loading without PE-g-MA compatiblizer respectively while the figure 6.5.1 (c) and (d) shows the result of as-received and acid-functionalized OFA loading with PE-g-MA compatiblizer respectively.

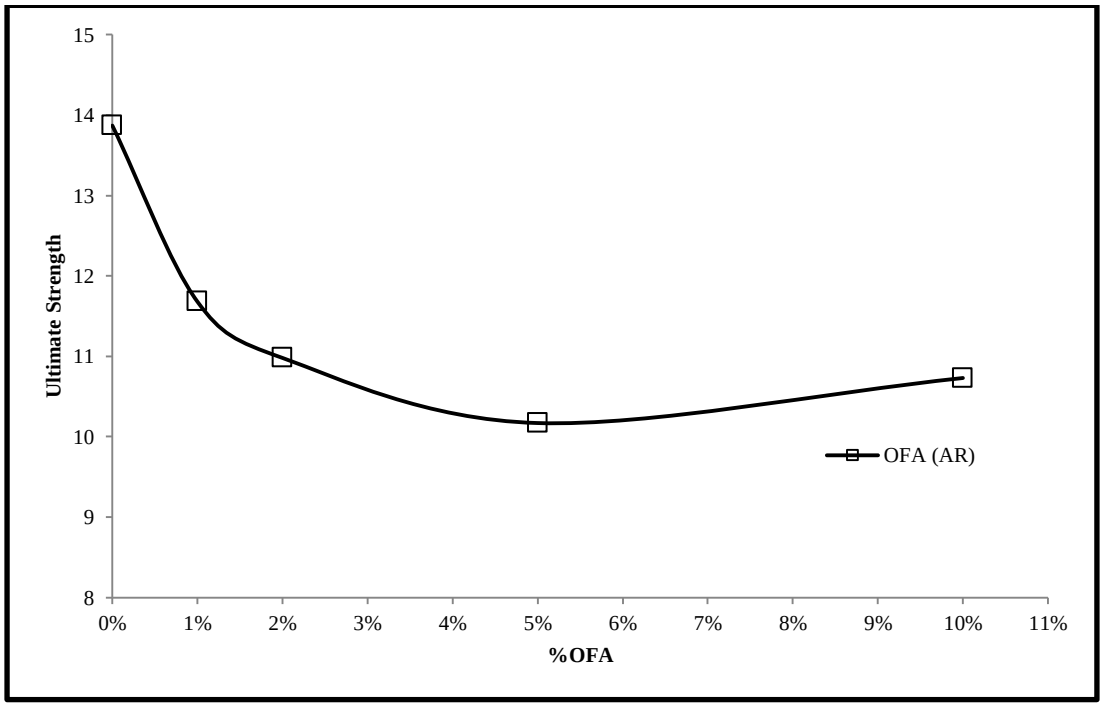

Figure 6.5.1(a): Effect of OFA Loading on Ultimate Strength

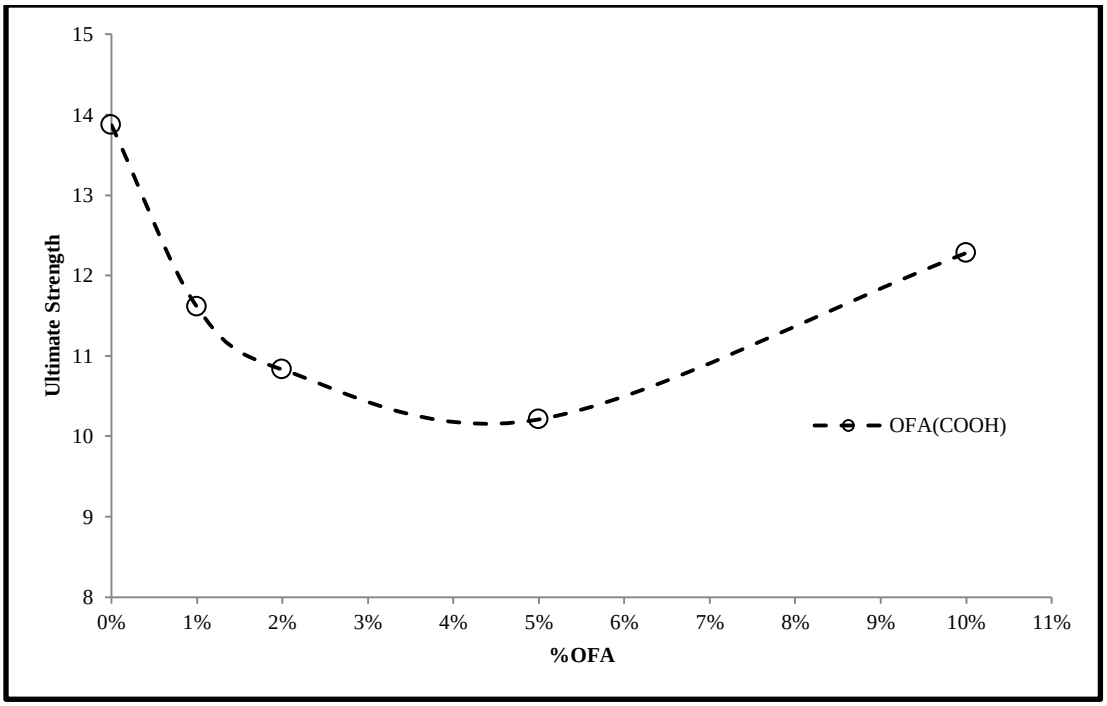

Figure 6.5.1(b): Effect of COOH-OFA Loading on Ultimate Strength

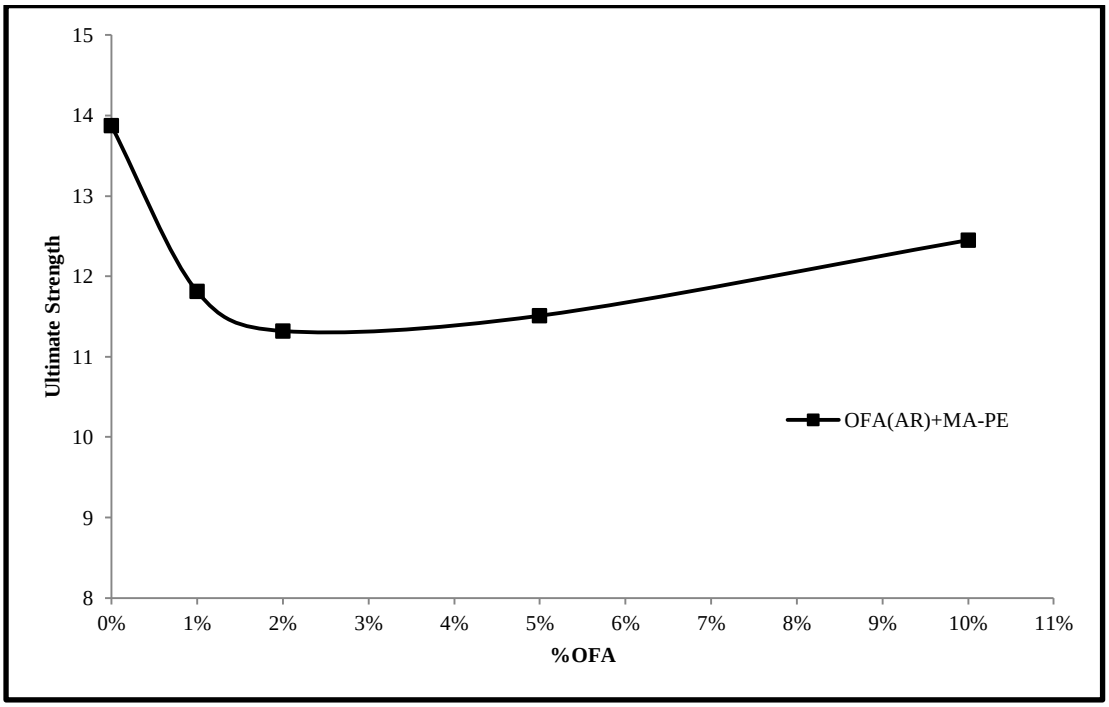

Figure 6.5.1(c): Effect of OFA Loading with 2%PE-g-MA on Ultimate Strength

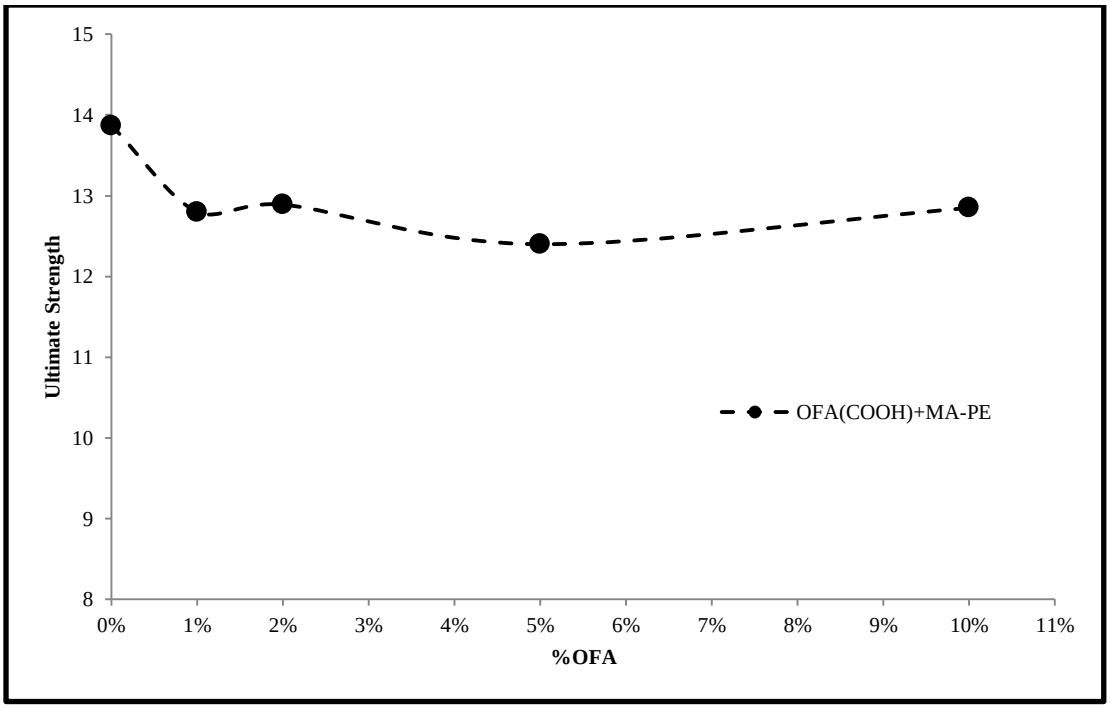

Figure 6.5.1(d): Effect of COOH-OFA Loading with 2%PE-g-MA on Ultimate Strength

6.5.2: Effect of OFA Functionalization on Ultimate Strength

Effect of OFA functionalization with and without PE-g-MA compatiblizer on Ultimate Strength of composites is shown in figure 6.5.2 (a-b). Figure 6.5.2 (a) shows the effect of functionalization without PE-g-MA compatiblizer. It is observed that at 1, 2 and 5% loading of both modified and unmodified OFA, Ultimate Strength decreased up to same extent. At 10% loading, functionalization shows improvement due to increase in elastic strength. Figure 6.5.2 (b) shows the effect of functionalization in the presence of PE-g-MA. It is observed that at each loading, functionalized OFA shows better results as compare to as-received OFA with compatiblizer. It is observed that by the combination of modified filler and compatiblizer, better results are obtained as compare to others conditions and Ultimate Strength becomes stable.

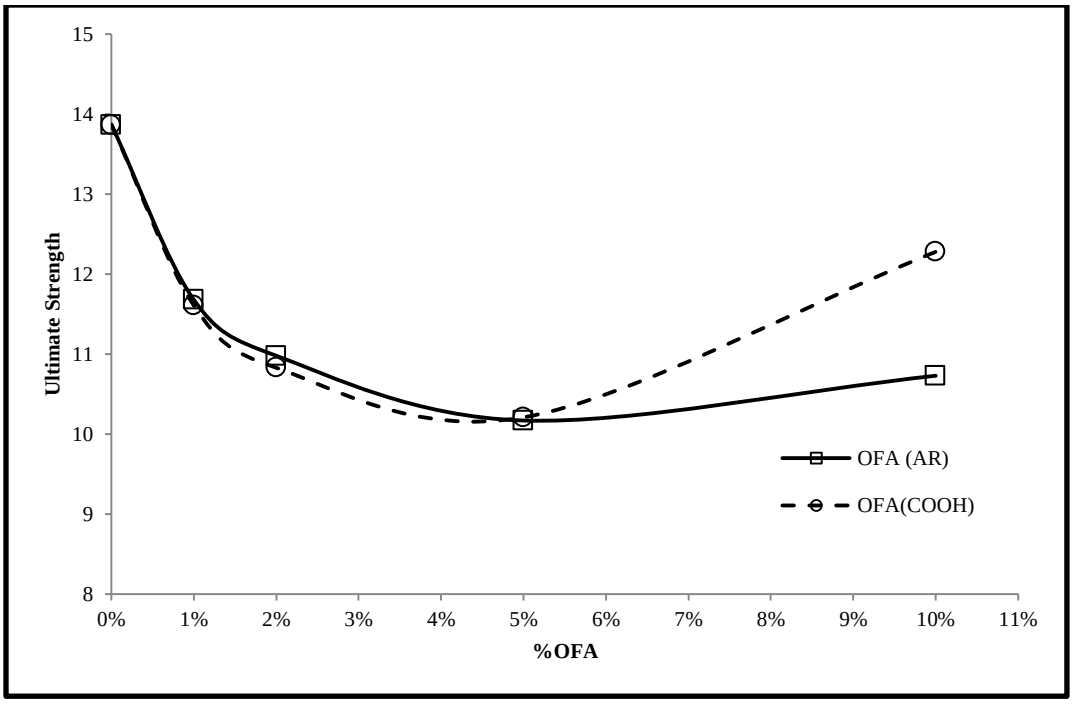

Figure 6.5.2(a): Effect of OFA functionalization without PE-g-MA on Ultimate Strength

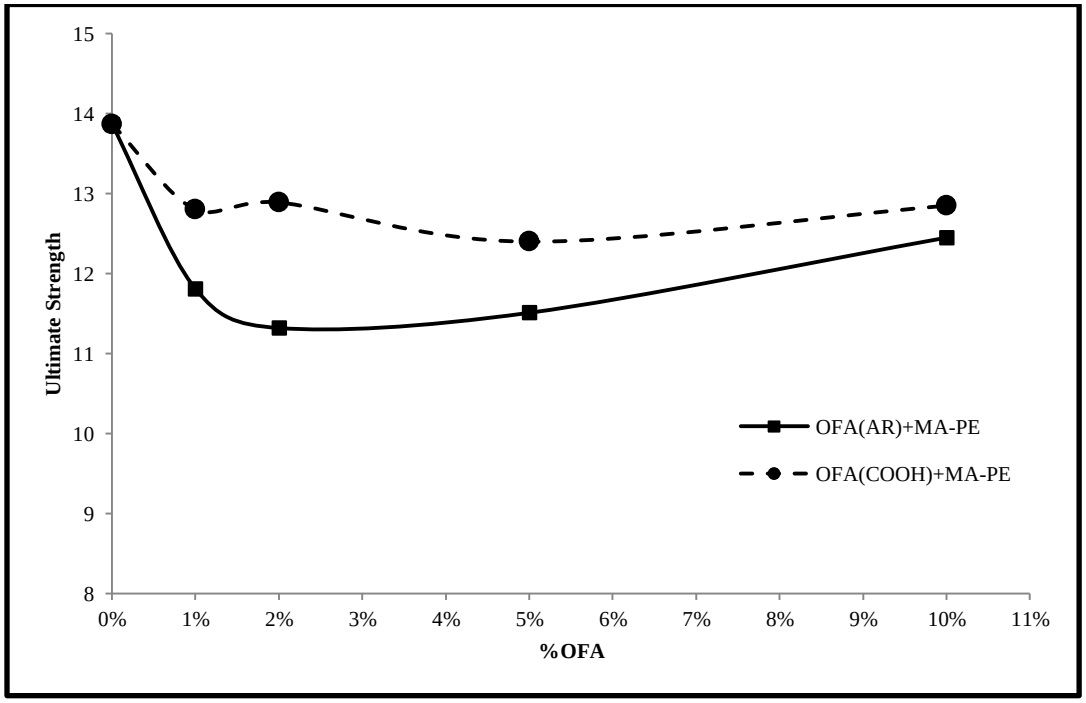

Figure 6.5.2(b): Effect of OFA functionalization without PE-g-MA on Ultimate Strength

6.5.3: Effect of PE-g-MA Compatiblizer on Ultimate Strength

Effect of Polyethylene-grafted-Maleic Anhydride with and without OFA surface modification on Ultimate Strength of composites is shown in figure 6.5.3 (a-b). Figure 6.5.3(a) shows the effect of PE-g-MA compatiblizer with unmodified fly ash. It is observed that at initial loading i.e. 1 and 2 wt%, the Ultimate Strength of composites is similar by the addition of PE-g-MA. At higher loading, 5 and 10 wt%, as the PE-g-MA enhanced the dispersion and increased the strength, so better results are obtain with compatiblizer. Figure 6.5.3(b) shows the effect of PE-g-MA with modified fly ash. It is observed that at each loading, a considerable improvement is observed when PE-g-MA is used. It shows good interlinking between functionalized OFA and polymer matrix with compatiblizer. At 10% loading, as the functionalization already enhanced the elastic strength, so the effect of compatiblizer is less as compare to other loading.

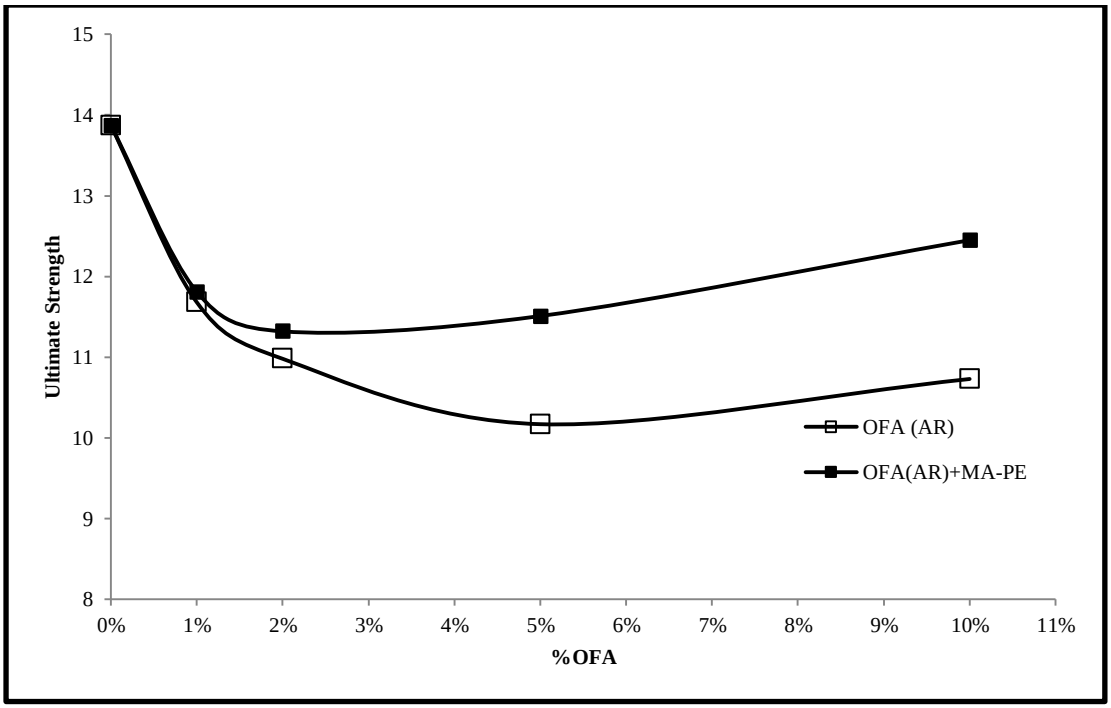

Figure 6.5.3(a): Effect of Compatiblizer with OFA Loading on Ultimate Strength

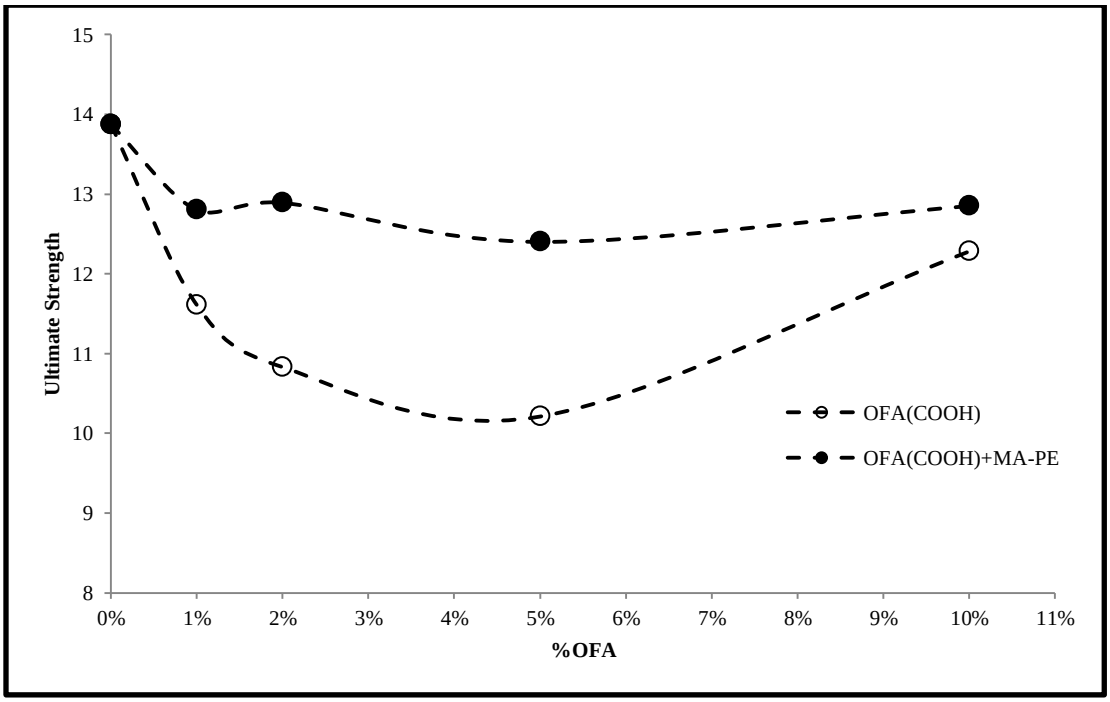

Figure 6.5.3(b): Effect of Compatiblizer with COOH-OFA Loading on Ultimate Strength

Part B: Thermal Behavior of LDPE/OFA Composite:

Thermal behavior of LDPE/OFA composite is observed by DSC QA-1000 instrument and the results are calculated by TA Universal Analyzer. Different properties have been calculated as Melting Point, Percent Crystallinity, Crystallization Peak and On-set Temperature. 2 specimens for each composite are analyzed and average values are reported. Comparison between modified and unmodified OFA loading is done and also the effect of PE-g-MA is observed.

6.6: Effect on Melting Point:

The DSC endothermic melting curves of LDPE/OFA composites at different loading with and without compatiblizer are shown in figure 6.6.1 (a) and (b) respectively. It is observed that the melting curves of pure LDPE and its composites are quite similar. There is no considerable effect of fillers is observed on melting point. All variation in the results is in the range of 1.4°C. The results of melting point are shown in table 6.6.

Table 6.6: Effect of OFA loading on Melting Point

Composite	**OFA Loading**					
		0%	**1%**	**2%**	**5%**	**10%**
LDPE/OFA	°C	110.9	110.4	110.6	111.2	111.1
LDPE/COOH-OFA	°C	110.9	110.2	110.3	110.7	110.6
LDPE/OFA + PE-g-MA	°C	110.9	110.7	110.9	110.6	109.8
LDPE/COOH-OFA + PE-g-MA	°C	110.9	110.6	111.1	110.6	109.9

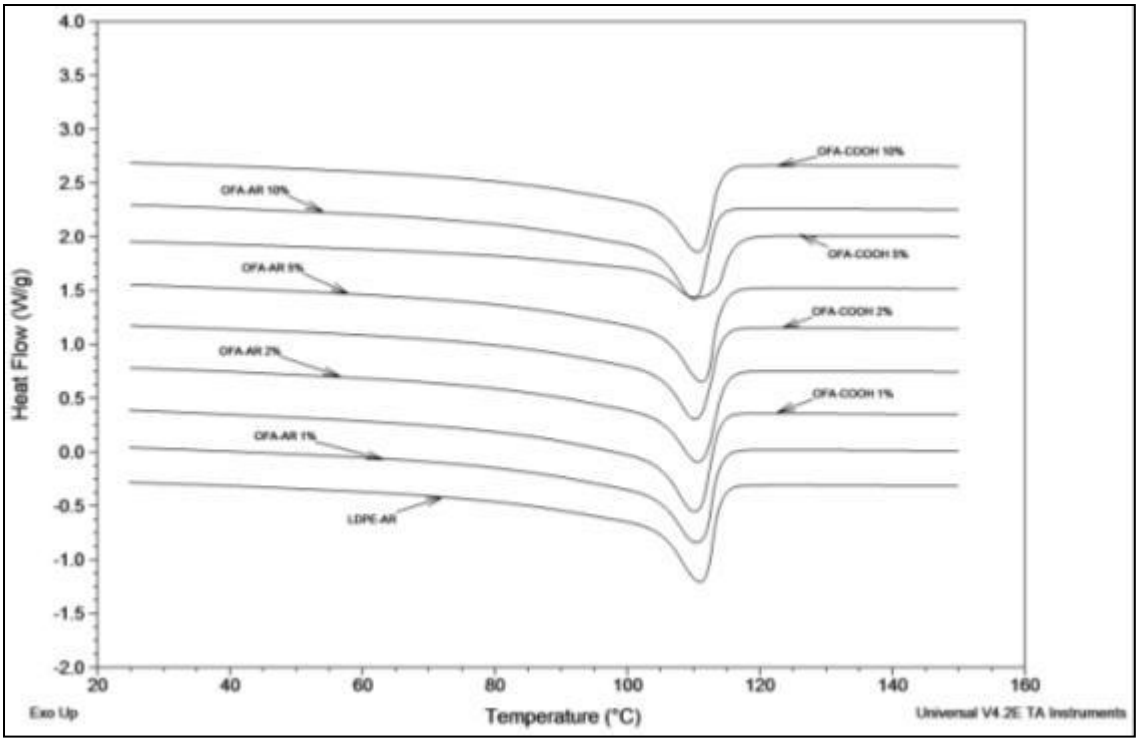

Figure 6.6.1(a): Endothermic Melting curves of LDPE/OFA composite without compatiblizer

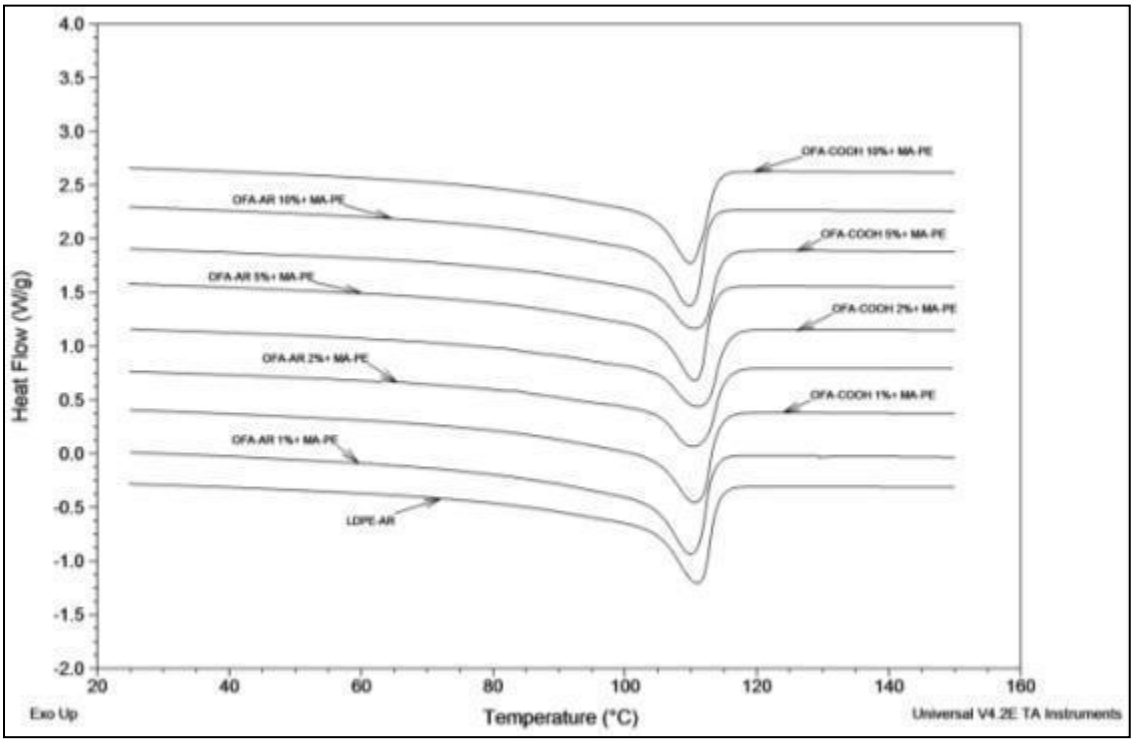

Figure 6.6.1(b): Endothermic Melting curves of LDPE/OFA composite with compatiblizer

The melting point of modified fly ash composites is slightly less as compare to unmodified fly ash composite. The results are more precisely demonstrated by figure 6.6.2. The effect of PE-g-MA compatiblizer on the as-received and acid-functionalized fly ash loading is shown in figure 6.6.3 (a) and (b), respectively. It is observed that at low loading, the melting point increased slightly however it decreased at higher loading. It may be due to agglomeration of fillers at higher loading so that the compatiblizer affects more on LDPE. As the PE-g-MA has low melting point as compare to pure LDPE, so the melting point of composite decreased. At lower loading, the compatiblizer affects more on filler so the effect of low melting point PE-g-MA decreased or remains almost same.

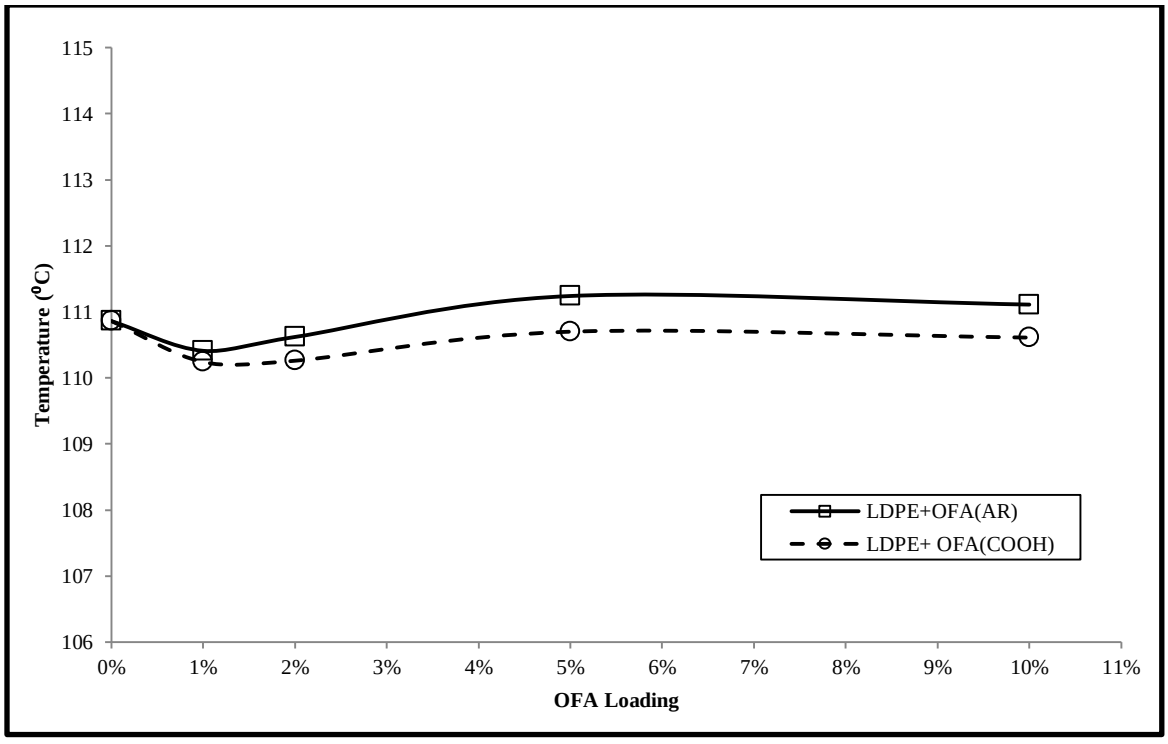

Figure 6.6.2: Effect of functionalization of OFA on Melting Point

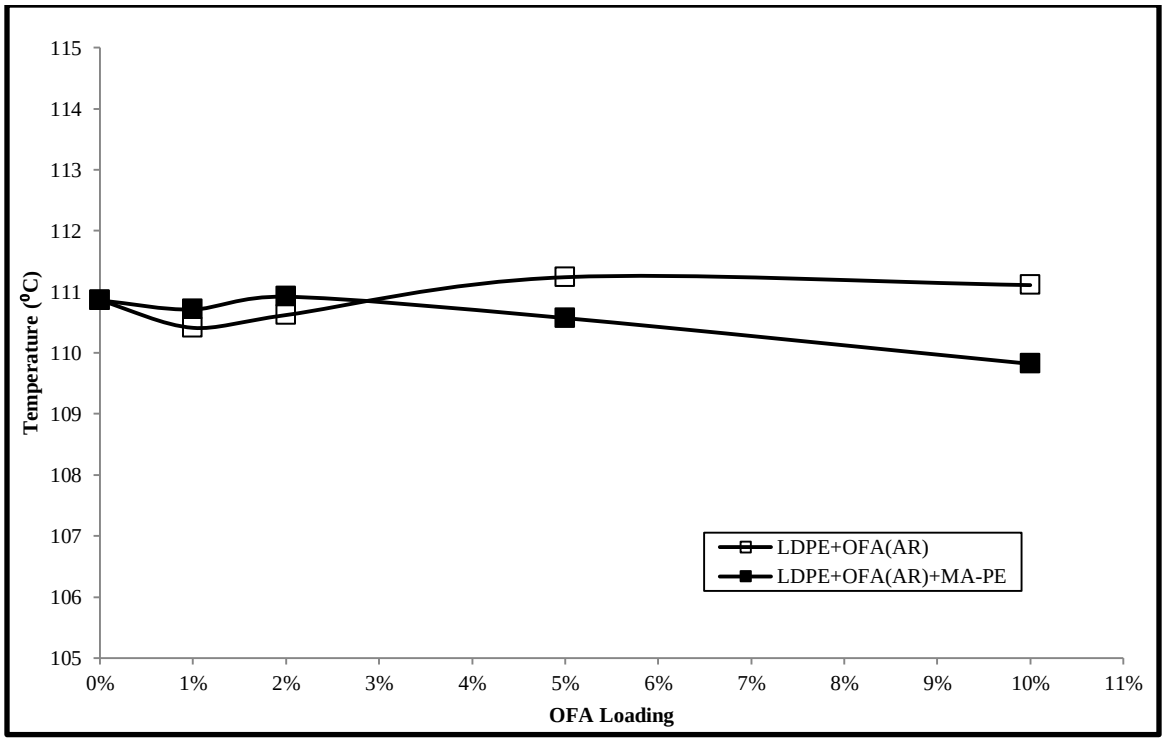

Figure 6.6.3(a): Effect of compatiblizer with OFA loading on Melting Point

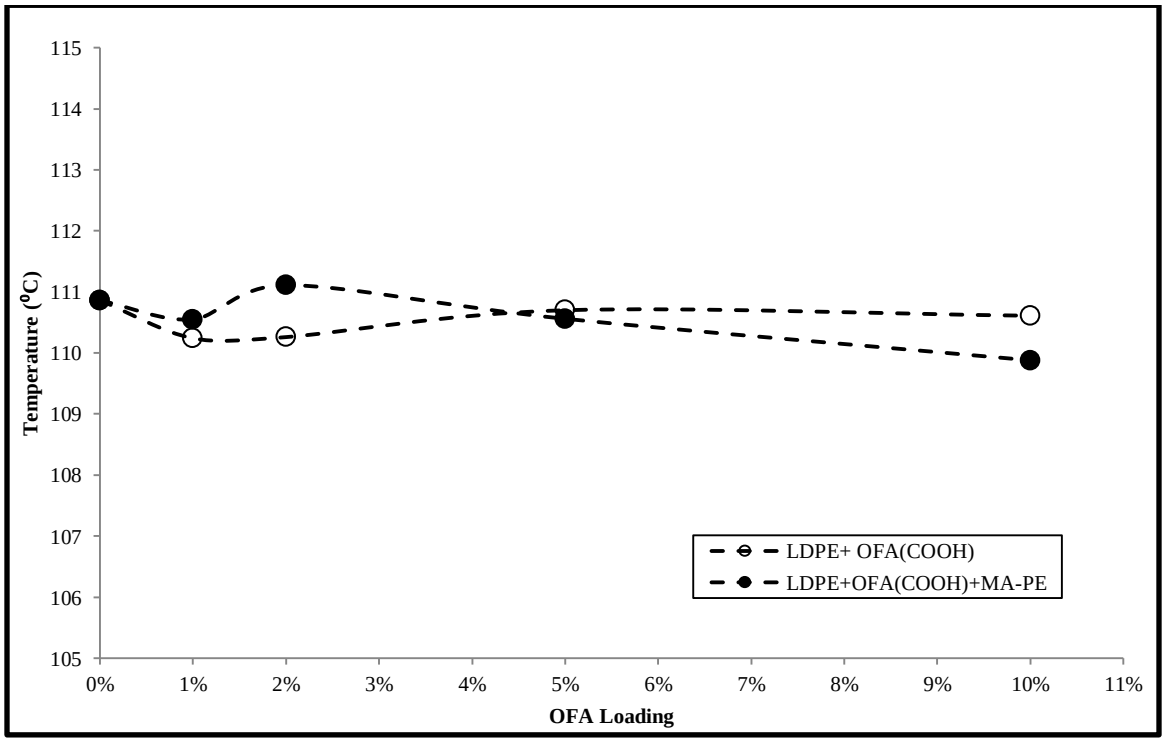

Figure 6.6.3(b): Effect of compatiblizer with COOH-OFA loading on Melting Point

6.7: Effect on %Crystallization:

Polymer crystallinity is the arrangement of its molecule into a regular structure. Pure LDPE is a semi-crystalline material having crystallinity between 33%-53% [49]. In this research, Universal Analysis software is used to calculate Percent Crystallinity based upon 293 J/g for the 100 % crystalline material. It is observed the percent crystallinity increased by addition of oil fly ash. The results of percent crystallinity are shown in table 6.7. The increment in percent crystallinity is relates with the dispersion of filler into the polymer matrix. Higher degree of crystallinity is achieved by with high dispersion which enhances the arrangement of molecules. Whereas the agglomeration of the fillers hinders in the arrangement of polymer molecules results in low crystallinity. As we observed the high degree of dispersion in achieved in case of modified fly ash which results in achievement of maximum crystallinity.

Table 6.7: Effect of OFA loading on %Crystallinity

Composite	**OFA Loading**					
		0%	**1%**	**2%**	**5%**	**10%**
LDPE/OFA	%	41.62	42.99	42.42	43.15	42.70
LDPE/COOH-OFA	%	41.62	43.62	41.14	53.46	45.84
LDPE/OFA + PE-g-MA	%	41.62	46.54	49.36	44.79	43.64
LDPE/COOH-OFA + PE-g-MA	%	41.62	48.95	45.41	54.21	46.71

Figure 6.7.1 shows the effect of functionalization on percent crystallinity. At initial loading, as both type of fillers showed almost similar dispersion, therefore similar percent crystallinity observed at 1 and 2% loading. As the modified fly ash showed high dispersion at 5% loading which results in maximum crystallinity. At 10% loading crystallinity decreased due to some agglomeration. It shows the optimum conditions are achieved at 5% modified fly ash loading. There is no considerable change is observed in case of as-received fly ash. Figure 6.7.2 (a) and 6.7.2 (b) shows the effect of PE-g-MA on percent crystallinity with unmodified and modified fly ash, respectively. It is observed that in both cases, the % crystallinity increased because of some improvement in degree of dispersion. The enhancement is more at lower loading as compare to high loading in both cases.

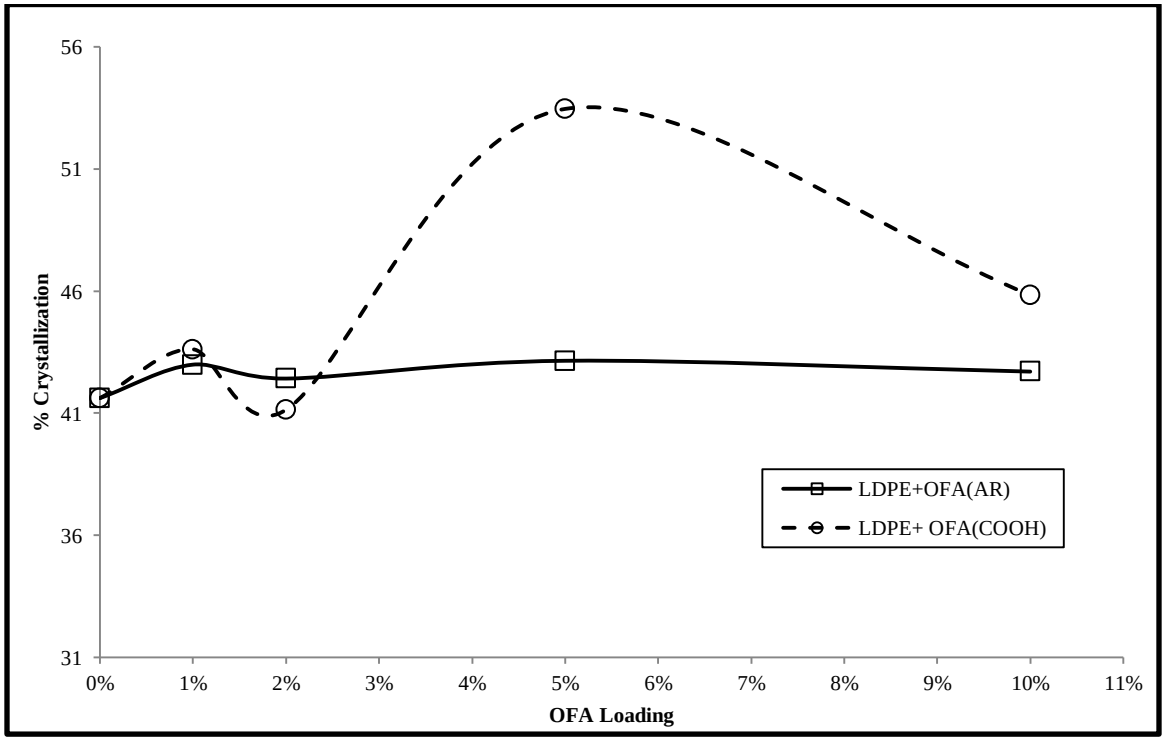

Figure 6.7.1: Effect of functionalization of OFA on %Crystallinity

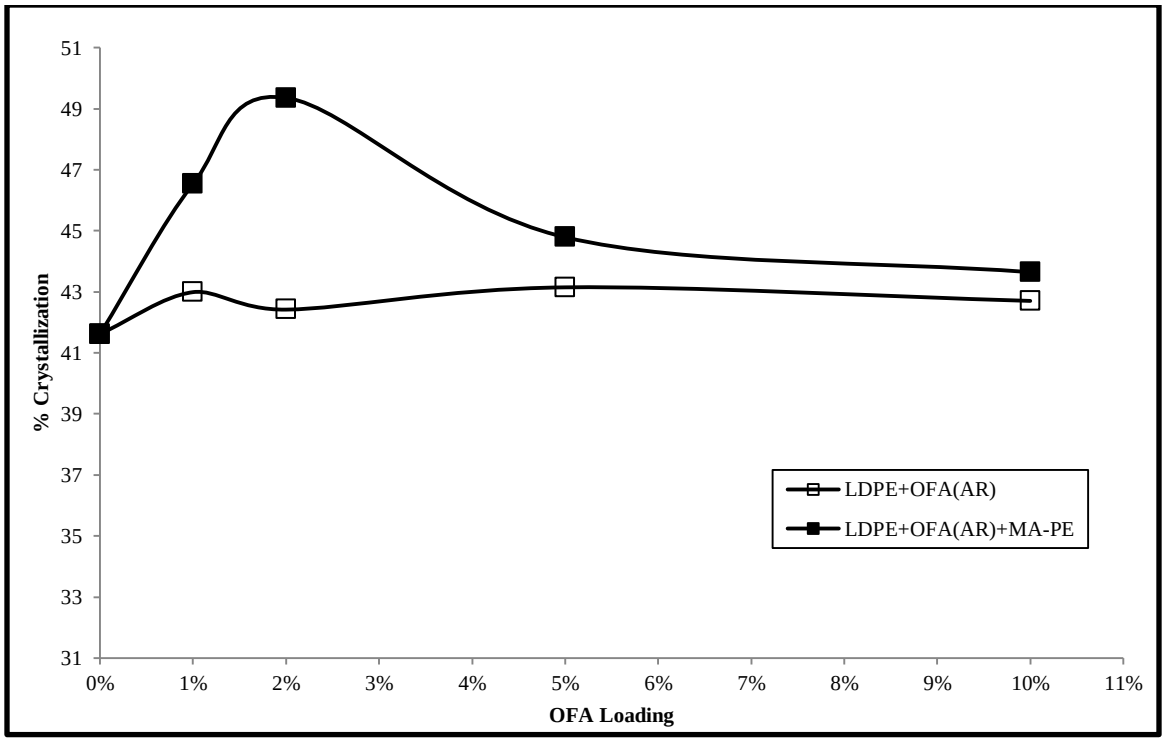

Figure 6.7.2(a): Effect of compatiblizer with OFA loading on %Crystallinity

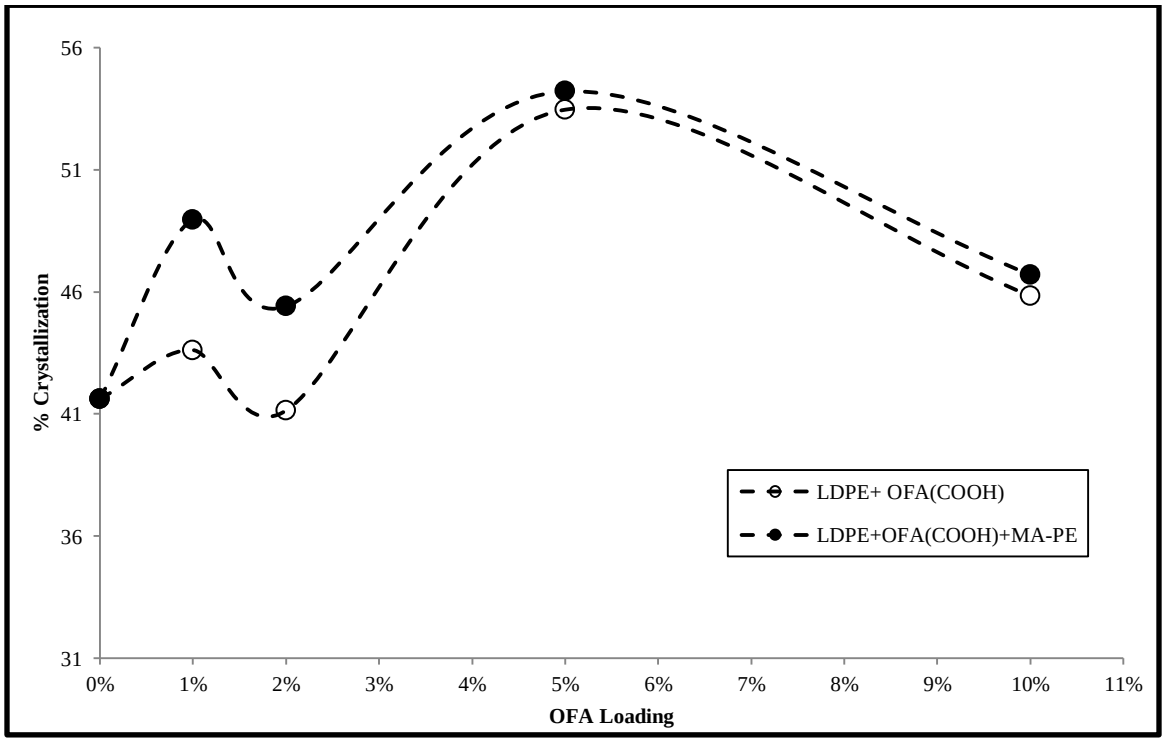

Figure 6.7.2(b): Effect of compatiblizer with COOH-OFA loading on %Crystallinity

6.8: Effect on On-Set Temperature:

On-set temperature is the temperature in cooling curve from where the polymer starts developing its crystalline structure. Figure 6.8.1 (a) and (b) shows the cooling curves of LDPE/OFA composite at different loading with and without compatiblizer, respectively. It is shown that the cooling curves of LDPE and its composites are quite similar. It is observed that On-set temperature increased by the addition of OFA. The results of the On-Set temperature are given in table 6.8.

Table 6.8: Effect of OFA loading on On-Set Temperature

Composite	**OFA Loading**					
		0%	**1%**	**2%**	**5%**	**10%**
LDPE/OFA	℃	98.2	99.7	99.8	99.4	99.7
LDPE/COOH-OFA	℃	98.2	99.8	99.6	99.1	99.3
LDPE/OFA + PE-g-MA	℃	98.2	99.9	99.5	99.2	98.9
LDPE/COOH-OFA + PE-g-MA	℃	98.2	99.7	99.3	99.3	99.3

Results showed that there is no considerable difference is achieved in On-Set temperature by increase in filler loading. Figure 6.8.2 shows the effect of functionalization on On-set temperature. At lower filler concentration i.e. 1 and 2% loading, both type of fillers gives almost same results. At 5% loading, the On-set temperature of functionalized fly ash is less and this difference decreased again at 10% loading. Also the addition of compatiblizer didn't make any change in the values of On-set temperature. The effect of compatiblizer on unmodified and modified fly ash is shown in figure 6.8.3 (a) and (b), respectively.

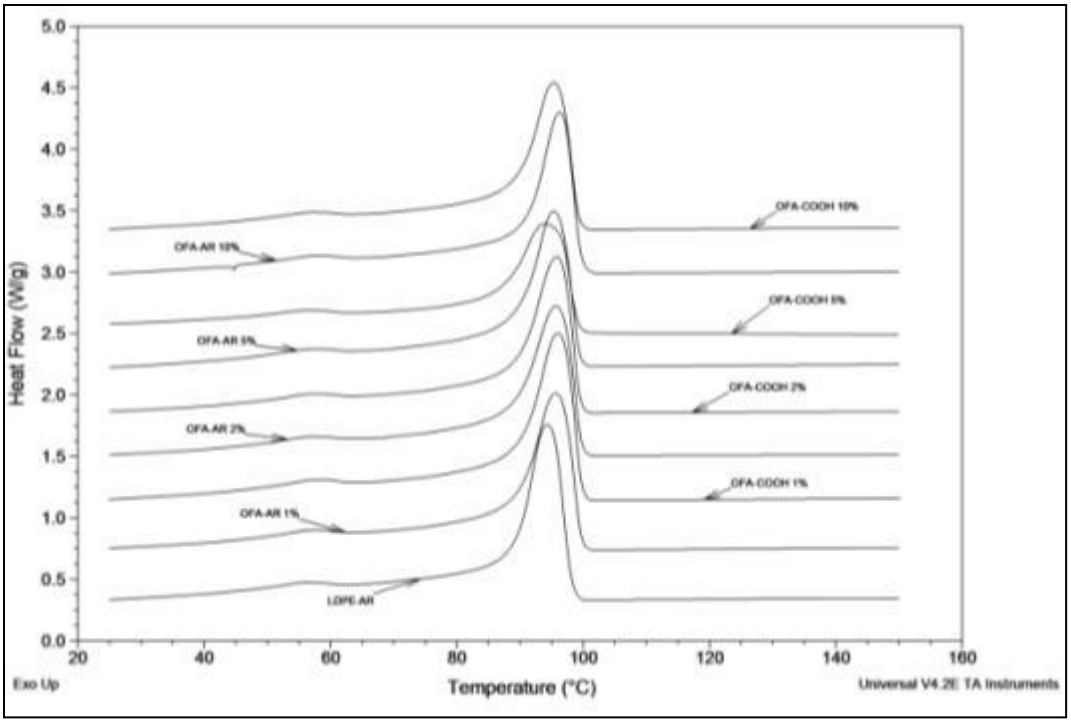

Figure 6.8.1(a): Exothermic Crystallization curves of LDPE/OFA composite without compatiblizer

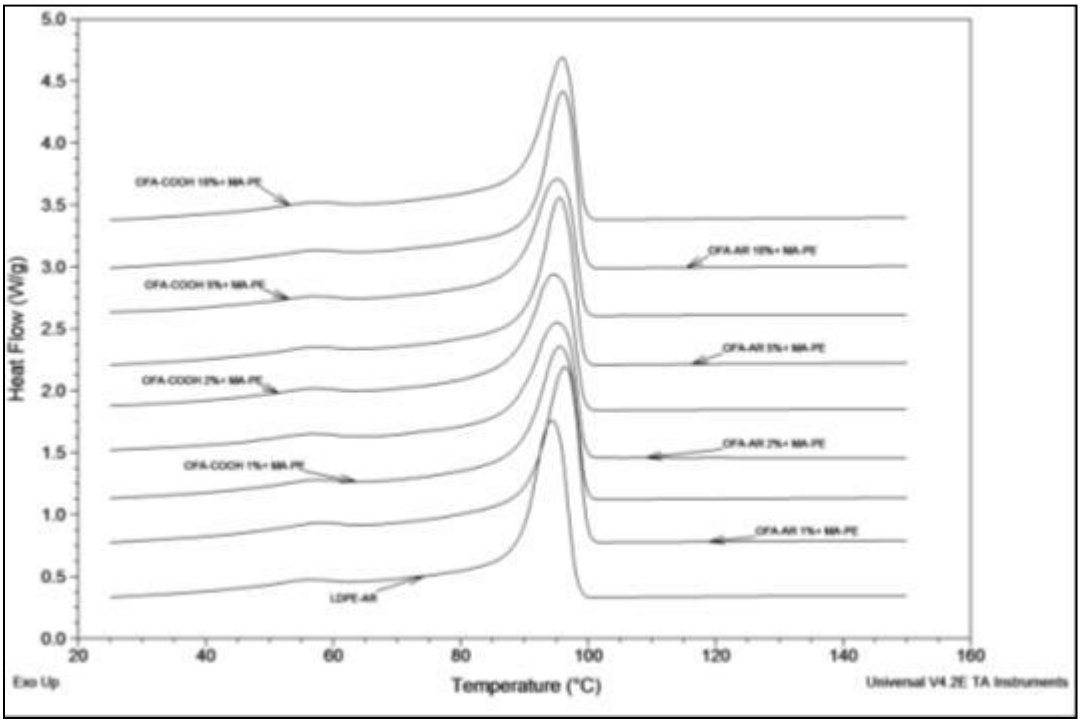

Figure 6.8.1(b): Exothermic Crystallization curves of LDPE/OFA composite with compatiblizer

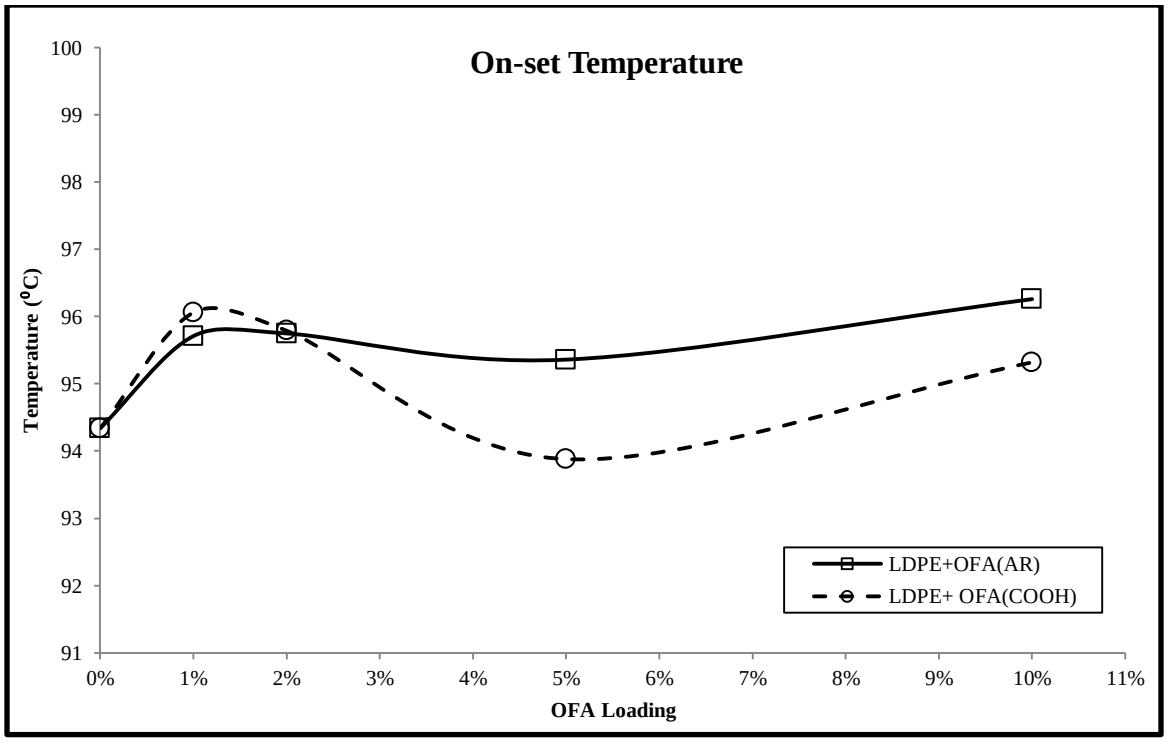

Figure 6.8.2: Effect of functionalization of OFA on On-set temperature

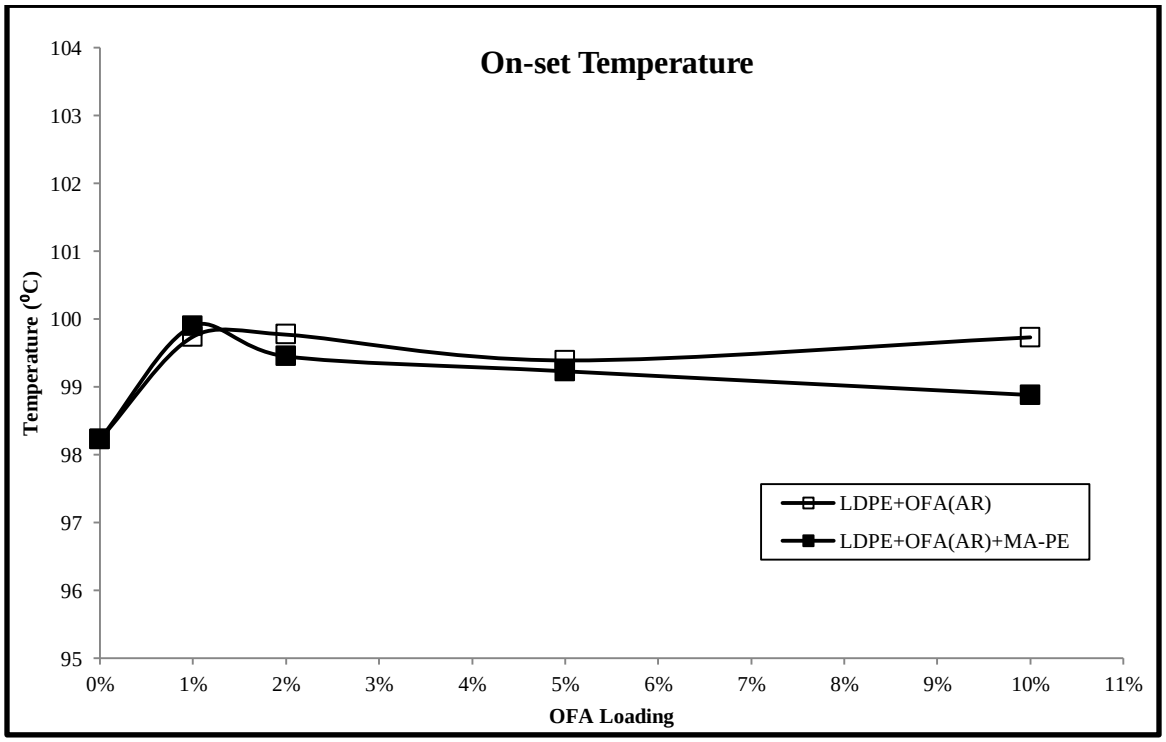

Figure 6.8.3(a): Effect of compatiblizer with OFA loading on On-set temperature

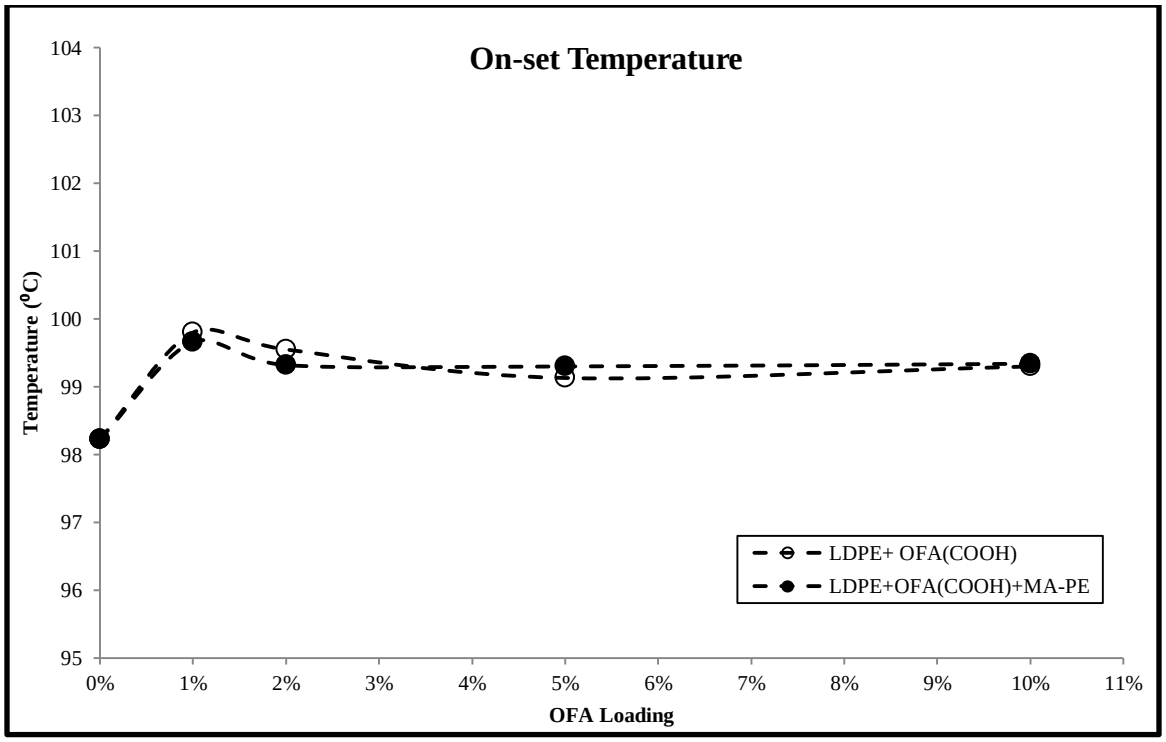

Figure 6.8.3(b): Effect of compatiblizer with COOH-OFA loading on On-set temperature

6.9: Effect on Crystallization Peak:

Crystallization peak is the maximum temperature observed in the exothermic cooling curve in cooling cycle. A random effect on crystallization peak is observed by the addition of OFA as a filler. In case of as-received fly ash, it increased by the filler loading and become almost constant. Whereas by the Acid functionalized fly ash loading, initially it increased but again decreased at higher loading. LDPE/OFA composites with PE-g-MA compatiblizer shows more uniform results for some extent as compare to composites without compatiblizer. The results of the Crystallization peak temperature are given in table 6.9

Table 6.9: Effect of OFA loading on Crystallization Peak

Composite		OFA Loading				
		0%	**1%**	**2%**	**5%**	**10%**
LDPE/OFA	°C	94.34	95.71	95.75	95.36	96.26
LDPE/COOH-OFA	°C	94.34	96.06	95.79	93.88	95.32
LDPE/OFA + PE-g-MA	°C	94.34	96.41	95.49	95.48	96.05
LDPE/COOH-OFA + PE-g-MA	°C	94.34	95.56	94.69	95.17	95.89

Figure 6.9.1 shows the effect of functionalization on the crystallization peak. At lower loading, both type of fillers showed the same results. However, at higher loading, the crystallization peak reduces in case of modified fly ash. Effect of PE-g-MA with unmodified and modified fly ash on the crystallization peak is shown in figure 6.9.2 (a) and (b). At 1% loading, the as-received fly ash shows a very slight increase in crystallization peak by the addition of compatiblizer but no considerable change is observed at other loadings. In case of modified fly ash, compatiblizer shows a decrement in the crystallization peak temperature but it increased at high concentration of filler as shown in the figure.

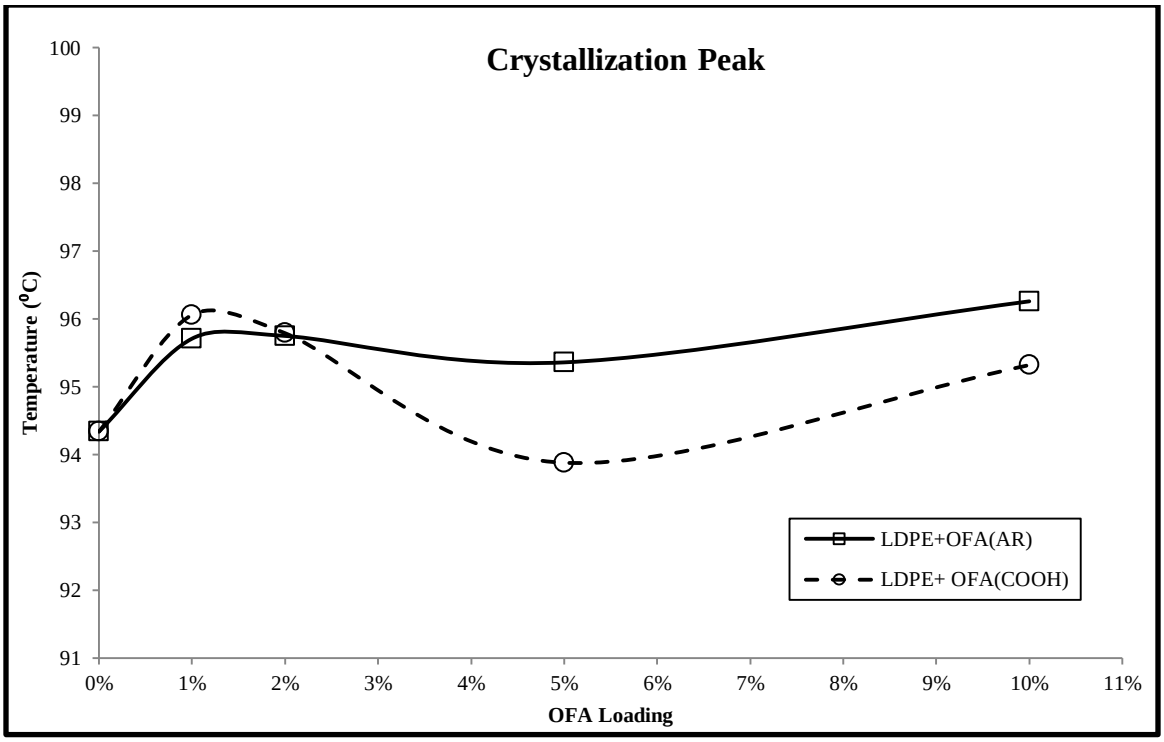

Figure 6.9.1: Effect of functionalization of OFA on Crystallization Peak

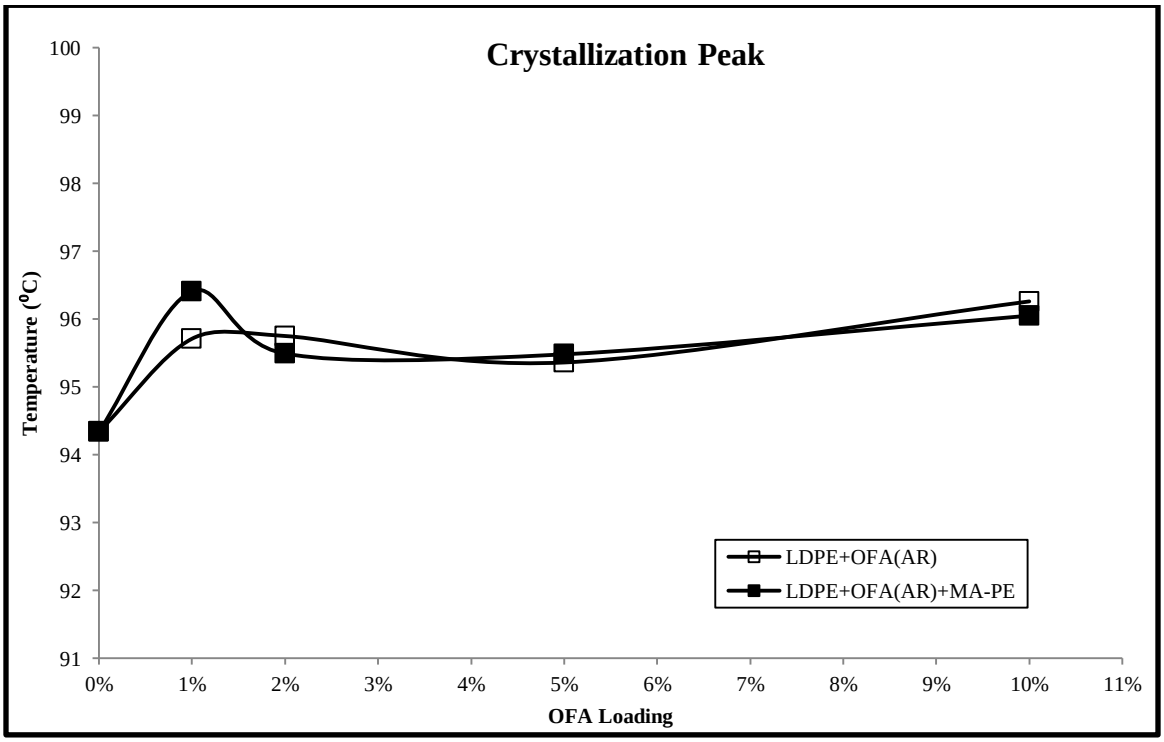

Figure 6.9.2(a): Effect of compatiblizer with OFA loading on Crystallization Peak

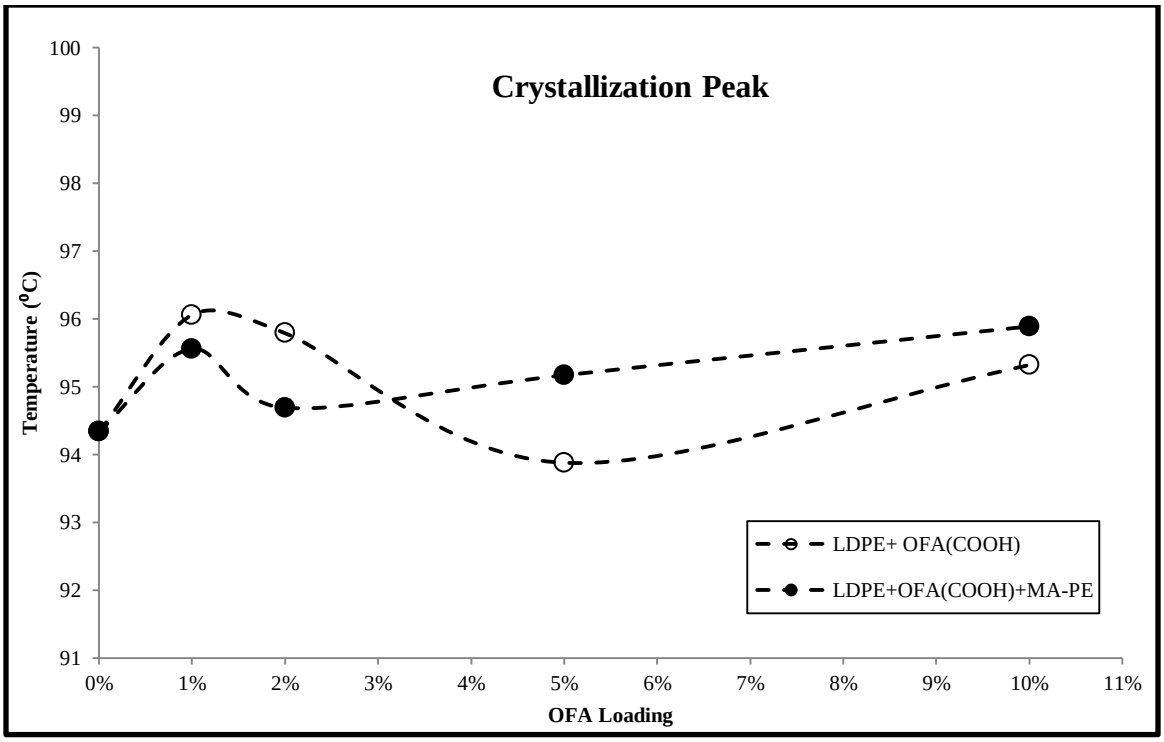

Figure 6.9.2(b): Effect of compatiblizer with COOH-OFA loading on Crystallization Peak

CHAPTER 7

CONCLUSION AND RECOMMENDATIONS

7.1. Conclusion:

The effect of fillers on the properties of polymers has been investigated for several decades. The most common particles which got the interests of scientists and engineers are carbon nanotubes, nanofibers, nanosphers, clays and metallic nanorods. The addition of these particles produces a dramatic enhancement in polymer composites. One of the big challenges of this field is the production of cheap, commercial level fillers to affect the polymer properties on cost effective basis. In this study, oil fly ash is used as a filler to improve the Low density Polyethylene performance. Surface modification of fly ash was done by acid treatment method in order to enhance the polymer-filler interaction. Optimization of different parameters is one of the major challenges of the research work. LDPE/OFA composites were prepared by melt mixing method and rheological, morphological, mechanical and thermal properties were investigated. Also the effect of Polyethylene-grafted-Maleic Anhydride (PE-g-MA) as a compatiblizer was observed.

Following conclusions are made by this research work:

- The functionalization of OFA surface is achieved by H_2SO_4:HNO_3 acid mixture with different composition and also the effect of air-oxidation is observed.
- FTIR results shows that the injection of air for oxidation during the surface modification method enhanced the functionalization of fly ash. Also it is observed that the attachment of carboxylic group to the surface of fly ash

increased with increase in the concentration of nitric acid into the acid mixture upto 15%. After that, decrement in attached acidic functional group and attachment of some unsaturated groups is observed.

- Spot Analysis shows that the carbon to oxygen ratio increased by the surface modification of fly ash. Percent content of oxygen is more in case of air oxidation method. Also the carbon to oxygen ratio increased with increase in nitric acid concentration in acid mixture.
- XRD analysis shows the increment in carbon crystalline structure by surface modification of fly ash. The improvement is increased by air oxidation and also by increased in nitric acid concentration into the acid mixture upto 15%.
- Rheological characterization of LDPE/OFA composites is done by ARES rheometer and properties are calculated by TA Orchestrator software.
- An increase in storage modulus and loss modulus is observed by the addition of fly ash.
- In case of as-received fly ash, good dispersion is achieved at 1 and 2% filler loading but some agglomeration is observed at 5 and 10% loading. However, the acid functionalized fly ash shows remarkable results even at high loading. It shows that the polymer-filler interaction increased by surface modification of filler and hence the dispersion increased. The optimum results are obtained at 5% loading of surface modified fly ash.
- Cross over point and cross over frequency increased with filler loading in case of as-received fly ash while it decreased after surface modification of filler. It is the clear evidence to better dispersion of acid-functionalized fly ash.

- Cole-Cole plot shows two phase system due to agglomeration of fillers at 5 and 10% loading of as-received fly ash. However, no such type of observation is observed in case of modified fly ash.
- Addition of PE-g-MA enhanced the dispersion of both modified and unmodified fly ash. However the properties of composites slightly decreased due to low viscosity of PE-g-MA itself.
- FE-SEM analysis is done to observe the distribution fly ash in the polymer matrix. Results shows that particles are more distributed in case of modified fly ash as compare to unmodified fly ash. A slight agglomeration is observed in as-received LDPE/OFA composite images.
- Mechanical analysis of LDPE/OFA composites is done by Instron Mechanical testing machine. Young's Modulus, Elongation to break, Toughness, Yield Strength and Ultimate Strength is calculated.
- The Young's Modulus of the polymer composite increased with increased in filler concentration. Also the PE-g-MA enhanced the results more by improving the dispersion of fillers. Maximum increment of 47.80% and 46.84% is observed with PE-g-MA at 10% unmodified and modified fly ash loading, respectively.
- The elongation to break and toughness decreased with increase in filler concentration. This shows that the polymer becomes stiffer by the addition of filler and its plasticity decreased. A dramatic change is observed from 2% to 5% loading. Modified fly ash and compatiblizer shows some good improvement as compare to unmodified fly ash.

- The yield strength of polymer composite an increase with increased in OFA concentration. It is observed that the modified fly ash shows better improvement as compared to unmodified fly ash. Also the PE-g-MA increased the modulus by an increase in the degree of dispersion of filler. Maximum increment of 37.35% is observed in case of modified fly ash with compatiblizer.
- Thermal analysis of LDPE/OFA composites was done by DSC QA-1000 instrument and results are calculated by TA Universal Analyzer. Melting Point, percent crystallinity, crystallization peak and on-set temperature is calculated.
- An increase in percent crystallinity of composite is observed by addition of filler. The increment is related to the degree of dispersion of filler. However, no considerable change in melting point and on-set temperature is observed. A random effect on crystallization peak is observed by increasing the filler concentration.
- Melting and crystallization curves of LDPE composites showed the similar trend as observed in Pure LDPE.

Form the above results, it is concluded that OFA can be used as a filler to enhance the properties of LDPE and reduce the amount of polymer in the composites. Finally, the use of chemically modified oil fly ash proved to be very useful for the improvement of the properties of polyethylene composites up to 10% by weight. The use of such waste material in expected to reduce the amount of polymer composite and reduce its impact on environment.

7.2. Recommendation:

In the light of above research work, we recommend the following future work for further investigation of this field:

- Different types of techniques can be used to attach different types of functional groups for the modification the OFA surface.
- The effect of OFA on the extensional rheology of the polymer can be investigated.
- The OFA can be used with different type of polymers to see the effect on different polymer structures.

APPENDIX A

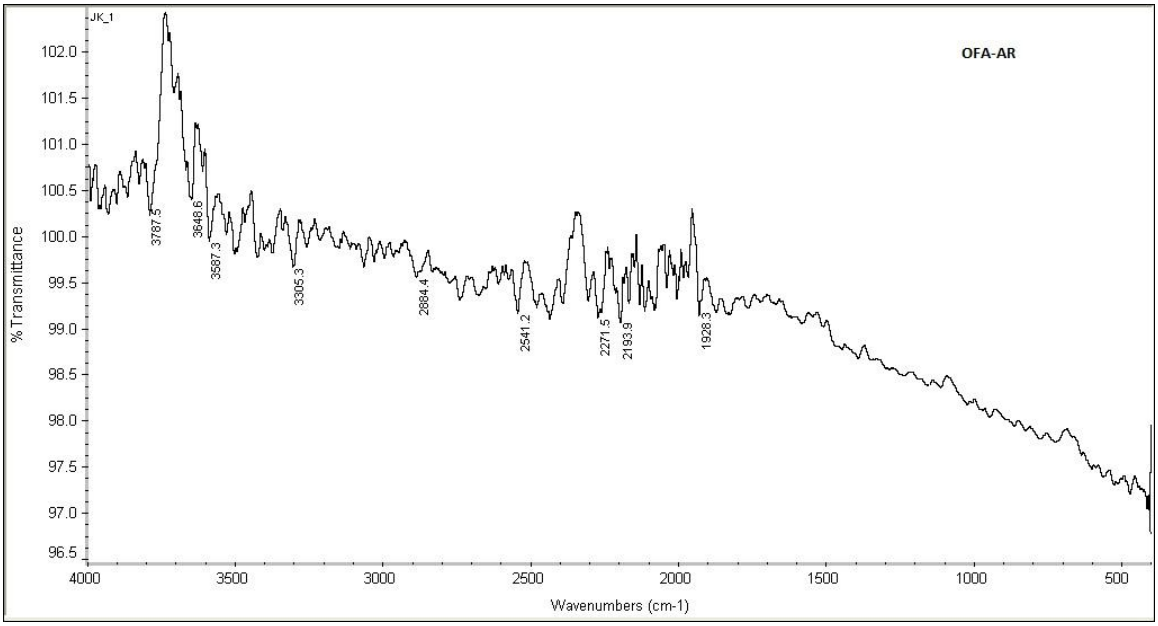

A-1: FTIR Spectra of as-received OFA

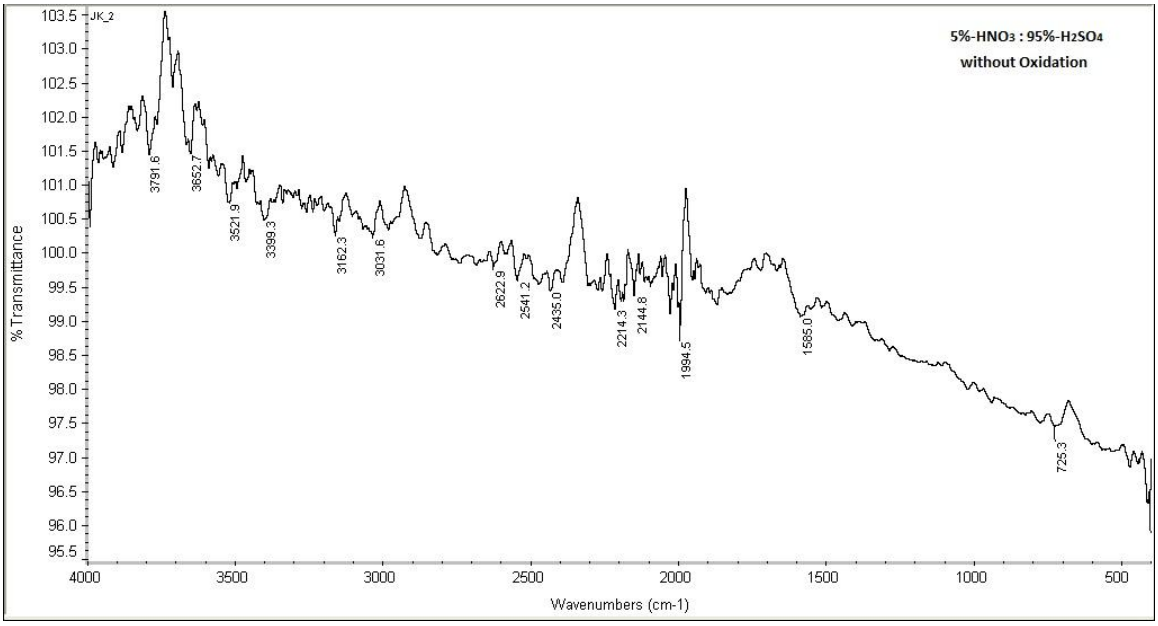

A-2: FTIR Spectra of OFA modified by 95%-H_2SO_4:5%-HNO_3 acid mixture without air-oxidation

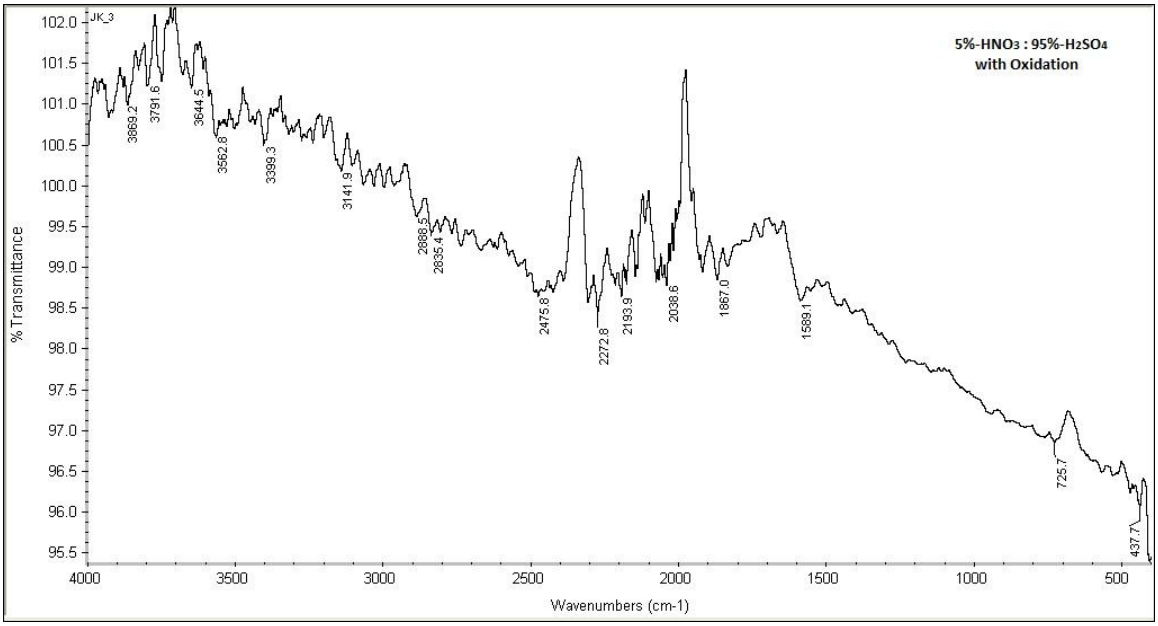

A-3: FTIR Spectra of OFA modified by 95%-H_2SO_4:5%-HNO_3 acid mixture with air-oxidation

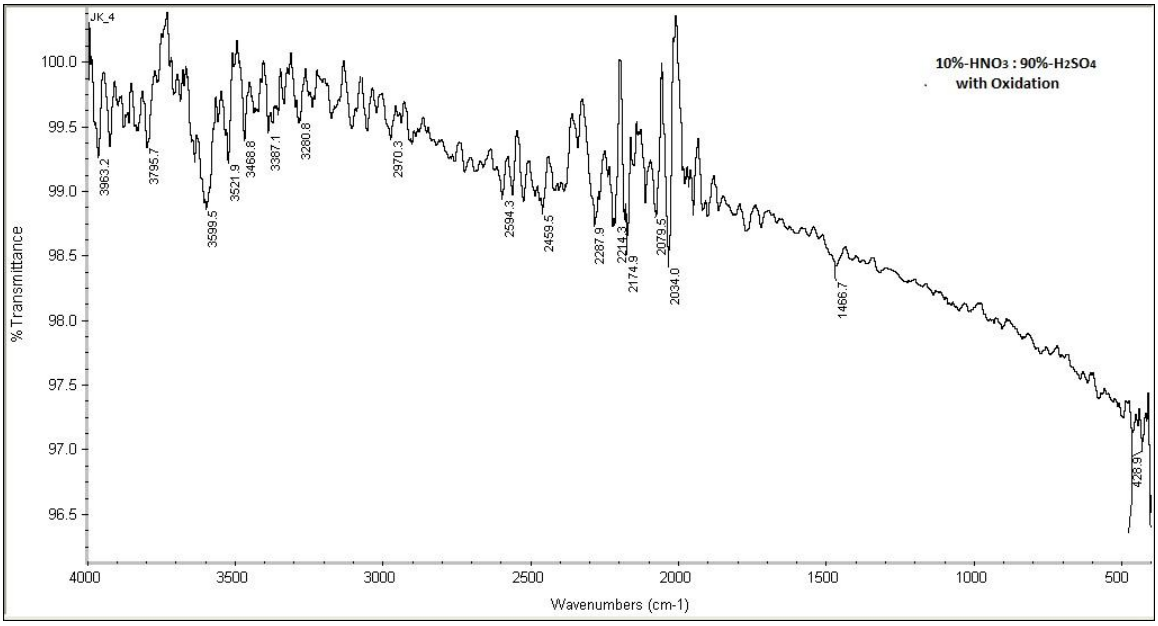

A-4: FTIR Spectra of OFA modified by 90%-H_2SO_4:10%-HNO_3 acid mixture with Air-oxidation

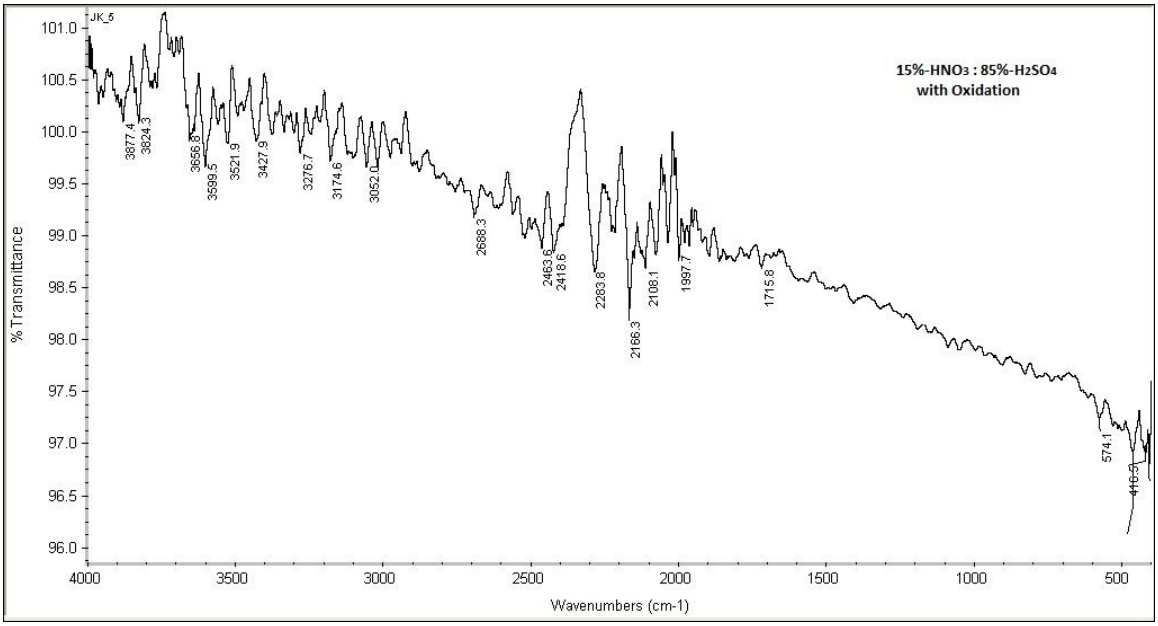

A-5: FTIR Spectra of OFA modified by 85%-H_2SO_4:15%-HNO_3 acid mixture with Air-oxidation

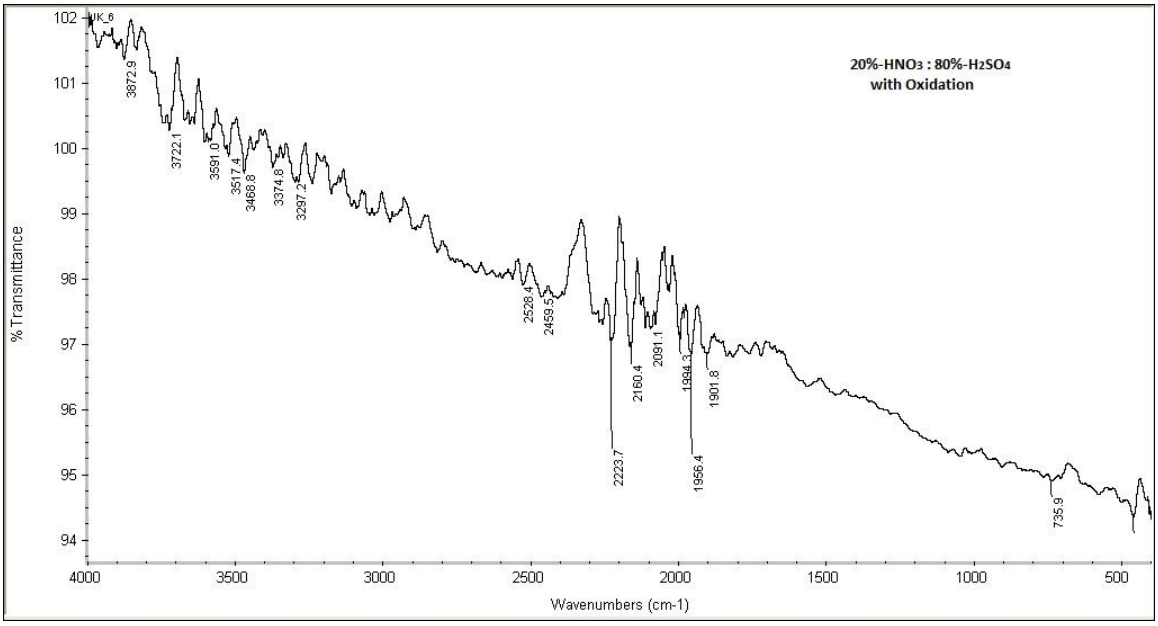

A-6: FTIR Spectra of OFA modified by 80%-H_2SO_4:20%-HNO_3 acid mixture with Air-oxidation

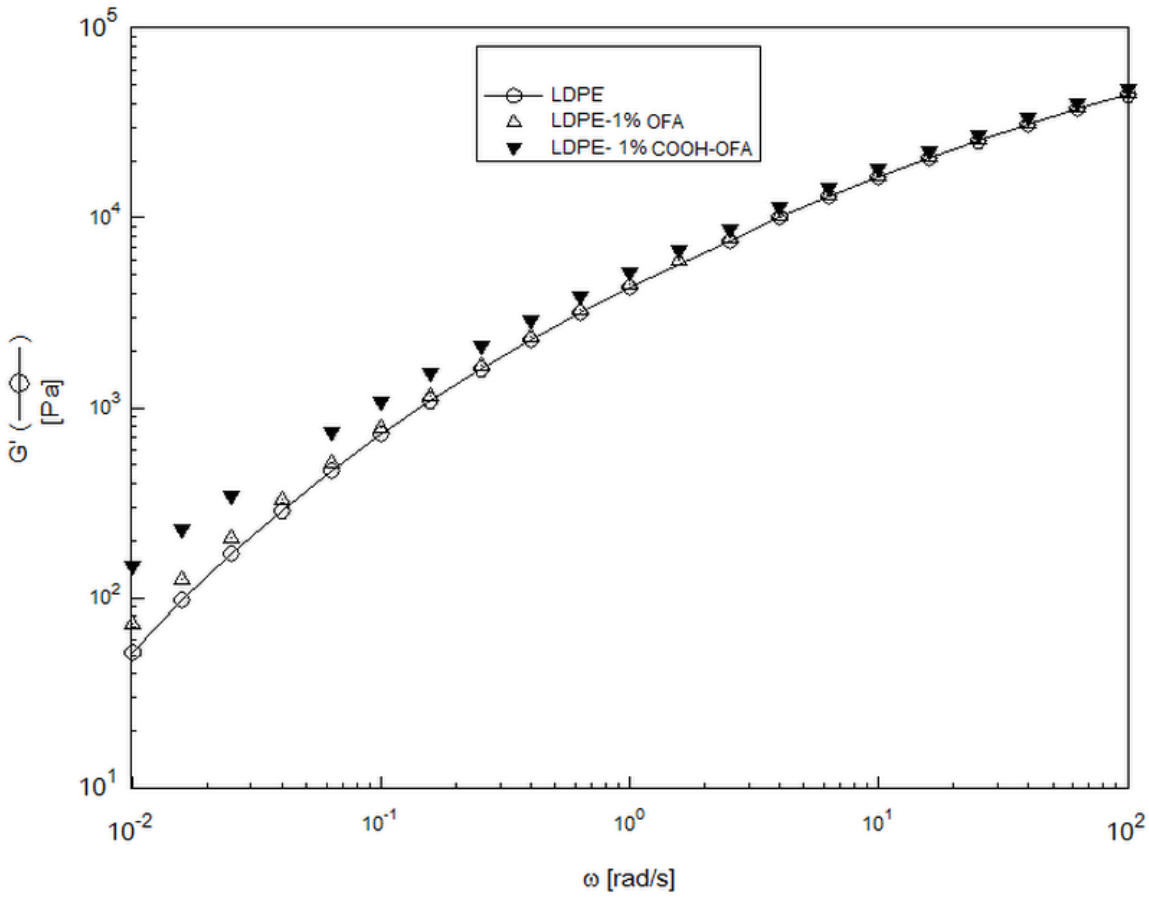

A-7: Effect of OFA-functionalization at 1% loading on Storage Modulus

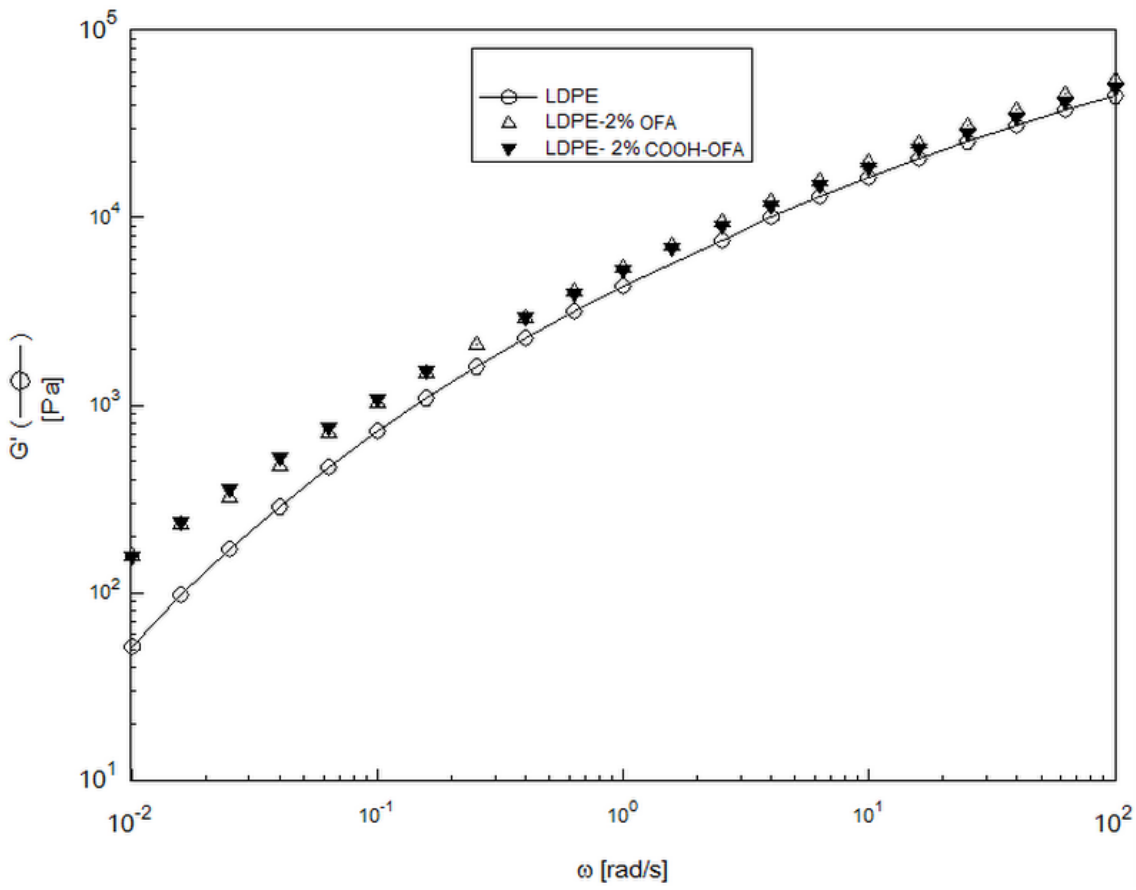

A-8: Effect of OFA-functionalization at 2% loading on Storage Modulus

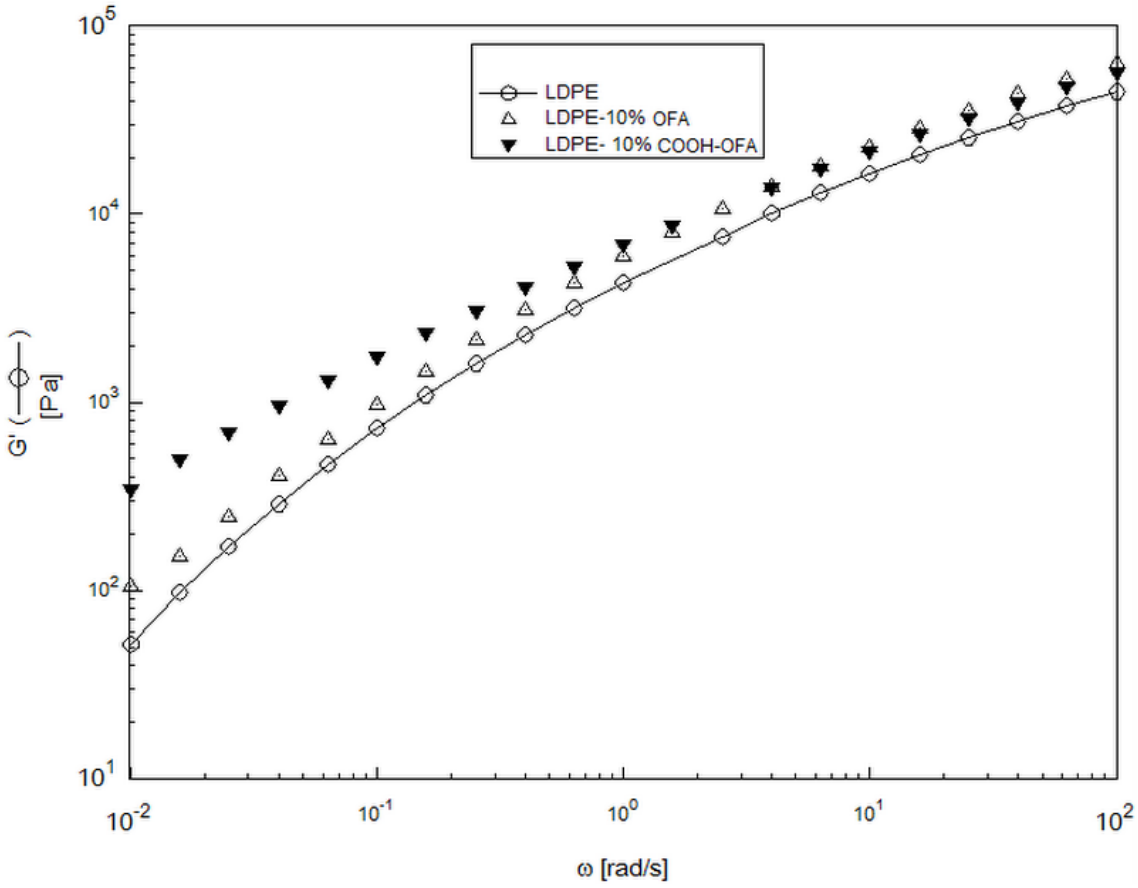

A-9: Effect of OFA-functionalization at 10% loading on Storage Modulus

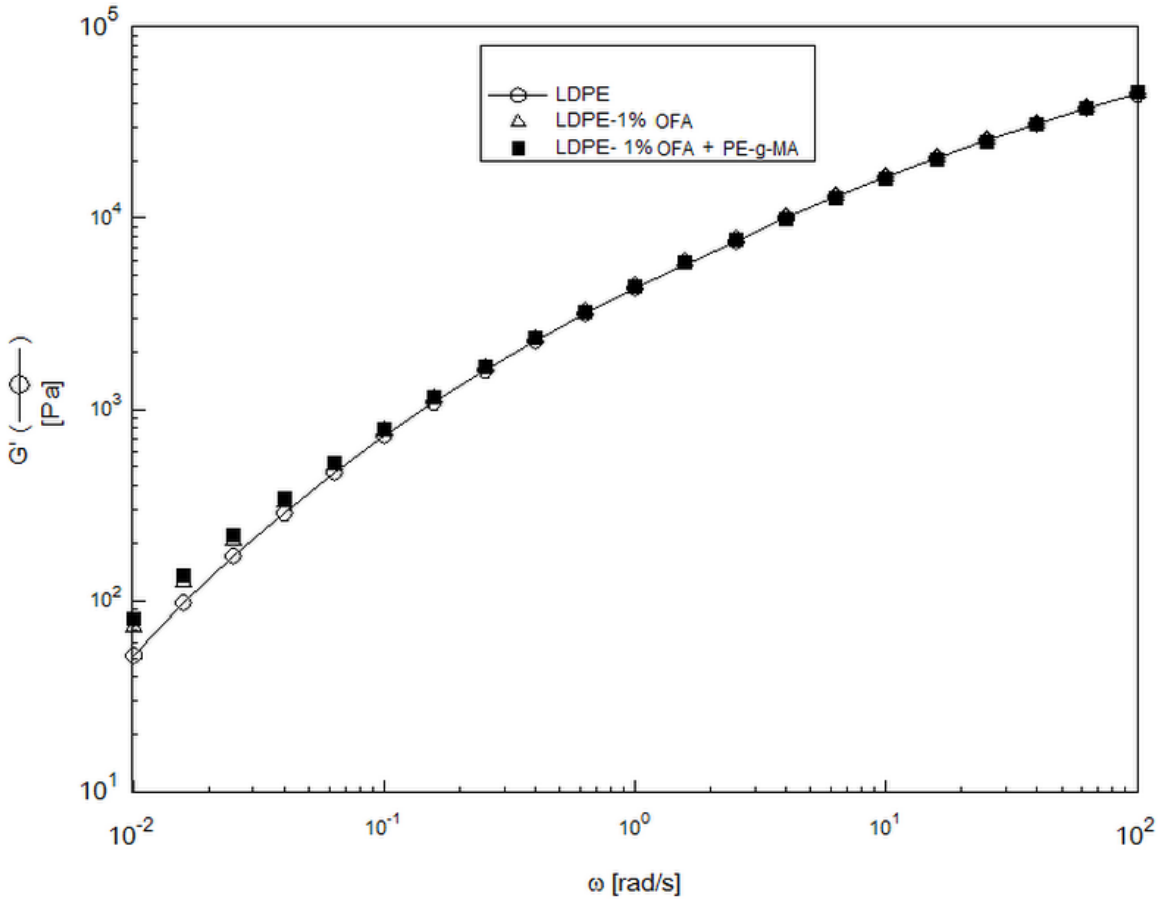

A-10: Effect of PE-g-MA at 1% OFA loading on Storage Modulus

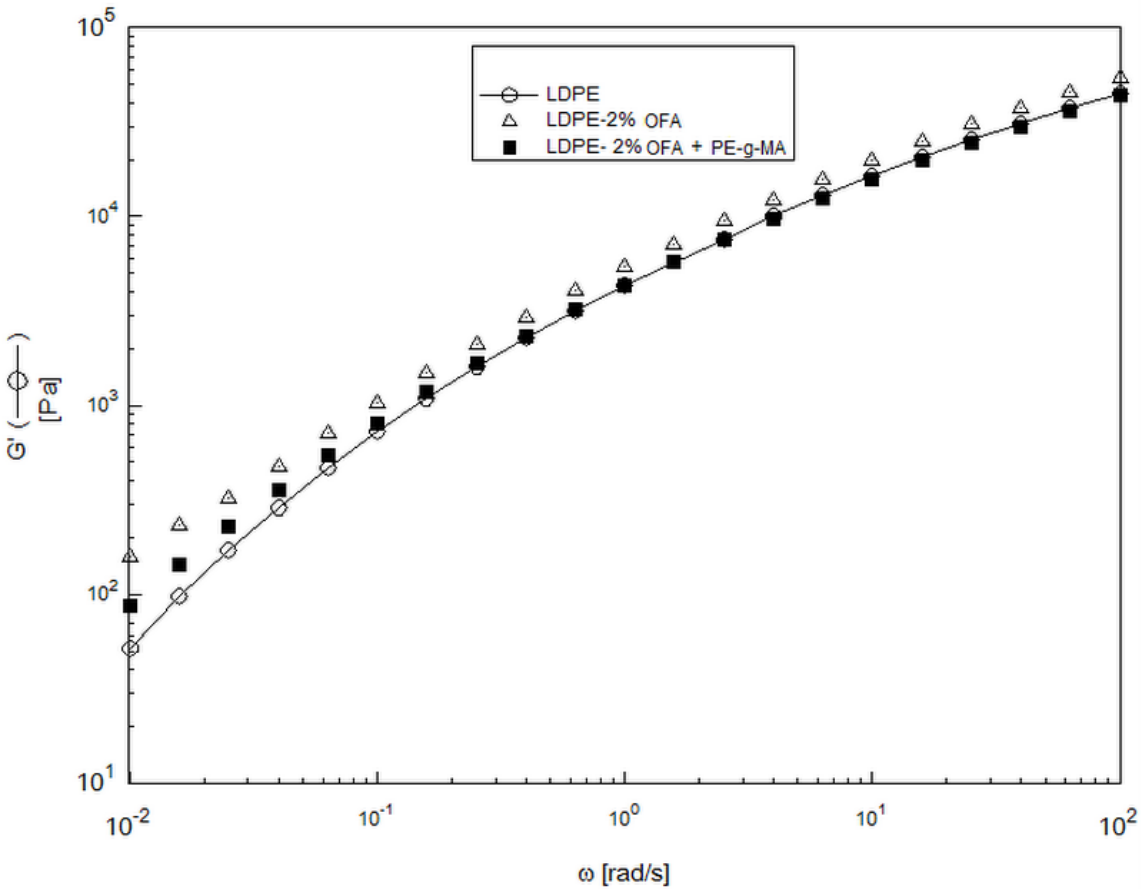

A-11: Effect of PE-g-MA at 2% OFA loading on Storage Modulus

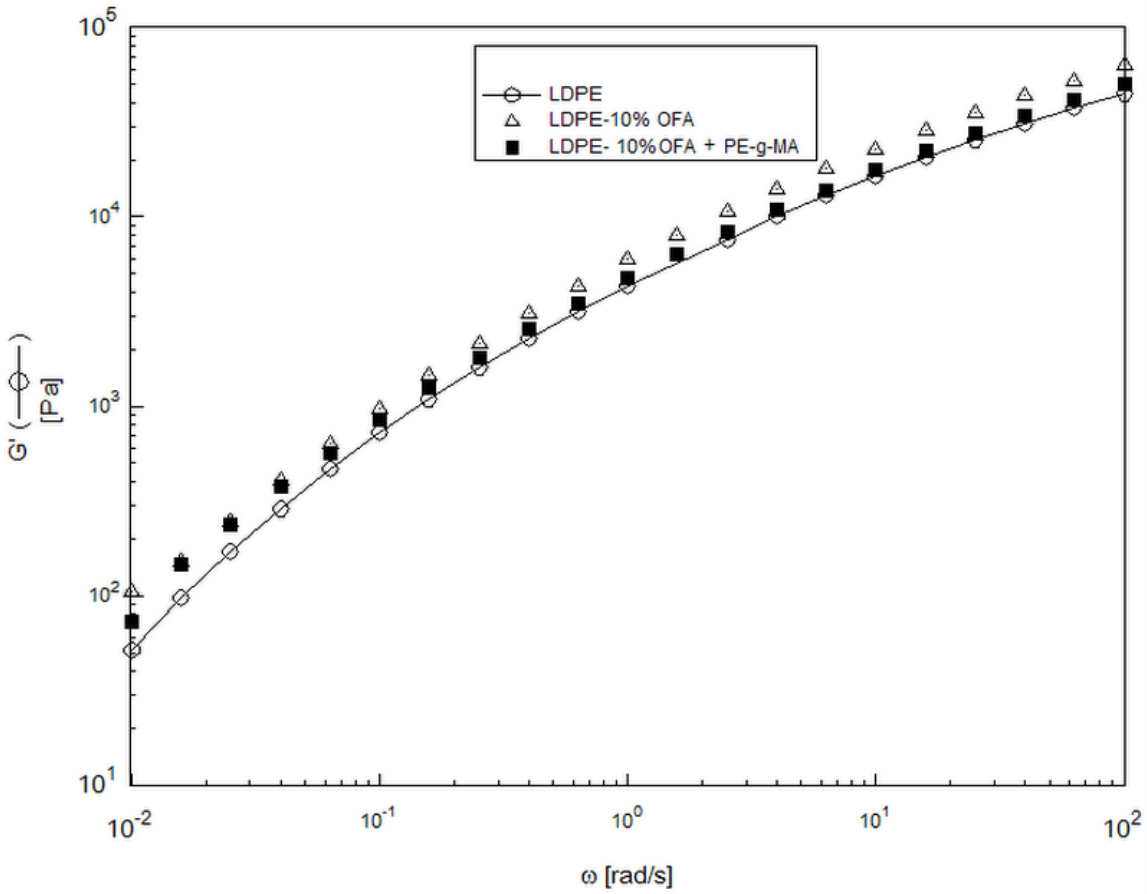

A-12: Effect of PE-g-MA at 10% OFA loading on Storage Modulus

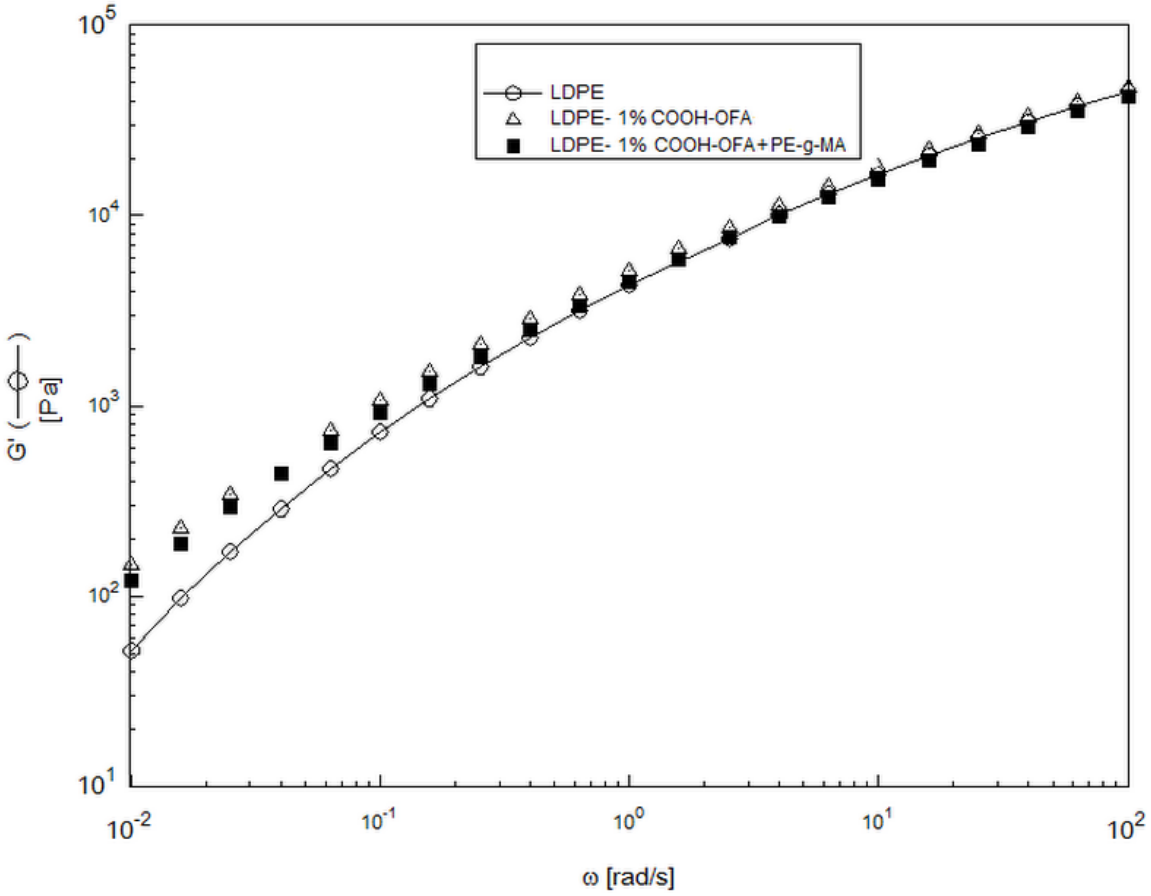

A-13: Effect of PE-g-MA at 1% COOH-OFA loading on Storage Modulus

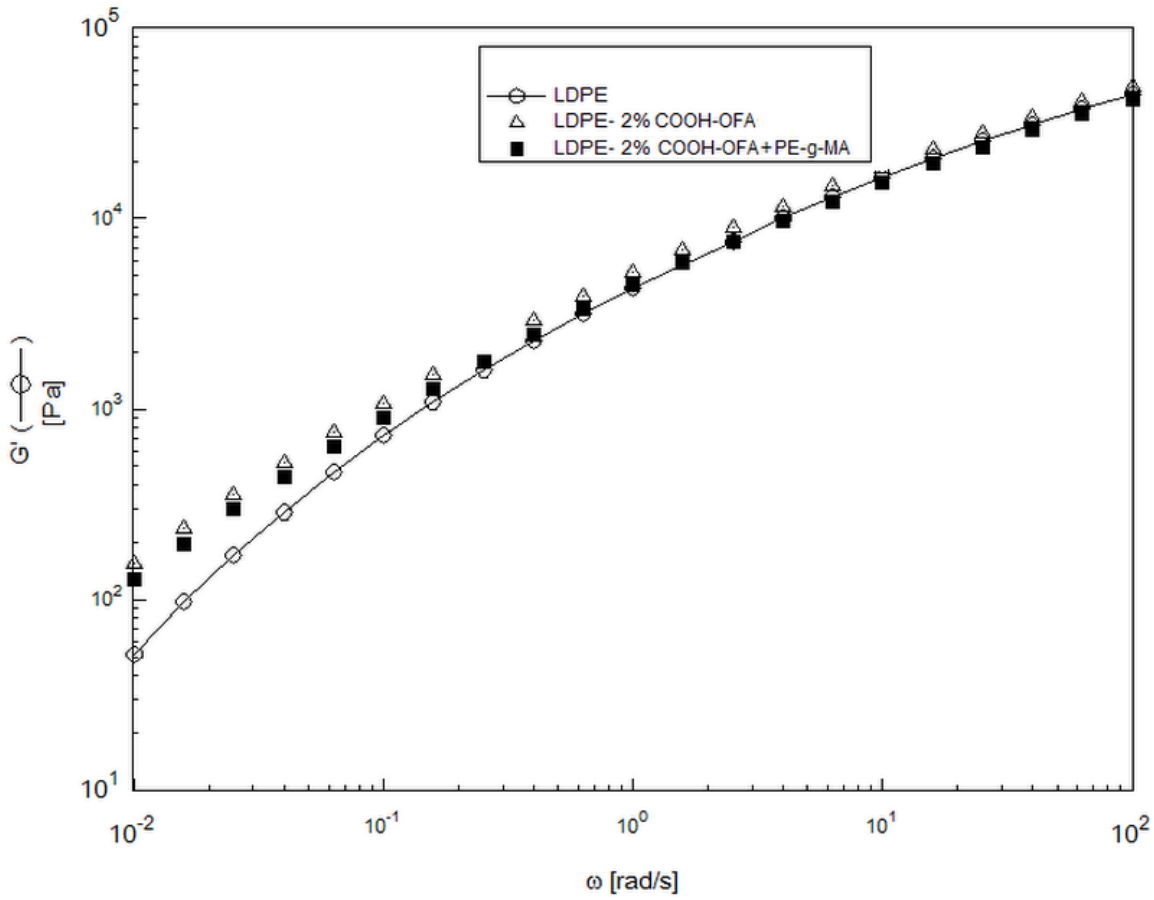

A-14: Effect of PE-g-MA at 2% COOH-OFA loading on Storage Modulus

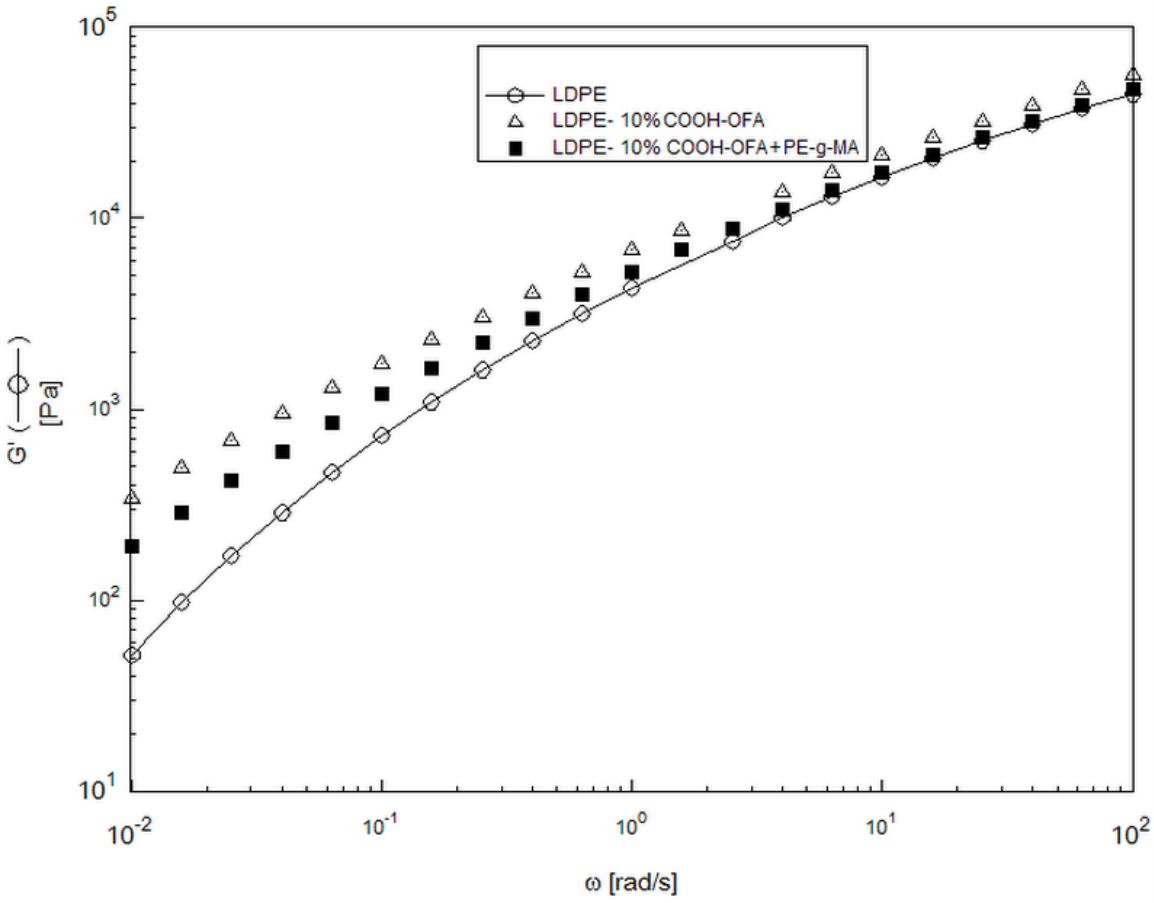

A-15: Effect of PE-g-MA at 10% COOH-OFA loading on Storage Modulus

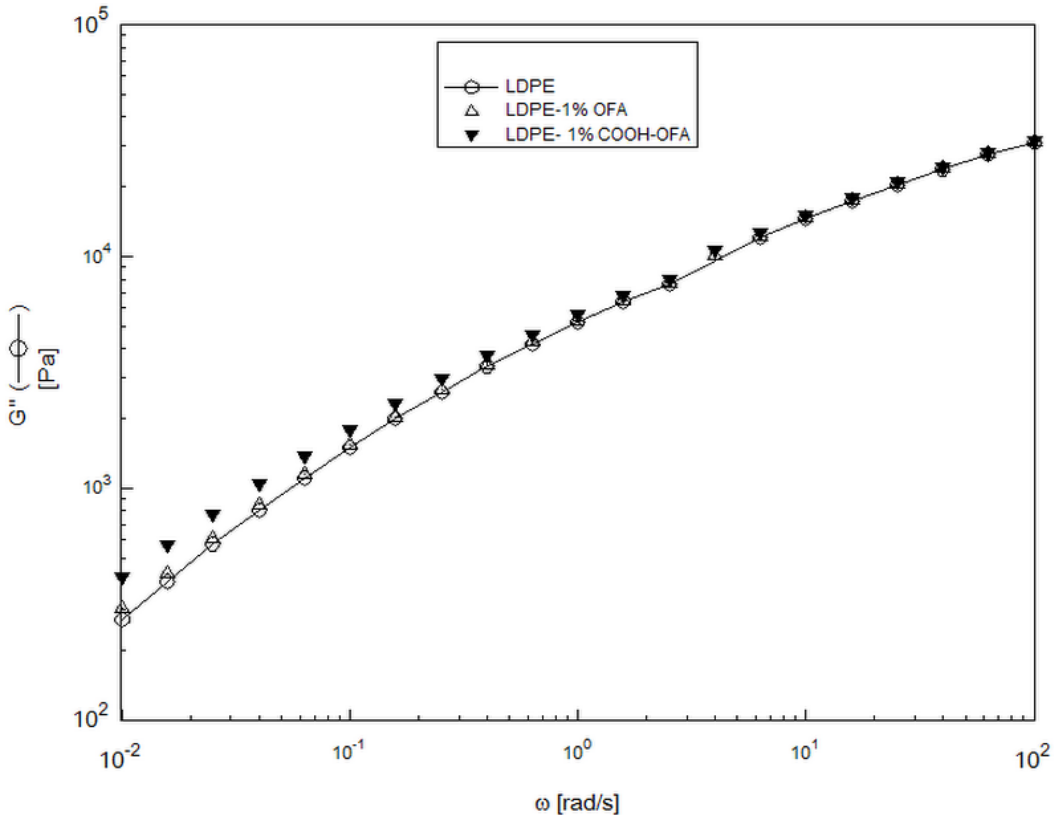

A-16: Effect of OFA-functionalization at 1% loading on Loss Modulus

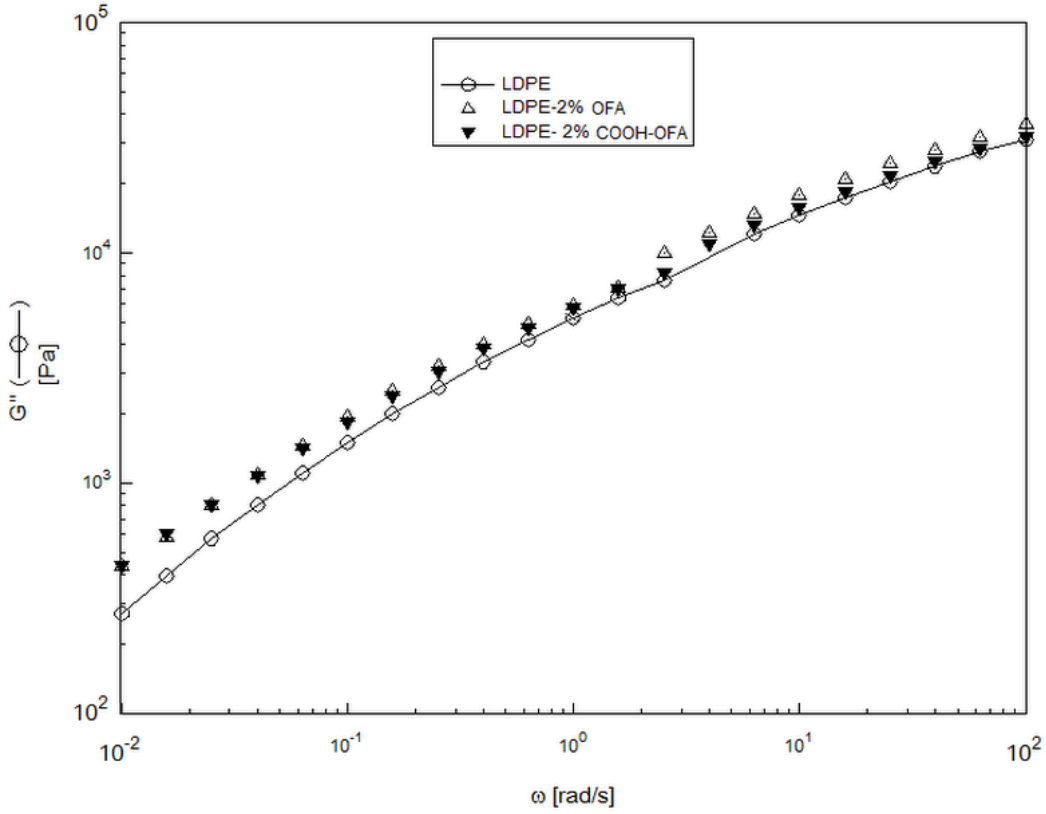

A-17: Effect of OFA-functionalization at 2% loading on Loss Modulus

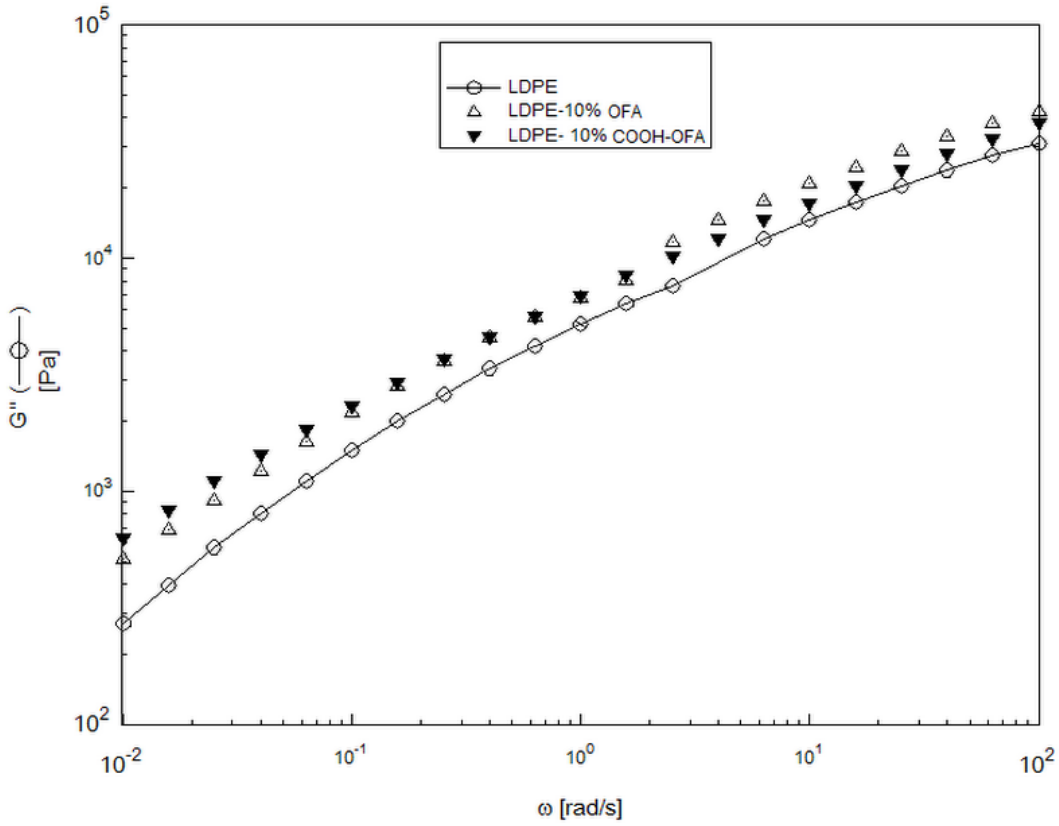

A-18: Effect of OFA-functionalization at 10% loading on Loss Modulus

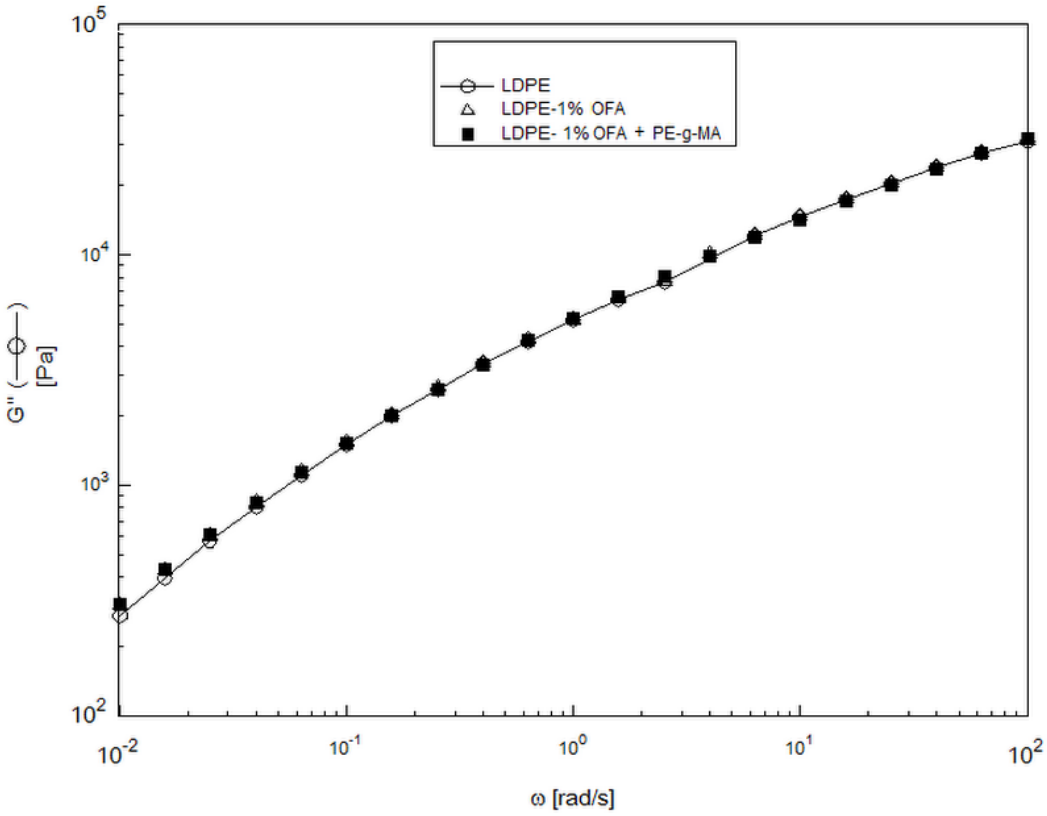

A-19: Effect of PE-g-MA at 1% OFA loading on Loss Modulus

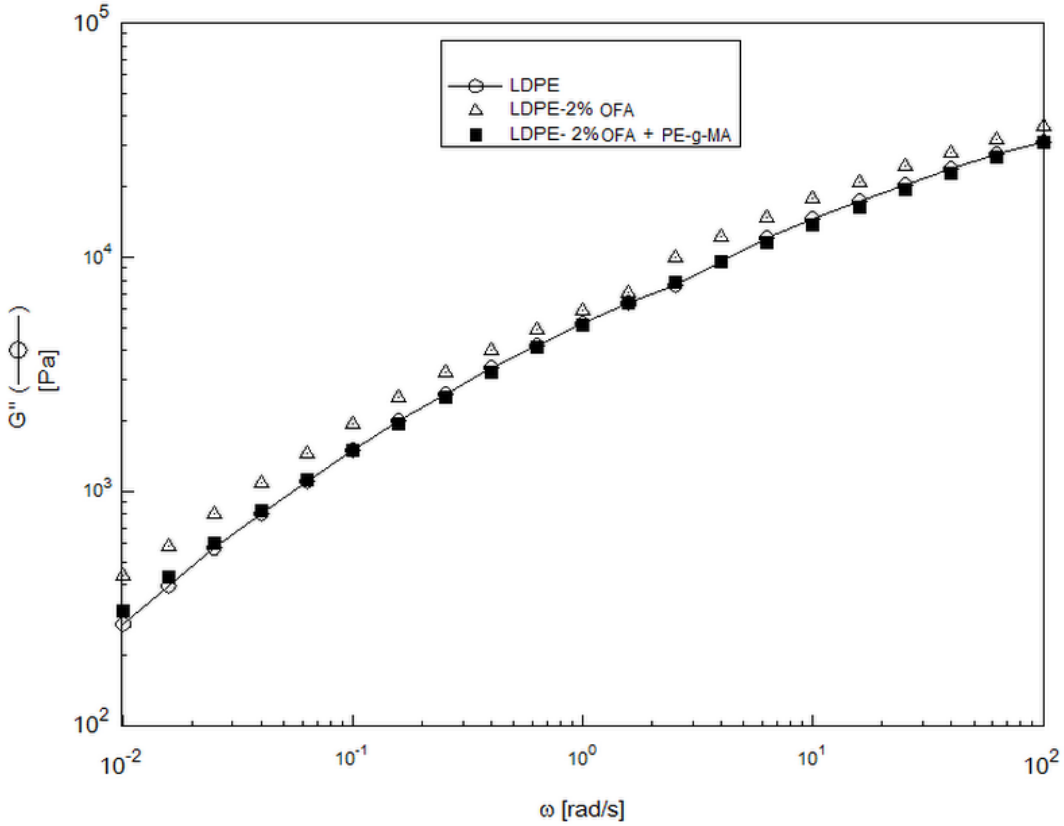

A-20: Effect of PE-g-MA at 2% OFA loading on Loss Modulus

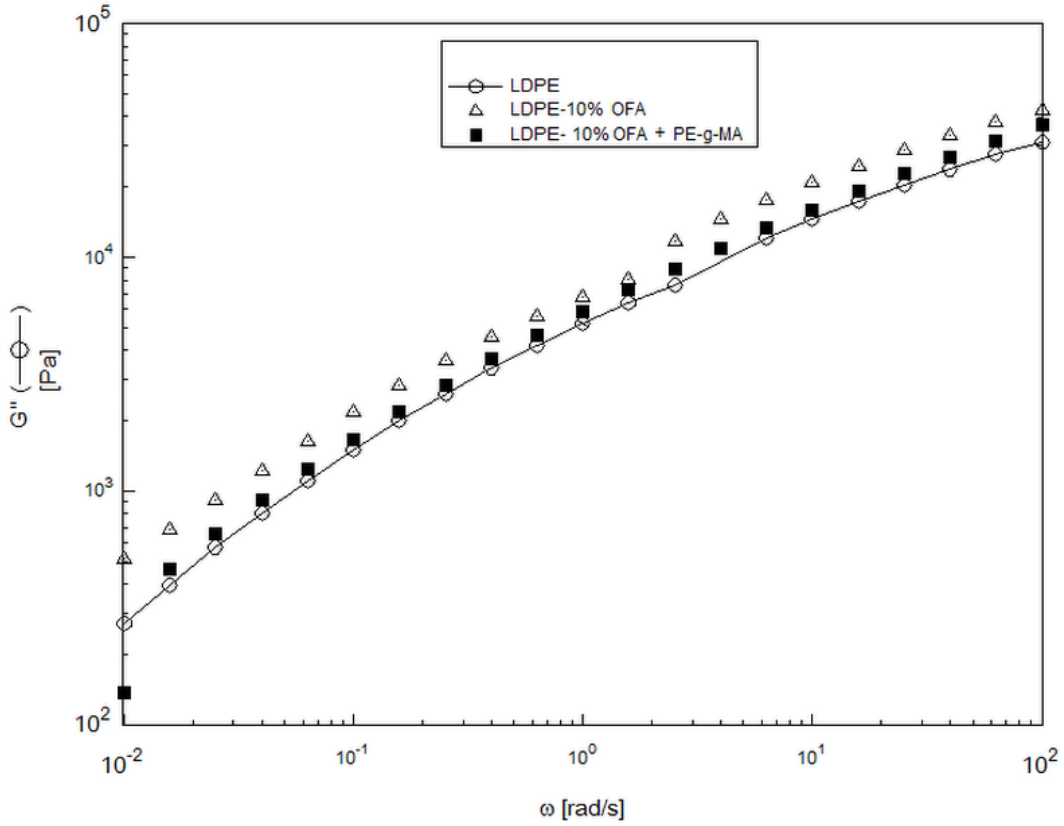

A-21: Effect of PE-g-MA at 10% OFA loading on Loss Modulus

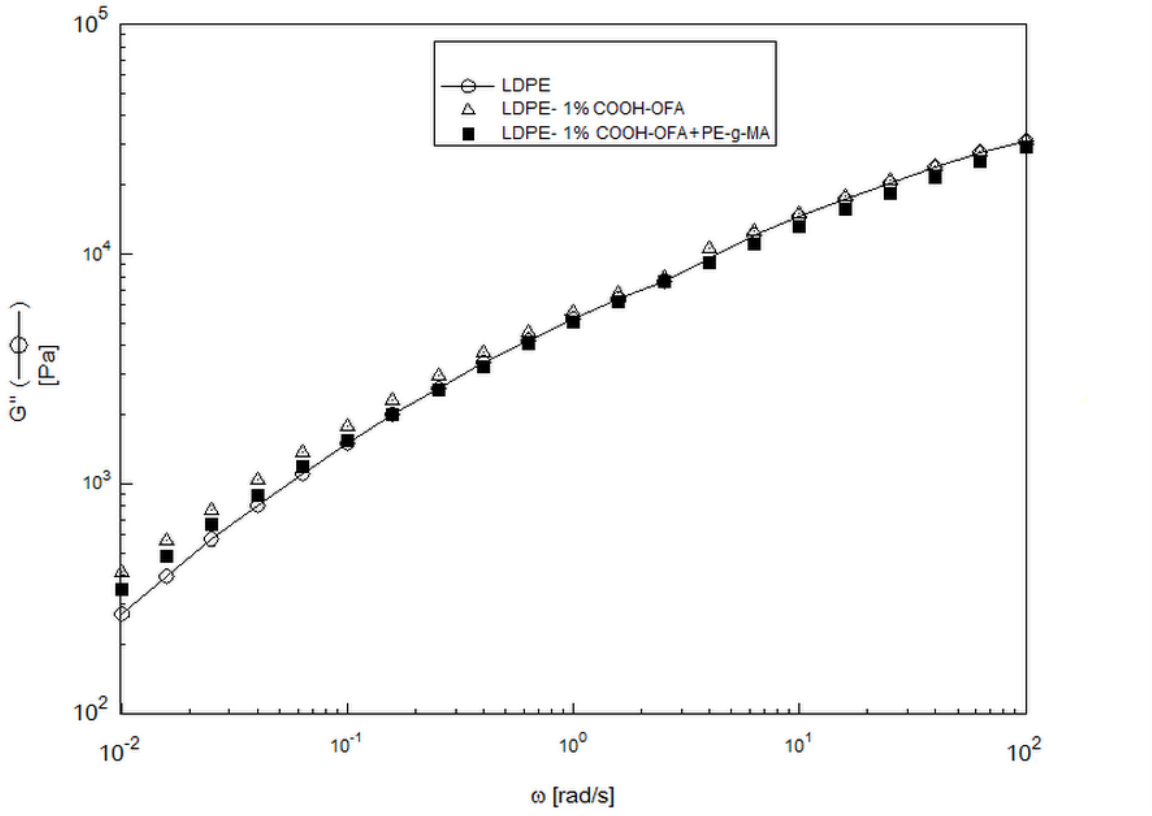

A-22: Effect of PE-g-MA at 1%COOH-OFA loading on Loss Modulus

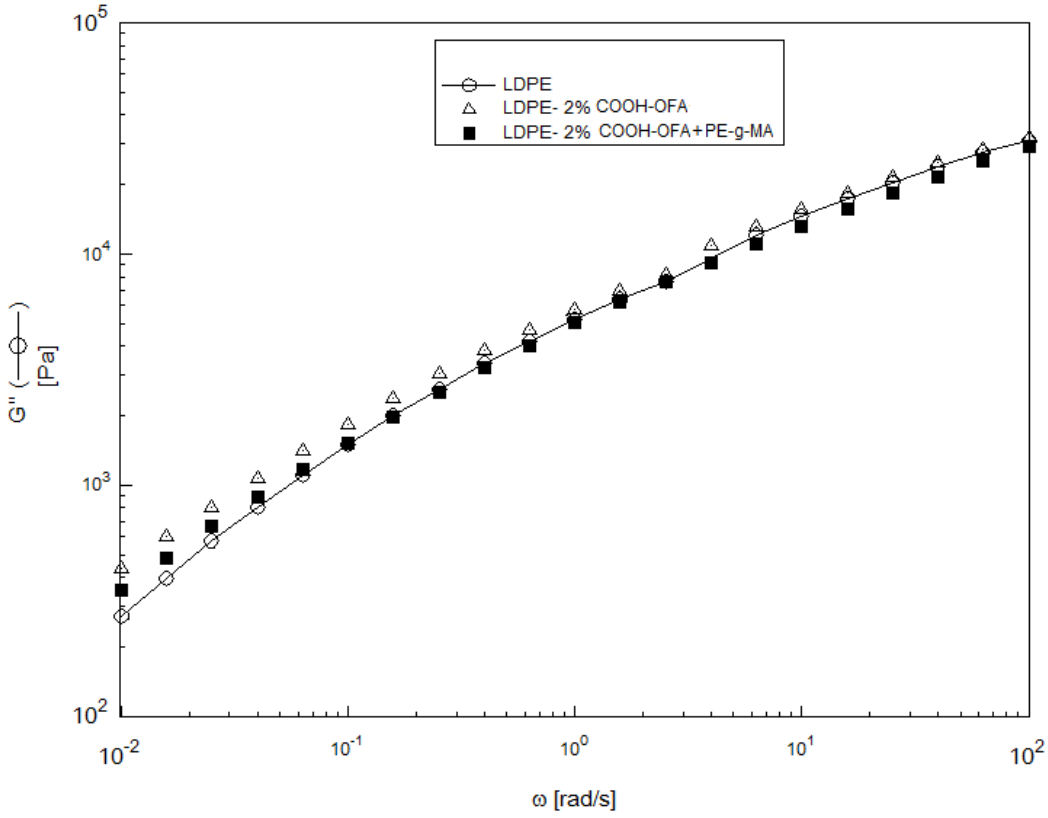

A-23: Effect of PE-g-MA at 2%COOH-OFA loading on Loss Modulus

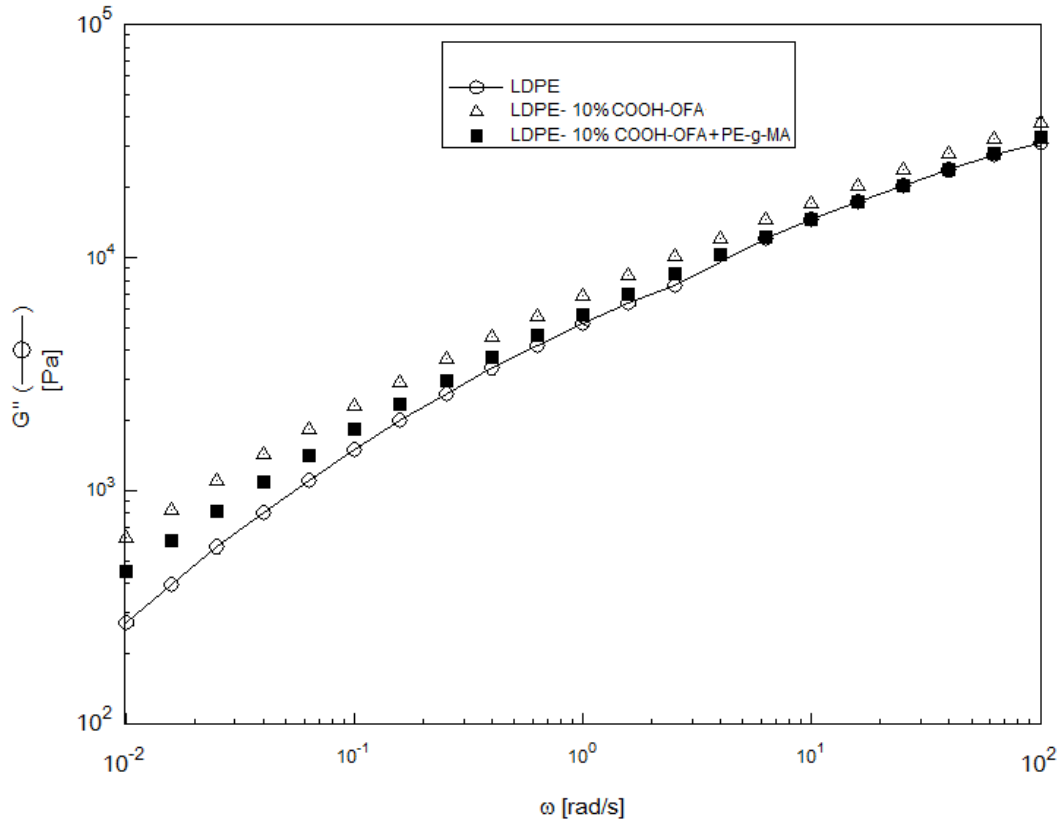

A-24: Effect of PE-g-MA at 10%COOH-OFA loading on Loss Modulus

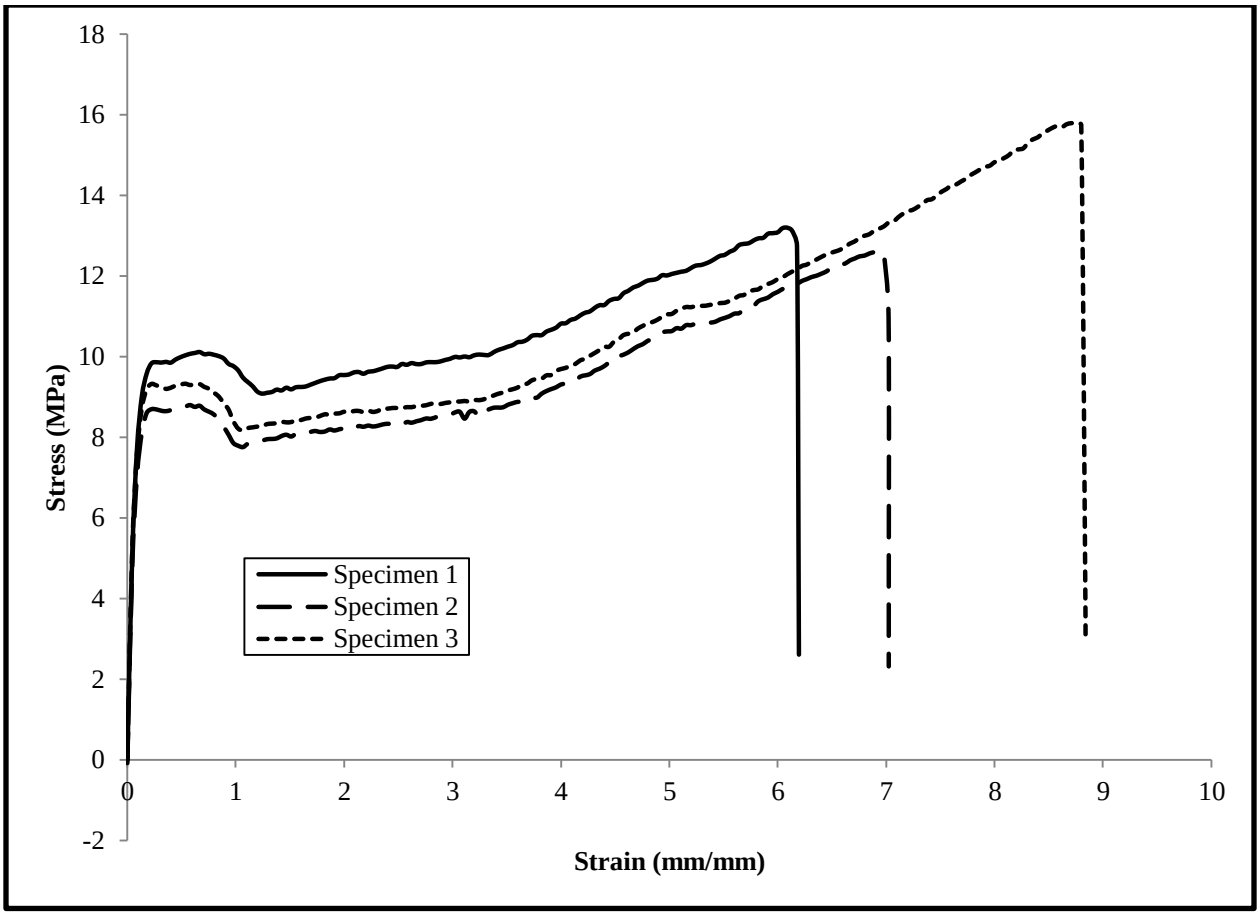

A-25: Stress-Strain Curve of as-received LDPE

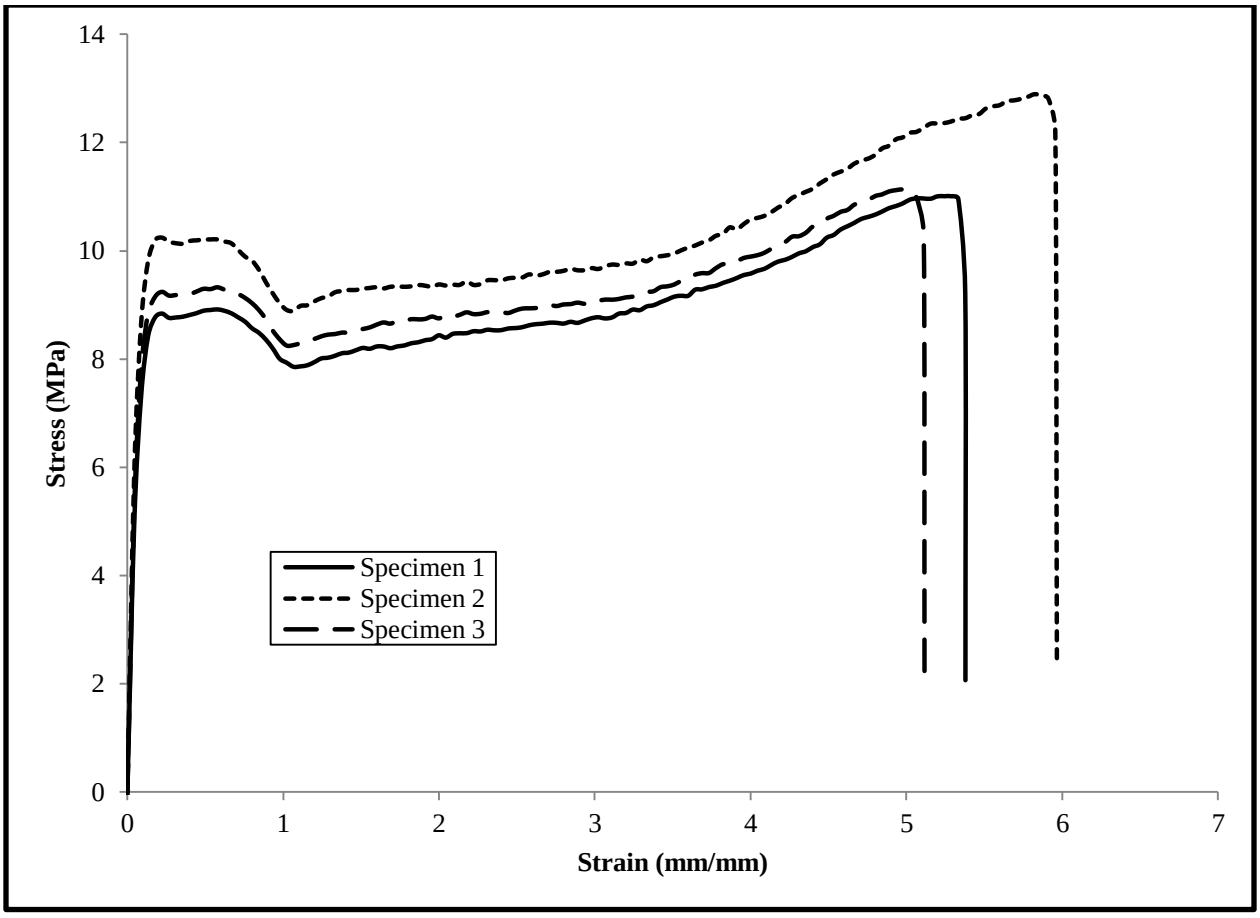

A-26: Stress-Strain Curve of LDPE/OFA composite at 1% unmodified fly ash loading without compatiblizer

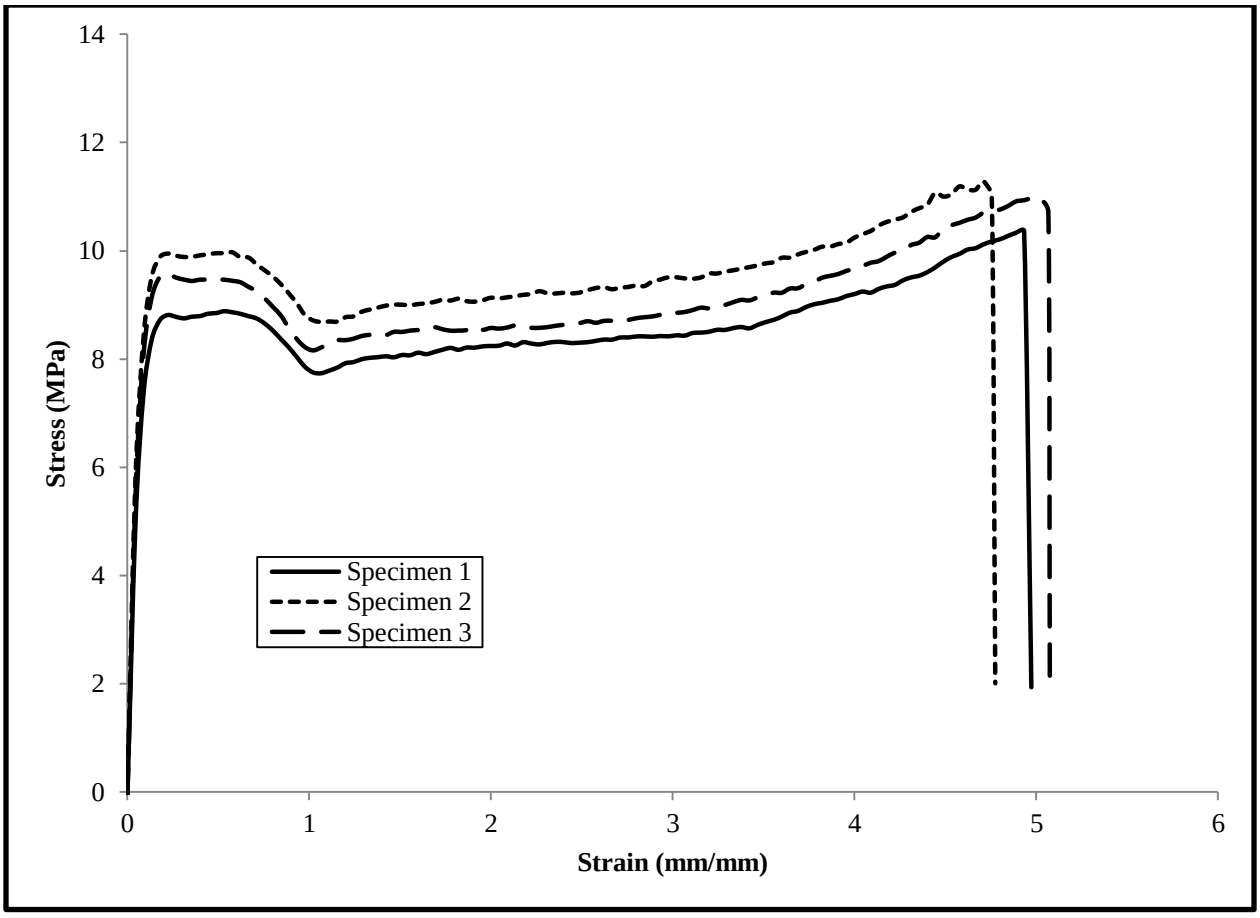

A-27: Stress-Strain Curve of LDPE/OFA composite at 2% unmodified fly ash loading without compatiblizer

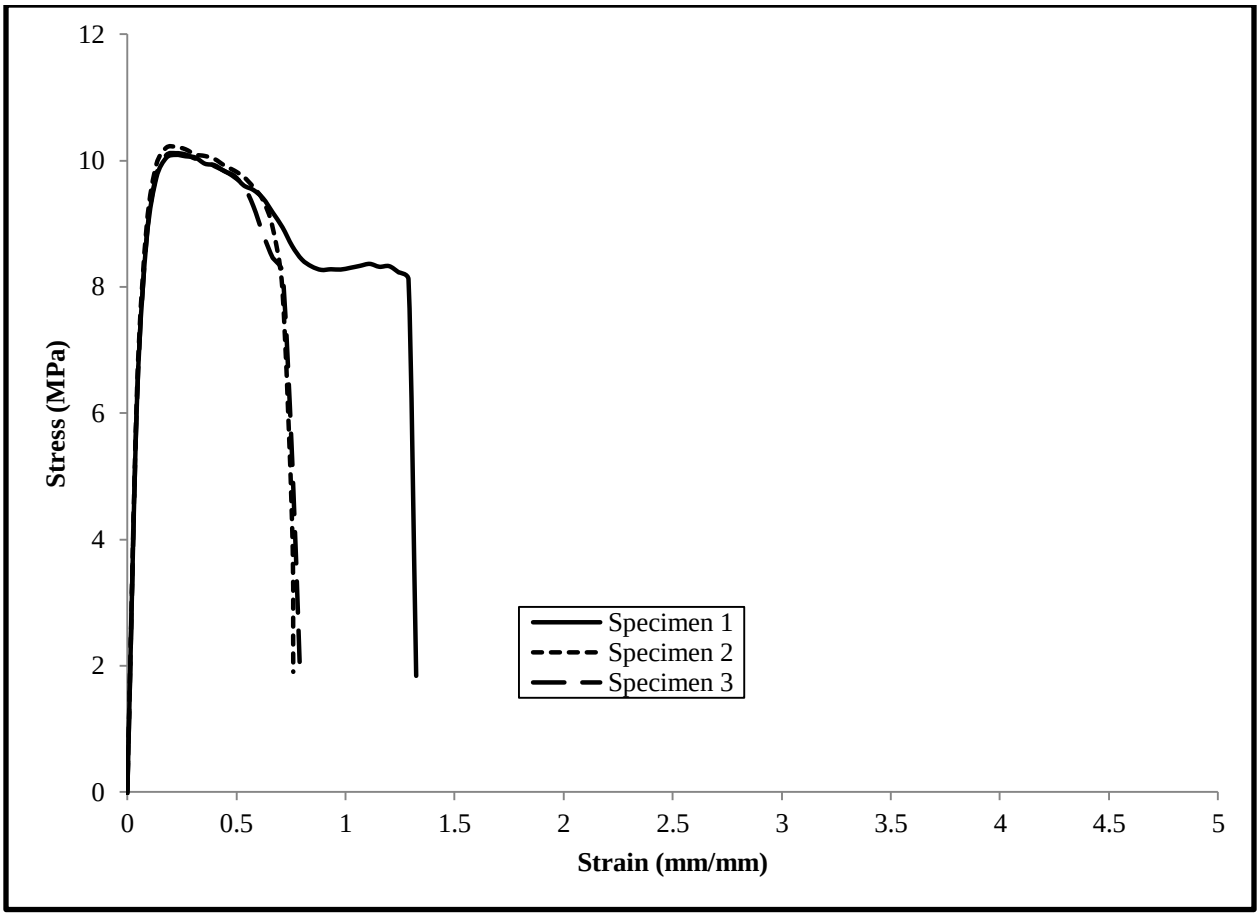

A-28: Stress-Strain Curve of LDPE/OFA composite at 5% unmodified fly ash loading without compatiblizer

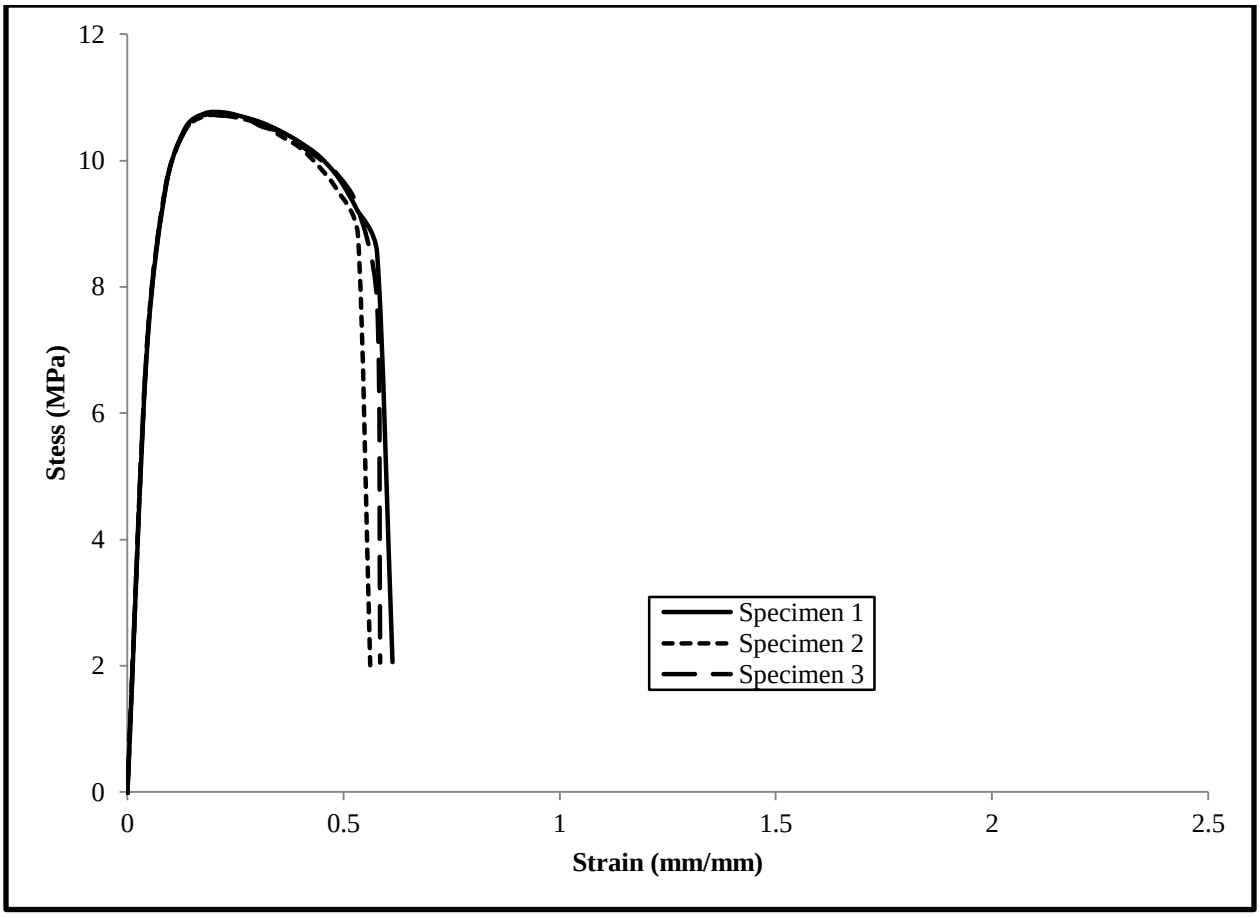

A-29: Stress-Strain Curve of LDPE/OFA composite at 10% unmodified fly ash loading without compatiblizer

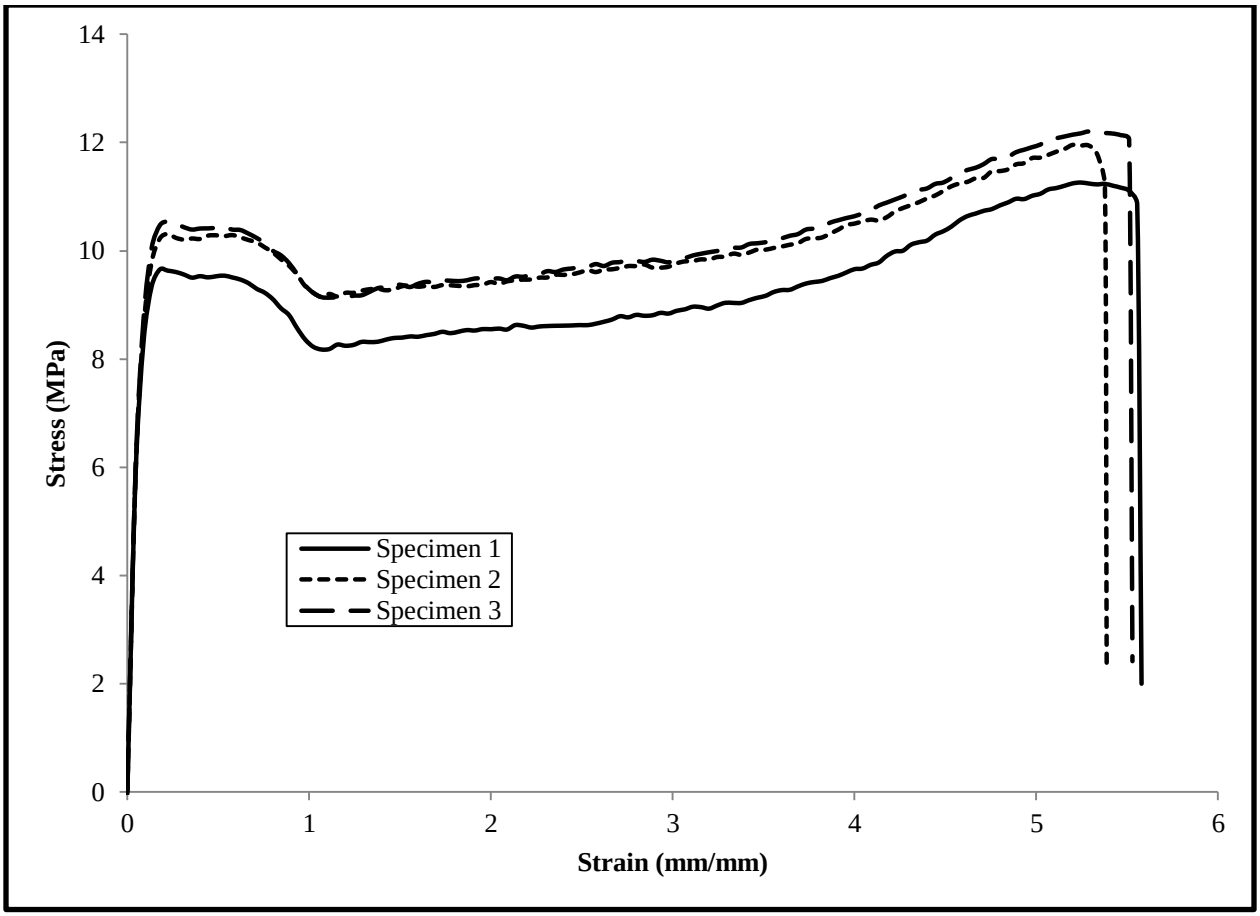

A-30: Stress-Strain Curve of LDPE/OFA composite at 1% unmodified fly ash loading with compatiblizer

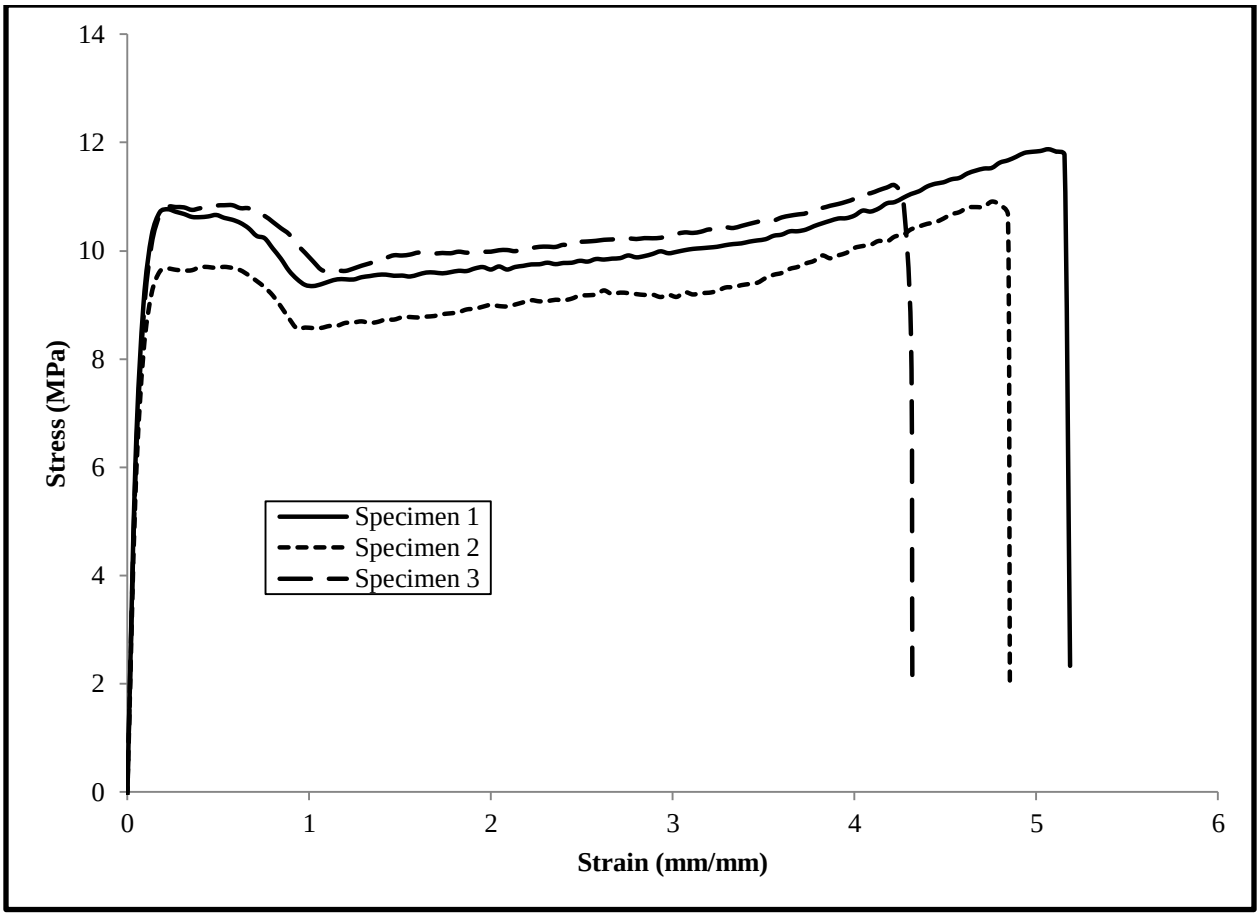

A-31: Stress-Strain Curve of LDPE/OFA composite at 2% unmodified fly ash loading with compatiblizer

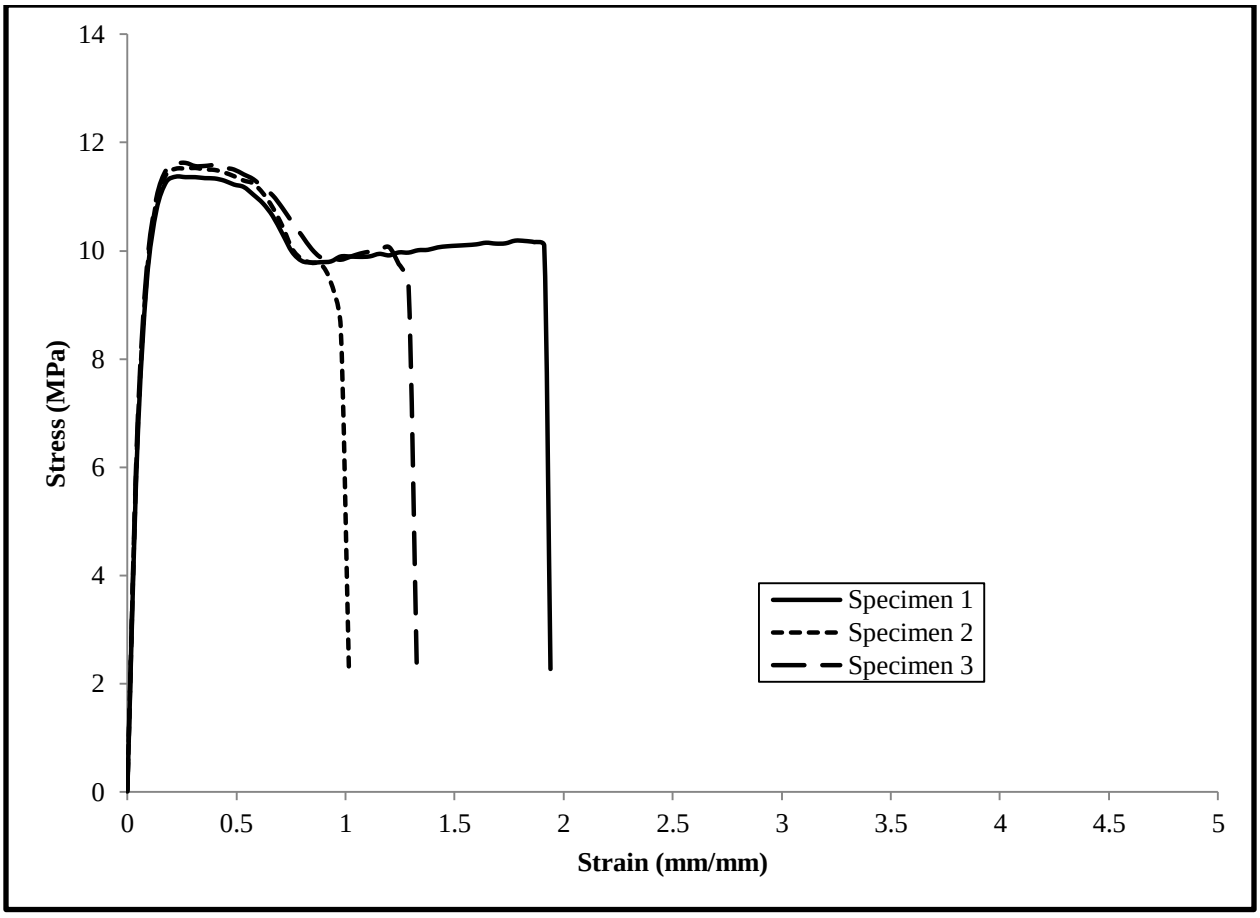

A-32: Stress-Strain Curve of LDPE/OFA composite at 5% unmodified fly ash loading with compatiblizer

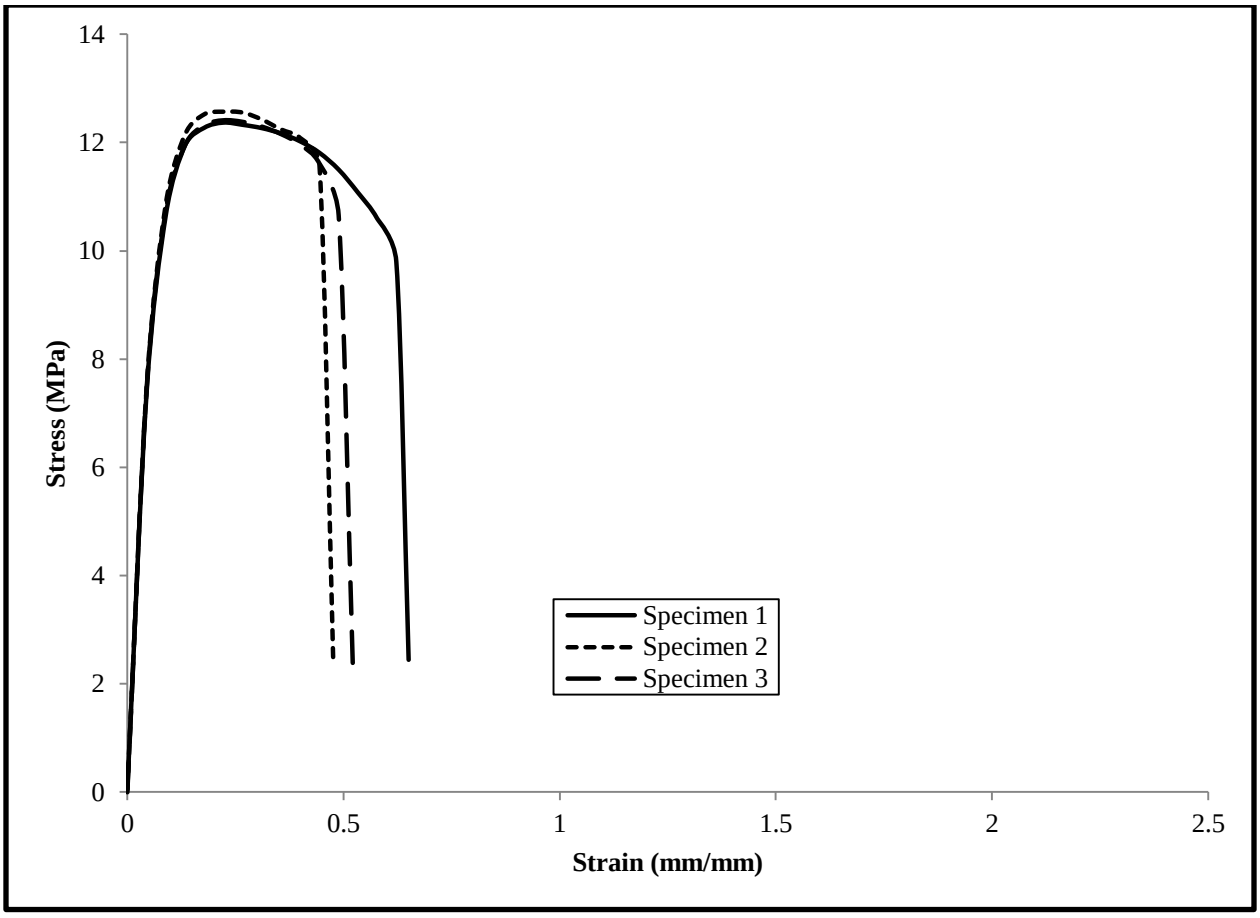

A-33: Stress-Strain Curve of LDPE/OFA composite at 10% unmodified fly ash loading with compatiblizer

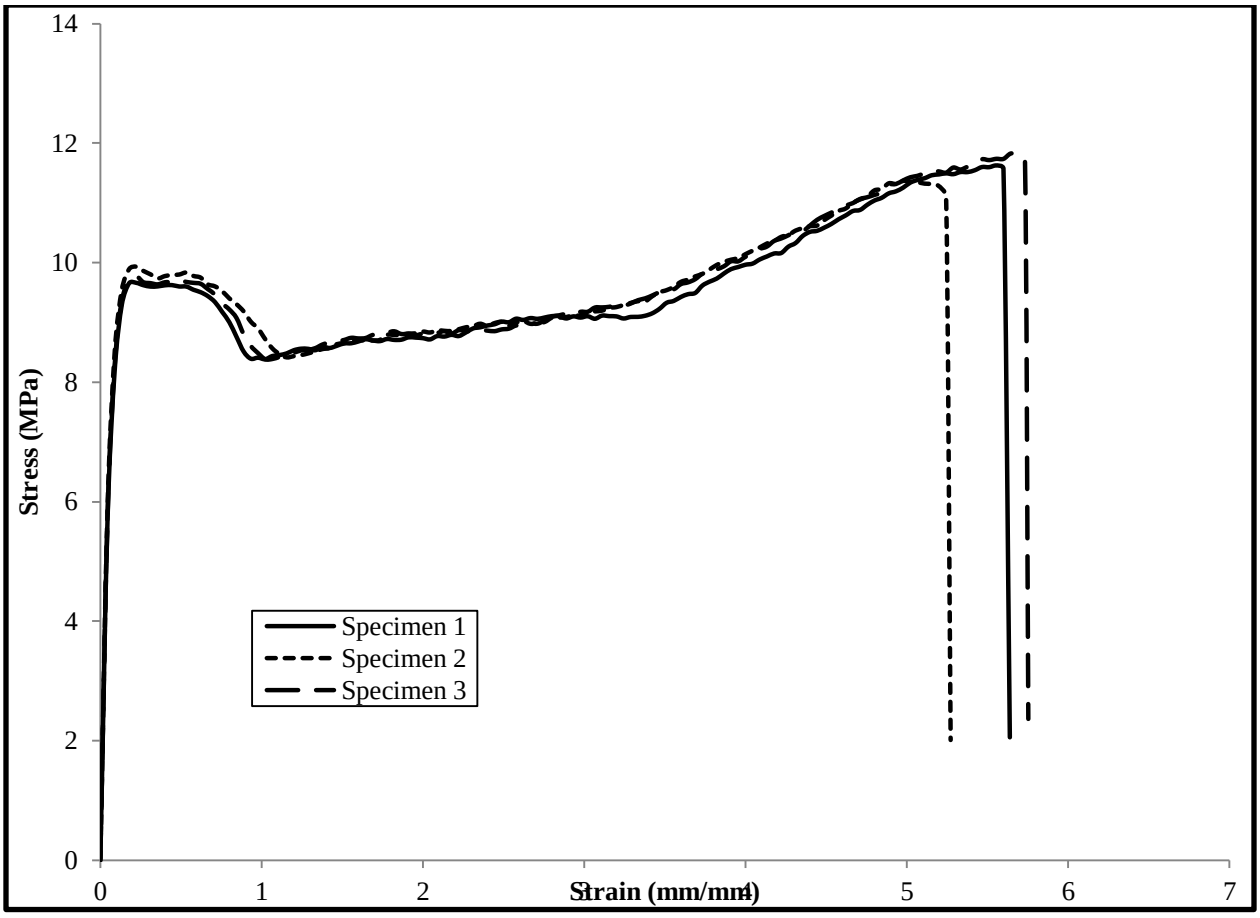

A-34: Stress-Strain Curve of LDPE/OFA composite at 1% modified fly ash loading without compatiblizer

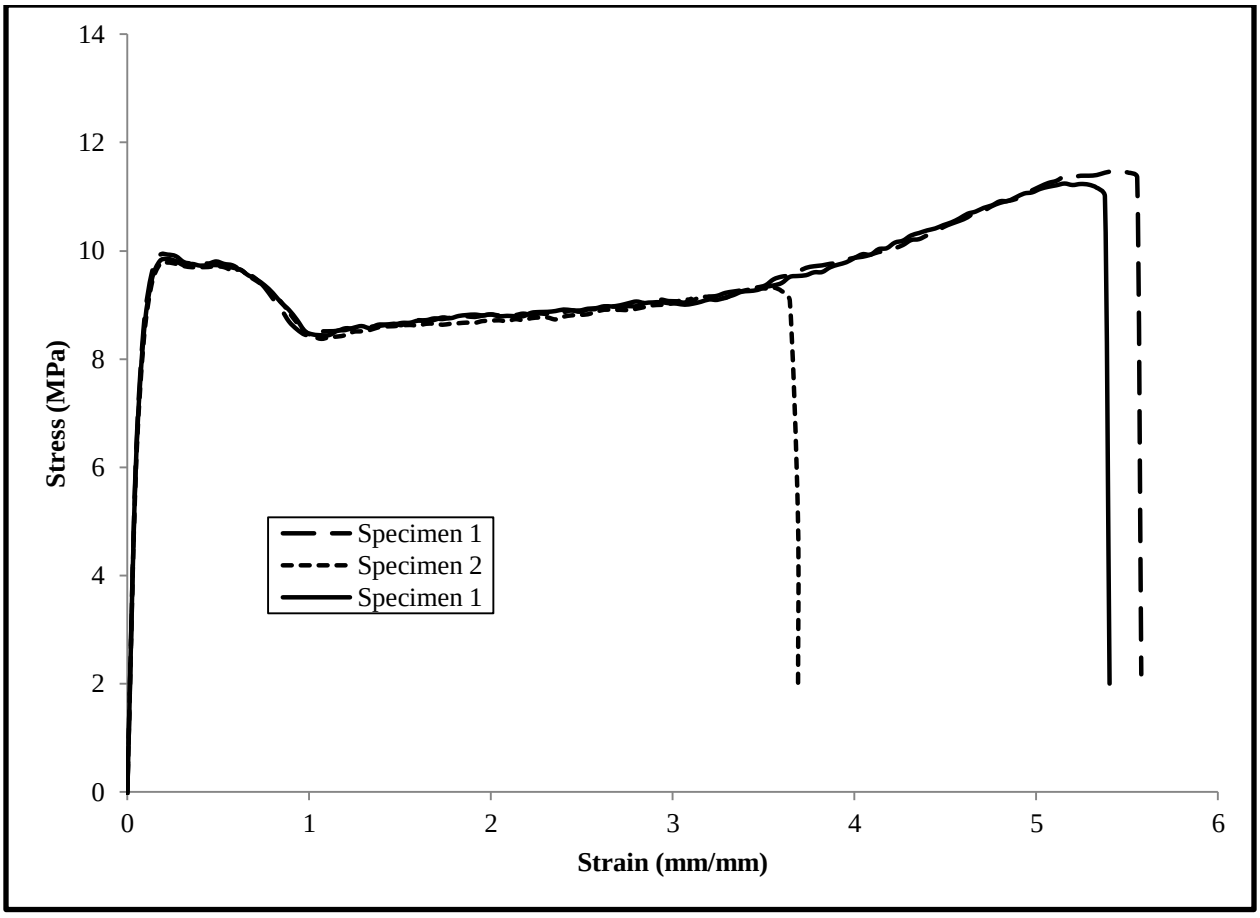

A-35: Stress-Strain Curve of LDPE/OFA composite at 2% modified fly ash loading without compatiblizer

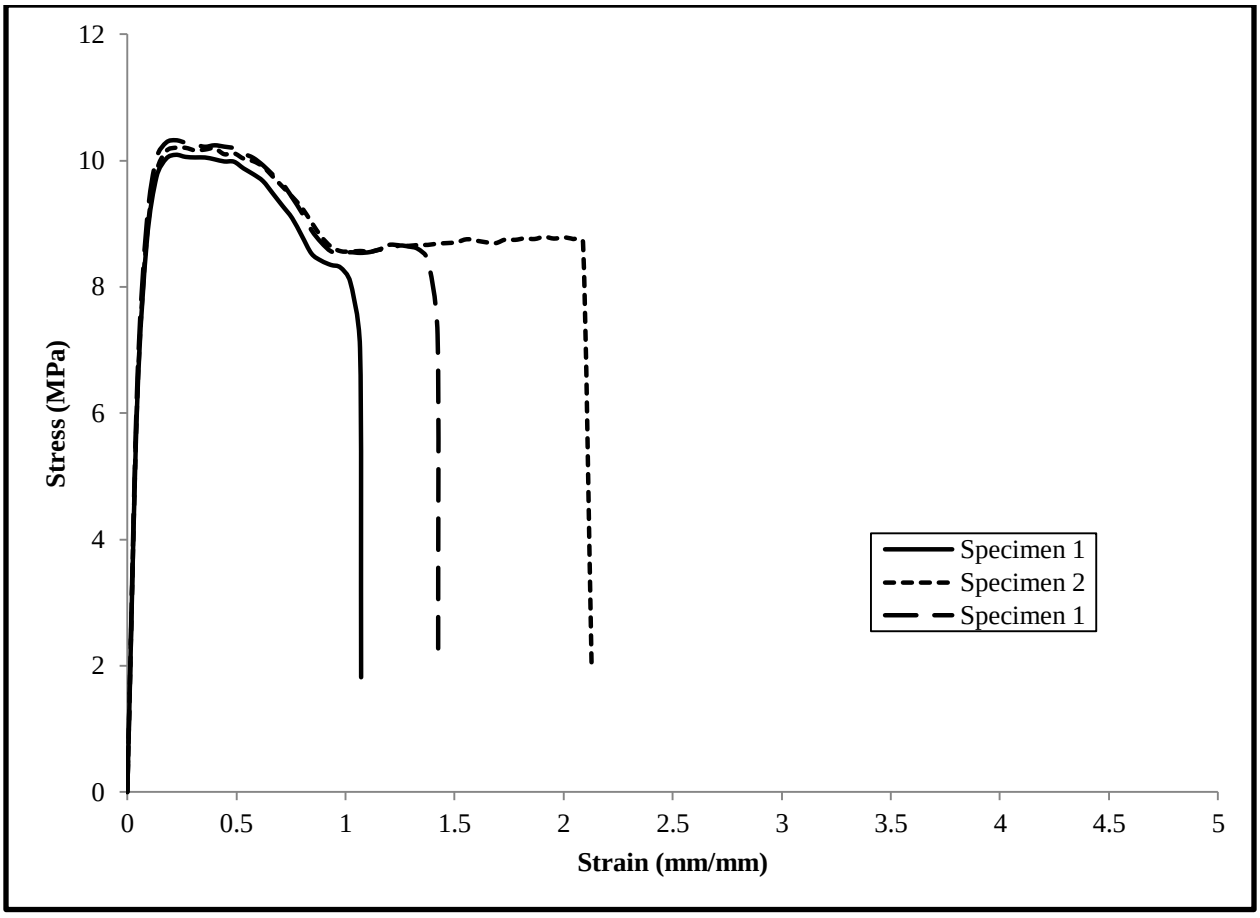

A-36: Stress-Strain Curve of LDPE/OFA composite at 5% modified fly ash loading without compatiblizer

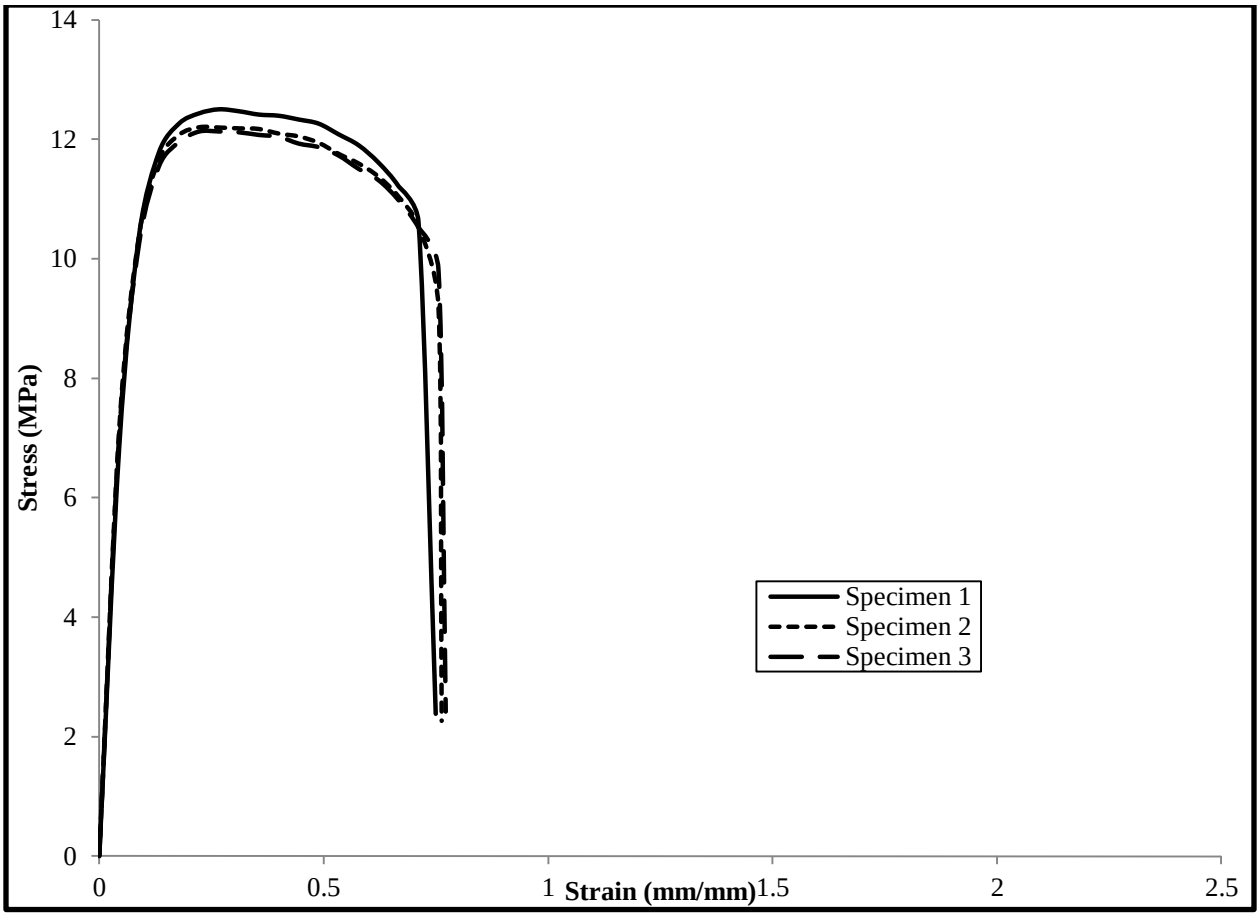

A-37: Stress-Strain Curve of LDPE/OFA composite at 10% modified fly ash loading without compatiblizer

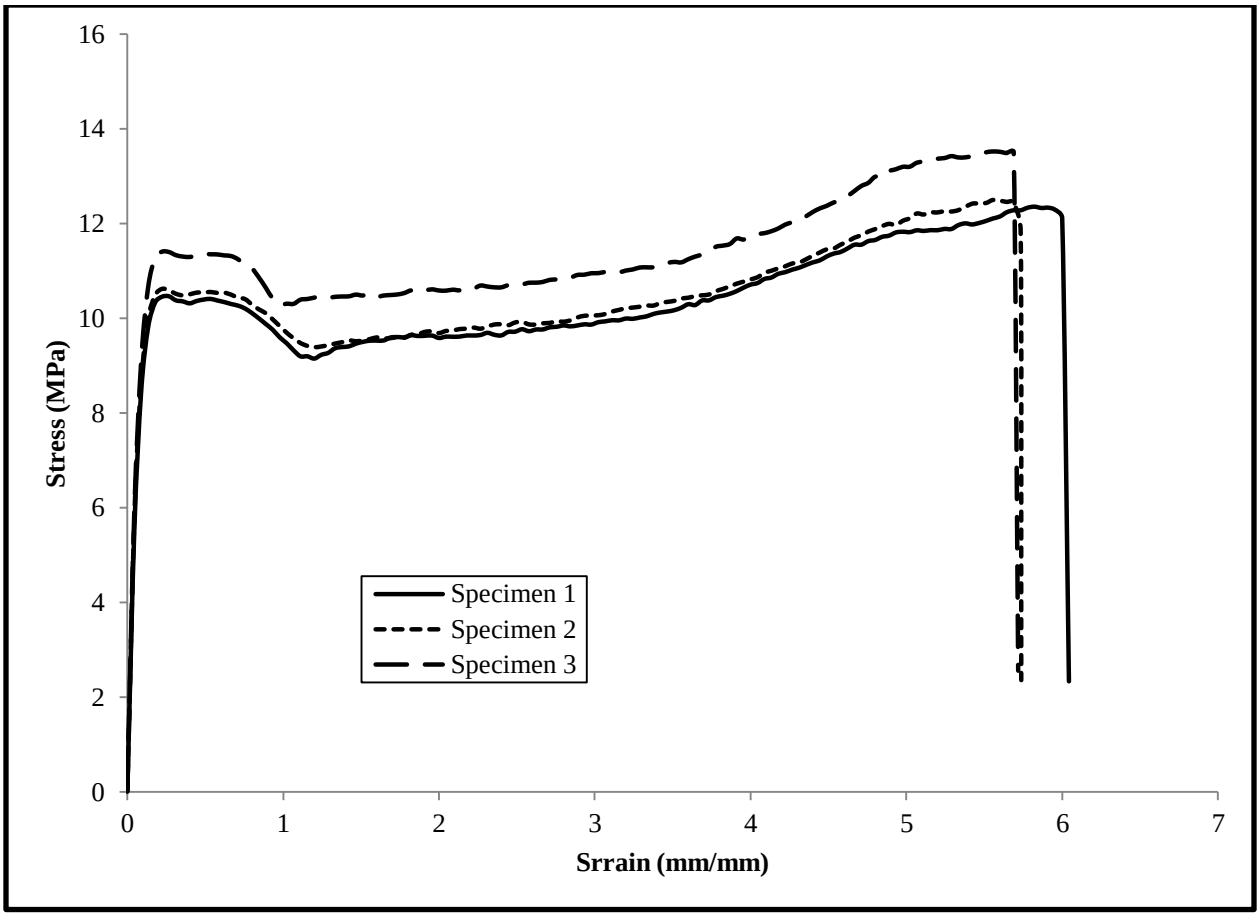

A-38: Stress-Strain Curve of LDPE/OFA composite at 1% modified fly ash loading with compatiblizer

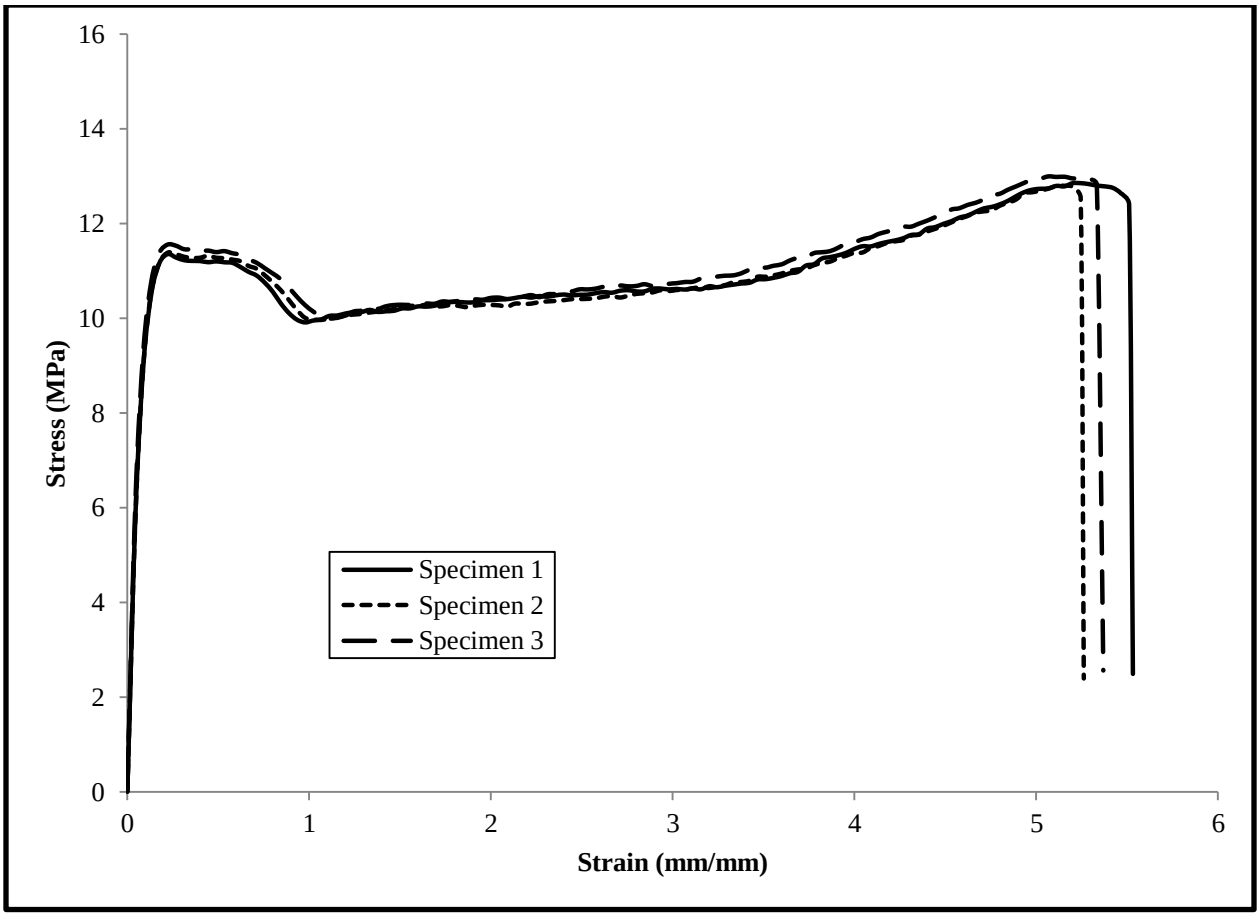

A-39: Stress-Strain Curve of LDPE/OFA composite at 2% modified fly ash loading with compatiblizer

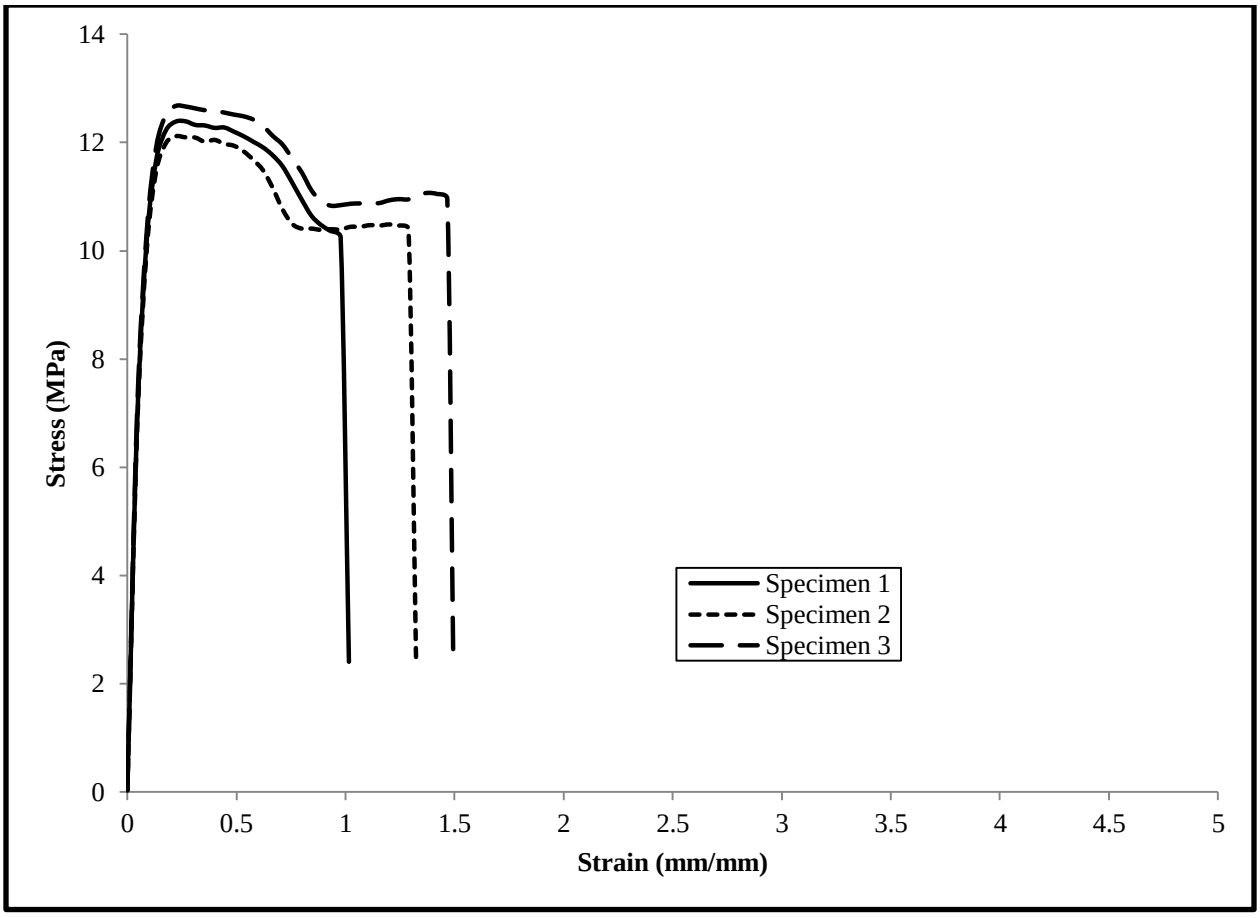

A-40: Stress-Strain Curve of LDPE/OFA composite at 5% modified fly ash loading with compatiblizer

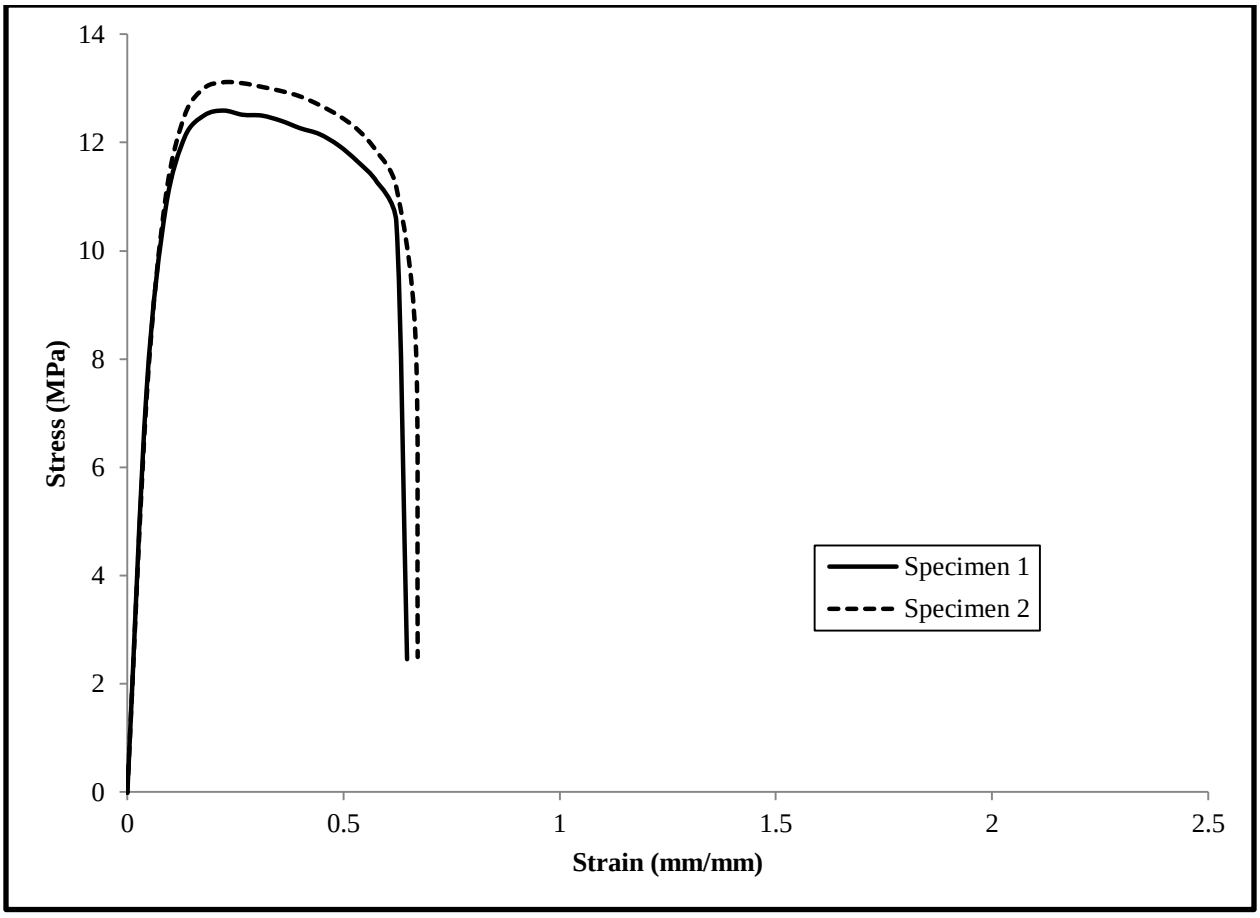

A-41: Stress-Strain Curve of LDPE/OFA composite at 10% modified fly ash loading with compatiblizer

REFERENCES

1. Chemical & Engineering News, 23 February 2009, "The Foul Side of 'Clean Coal," Volume 87, Number 08, pp. 44-47.
2. Chemical & Engineering News, 21 December 2009, "Year In Review," Volume 87, Number 51, pp. 24 – 29.
3. Woo-Teck, K. K. Dong-Hyun and K. Yung-Phil, "Characterization of Heavy Oil Fly Ash Generated from a Power Plant," Journal of Materials Online, 2005.
4. "Managing Coal Combustion Residues in Mines, Committee on Mine Placement of Coal Combustion Wastes," National Research Council of the National Academies, 2006.
5. "Human and Ecological Risk Assessment of Coal Combustion Wastes," RTI, Research Triangle Park, prepared for the U.S. Environmental Protection Agency, August 6, 2007.
6. Y.T. Riu B.G. Kim, Y.Y. Choi, S.Y. Hong S.K. Hwang and J.H. Park, "Properties and combustion characteristics of heavy oil fly ash," J. Korea Solid Wastes Engineering Society, 13, 236-246, 1996.
7. K.Q. Xiao, L.C. Zhang and I. Zarudi, "Mechanical and rheological properties of carbon nanotubes-reinforced Polyethylene composites," Composites Science and Technology, 67, 177-182, 2007.
8. L.-P. Cheng, D.-J. Lin and K.-C. Yang, "Formation of mica-intercalated-Nylon 6 nanocomposite membrane by phase inversion method," J. Membr. Sci. 172, pp. 157–166, 2000.

9. Yong Lei, Qinglin Wu and Craig M. Clemons, "Preparation and Properties of Recycled HDPE/Clay Hybrids," J. Appl. Poly. Sci. 103, 3056-3063, 2007.

10. Xing, Z, Fuel and Energy Abstr, 37,185, 1996.

11. J. Y. Hwang, X. Sun, Z. Li, "Unburned Carbon from Fly Ash for Mercury Adsorption: I. Separation and Characterization of Unburned Carbon," Journal of Minerals & Materials Characterization & Engineering, Vol 1, 39-60, 2002.

12. J. Y. Hwang, "Beneficial Use of Fly Ash," Michigan Technological University, Institute of Materials Processing, 1999.

13. Abu-Rizaiza, A.S., "Characteristics of Fly Ash from Residual Oil Combustion at Rabigh Electric Power Plant," Journal of Environmental Science, Institute of Environmental Studies and Research, Ain Shams University, Vol. 8, 2004.

14. Daous, M.A., "Utilization of Cement Kiln Dust and Fly Ash in Cement Blends in Saudi Arabia," Journal of King Abdulaziz University: Engineering Sciences, Vol. 15, No. 1, pp. 33-45, 2004.

15. Suryasarathi Bose & P.A.Mahanwar, "Effect of Fly Ash on the mechanical, thermal, dielectric, rheological and morphological properties of filled Nylon 6," Journal of Minerals & Materials Characterization & Engineering, Vol. 3, No.2, pp 65-89, 2004.

16. U. Atikler, D. Basalp, F. Tihminlioglu, "Mechanical and Morphological Properties of Recycled High-Density Polyethylene, Filled with Calcium Carbonate and Fly Ash," J Appl. Polymer Sci. 102, 4460–4467, 2006.

17. Woo-Teck, K., K. Dong-Hyun, and K. Yung-Phil, "Characterization of Heavy Oil Fly Ash Generated from a Power Plant," AZ Journal of Materials on Line, 2005.

18. Yang Yu-Fen, Gai Guo-Sheng, Cai Zhen-Fang and Chen Qing-Ru, “Surface Modification of Purified Fly Ash and application in polymer,” Journal of Hazardous Materials B133, 276–282, 2006.
19. Kishore, SM Kulkarni, D Sunil and S Sharathchandra, “Effect of surface treatment on the impact behavior of fly-ash filled polymer composites,” Polym. Int 51:1378–1384, 2002.
20. Thongsang and N. Sombatsompop, “Effect of NaOH and Si69 treatment on the properties of Fly Ash/Natural Rubber Composites,” Polymer Composites, 27:30-40, 2005.
21. Ya-Ping Sun, Kefu Fu, Yi Lin, Weikie Huang, “Functionalized Carbon Nanotubes: Properties and Applicatons,” Accounts of Chemical Research, 35, 1096-1104, 2002.
22. Chen J. Hamon, M. A. Hu, H. Chen, Y., Rao, A. M. Eklund, P.C. Haddon, R. C., “Solution properties of single-walled carbon nanotubes” Science, 282, 95, 1998.
23. Chen, J. Rao, A. M. Lyuksyutov, S. Itkis, M. E. Hamon, M. A. Hu, H. Cohn, R. W. Eklund, P. C. Colbert, D. T. Smalley, R. E. Haddon. R. C., “Dissolution of full-length single-walled carbon nanotubes,” J. Phys. Chem. B, 105, 2525-2528 2001.
24. Hyun Y. H. Lim S. T. Choi H. J. Jhon M. S., "Rheology of Poly(ethylene oxide)/Organoclay Nanocomposites", Macromolecules, 34, 8084-8093, 2001.
25. Wu D.; Wang X.; Song Y.; Jin R., "Nanocomposites of Poly(vinyl chloride) and Nanometric Calcium Carbonate Particles: Effects of Chlorinated Polyethylene on Mechanical Properties, Morphology, and Rheology", J Appl. Polym. Sci., 92, 2714–2723, 2004.

26. N. Sombatsompop, S. Thongsang, T. Markpin, E. Wimolmala, "Fly Ash Particles and Precipitated Silica as Fillers in Rubbers. I. Untreated Fillers in Natural Rubber and Styrene–Butadiene Rubber Compounds," J Appl Polym Sci 93, 2119-2130, 2004.
27. J. Y. Hwang, "B. Plastic Filler Applications of Fly Ash," Michigan Technological University, Beneficial Use of Fly Ash.
28. Chen G. X.; Kim E. S.; Yoon J. S., "Poly(butylene succinate)/Twice Functionalized Organoclay Nanocomposites: Preparation, Characterization, and Properties," J. Appl. Polym. Sci., 98, 1727–1732, 2005.
29. Lim Y. T.; Park O.O., "Rheological evidence for the microstructure of intercalated polymer/layered silicate nanocomposites," Macromol. Rapid Commun., 21**,** 231–235, 2000.
30. McNally T, P. Potschkeb, P. Halley, M. Murphy, D. Martin, S.E.J. Bell, G.P. Brennan, D. Bein, P. Lemoine, J.P. Quinn, "Polyethylene multiwalled carbon nanotube composites," Polymer, 46, 8222, 2005.
31. Ahmad Mohaddespour, Seyed Javad Ahmadi, Hossein Abolghasemi and Shahryar jafarinejad, "Thermal stability, mechanical and adsorption resistant properties of HDPE/PEG/Clay nanocomposites on exposure to electron beam," CHE, Tehran University, e-polymers journal, 2008.
32. S. H. Bidkar, A. G. Patil, U. R. Kapadi, D. G. Hundiwale, "Flyash as a Co-Filler for Elastomer Composites," North Maharashtra University, Jalgaon, International Journal of Polymeric Materials, 55:135–145, 2006.

33. Bing-Xing Yang, Jia-Hua Shi, K.P. Pramoda, Suat Hong Goh, “Enhancement of the mechanical properties of polypropylene using polypropylene-grafted multiwalled carbon Nanotubes,” Composites Science and Technology, 68, 2490-2497, 2008.

34. Yang BX, Pramoda KP, Xu GQ, Goh SH., “Mechanical reinforcement of polyethylene using polyethylene-grafted multiwalled carbon nanotubes,” Adv. Functional Material 2007.

35. Michael J. O'Connell, Peter Boul, Lars M. Ericson, Chad Huffman, Yuhuang Wang, Erik Haroz, Cynthia Kuper, Jim Tour, Kevin D. Ausman, Richard E. Smalley, “Reversible water-solubilization of single-walled carbon nanotubes by polymer wrapping,” Chemical Physics Letters, 342, 265-271, 2001

36. Ami Eitan , Kuiyang Jiang, Doug Dukes, Rodney Andrews, Linda S. Schadler, “Surface Modification of Multiwalled Carbon Nanotubes: Toward the Tailoring of the Interface in Polymer Composites,” Chem. Mater., 15, 3198-3201, 2003.

37. Gregg, S.; L.Sing, Adsorption, surface area and porosity. 2nd ed.; Academic Press: Lond.

38. Ibnelwaleed A. Hussein and Michael C. Williams, “Rheological Study of Heterogeneities in Melt Blends of ZN-LLDPE and LDPE: Influence of Mw and Comonomer Type, and Implications for Miscibility," Rheologica Acta, 43 (6), 602-614, 2004.

39. Yaofa, J.; Elswick, E. R.; Mastalerz, M., Progression in sulfur isotopic compositions from coal to fly ash: Examples from single-source combustion in Indiana. International Journal of Coal Geology 2008, 73, (3-4), 273-284.

40. 15. Speight, J. G., Handbook of coal Analysis. John Wiley and Sons.on, 1982.

41. Reyad A Awwad Shawabkeh: "Synthesis and characterization of activated carbo-aluminosilicate material from oil shale," Microporous and Messopourous, 2004.
42. T. Yang, A. Lua, "Characteristics of activated carbons prepared from pistachio-nut shells by physical actication," J. of Coll. and Interface Science. 267, 408-417, 2003.
43. A. Puziy, O. Poddubanaya, A. Martinez-Alonso, F. Suarez-Garci, J. Tascon, "Synthetic carbons activated with phosphoric acid III. Carbons prepared in air," Carbon 41, 1181-1191, 2003.
44. J. Guo, A. Lua, "Textural and chemical characterizations of activated carbon prepared from oil-palm stone with H_2SO_4 and KOH impregnation," Microporous and Messoprous Materials, 32, 111-117, 1999.
45. Ibnelwaleed A. Hussein, Mohammed H. Iqbal, Hamad I. Al-Abdul Wahhab, "Influence of Mw of LDPE and vinyl acetate content of EVA on the Rheology of Polymer Modified Asphalt," Rheologica Acta, 45(1), 92-104, 2005.
46. Mohammad H. Iqbal, Ibnelwaleed A. Hussein, Hamad I. Al-Abdul Wahhab, Mohamed B. Amin, "Rheological Investigation of the Influence of Acrylate Polymers on the Modification of Asphalt," J. Applied Polymer Science, 102(4), 3446-3456, 2006.
47. Peyman Ezzati, Ismaeil Ghasemi, Mohammad Karrabi, and Hamed Azizi, "Rheological Behaviour of PP/EPDM Blend: The Effect of Compatibilization," Iranian Polymer Journal, 2008.
48. Chen Y, Li H, "Phase Morphology evolution and compatibility improvement of PP/EPDM by ultrasound irradiation," Polymer, 2005.
49. Polymer Data Handbook", Oxford University Press

VITAE

- Muhammad Jamal Khan
- Born in Karachi, Pakistan on 20th May, 1984
- Received B.Sc. (H) in Applied Chemistry & Chemical Technology from University of Karachi, Pakistan in December, 2004
- Received M.Sc. in Applied Chemistry & Chemical Technology from University of Karachi, Pakistan in January, 2006
- Worked in Pakistan State Oil Company, Karachi, Pakistan as a Quality Assurance Officer from March, 2006 to September, 2008
- Joined King Fahd University of Petroleum & Minerals, Dhahran, Saudi Arabia as a Research Assistant in October, 2008
- Completed M.S. in Chemical Engineering from King Fahd University of Petroleum & Minerals, Dhahran, Saudi Arabia in November 2010
- E-mail: 101.jamal@gmail.com
- Present Address: P.O. Box 8602, King Fahd University of Petroleum & Minerals, Dhahran- 31261, Saudi Arabia
- Permanent Address: H. No. J-11/2, Pak Jamhooria Colony, near P.N.S. Shifa Hospital, Karachi-75530, Pakistan